Development of konjac glucomannan hydrogel for wound healing.

Munira Shahbuddin
Supervisors:
Prof. Sheila MacNeil
Prof. Stephen Rimmer

Submitted for the degree of Doctor of Philosophy
Department of Materials Engineering and Science.
October 2013

Acknowledgement

In the name of Allah, The Most Merciful and The Most Beneficient.

A wonderful thank you is due to my darling husband, Nik Nooruhafidzi M. Noor whose love, patience and company are the strongest motivation. Also, I would like to thank my family and friends for their support and love.

Finally, I must express my deepest gratitude to my parents, Shahbuddin M. Fiah and Latifah A. Kahar, for their unconditional love and patience; to them I dedicate this book.

Munira Shahbuddin

Abstract

The research presented in this thesis explores the potential uses of KGM and the development of KGM containing hydrogels for wound healing applications. The work involved characterization of five different species of *Amorphophallus* and investigating the biological activity of KGM and different molecular weight fractions of KGM on skin cells. KGM stimulated fibroblast (but not keratinocyte) proliferation and these effect were influenced by the species, Glc:Man ratio, % of glucomannan, molecular weight and the treatments of KGM. KGM also had the ability to maintain fibroblasts and ADMSC viabilities in unchanged medium for 20 days. The involvement of carbohydrate binding receptors on skin cells was also investigated to obtain a better understanding of the biological activity of KGM. KGM also had the potential for cell transportation where examination subjected to shear stress showed positive result. Following these, two sets of KGM hydrogels; crosslinked KGM and interpenetrating network (IPN); (semi IPN and graft-conetworks) were then developed and characterized using FTIR, DSC, SEM and ^{13}C solid state NMR spectroscopy and their water content were examined. The crosslinked KGM was synthesized at various concentrations of KGM and Ce(IV), while the IPNs were made of KGM and poly(N-vinyl pyrrolidinone) (P(NVP)) crosslinked with poly(ethylene glycol diacrylate) (PEGDA) using photopolymerisation. Graft-conetwork hydrogels' EWC of 85-90% was very stimulatory to fibroblast proliferation and the migration of both keratinocytes and fibroblasts while semi IPN with the highest EWC of (90-95%) and water content did not. Differences in the chemistry and water properties of the hydrogels had significant influences in their biological activities. Examination on 3D tissue engineered skin and wound models showed that the KGM containing hydrogels were able to decrease the extent of skin contracture without affecting the reepithelisation process. Taken together these data support a potential role for KGM and KGM containing hydrogels in wound healing.

Abbreviations.

ALI	Air-liquid interface
ADMSC	Adipose Derived Mesenchymal Stem Cell
ATR	Attentuated Total Reflactance
BSA	Bovine serum albumin
BSE `	Bovine spongioform encephalitis
CEA	Cultured epithelial autograft
DAPI	4',6-Diamidino-2-phenylindole
DED	De-epithelised acellular dermis
DEGBAC	Diethyleneglycol bisallylcarbonate
DEGDMA	Diethyleneglycol dimethacrylate
DMEM	Dulbecco's modified eagles medium
DMSO	Dimethyl siloxane
DSC	Differential scanning calorimetry
ECM	Extracellular matrix
EGDMA	Ethylene glycol dimethacrylate
EGF	Epidermal growth factor
EtOH	Ethanol
EWC	Equilibrium water content
FCS	Foetal calf serum
FGF	Fibroblast growth factor
FTIR	Fourier transform infrared
GAG	Glycosaminoglycan
GPC	Gel Permeation Chromatography
HA	Hyaluronan
HCl	Hidrochloric acid
H&E	Haematoxylin and Eosin
HMW	High molecular weight
IL	Interleukin
KGF	Keratinocyte growth factor
KGM	Konjac glucomannan
KcM	Keratinocyte mannose receptor

LMW	Low molecular weight
MMP	Matrix metalloproteinase
MMR	Macrophage mannose receptor
MTS	3-(4,5-dimethylthiazol-2-yl)-5-(3-carboxymethoxyphenyl)-2-(4-sulfonyl)-2H-tetrazolium
MTT	3-(4,5-Dimethylthiazol-2-yl)-2,5-diphenyltetrazolium bromide
Mw	Average molecular weight
NMR	Nuclear magnetic resonance
NVP	N-vinyl pyrrolidinone
PAA	Poly(acrylic acid)
PAAm	Poly(acrylamide)
PBS	Phosphate buffered saline
PDGF	Platelet derived growth factor
PEG	Poly(ethylene glycol)
PEO	Poly(ethylene oxide)
P(EF-co-EG)	Poly(ethyl fumarate-co-ethyl glycol)
PHEMA	Poly(hydroxyethylmethacrylate)
PNIPAAm	Poly(N-isopropylacrylamide)
P(NVP)	Poly(vinyl pyrrolidinone)
P(NVP-co-PEGDA)	Poly(vinyl pyrrolidinone-co-poly(ethylene glycol diacrylate)
PVA	Poly(vinyl alcohol)
RGD	Arginine-glycine-aspartic acid (cell adhesion peptide)
SD	Standard deviation
SDS	Sodium dodecyl sulphate
SEM	Scanning Electron Microscopy
TCP	Tissue culture polystyrene
TE	Tissue engineered (skin)
Tg	Glass transition temperature
Tm	Melting temperature
TGF-α	Transforming growth factor α
UV	Ultraviolet
VEGF	Vascular endothelial growth factor
Wt%	Weight %

Publications

Papers

1. Shahbuddin, M., Shahbuddin, D., Bullock, A.J., Ibrahim, H., Rimmer, S., MacNeil, S., **High molecular weight plant heteropolysaccharides stimulate fibroblasts but inhibit keratinocytes**, Carbohydrate Research (2013). Volume 375, 28 June 2013, Pages 90–99

2. Shahbuddin, M., Bullock, A.J., Rimmer, S., MacNeil, S., **Glucomannan-poly(N-vinyl pyrrolidinone) bicomponent hydrogels for wound healing**. Submitted to Journals of Materials Chemistry-B (2013). (accepted, awaiting publication).

3. Shahbuddin, M., Bullock, A.J., Rimmer, S., MacNeil, S., **Glucomannan hydrogels inhibit the contraction of tissue engineered skin without disrupting reepithelisation and promoted fibroblast proliferation in dermal area.** (in preparation).

Published abstracts

1. Shahbuddin, M., Rimmer, S., MacNeil, S., The biological effect of konjac glucomannan on skin cells (2010) Biomaterials & Tissue Engineering Group, The 12th Annual White Rose Work in Progress Meeting, Leeds, United Kingdom.

2. Shahbuddin, M., Rimmer, S., MacNeil, S., The potential use of konjac glucomannan for wound healing and cell transportations. European Cells and Materials Vol. 22. Suppl. 3, 2011 (page 43).

3. Synthesis and preparation of Konjac glucomannan hydrogel for wound healing. World Tissue Engineering and Regenerative Medicine Symposium (TERMIS), Vienna, Austria September 5-8th 2012.

Table of contents

Chapter 1. Introduction

1.1 Historical overview of the treatment of wounds.

Historically, wounds have been treated with natural substances such as cobwebs, leaves, tree bark, resin and honey due to their availability, cooling and soothing effects (Forrest 1982). The use of cloth, honey, milk, and resin in the treatment of wounds can be traced from ancient Egypt and Mesopotamia to the Arabs via Greeks and Romans. *The Edwin Smith Surgical Papyrus* which was written around 1700 BC is one of the earliest known documentations on the treatment of wounds encountered during battle fields in Eqypt (Breasted 1930). Mixtures of honey and lard or honey and resin were used as wound healing agents in Egypt due to their properties that prevent infection from entering the wound site as well as sealing off the wound from getting exposed. The Egyptians were also among the first people to introduce the use of minerals such as silver, sulphur and mercury in wound treatment (Forrest 1982). The treatment of topical wounds using water or milk and subsequently covered cloth pasted with honey and resin was recorded by The Mesopotamians on a clay scripture dated back in 2500 BC (Forrest 1982).

Treatment with salves to promote suppuration was suggested by Hippocratus (460-377 BC) in order to remove necrotic materials and to reduce inflammation (Leo 1961; Forrest 1982). Then, Guy de Churliac (1300-1368) in Cyrugia Magna proposed the five principles of wound treatment, the removal of wound debris, reapproximation of the separated parts, maintenance of wound conditions, conservation and the treatment of complications, which became the basis of today's wound treament (Leo 1961).

In the late 19th century, Joseph Lister, adopted the idea of antiseptic surgery which led to significant reductions in the post operative infections (Hanninen and Farago 1983). Use of simple hygienic practices and sterilization made a huge difference in the prevention of

infection. Based on this practice, Robert Wood Johnson I began the production of gauze and wound dressings treated with iodine in the 1870s, that later emerged as a step forward in the production of antiseptic dressing (Hanninen and Farago 1983). 50 years on, the discovery of an antibiotic called penicillin from Penicillium mold by Sir Alexander Fleming at St. Mary University laboratory, London epitomized a revolution in modern wound treatment.

Technological advances in polymerisation in the early 20th century provided new materials for wound treatment. Fibrous synthetic materials such as nylon, polyurethane, polyester and polypropelene are some of the polymers used as wound dressings. Povidone, which is a polymer of *N*-vinylpyrrolidone soaked in iodine was widely used to treat wounded soldiers in World War II.

Chronic non-healing wounds have become a major economic burden to many countries due to the debilitating cost of treatment. Winter et. al 1962 then proposed that a moist wound environment promoted faster re-epithelization rates of the exposed tissues in both porcine and human model compared to dry wound. These findings then led to the introduction of semi occlusive dressings for the treatment of wounds in the 1970's (Janzekovic 1970).

Emergence of tissue engineering and regenerative medicine with improvements in composite and hybrid polymers expanded the range of new materials. Introduction of gene and protein based therapies to impaired wound healing from diseases such as diabetes and infections have significantly improved conditions and promote healing progression. The next generation of ideal biomaterials for wound dressing should be biologically active that selectively interact with specific integrins, lectins, cytokines and growth factors expressed by target cells in surrounding tissues required for the repair of the damaged tissue (Griffith and Naughton 2002). The knowledge of the involvement and the functions of lectins and growth factor receptors in many cellular physiological events such as proliferation, adhesion, migration and differentiation could enable the design of synthetic materials to modulate cell functions

for tissue regeneration. (Wollenberg, Mommaas et al. 2002; McGreal, Miller et al. 2005; Irache, Salman et al. 2008).

1.2 The use of sugar for wound treatment.

Sugars such as granulated sugar, starch (amylose), honey and cellulose have the same chemical structure of $C_6H_{12}O_6$ with differences in molecular weight and stereochemistry. The use of sugar in medicines to treat wounds and ulcers has been reported extensively in the last few centuries by Scultetus in 1679 and Zoinin in 1714 (Pieper and Caliri 2003).

Sugars help to reduce exudation and edema, enhance nutrients in healing tissue, stimulate granulation tissue, lower the wound pH, induce a bacteriostatic effect, and encourage growth of epithelial tissue (Knutson, Merbitz et al. 1981; Silvetti 1981; Chirife, Scarmato et al. 1982; Kilic 2001; Moore, Smith et al. 2001). Knutson and colleagues performed the largest series of wound treatments using granulated sugar soaked into gauze in povidone-iodine on 605 patients with traumatic wounds, burns and ulcers and showed reduction of the healing time by 25% compared to controls with minimal and no scarring (Knutson, Merbitz et al. 1981). Similar findings were also reported by Herzage, where a reduction in odor and a decrease in purulent secretions in infected wounds were reported (Chirife, Scarmato et al. 1982).
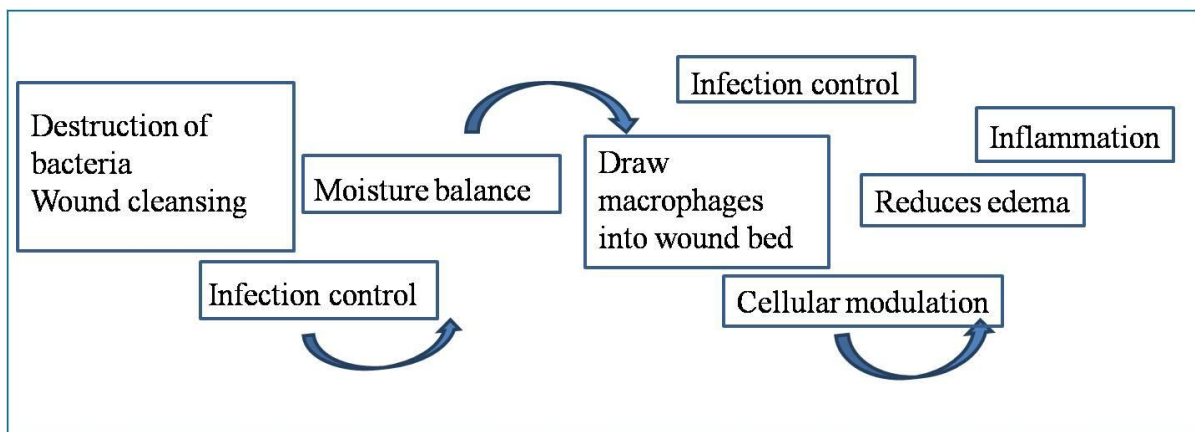
Figure 1.1   Physiological rational for the use of sugar for wound healing. Adapted from J. Diabetes Sc. Technol. Vol 4, Issue 5, September 2010 (Biswas, Bharara et al. 2010)

Kilic and colleagues specifically used granulated sugar paste to treat his patients with diabetic foot ulcers (DFU) by changing the dressings twice daily. He noted a decrease in odor, inhibition of bacterial growth, reduction of edema and debridement of necrotic tissue which was similar to that reported by Knutson et. al. (Kilic 2001). An interesting study on DFU with multiple resistance to topical applications, allergic to systemic antibiotic and had four multi pathogen-infected venous stasis ulcers that were recurrent for 17 years was conducted by Lisle (Lisle 2002). All wounds were completely healed at the end of treatment, where they had shown similarities to the findings by Kilic, Knutson and Herszage's groups with additional findings on the suppression of methicillin resistant *S. aureus, β-hemolytic strepcocci* and mixed bacteria from entering flora in the wound (Lisle 2002).

Similar observations were reported with the use of high molecular weight polysaccharide powders containing 3-5% ascorbic acid (Silvetti 1981). Silvetti claimed that a high molecular weight polysaccharide prevented the growth of bacteria in wounds by lowering the water content below 0.65% through osmosis, which supported the finding by Chirife et. al. (Silvetti 1981; Chirife, Scarmato et al. 1982). Both studies described the positive effect of low pH and osmosis to improve wound healing conditions.

The binding of water creates a template suitable for cell migration and proliferation (Brenda, Marques et al. 1995; Topham 2002), encouraging the production of hyaluronic acid from glucose and simultaneously suppresses the formation of fiber forming collagen that contributes to scarring (Topham 2002; Pieper and Caliri 2003). Specific interactions of sugar with different cell types also encourages the excretion of essential cytokines and growth factors that can improve conditions of wound healing (Topham 2002).

1.3 Hydrogel.

Hydrogels are defined as three dimensional (3D) 'solid like solution' materials with the ability to absorb large amounts of water while maintaining their dimensional stability (Peppas and Sahlin 1996). The integrity of the hydrogels can be maintained either by physical or chemical crosslinking (Brannon-Peppas and Peppas 1990). Hydrogel formation is influenced by chemically crosslinked network of hydrophilic polymers in which the thermodynamic forces of swelling are counterbalanced with elastic and refractive forces of the crosslinking in the material (Hoffman 2002).

Hydrogels are widely used in biopharmaceutical and wound applications due to their properties which include biocompatibility and the ability to copolymerize with other synthetic or natural polymers due to the functional groups on the polymer backbone that offer a wide range of formulation possibilities (Hoffman 2002). The amount of water absorbed in hydrogels is related to the presence of specific groups such as $-COOH$, $-OH$, $-CONH_2$, $-CONH-$ and $-SO_3H$ (Dergunov and Mun 2009). Other factors such capillary effect, pH, osmotic pressure, temperature and ionic strength of water solution in contact with the polymer also influence hydrogel's absorption (Brannon-Peppas and Peppas 1990; Hoffman 2002; Dergunov and Mun 2009). The ability of hydrogels to absorb and release water in a reversible manner and in response to specific environmental stimuli have made hydrogels appealing for applications in various engineering field, ranging from personal care products to drug delivery and as catalysts and biosensors. In the tissue engineering and biomaterials fields, hydrogels represent an ideal environment to support cellular proliferation and migration as they permit the diffusion of nutrient and waste (Brannon-Peppas and Peppas 1990) and also their structural and hydration properties that mimic human tissue (Cha and Pitt 1990; Peppas, Langer et al. 1995).

1.3.1 Classifications of hydrogels.

Hydrogels can be classified in several ways, depending on the method of preparation, the origin of the hydrogel, ionic charges, sources, nature of swelling with changes in the environment, rate of biodegradation or the nature of crosslinking (Hoffman 2002; Kolybaba 2003; Rimmer 2011). One of the important classifications is based on their crosslinking nature and preparation methods such as physical and chemical hydrogels, homo, co- and interpenetrating polymers. Physical hydrogels are the type of hydrogels where the chains are connected by electrostatic forces, hydrogen bonds, hydrophobic interactions between oppositely-charged biopolymers or chain entanglement (Hoffman 2002). Chemical hydrogels are the type of hydrogels where the chains are linked to each other with covalent bonds at specific sites of the polymer molecular backbone using crosslinkers (Hoffman 2002). Physical and chemical hydrogels can be produced from either natural or synthetic polymers (Farris, Schaich et al. 2009). Interpenetrating polymers or networks (IPN) are generally formed of two or more polymer networks that may be crosslinked by chemical or physical bonds. IPN may be formed simultaneously (from monomer A and monomer B) or sequentially (from polymer A and monomer B) (Farris, Schaich et al. 2009). IPN can also be formed by the swelling of a first network in a solvent containing monomers which then form the second intermeshing network structure (Zhao, Cao et al.).

The double networks of IPN would either be hydrophilic and hydrophobic or hydrophilic and hydrophilic. There are two types of IPNs: full IPNs with both networks crosslinked and semi IPNs in which only one network is crosslinked but the second network is not. The advantage of IPN in the development of hydrogel lies in the sharing properties of combination network.

Noninionic Hydrogels

Cationic Hydrogels

Anionic Hydrogels

Ampholytic Hydrogels

Ionic charge

Biodegradable Hydrogels

Non-biodegradable Hydrogels

Biodegradability

Smart Hydrogels

Physical properties

Conventional Hydrogels

Physical crosslinked Hydrogels

Chemically crosslinked Hydrogels

Crosslinking

Hydrogels

Natural Hydrogels

Hybrid Hydrogels

Source

Synthetic Hydrogels

Preparation method

Homopolymers

Copolymers

Interpenetrating Polymers

Triblock Copolymers

Multiblock Copolymers

Figure 1.2 Classifications of hydrogels. *Adapted from Alpesh, P. and K. Mequanint, Hydrogel Biomaterials, Biomedical Engineering - Frontiers and Challenges, 2011*. (Alpesh and Mequanint 2011).

In general, polymers consist of repeating monomers (homopolymer) or chemically different polymers (copolymer) or compositions of more than three crosslinked monomers (multipolymers) that can be organized in different ways to make random copolymers, alternating copolymers, block copolymers or graft copolymers (Rimmer 2011). The term homopolymer hydrogels is defined as one type of hydrophilic monomers crosslinked with each other in a network whereas copolymer hydrogels are formed by the crosslinking of two comonomers, one of which must be hydrophilic (Hoffman 2002). On the other hand, multipolymer hydrogels are produced from three or more comonomers reacting together.

1.3.1.1 Synthetic polymers

Synthetic polymers are widely used in biomedical applications because of their wide range of chemistry with specific molecular weights, chemical structures, degradable or non-degradable structures and with specific crosslinking and can be produced in large quantities and low cost of production (Hoffman 2002). Examples of synthetic polymers are as shown in Figure 1.3.

PEG based hydrogels are gaining attention due to their limited immunological reaction and biocompatibility of their degradation products (Bae, Gemeinhart et al. 2010). Poly(ethylene oxide) (PEO) which is an FDA approved biocompatible, and hydrophilic semicrystalline polymer is one of the most commonly used polymers for tissue engineering due to its similarity and flexibility to human tissue (Lee and Mooney 2001). The chemical structure of PEO is similar to poly(ethylene glycol) PEG and both of these polymers can be

photocrosslinked by modifying each other's polymer end with either methacrylate or acrylates using appropriate photoinitiator. Block co-polymerisation of PEO or PEG also can be formed with poly(lactic acid) (PLA) and poly(glycolic acid) (PGA) or a combination of poly(lactic-glycolic acid) (PLGA) to make thermally responsive and reversible polymers.

PLA, PGA and PLGA are most commonly used synthetic polymers in tissue engineering (Cha and Pitt 1990; Peppas and Sahlin 1996). However, the degradation of PLA and PGA was reported to cause destruction to proteins due to high local acidity (Cha and Pitt 1990).
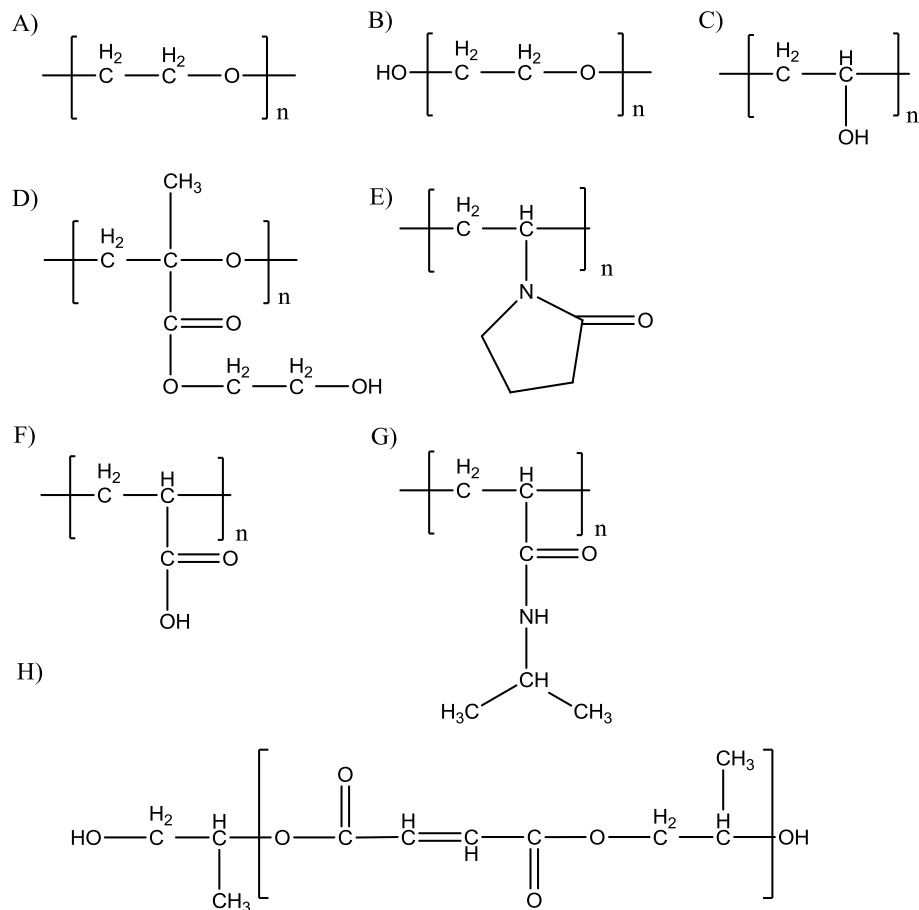
Figure 1.3   Representative chemical structure for synthetic polymers; A-E) neutral polymers : A) PEO, B) PEG, C) PVA, D) P(HEMA), E) PVP, F-H) responsive polymers: F) PAA, G) P(NIPAAM) and H) PPF.

Another example of widely used synthetic hydrogel for biomaterials is poly(2-hydroxylethyl methacrylate) (PHEMA) which is a common constituent in contact lenses (Corkhill, Hamilton et al. 1989) (Figure 1.3 (D)). These lenses showed excellent wettability with 38% water content and were comfortable to wear compared to hard contact lenses (Wichterle and Lim 1960). Modification by addition of various hydrophilic monomers such as NVP and glycerol methacrylate (GMA) helped to improve its swelling and mechanical properties (Lloyd, Faragher et al. 2001). PHEMA is also used in drug delivery and tissue engineering applications (Peppas and Sahlin 1996).

Poly(*N*-vinyl pyrrolidone) P(NVP) is also known as povidone and is a common constituent in wound dressings for its compatibility and hydrability (Figure E) (Higa, Rogero et al. 1999). It is a water soluble homopolymer of N-vinyl-2-pyrrolidone. P(NVP) polymers have the ability to absorb water, where the absorption center is the amide group (Levy and Frank 1955). The polymer has been widely used in various biomedical applications due to its hydrophilicity and biocompatibility ever since it was developed in the 1930's by Professor Walter Repper and his colleagues in Germany at I.G Farben (Robinson, Sullivan et al. 1990). In World War II, P(NVP) was used as a blood plasma substitute and extender but was declared unsafe for such use by the FDA due to the risk of its accumulation in the body that could lead to the formation of granuloma (Robinson, Sullivan et al. 1990). The report also mentioned the polymer interference with blood coagulation, haemostasis, blood typing and crossmatching (Robinson, Sullivan et al. 1990).

The use of P(NVP) in clinical applications has been slightly controversial due to the FDA report and contradictory results (Robinson, Sullivan et al. 1990; Vijayasekaran, Chirila et al. 1996). The presence of the polymer in rabbit eyes caused severe inflammatory reactions after it was injected into rabbit eyes (Vijayasekaran, Chirila et al. 1996). Despite that, WHO

granted permission for the use of P(NVP) as a binder for tablets with acceptable daily intake of 0-5 mg.mL^{-1} (Robinson, Sullivan et al. 1990).

P(NVP) has the ability to be polymerised with free-radical initiators to make a non-ionic, hydrophilic polymer. Its solubility factor is due to some degree of compensation between the strong hydrogen bonding capability, specifically between the cyclic amide group and water protons and the NVP polymer backbone and cyclic methylene groups (Moshaverinia, Roohpour et al. 2009).

Poly(ethyl fumarate-co-ethyl glycol) (P(EF-co-EG)) is a newer, promising synthetic block copolymer which consists of linear, hydrophobic poly(propylene fumarate) (PPF) and hydrophilic poly(ethyl glycol) PEG (Figure H) (He, J. Yaszemski et al. 2000). It has been used as a biodegradable, injectable carrier for bone and blood vessel engineering where the degradation takes place via hydrolysis through the ester linkages (Suggs and Mikos 1999).

1.3.1.2 Natural polymer.

Naturally derived polymers are usually biocompatible (Bundle and Young 1992). These polymers can be derived from bacterial celluloses, plants' polysaccharides (i.e. konjac glucomannan, pectin, dextran) or animal (hyaluronic acid (HA), collagen) (Rault, Frei et al. 1996 ; Mano, Silva et al. 2007; Cascone, Barbani et al. 2001). The similarity in the chemical structures of bioactive glycosamino glycan (GAG) molecules present in the ECM with naturally derived polymers makes it widely used in formulations with synthetic polymers for biomaterials. Mechanical and degradation properties of plant extracted polymers make them useful as dressings for wound treatment. (Brenda, Marques et al. 1995).
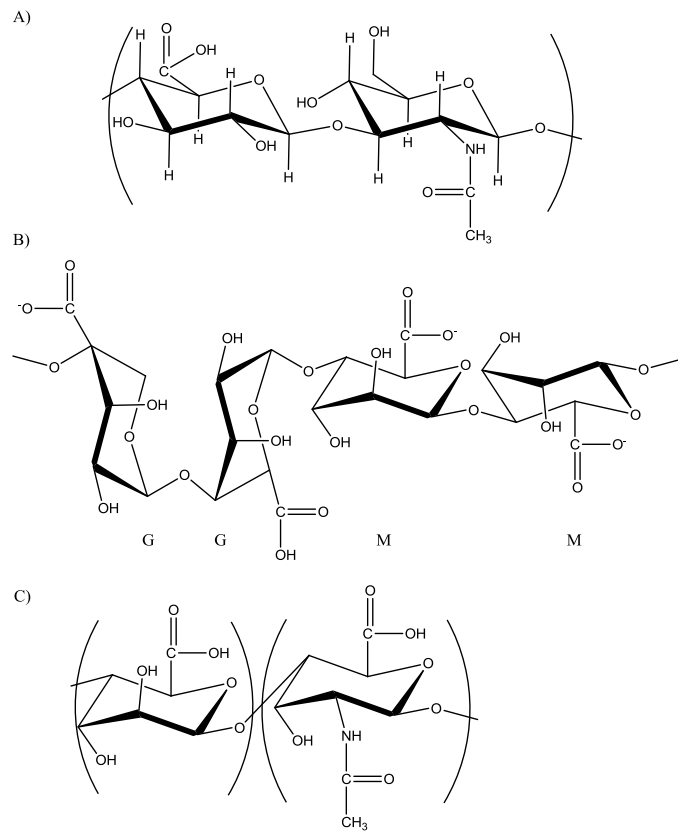
Figure 1.4 Structure of naturally derived polymers: (A) HA, (B) alginate and (C) chitosan.

Table 1.1   Examples of plant derived polymers for biomaterials

Source	Type	Biological activities	Use	Reference
Plant	Carrageenan	Biocompatibility.	As thickner or gelling agent in food industry. Filling in dental treatment and in formulation of biomaterials.	(Tye 1989)
	Pectin	Binds to cholesterol and help to reduce blood cholesterol level	As thickner or gelling agent in food industry. Dietary fiber.	(Farris, Schaich et al. 2009)
	Glucomannan	Improve insulin sensitivity and also promote wound healing.	Wound dressings, dietary fiber and cell encapsulation.	(Vuksan, Sievenpiper et al. 2000; Alonso-Sande, Teijeiro-Osorio et al. 2009)
	Alginate	Support tissue regeneration and able to support cell transportation.	Wound dressings, injectable hydrogel and cell encapsulation.	(Lee and Mooney 2001; Bo Chen, Bernice Wright et al. 2012)
	Xanthan gum	Tissue regeneration.	As biomaterial to improve mechanical strength in formulation with other polysaccharide hydrogel.	(Fan, Wang et al. 2008)
	Amylose	Anti-tumor, support tissue regeneration and biocompatible.	As biomaterials for tissue engineering and drug delivery vehicle.	(Esseku and Adeyeye 2010; Toita, Morimoto et al. 2011)

Table 1.2 Examples of animal derived polymers for biomaterials.

Source	Type	Biological activities	Use	Reference
Animal	Collagen	Promotes cell attachment, migration, proliferation and migration.	Has been developed into scaffolds for tissue engineering and for treatment of, cartilage and periodontal ligament.	(Yannas, Tzeranis et al. 2010) (Sylvester, Yannas et al. 1989) (Eichler and Carlson 2006)
	Fibrin	Supports keratinocytes and fibroblasts growth and enhances cellular motility in the wound	Use in wound healing treatment or coating on surface of biomaterials to support cell growth.	(Currie, Martin et al. 2003)
	Hyaluronic acid	Enhances bone formation, wound healing and cell functions.	Biomaterials and scaffolds for tissue engineering.	(Matsuda, Suzuki et al. 1990; Kuroyanagi, Kubo et al. 2004; Peattie, Nayate et al. 2004)
	Glycosamino glycan	Biological activities as with ECM and support cell attachment, proliferation and differentiation.	Scaffolds for tissue engineering.	(Yannas, Tzeranis et al. 2010)
	Silk	Supports cellular adhesion, proliferation and differentiation and it also promotes tissue repair in vivo	Wound dressing, biomaterials and drug delivery vehicle.	(Liu, Miao et al.) (Perez-Rigueiro, Elices et al. 2007)

Source	Type	Biological activities	Use	Reference
Bacterial or fungi extracted cellulose	β-D-1-3 Glucans	Anti-inflammatory, anti-tumorgenesis,	Use as vehicle in drug delivery system, drug encapsulation and for treatment of specific disease.	(Bohn and BeMiller 1995)
	Glucomannan	Photoprotective effect against UVA and UVB on skin	Use in cosmetic formulation.	(Ruszova, Pavek et al. 2008)
	Mannan containing polysaccharide	Anti-tumor	Use in chemotherapy to improve drug efficacy.	(Wasser 2003)

Table 1.3 Examples of bacterial or fungi extracted polymers for biomaterials

1.3.1.2 i. Konjac glucomannan

Figure 1.5   *Amorphophallus konjac* C. Koch.

Konjac glucomannan (KGM) is a perennial herbaceous herb which belongs to the Aracea family and *Amorphophallus* species (Figure 1.5). There are about 200 *Amorphophallus* species that grow in tropical Africa, Madagascar, tropical and subtropical Asia, the Malay Archipelago, Melanesia and Australia (Mayo, Bogner et al. 1997). KGM is widely used by Chinese and Japanese as traditional medicine in the treatment of asthma, coughs, hernia, burns, and dietary fiber in the treatment of diabetes and obesity (Alonso-Sande, Teijeiro-Osorio et al. 2009). KGM helps to decrease total cholesterol and low density lipoprotein and to maintain high density lipoprotein and increase insulin sensitivity from the pancreas (Vuksan, Jenkins et al. 1999; Vuksan, Sievenpiper et al. 2000).

KGM belongs to the group of immunomodulatory polysaccharides which includes galactomannans, heteroglycans, glucans, arabinogalactans and other mixed polysaccharides (Bohn and BeMiller 1995; Wasser 2003; Miadoková, Svidová et al. 2006). Consumption of KGM has also been beneficial to the gastrointestinal tract by enhancing the growth of bifidobacteria (Connolly, Lovegrove et al.). In recent years, the United States and Europe have introduced KGM as a food additive and dietary supplement, mainly for the treatment of obesity, constipation and indigestion (Martino, Martino et al. 2005). Clinical studies reported that supplementation with KGM helps to regulate systemic inflammation in the gastrointestine (Connolly, Lovegrove et al. ; Yeh, Lin et al.).

The active ingredient in *Amorphophallus konjac* is glucomannan (GM) which is also a major structural component of yeast, bacterias and other plants with similar physical properties containing α or β 1,4 or 1,6 glycosidic chains of D-glucose and D-mannose. (Wasser 2003; Ruszova, Pavek et al. 2008). It was reported that polymers containing mannose (mannans) exhibit significant biological activity when administered to mammals (Tizard, Carpenter et al. 1989).

1.3.1.3 Blend and copolymerisation of natural and synthetic polymer.

The combination of two or more polymers from natural or synthetic resources by physical or chemical methods bring together a number of different physical, mechanical and biological properties of different polymers for the development of specific polymer function (Hoffman 2002). Both natural and synthetic polymers have their own advantages and disadvantages (Ko, Ratner et al. 1981; Hoffman 2002). The properties of the blend is dependent on the degree of compatibility and miscibility of the polymer at a molecular level (Hoffman 2002).

The combination of synthetic with natural polymers for tissue engineering and biomaterial applications has gained a lot of attention due to biologically active ingredients in naturally derived polymers that have the potential to enhance cells' physiological impact on cellular level interacting via carbohydrate recognition proteins (lectin) (Holgersson, Gustafsson et al. 2005).

1.4 Synthesis and preparation of hydrogels.

Hydrogels can be prepared physically or chemically and a schematic method for the preparation of hydrogels is shown in Figure 1.6.

1.4.1 Physical method.

The physical method usually involves hydrophobic association among the macromolecules, as the macromolecules gradually lose their water by hydration to form the hydrogel network (Brannon-Peppas and Peppas 1990). Physically crosslinked hydrogels possess physical junction domains that associate with chain entanglement, hydrophobic interaction, hydrogen bonding, crystallinity and/or ionic complexation. Certain polysaccharides can gelate by itself when immersed in water and from heating. The degree of polysaccharide gelation depends on the degree of substitution which is defined as the average number of etherified hydroxyl

groups in a glucose unit. These units can be controlled to a certain extent in order to obtain the desired solubility and viscosity in aqueous solution. The degree of substitution polysaccharide solution can be properly adjusted to obtain specific formulation for gelation at body temperature, which is potentially useful for biomedical application (Chen 2003). The use of physical crosslinking method is gaining interest due to ease of fabrication and bulk polymerisation, (Xiao, Gao et al. 2000; Pavlov, Mano et al. 2004) and the avoidance of using crosslinking agents that are often toxic (Alpesh and Mequanint 2011). However, the major disadvantage of physical polymerisation is their weak mechanical properties in the swollen state (Alpesh and Mequanint 2011).
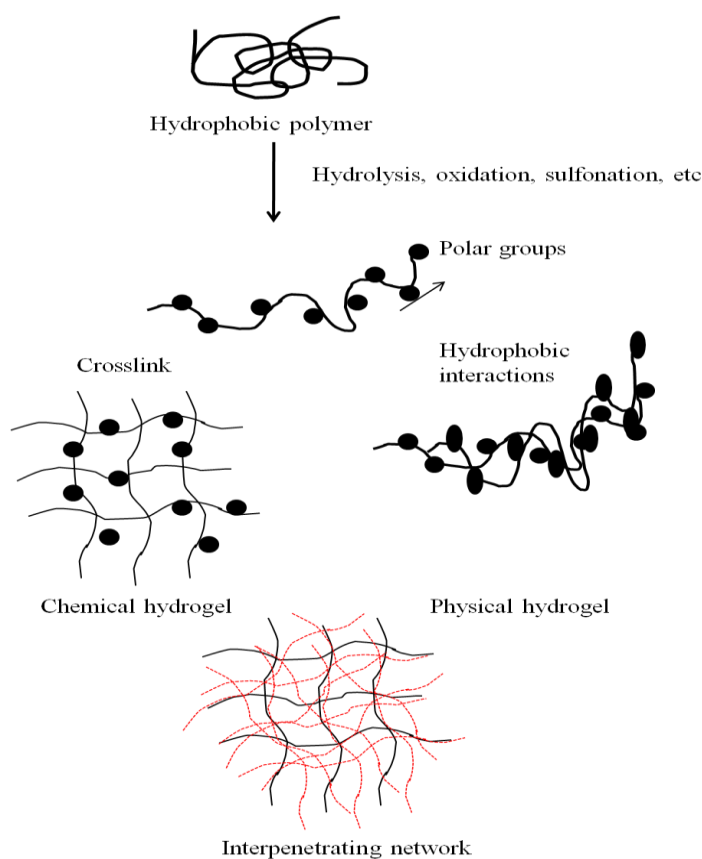
Figure 1.6   Schematic method for the formation of physical and chemical hydrogels (Adapted from *Advanced Drug Delivery Reviews,* 54, Allan S. Hoffman, 'Hydrogels for biomedical applications', 10, 2002).

1.4.2 Chemical method.

Chemical methods can be used to prepare a stable, stiff network of hydrogels by introduction of crosslinking at the functional groups of the polymer backbone. The degree of crosslinking, as defined by the number of crosslinking sites per unit volume of the polymer network affects the strength and degradation of the polymer (Berger, Reist et al. 2004).

There are a number of crosslinking agents and catalysts that can be used to make hydrogels. These agents are divided into 2 categories; reversible and non reversible crosslinkers. Examples of reversible crosslinkers are dialdehydes and polyaldehyde, the non reversible crosslinkers are epichlorohydrin and other epoxides, triphosphates and divinyl sulphone. One of the drawbacks in using aldehydes (reversible crosslinker) is toxicity in its unreacted state. Though it is possible to reduce or eliminate the toxicity of a crosslinker by extensive washing with ethanol and distilled water, the issue of toxicity will remain in question in order to preserve the biocompatibility of the hydrogel.

1.4.2.1 Polymerisation.

Polymerisation is a process by which small molecules called monomers react together in a chemical reaction to form a large molecule consisting of repeating units (Langer 1995). These chains may consist of repeating monomers (homopolymer) or chemically different monomers (copolymers). The monomers can be arranged into random, alternating, block or graft copolymers.

There are five types of polymers: homopolymer, copolymer, random copolymer, alternating copolymer, block copolymer and graft copolymer. Their arrangements and chemical diversities are shown in Figure 1.7.

Homopolymer – A polymer of the same repeating unit in the chain

$$M + M \rightarrow MMMMMMMMMM$$

Copolymer – A polymer with two or more different polymers in the chain

$$M + N \rightarrow MNMNNNMMMNN$$

Random copolymer – A random arrangement of two or more monomers along the polymer chain.

$$M + N + A \rightarrow MAANMAAMMMANNNAAAA$$

Alternating copolymer – Alternating arrangement of two monomers along the polymer chain.

$$M + N \rightarrow MMMMNNNNMMMMNNNNMMMM$$

Block copolymer – Blocks of two monomers in the polymer chain

$$M + N \rightarrow MMNNMMNNMMNN$$

Graft copolymer – Formation of branches from two or more monomers along the polymer backbone.

```
                              M
                              N
                              M
                              N
              MMMMMNNNMMMNNNN
                M       M
                N       N
                N       N
                N       N
```

Figure 1.7   Chemical diversity of polymer chains.

Bulk polymerisation is a process where the reaction mixture contains only initiator and monomer, without the presence of solvent. Solution polymerisation is a process where the reaction mixture contains solvent, initiator, and monomer. Suspension polymerisation is defined as a process where the reaction mixture contains an aqueous phase, water-insoluble monomer, and initiator soluble in the monomer droplets. Emulsion polymerisation requires an

emulsifying agent and is a similar process to suspension polymerisation except that the initiator is soluble in the aqueous phase rather than in the monomer droplets (Odian 2004).

Specifically, there are two types of polymerisation; step and chain growth polymerisation. The type of polymerisation is dependent on the method and chemicals used in the reactions. Step growth polymerisation is a stepwise reaction that usually proceed by the reactions between two different functional groups such as hydroxyl and carboxyl, or isocynate and hydroxyl group (Odian 1981). . The process includes the formation of urethanes (Yeganeh and Mehdizadeh 2004), esterification, amidation, aromatic substitution and others (Odian 1981). The process produces condensate and is also called condensation polymerisation (Odian 1981). These processes are divided into two groups which are depending on the type of monomers used (Odian 1981). The groups involve i) two different bifunctional monomers in which each monomer possesses only one type of functional group and ii) a single monomer containing both types of functional groups (Odian 1981). In this process, the obtained polymer could contain functional groups as part of its backbone chain or lose some of the atoms in the repeating unit (Odian 1981) The two groups of reactions are represented in a general manner which is shown in Figure 1.8.

$$nA\text{-}A \ + \ nB\text{-}B \ \rightarrow \ (\!\!-A\text{-}AB\text{-}B\!\!-\!)_n \qquad (i)$$

$$nA\text{-}B \rightarrow \ (\!\!-A\text{-}B\!\!-\!)_n \qquad\qquad (ii)$$
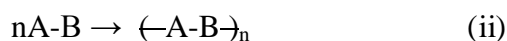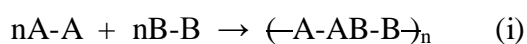
Figure 1.8 Representation of two different groups of reaction in step polymerisation.

.

Other type of polymerisation is called chain growth polymerisation, also known as addition polymerisation (Odian 1981). It involves the binding of molecules that incorporate double or triple chemical bonds. These monomers form the repeating chain by breaking its chemical

bonds and then linking up with other monomers. Examples of such polymerisation are poly(ethylene), poly(propelene) and poly(vinyl chloride) (Hoffman 2002). Some free radical polymerisation must take place in high temperature and pressure, such as poly(ethylene) with approximate 300°C and 2000 atm (Chenal, Olonde et al. 2007). Other forms of chain growth polymerisation are cationic addition polymerisation and anionic chain polymerisation. These methods are not popular due to stringent reaction condition such as lack of water and oxygen. These methods provide alternatives to the free radical method and are ideally suited for living polymerisation (Chenal, Olonde et al. 2007).

Free radical polymerisation is one of the methods for chain growth, also known as anionic, cationic and coordination polymerisation. The chains form a polymer from successive addition of free radical building blocks The formation of free radicals can be obtained by a number of different mechanisms which usually involves the use of separate initiator molecules (Rimmer 2011). This process can be initiated thermally or by irradiation using UV initiators such as peroxy, percarbonate or azo (Rimmer 2011). Thermal polymerisation is suitable for thick specimens whilst UV and other irradiation techniques are suitable for thinner devices such as contact lenses.

The polymerisation is controlled by three processes: chain initiation, chain propagation and chain termination. During the initiation process, a radical is created from initiating monomer and transferred from the initiator molecules to the monomer units. Radical initiation works best on carbon-carbon double bond of vinyl monomers and the carbon-oxygen double bond in aldehyde and ketone (Odian 2004). Electron beam and gamma irradiation can also generate radicals directly from monomers, without the use of a photoinitiator. The degree of crosslinking is dependent on irradiation dose and polymer concentration (Rimmer 2011). This technique is preferable for the synthesis of hydrogels for medical applications where small

traces of toxicity are not tolerated. The advantages of these procedures are that it does not involve the addition of chemical reagents while simultaneously sterilising the polymer. Although high energy radiation usually leads to chain scission of the polymer, crosslinking will prevail after the degradation under mild conditions (Rimmer 2011).

Photopolymerisation has gained increased attention in biomedical applications because of its minimally invasive procedure and rapid polymerisation following brief exposure to ultraviolet light (Langer and Peppas 1981). UV polymerisation requires photoinitiators in which production of radicals is initiated by homolytic scission of alkyl carbonyl bond. Examples of the mechanisms involve the cleavage at C-C, C-Cl, C-O or C-S bonds to form radicals when exposed to UV (Figure 1.9) (Nguyen and West 2002), abstraction of an H donor molecule to generate a ketyl radical and a donor radical from aromatic ketone (Liu and Bhatia 2002) and generation of protonic acids by cationic photopolymerisation(Kamigaito, Maeda et al. 1993). This type of polymerisation is widely used for biomaterials as it also provides effective sterilization (Rimmer 2011).
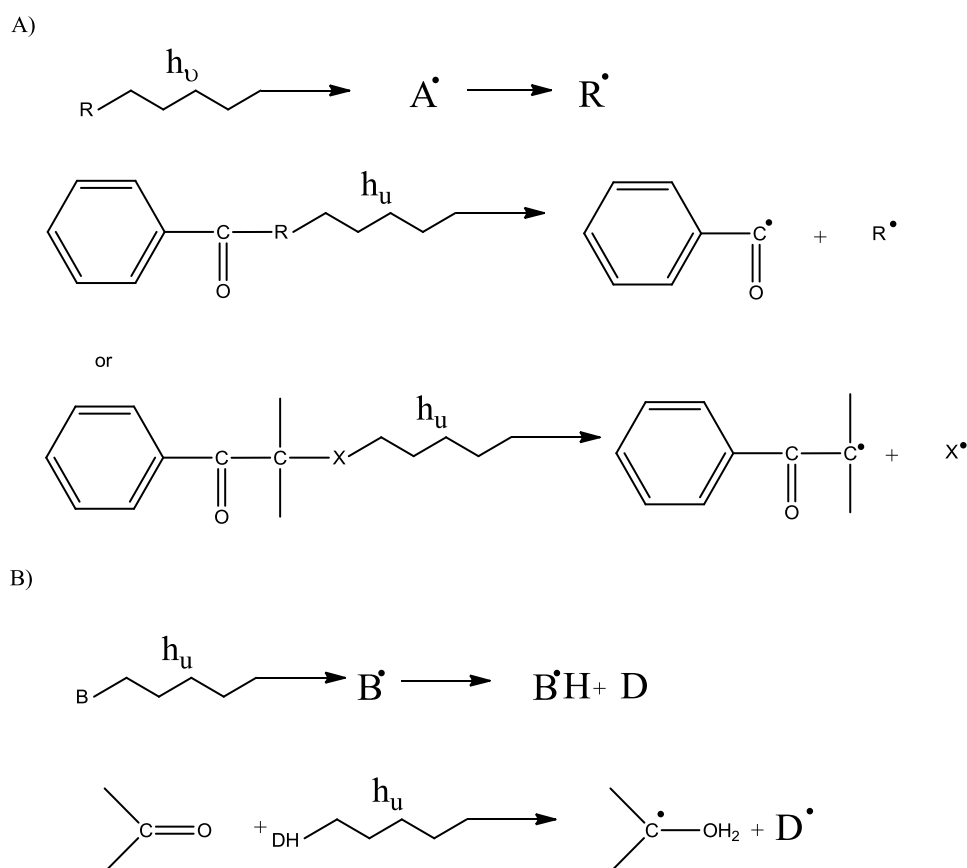
Figure 1.9   Photoinitiation mechanisms (A) – photocleavage, (B) hydrogel abstraction. *Adapted from Biomedical hydrogels, Biochemistry, manufacture and medical applications* (Rimmer 2011) and *Biomaterials,* Vol 23, Issue 22, *Photopolymerizable hydrogels for tissue engineering application* (Nguyen and West 2002).

Although this method provides effective sterilization, the use of a photoinitiator raises concern of cytotoxicity due to its small molecules contaminants which it is essential to thoroughly remove by washing. As for hydrogels, the swelling nature can facilitate removal of the potential toxins from unreacted monomers.

1.5 Human skin.

It is of outmost importance to understand the structure of the skin and the underlying mechanisms of normal and abnormal wound healing in designing hydrogels for wound treatment.

1.5.1 Functional significance.

Skin is an immunologically competent organ with the largest surface area covering the entire human body. It serves as a protective boundary between the human body and the external environment. As a physical barrier, skin plays significant and collaborative roles in the biomechanics, protection and thermoregulatory function (Metcalfe and Ferguson 2007). It helps to regulate body temperature by preventing water loss from internal tissues and protecting the sensitive organs from excessive heat and cold by sweating, and acts as a filter to prevent bacteria, viruses and harmful chemicals from entering the body (Jones, Currie et al. 2002).

As part of its protective function, skin is capable of sensing and mounting appropriate responses to pathogen invasions and physical stress by both innate and adaptive immune responses (Williams and Kupper 1996). Skin synthesizes important chemicals such as melanin and carotenes, which give the skin its color. It metabolizes vitamin D, which is important for calcium adsorption and development of bones, in the epidermis when it is exposed to sunlight.

1.5.2 Structural details.

Skin is composed of three layers – the epidermis or the epithelial layer, the dermis that contains a complex nerve and blood supply and the subcutaneous layer which is mainly composed of fat and loose connective tissues. A schematic representation of human skin is shown in Figure 1.10.

The epidermis is thin and highly stratified, composed mainly of keratinocytes and melanocytes in the lower epidermal layer. It is subdivided into 4 layers (Figure 1.11): stratum corneum (the cornified layer), stratum granulosum (the granular layer), stratum spinosum (the spinous layer) and stratum basale (the basal layer) (Gilbert 2003).

The outermost cornified layer of epidermis provides the physical barrier and is composed mainly of dead keratinocytes while the keratin and desmosomes underneath physically support the integrity of the epidermis (Falanga, Faria et al. 2007)
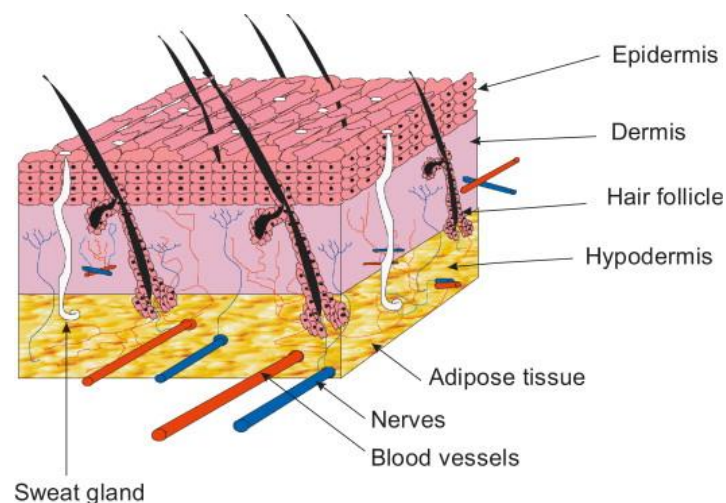
Figure 1.10   A schematic representation of human skin. Adapted from (Metcalfe and Ferguson 2007).

The spinous layer contains the major antigen presenting cells called Langerhan cells, which express major histocompatibility complex (MHC) that is important in the defence mechanism against pathogens and irritants (Wagner and Sohnle 1995).

The bottom layer of the epidermis contains melanocytes which are responsible for synthesis and distribution of melanin pigments (Yamaguchi, Hearing et al. 2005). It also contains keratinocytes that are capable of proliferating to either new basal cells or terminally differentiated keratinocytes. The differentiated keratinocytes will undergo changes such as the shrinking of nucleus and cytoplasm packed with keratins before travel to the outermost layer to form the protective layer (Yamaguchi, Hearing et al. 2005; Metcalfe and Ferguson 2007).

The second layer, i.e. the dermis is an organized structure of thick elastin and collagen fibers that are filled with a viscous fluid made up of glycosaminoglycans and hyaluronan. It is relatively acellular and composed of extracellular matrices that are primarily produced and maintained by fibroblasts which are the major type of cells in the dermis.

The dermis contains a complex vascular arrangement of blood vessels and adnexal structures with origin of hair follicles, sweat glands and sebaceous glands. It also has abundant endothelial cells which are important for angiogenesis and maintaining the blood vessels, hemapoetic cells such as macrophages and lymphocytes, smooth muscle cells, adipocytes, sensory neurons and cells of sweat glands. These cells collaboratively help to maintain homeostasis within the skin.

The subcutaneous layer, or hypodermis, is the third layer of the skin. It is a layer of fat and loose connective tissues that houses larger blood vessels and nerves. The integrity of this layer is important to maintain heat and prevent water loss as well as to protect the body against mechanical trauma. The size of this layer varies throughout individuals. The

overdeveloped subcutaneous layer leads to obesity while the loss and declination of this layer cause wrinkles and sagging.
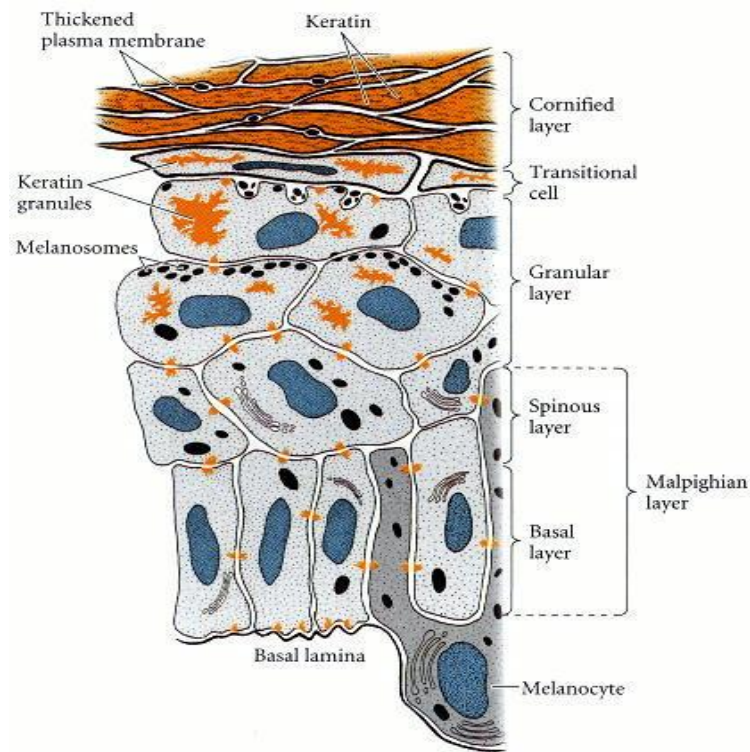
Figure 1.11 Schematic representation of the human epidermal layer. There are four main layers, cornified layer, granular layer, spinous layer and basal layer. The outermost layer, or the cornified layer is composed mainly of dead keratinocytes while the keratin and desmosomes inside the layer support the integrity of the dermis. The granular and spinous layers are composed mainly of differentiated keratinocytes while the bottom layer, the basal layer, contains proliferating keratinocytes. Image from Gilbert, 2003 (after Montagna and Parakkal, 1974).

1.6 Wounds.

A wound is a type of injury in which the epithelial integrity of skin is ripped and torn apart which may cause a disruption of the skin structure and the function of the underlying normal tissue. Wounds are divided into two categories, open and closed wounds. There are several types of open wounds such as incision, abrasion, laceration, puncture, gunshot and

penetration wound. A closed wound happens when a blunt force trauma causes contusion and damages part of the skin structure. A closed wound is as dangerous as an open wound. It can be classified as contusion, hematomas, crush injuries and chronic and acute wound. The chronic and acute wound in this category happens slowly and damages the tissue from within. These include pressure, venous and diabetic ulcers (Joseph 2004).

1.6.1 The conditions of wounds.

There are about five types of wound, necrotic, sloughy, granulating, epithelizing and infected wounds which are shown in Figure 1.12.

Figure 1.12   The types of wound. The pictures show (A) necrotic wound, (B) sloughy wound, (C) granulating wound, (D) epithelising wound and (E) infected wound. Pictures were taken from 3M wound resources center with Wound Healing Research Unit, Cardiff. (http://solutions.3m.co.uk/wps/portal/3M/en_GB/skin-care/wound-resource-centre/image-library/).

A necrotic wound appears to be black and devitalized, due to the death of tissues from dehydration and dry wound condition. Under normal physiological healing, dead tissue will become soft and easily shed from the wound site as slough through autolysis. The treatment of necrotic wounds requires hydrogels such as Tegaderm™ hydrocolloid dressing, used to provide and maintain moisture, and to promote autolytic debridement in order to remove the hardened tissue. Sometimes enzymes were also used in order to clean wounds by dissolving tissue debris and slough (Queen, Evans et al. 1987).

A slough wound is the type of wound that has thick layers of sloughy tissue. A slough wound slows granulation, thus prolonging the healing process. Sloughy layers need to be removed either by surgery, enzyme preparation or larval therapy. The use of enzyme is a commonly used form of debridement as the enzyme breaks down and separates tissue. In moist conditions, the enzymes help to soften and liquefy hardened tissue. Dressings such as hydrogels and foam dressings are commonly used for the treatment (Eaglstein 2001).

Infection of the wound occurs when bacterial colonization in and around the wound site increases to a critical level leading to the deterioration of wound condition. The signs of infection include redness, heat, swelling, pain, high level of exudation, discoloration of granulation tissue and delay of healing. Usually antiseptic and antibody are used with the dressings during treatment (Eaglstein 2001).

A chronic wound is the type of wound that does not heal orderly through the set of stages in a period of time that wound usually heal within. Chronic wounds usually involve the wound becoming stuck in one or more stages in the wound healing process. For example, a prolonged inflammatory stage impairs the balance of production and degradation of molecules such as collagen. An imbalance in the amount of vital molecules, proteins and nutrients slows healing (Marvin E 1998; Joseph 2004).

Chronic wounds cost an estimated £2.3 – 3.1 billion annually and represent a significant burden to patients, health care professionals and the National Health Service (NHS) (Posnett et al.). Chronic wounds result from impairment in physiological and mechanical factors causing the delay in healing response that fail to proceed according to the usual stepwise progression. Some chronic wounds may not heal or take years to heal. To effectively manage these problems, one must understand the normal healing process and the causes of the delay (Joseph 2004).

Infection, hypoxia, trauma and systemic problems such as diabetes mellitus,

immunodeficiency and malnutrition are often the cause of a prolonged inflammatory phase in wound healing. These factors are interlinked to each other as interplay of healing stages are overlapping and required the involvement of different types of cell (Fahie and Shettko 2007).

Infection happens when more than 10^5 organism per gram of tissue colonizes the wound. This affects the wound healing process by increasing the demand for proinflammatory cytokines such as macrophages. Prolonged secretion of a high level of proinflammatory cytokines causes the impairment of fibroblast proliferation, neovascularization and degradation of granulation (Schwentker, Vodovotz et al. 2002).

Hypoxia is one of the main causes of delayed healing. Oxygen is required for collagen deposition and fibril crosslinking with hydroxylated proline to ensure a stable foundation for reepithelisation. Hypoxia can be caused by systemic diseases such as diabetes mellitus which cause erythrocytes to become less pliable and less able to deliver oxygen to the wound (Gouin and Kiecolt-Glaser ; Angele, Knöferl et al. 1999).

Diabetes also causes complications and damage in nerves, arteries and immune systems which lead to a delay in wound healing. Most common complications of diabetes are nerve damage and artery problems such as peripheral arterial disease which happens from blockage in the blood vessels due to fatty acid deposits. Diabetic conditions also cause impairment to our body systems as the fluctuations in sugar concentrations in blood reduces the body's natural ability to fight infection. This contributes to cells' inability to bind with insulin and causes a disruption in glucose transportation into cells for metabolic activities, depriving cells of nutrients and leading to many physiological problems.

1.6.2 Mechanism of wound healing.

Wound healing is a complex, physiological self repairing process in which injured skin (or other organ tissues) undergoes progressions of physiological events to restore its functional

normality (Joseph 2004). Human skin has one of the greatest abilities to regenerate itself compared to other tissues in our body. The normal healing process starts as soon as the tissue is injured where the blood components come into contact with collagen and ECM at the site of injury, releasing clotting and growth factors (Joseph 2004). This progression is divided into three sequential and overlapping phases; inflammatory, proliferative and remodeling which can be characterized by secretion of distinctive cytokines by specific cells.

1.6.2.1 Inflammation.

The inflammatory phase plays an important role in fighting infections, clearance of debridement and induction of the proliferative phase (Joseph 2004). During the time of injury, hemostasis or clotting cascade takes place by a way of a fibrin clot. Simultaneously, the cells launch chemokines and cytokines to attract cells to phagocytose debris, bacteria and damaged tissue that give recognizable cardinal signs of inflammatory response such as redness, warmth, swelling, pain and loss of function. The inflammatory phase can be divided into four subphases: coagulation, vasoconstriction and vasodilation, polymorphonuclear neutrophils and macrophages (Braun and Werner 2006).

i. Coagulation.

Coagulation is part of hemostasis and is started as soon as the injury takes place, triggering inflammatory factors by initiating extrinsic coagulation cascade to activate factor VII. Factor VII is an essential blood clotting factor for hemostasis. Exposure of tissue factors such as thrombokinase with blood leads to the formation of a fibrin plug by mediating crosslinking of fibrin and fibronectin. The fibrin plug acts as a structural support to prevent blood loss and also as a matrix for migratory cells. It allows platelets to adhere and express glycoproteins on their cell membranes. Glycoproteins allow them to stick to each other and aggregate (Joseph 2004). Platelets secrete

adenosine diphosphate, tissue growth factor-β (TGF-β) and platelet derived growth factor (PDGF) to act on surrounding cells and stimulate chemotaxis of neutrophil, monocytes and fibroblasts to the wound site, thus promoting the increase of cell proliferation and migration (Joseph 2004).

ii. Vasoconstriction and vasodilation

Vasoconstriction of blood vessels happens immediately after a blood vessel is breached, causing the ruptured cell membranes to release inflammatory factors such as thromboxane and prostaglandin. This is to prevent blood loss and a mechanism to aid the injured site by collecting inflammatory cells and factors. Vasoconstriction lasts five to ten minutes and is followed by a widening of blood vessels. This peaks at about twenty minutes post-wounding (Joseph 2004).

Histamine is the main cause of vasodilation as it causes the blood vessels to become porous and facilitates the entry of the inflammatory cells like leukocytes from the blood stream into the wound site (Joseph 2004).

iii. Polymorphonuclear Neutrophils (PMNs)

PMNs arrive at the wound site within hours of injury and begin to dominate the cells in the wound for the first forty eight hours of injury together with white blood cells (WBC). They are the first to begin bactericidal activity using inflammatory mediators and oxygen free radicals in what is called a 'respiratory burst'. Normal wound healing can occur without PMNs and they normally undergo apoptosis after completion of their tasks, and are engulfed and degraded by macrophages (Joseph 2004).

iv. Macrophages

Unlike PMNs, macrophages are essential to wound healing as they are involved in

debridement, fibroblasts proliferation and angiogenesis. After 24-36 hours as PMNs begin to decrease, circulating monocytes will enter the wound and mature into tissue macrophages. These macrophages are important to the debridement of damaged tissue at a microscopic level by phagocytozing bacteria and debris. Also, in the process of debridement, they produce a wide range of important substances such as interleukin-1 (IL-1) and basic fibroblast growth factor (bFGF) (Metcalfe and Ferguson 2007).

At this stage, IL-1 and bFGF are important to the proliferation of inflammatory cells and promotion of angiogenesis through endothelial cell replication. Towards the end of the inflammatory phase, creation of granulation tissues (eicosanoids) in the wound will strongly influence fibroblast proliferation and synthesis of collagen as well as promoting the influx of keratinocytes and endothelial cells into the wound (Li, Zhang et al. 2003; Yamaguchi, Hearing et al. 2005).

1.6.2.2 Proliferative Phase.

The proliferative phase is characterized by angiogenesis, collagen deposition, granulation tissue formation, reepithelisation and wound contraction. It begins when mononuclear cells continuously replace white blood cells (WBC) and macrophages. Two to three days after injury, fibroblasts from the wound margin will migrate inward over the fibrous matrix which is formed during the inflammatory phase. At the same time, formation of new blood vessels (angiogenesis) by endothelial cells takes place and this step overlaps with other proliferative stages such as fibroplasia over time (Joseph 2004).

i. Angiogenesis (Neovascularisation).

Angiogenesis or neovascularization is a regeneration of new blood vessels. The process is normal and vital in wound healing and concurrently happens with fibroblast proliferation and endothelial cell migration. Cooperative regulation of vascular

endothelial growth factor (VEGF), angiopoietic, fibroblast growth factor (FGF) and transforming growth factor-β (TGF-β) are essential as they facilitate endothelial expansion to angiogenesis, creating vessels in granulation tissues (Li, Zhang et al. 2003). This process is directly stimulated by hypoxic conditions, which is a low oxygen environment, and the presence of lactic acid. Production of angiogenic factors by macrophages and the other growth factors producing cells will stop when they are no longer in a hypoxic and lactic acid filled environment, leading to the reduction of endothelial migration and proliferation (Li, Zhang et al. 2003). At the end of this stage when tissue is perfused with adequate nutrients and environment, the blood vessels that are no longer needed will die by apoptosis (Li, Zhang et al. 2003).

ii. Fibroplasia and granulation tissue formation.

Fibroplasia and granulation tissue formation starts as the inflammatory phase ends and occurs with angiogenesis. At this stage fibroblasts are beginning to accumulate in the wound and will become the dominant type, peaking at one to two weeks. Fibroblasts use fibrin linked fibers to migrate across the wound and then begin to assemble collagen molecules into the fibers (Joseph 2004).

Fibroblasts are also one of the important components in granulation tissues that appear after the inflammatory phase. As angiogenesis stops, granulation tissues containing newly formed blood vessels, endothelial cells, myofibroblasts and components of a new provisional extracellular matrix (ECM) will grow continuously until the wound bed is covered (Gouin and Kiecolt-Glaser ; Joseph 2004; Metcalfe and Ferguson 2007).

Provisional ECM is different to ECM found in non-injured tissue and this will later be replaced by fibroblasts in the next phase of healing (Joseph 2004).

ii.i Collagen deposition.

Fibroblasts are the major contributor to collagen synthesis and deposition of collagen in fibril linked fibers increase the strength of the wound, facilitating cells involved in angiogenesis, inflammation and construction of connective tissues to adhere, grow and differentiate.

The type III collagen and fibronectin are produced between ten hours and three days after injury and their deposition peak length from one to three weeks depending on the size of the wound (Joseph 2004).

1.6.2.3 Maturation and Remodelling.

Remodelling begins when collagen deposition is adequate for reepithelisation to mature and production of collagen type III is gradually replaced by collagen type I (Isaac, Mathor et al. 2009). The tensile strength of the wound will increase over time and will become as much as 80% as strong as normal tissue at least 12 weeks after injury.

i. Epithelisation.

Reepithelisation takes place from the formation of granulation tissues in an open wound that allows epithelial cells and keratinocytes to migrate across the newly formed tissue to form a barrier between the wound and the surrounding tissue. (Braun and Werner 2006). In this stage, keratinocytes do not undergo proliferation yet but its migration from wound edges across the wound site is important to allow formation of epithelial cells that would later assist in further healing stages.

Before migration, keratinocytes will change their shape into longer, flatter morphologies thus extending their cellular processes such as further formation of actin filament and lamellipodia. The migration is mediated by the lack of contact inhibition and chemicals such as nitric oxide (Schwentker, Vodovotz et al. 2002). They use

fibronectin linked fibrin formed during the inflammatory phase to move across the wound site. During this stage, epithelial cells are forming at wound edges to provide a base for keratinocyte proliferation. The epithelial cells are also important to remove debris (debridement) and contagions.

Keratinocyte migration will continue until cells from other wound edges meet to form a contact inhibition which causes them to stop migrating. As this happen, they will secrete proteins that form the new basement membrane and established desmosomes and hemidesmosomes to anchor the layer to the basement membrane (Eves, Beck et al. 2005).

ii. Contraction.

Wound contracture is a 'the dimunition of area of a wound that occurs from centripetal movement of the whole thickness of the surrounding tissue' (Abercrombie, Flint et al. 1956; Yannas 2005). Contraction is vital for wound healing and it commences approximately 4 to 5 days after wounding at an everage of 0.6-0.7 mm.day^{-1} depending on tissue type and wound shape (Lawrence 1998). The contraction appears to be mediated by fibroblastic lineage when fibroblasts differentiate into myofibroblasts (Eichler and Carlson 2006) but the exact nature of myofibroblast interaction with ECM has yet to be determined (Tejero-Trujeque 2001). The process begins 4 to 5 days after wounding and continues for 12-15 days depending on tissue type and wound shape (Lawrence 1998). It can also last up to several weeks depending on the severity of the wound and prolonged contraction can cause severe limitation of functions and skin deformation.

1.7 Wound management.

The ideal wound management should be cost effective, avoid infections, allow exchange of water vapor, and allow healing without delay or damaging the newly formed tissue (Queen, Evans et al. 1987). Some diseases such as diabetes and ischemia and conditions such as malnutrition, aging and local infection could cause a delay in wound healing. Supplementation with appropriate diets would be necessary to assist healing progression with such conditions (Vuksan, Sievenpiper et al. 2000; Vuksan, Sievenpiper et al. 2001; Phan, Sun et al. 2003). Infection is a major complication of burn injury, is responsible for more than 50% of hospital deaths, and it is necessary that wound management should be done aseptically and in sterile conditions (Church, Elsayed et al. 2006). Wounds should also be managed properly and according to severity. Moist wound treatment is reportedly beneficial compared to dry condition (Winter 1962).

1.7.1 Managing exudates.

Exudate has been described as wound fluid, wound drainage or an excess of normal fluid that accompanies inflammatory reaction after initial wounding (Adderley 2010). Exudate leaks from the body tissue from permeable capillaries as a part of inflammatory response. Exudate consists of water, nutrients, electrolytes, inflammatory mediators, white cells, protein digesting enzymes and growth factors and functions to promote healing by supplying the essential nutrients that promote cell metabolism, migration and allowing separation of damaged or dead tissues from good tissue (White and Cutting 2006; Adderley 2010).

The production of exudates depends on the size of the wound, with larger (or deeper and wider) wounds producing a larger amount of exudate. As healing progresses, the amount of exudate normally decreases. However excessive amounts of exudate can cause undesired problems such as increased risk of infection to the wound.

Exudate varies from types of wound, where a chronic wound's exudate is more likely to contain bacteria and dead white cells, along with high level of inflammatory mediators and protein digesting enzymes that would be detrimental to wound healing (Adderley 2010; Wade, Wolf et al. 2010). Chronic wound exudate can also cause skin irritation and allergic reactions to the area around the wound (Hampton 2004).

Dressings that contain topical antimicrobial such as silver or iodine were used to reduce the levels of microbial contamination and to reduce exudate to a normal level (Bradshaw 2011). A broader system antibiotic is required to treat wounds with a high level of exudate that accompanies the symptoms of chronic wound infections (White and Cutting 2006).

Management focusing on the palliative symptom management such as absorbent dressings and topical antimicrobials can be used to treat the underlying cause of the heavy exudate thus helping to reduce the risk of infection (Bradshaw 2011).

Excessive exudate also brings discomfort to patients' lives as it can lead to soiling of clothing and bedding, malodour and loss of nutrients (Wade, Wolf et al. 2010). It also can cause maceration and excoriation of the surrounding wounded skin which can be very painful and impair patient's quality of life (Hampton 2004).

The ideal dressing should be able to remove excess exudates from the wound site and surrounding skin while maintaining the moisture within the dressing at the wound bed (Bale 1997). The dressing should be also easy to remove and cost effective (White and Cutting 2006). There are various designs of dressing that would be able to absorb exudates into the dressing matrix through different type of mechanisms such as foams, hydrogels and gauze dressings and these can be either biodegradable or non-biodegradable. There is no strong evidence to suggest that one particular type of dressing is better than another at managing exudate or promoting healing as there is currently no standard approach in use (White and Cutting 2006).

However, biodegradable hydrogels can sometimes be effective skin protection to a wound with excessive exudates as it will able to absorb, protect from maceration and excoriation and also reduce the risk of damaging newly formed tissues (Winter 1962). However, the toxicity of a degradation product is also a considerable factor as certain low molecular weight monomers may elicit an inflammatory response (Li, Rodrigues et al. 2012).

Managing exudates is one of the important criteria in the management of wound that selection of appropriate materials and dressing change intervals are very important to minimize the risk of maceration and help to improve healing condition.

Assessment of the effectiveness of the care should always be reassessed at regular intervals using appropriate materials such as biodegradable, non-biodegradable or foam dressings.

1.8 Materials for wound treatment.

It is accepted that due to the distinct characteristics of different types of wounds, conditions and stages of healing, there is no single dressing that can be efficiently applied in all situations. Conventional wound dressings rely on synthetic or natural materials that require frequent replacement to provide protection from the external environment and maintain the moisture conditions of the wound. The ideal criteria for wound dressings are summarized in Table 1.4.

 Current treatments do not provide the optimum therapy because of the lack of understanding of pathophysiology and molecular biology of different type of wound conditions. To date no commercially available wound dressings possess all of the properties in Table 1.4 nor are able to fully replace the functional and anatomical properties of native skin.

Polymeric materials with distinct chemical, physical and biological properties are used in the production of wound dressings of different designs, dimensions and shapes with different functional properties. The simplest way to classify the products is by consideration of its origin: synthetic or naturally based poly/co-polymers where this can be obtained by mixture

of both natural and synthetic or homogenous mixture using chemical or physical modification.

Table 1.4 Ideal criteria for the materials used in wound treatment. (Atiyeh, Hayek et al. 2005; MacNeil 2007; Shevchenko, James et al. 2010).

Economy	Physical	Biological
Low cost	Biocompatible	Reduce risk of infection
Readily available	Tensile strength to resist fragmentation and good elasticity.	Non-antigenicity
Minimize the cost of wound care	Prevent heat and fluid loss.	Grow with the child
Long shelf life	Impermeable to exogenous microorganism	Reduce healing time.
	Allow vapor transmission	
	Controlled degradation	
	Translucent, which allows direct observation of healing progress.	

There are a number of bioengineered skin replacement products that are currently under investigation, some of which have entered stage II-III clinical trials and could possibly be on the market shortly (Shevchenko, James et al. 2010). These materials are classified according to their structure, origin, function and biological activities as summarized in Table 1.5.

Table 1.5 Classification of currently available skin substitute products (modified from (Shevchenko, James et al. 2010).

Anatomical structure	Dermo-epidermal (composite), epidermal and dermal
Duration of the cover	Temporary, semi-permanent and permanent
Type of biomaterials	- biological: autologous, allogenic and xenogenic.

Skin substitute composition regarding cellular component: Primary biomaterial loading with cellular component occurs:	- synthetic: biodegradable and non-biodegradable. Acellular and cellular *In vivo* and *in vitro.*

There are three types of skin grafts that can be used for wound treatment, autograft, allograft and xenograft which are obtained from different sources.

i. Autograft.

Autograft is a skin graft taken from the patient's own uninjured skin, usually from the back side of a torso or from the bottom part of the body. It is the most reliable and remains the safest substitute for wound treatment because there are no issues with immunorejection. The disadvantages with autograft are the lack of adequate skin for severely burned patients and irregular healing pattern in recipient's area as well as increased morbidity associated with the skin harvesting from patient's own body (Garfein, Orgill et al. 2003).

ii. Allograft.

Allograft is a skin graft taken from the same species such as human cadaver allograft skin (HCAS). It provides the option of readily available skin grafts for temporary biological dressing. However, HCAS has several drawbacks that include the limitation of supply, poor quality of grafts, inconvenience of harvesting skin in mortuary, prolonged immune rejection and potential viral contamination from patients (Hansbrough, Mozingo et al. 1997). The use of immunosuppressant to reduce the effect of rejection is required to allow autologous cells to populate into the skin grafts (Hansbrough, Mozingo et al. 1997). Despite claims of immunorejection and risk of transmissible viral diseases, dermal allografts prepared in a lyophilized form have been shown to incorporate with autologous skin without rejection

(Garfein, Orgill et al. 2003).

iii. Xenograft.

Xenograft is the type of skin graft taken from other species such as pig, frog, lizard, dog and rabbit to provide a biologically active dermal matrix as a temporary replacement for skin loss. Problems associated with xenograft involve immunological rejection over time which causes the delay of engraftment (Yoshihiro T. et al. 2004). It is important to note that xenograft and allograft do not allow a true closure of the wound and are only suitable as a means of temporary wound covering. This is because keratinocytes and fibroblasts from patients minimally repopulate foreign substances such as xenograft and allografts, causing the original grafts to deteriorate and survive indefinitely.

Allogenic and xenogenic grafts have drawbacks due to the immunological response to non-self material which can cause the retardation of the wound healing process (Fodor 2003). These materials are also in limited supply and the operation to obtain allogenic skin causes donor side morbidity and there are difficulties in matching the topology of the graft with the injured site (Lionelli and Lawrence 2003; Metcalfe and Ferguson 2007). Table 1.6 summarizes the materials that are either commercially available or in development used for skin, epidermal and dermal substitute for the treatment of wound (Atiyeh, Hayek et al. 2005; Shevchenko, James et al. 2010).

Table 1.6   Commercially available or in development materials for skin substitute for the treatment of wound.

	Name and Manufacturer or investigating group	Incorporated human cells	Primary cellular loading occur	Cell source	Scaffold source	Scaffold materials	Duration of cover	Reference
Skin substitute	Allograft (Cadaveric)	Native	Native	Allo	Allo	Native human skin with dermal and epidermal cells.	Temporary	(Shevchenko, James et al. 2010)
	Apligraf Organogenesis Inc. Canton, Massachussetts. MA. U.S.A	Cultured keratinocytes and fibroblasts	*In vitro*	Allo	Xeno	Bovine collagen	Temporary	(Shevchenko, James et al. 2010)
	Orcel Ortec International Inc. New York, NY. U.S.A	Cultured keratinocytes and fibroblasts	*In vitro*	Allo	Xeno	Bovine collagen sponge	Temporary	(Shevchenko, James et al. 2010)
	Polyactive HC Implants BV, Leiden	Cultured keratinocytes and fibroblasts	*In vitro*	Auto	Synthetic	Poly(ethylene oxide terepthalate)/Poly (butylene terepthalate)	Temporary	(Shevchenko, James et al. 2010)
	E-Z Derm Brennen Medical Inc. MN. U.S.A.	-		Auto	Xeno	Chemically crosslinked porcine collagen	Temporary	(Healy and Boorman 1989)

Table 1.7   Commercially available or in development materials for epidermal substitute for the treatment of wound.

	Name and Manufacturer or investigating group	Incorporated human cells	Primary cellular loading occur	Cell source	Scaffold source	Scaffold materials	Duration of cover	Reference
Epidermal substitute	Bioseed-S BioTissue Technologies, GmbH, Freiburg, Germany	Cultured keratinocytes (subconfluent cell sheet).	*In vitro*	Auto	Allo	Fibrin sealant	Permanent	(Shevchenko, James et al. 2010)
	Cryoceal XCELLentis, Gent, Belgium merged with CellTrans Ltd, Sheffield, U.K.	Cryopreserved keratinocytes	*In vitro*	Auto	Allo		Temporary	(Shevchenko, James et al. 2010)
	Lyphoderm XCELLentis, Gent, Belgium merged with CellTrans Ltd, Sheffield, U.K.	Lyophilized neonatal keratinocytes	*In vitro*	Auto	Allo		Temporary	(Shevchenko, James et al. 2010)
	Epicel Genzyme Biosurgery, Cambridge, MA, USA.	Cultured keratinocytes	*In vitro*	Auto	-	-	Permanent	(Shevchenko, James et al. 2010)
	MySkin CellTran Ltd. Sheffield, U.K.	Cultured keratinocytes (subconfluent cell sheet).	*In vitro*	Auto	Synthetic	Silicone support layer with surface coated with specific formulation.	Permanent	(Shevchenko, James et al. 2010)

Table 1.8   Commercially available or in development materials for dermal substitute for the treatment of wound.

	Name and Manufacturer or investigating group	Incorporated human cells	Primary cellular loading occur	Cell source	Scaffold source	Scaffold materials	Duration of cover	Reference
Dermal substitute	Collagen-GAG-Chitosan dermal matrix INSERM, U533, Universite' Paris 7, IUH, Paris, France	Cultured dermal fibroblasts	*In vitro*	Allo	Xeno	Bovine collagen 1/ Chondroitin-4/ 6-sulfate/ chitosan lyophilized dermal matrix	Temporary	(Shevchenko, James et al. 2010)
	Collagen-GAG Fibers and Polymers Laboratory, Massachusetts Institute of Technology, Bldg. Cambridge, MA. U.S.A	-	*In vitro*	Allo	Xeno	Bovine collagen/ GAG	Temporary	(Yannas, Lee et al. 1989; Yannas, Tzeranis et al. 2010)
	Permacol™ Tissue Science Laboratories Inc. Andover, MA, U.S.A	-	*In vitro*	Auto	Xeno	Crosslinked collagen from porcine	Temporary	(MacNeil 2007)
	Biodegradable polyurethane Microfibers, Department of Materials Science and Engineering, University of Delaware, Newark, DE, U.S.A		*In vivo*	-	Synt	Biodegradable polyurethane microfibres	Permanent	(Shevchenko, James et al. 2010)
	Silk fibroin and alginate College of Veterinary Medicine and School of Agricultural Biotechnology, Seoul National University, Seoul, South Korea	-	*In vivo*		Xeno + Synth	Silk fibroin/ Alginate blended sponge	Permanent	(Shevchenko, James et al. 2010)

Table 1.9   Commercially available or in development materials for dermal skin construct for the treatment of wound.

	Name and Manufacturer or investigating group	Incorporated human cells	Primary cellular loading occur	Cell source	Scaffold source	Scaffold materials	Duration of cover	Reference
Dermal skin construct	Alloderm LifeCell Corporation, Branchburg, NJ. U.S.A	-	*In vivo*	-	Allo	Human acellular lyophilized dermis	Temporary	(Shevchenko, James et al. 2010)
	Surederm HANS BIOMED Corporation, Seoul, Korea	-	*In vivo*	-	Allo	Human acellular dermis	Temporary	(Shevchenko, James et al. 2010)
	Matriderm Dr. Suwelack Skin and Health Care, AG, Billerbeck, Germany	-	*In vivo*	-	Xeno	Bovine non crosslinked lyophilized dermis, coated with α-elastin hydrolysate	Temporary	(Shevchenko, James et al. 2010)
	Integra Integra LifeSciences Corporation, Plainsboro, NJ. U.S.A.	-	*In vivo*		Synthetic + Xeno	Silicone, collagen and glycosamino glycans	Temporary	(Wolter, Noah et al. 2005)
	Tegaderm – nanofibre contstruct Nanoscience and Nanotech Initiative, Division of Bioengineering, National University of Singapore, Singapore.	Cultured dermal fibroblasts	*In vitro*	Allo	Synthetic + Xeno	Poly (ε-caprolactone/ gelatine nanofibrous scaffold electrospun on polyurethane dressing	Temporary	(Shevchenko, James et al. 2010)

1.9 Carbohydrate-protein interactions.
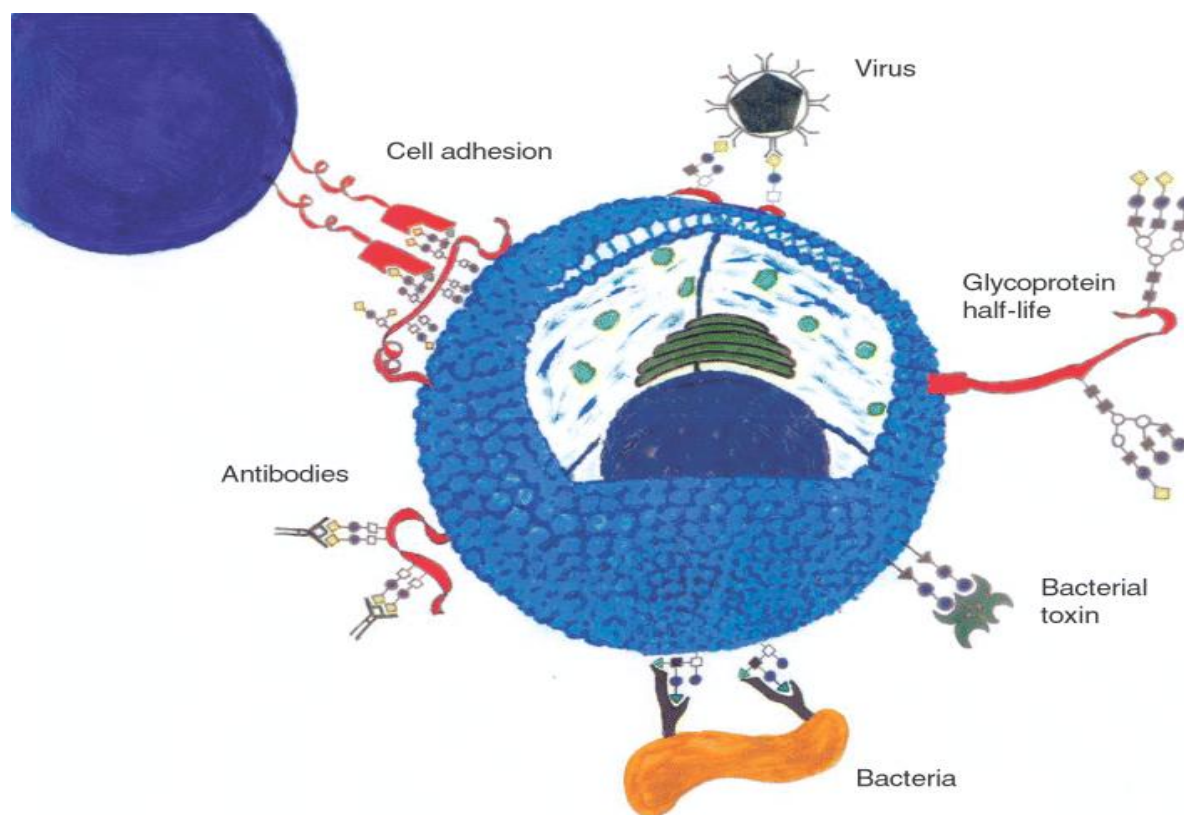
Figure 1.13 Schematic drawing illustrating protein-carbohydrate interactions at the cell surface mediating cell-cell binding, cell-pathogens (bacteria, viruses and toxins) adhesion and cell-antibody binding (Holgersson, Gustafsson et al. 2005).

Carbohydrate recognition by proteins is mediated by cellular responses which is shown in Figure 1.13. Oligosaccharides are functional components of many proteins associated with cellular communication, adhesion, migration and tuning with enzymatic activities (East and Isacke 2002).

Mannose receptors (MR) in skin fibroblasts are one of the receptors that are responsible for virus, bacteria and parasite invasions in skin via endocytosis and pinocytosis (Hespanhol, Soeiro et al. 2005). MR roles in innate immune response were not truly effective as they are generally involved in the process and presentation of glycoproteins and antigen (Lee, Evers et al. 2002). The expression of MRs vary with type and cell functions such as cell-cell

communication, (i.e. attachment of sperm to oocytes (Ofer et al.1976), pathogen recognition in innate immune response (Lee, Evers et al. 2002), antigen transporation and presentation (Taylor, Gordon et al. 2005) and clearance of glycoprotein (Lee, Evers et al. 2002). MR is also important for the regulation of myoblast motility and muscle growth where MR -/- cells were shown to have impaired migratory speed and myoblast fusion (Jansen and Pavlath 2006). Exploitation of the mannose targeting system could be a way to overcome insulin resistant conditions, where mannose specific receptors on the cell surface could be used to transport nutrients into cells for metabolic activity (Chen, Liu et al. 2005).

1.9.1 Mannose Receptors.

The mannose receptor (MR) is a 175 kDa transmembrane receptor that comprises of an N-terminal cysteine rich domain, a fibronectin type II (FNII) domain, eight or ten tandemly arranged C-type domains (CTLD), a transmembrane domain and a cytoplasmic domain. Also known as macrophage MR (MMR), it obtained its name due to its lectin activity for sugars terminated mannose, fucose or N-acetylglucosamine (Taylor, Gordon et al. 2005). In addition to MMR, there are other members in the mannose receptor family, comprising of Endo180, the M-type phospholipase A_2 receptor (PLA_2R) and DEC205 (East and Isacke 2002) The grouping of the mannose receptor family is based on the overall structural conservation which is shown in Figure 1.14, with each family having a unique number of C-type lectin superfamily. Figure 1.15 shows the 4 members of mannose receptor family.

Expression of Mannose Receptors (MRs) had been reported on human dermal fibroblasts and keratinocytes (Szolnoky, Bata-Csorgo et al. 2001; Wollenberg, Mommaas et al. 2002; Hespanhol, Soeiro et al. 2005). MRs are involved in many cellular responses such as innate immunity response (Taylor, Gordon et al. 2005), the migration of myoblasts and muscle regeneration (Jansen and Pavlath 2006), the clearance of glycoconjugates (Lee, Evers et al.

2002), tissue regeneration (Honardoust, Jiang et al. 2006) and in the mechanism of defence from pathogens (Hespanhol, Soeiro et al. 2005). MR are also involve in the re-epithelisation and connective tissue remodeling, during wound healing (Honardoust, Jiang et al. 2006).

Endo 180 is related to macrophage mannose receptor (MMR) which is expressed in fibroblast, endothelial cells and macrophages (Sheikh, Yarwood et al. 2000). Characteristics of MRs, keratinocyte mannose receptor (KcMR) and MMR are different in molecular weight and structure which may define their differences in biological activities (Szolnoky, Bata-Csorgo et al. 2001). The expression of keratinocyte and fibroblast MR in culture was found to be dependent on the supplementation of 10% FBS, where the expression was significantly increased by approximately two fold (Honardoust, Jiang et al. 2006). Inhibition of MR by mannan and mannan-BSA complex were found to inhibit *Leishmania* and *Candida* infection of fibroblasts and keratinocytes by blocking the adherence of these pathogens onto the cell surface (Szolnoky, Bata-Csorgo et al. 2001; Hespanhol, Soeiro et al. 2005).

MR is well defined on human macrophages and its involvement in the mediation of endocytic clearance of glycoprotein, regulation of myoblast motility and immune response has been reported (Taylor, Gordon et al. 2005). Table 1.11 describes the differences between K$_c$MR and MMR

Table 1.11   Comparison of KcMR with MMR, adapted from Szolnoky et al.(2002).

	KcMR	MMR
Number of sites per cell	1×10^4	2×10^4
K$_D$(M)	1.8×10^{-8}	10^{-8}
Internalization	Not efficient	Efficient
Ca^{2+} dependency	Dependent	Dependent
Sensitivity to proteolysis	Rapid	Rapid
Recovery after proteolysis	Rapid	Rapid
Molecular weight	~ 200 kDa	~ 175 kDa
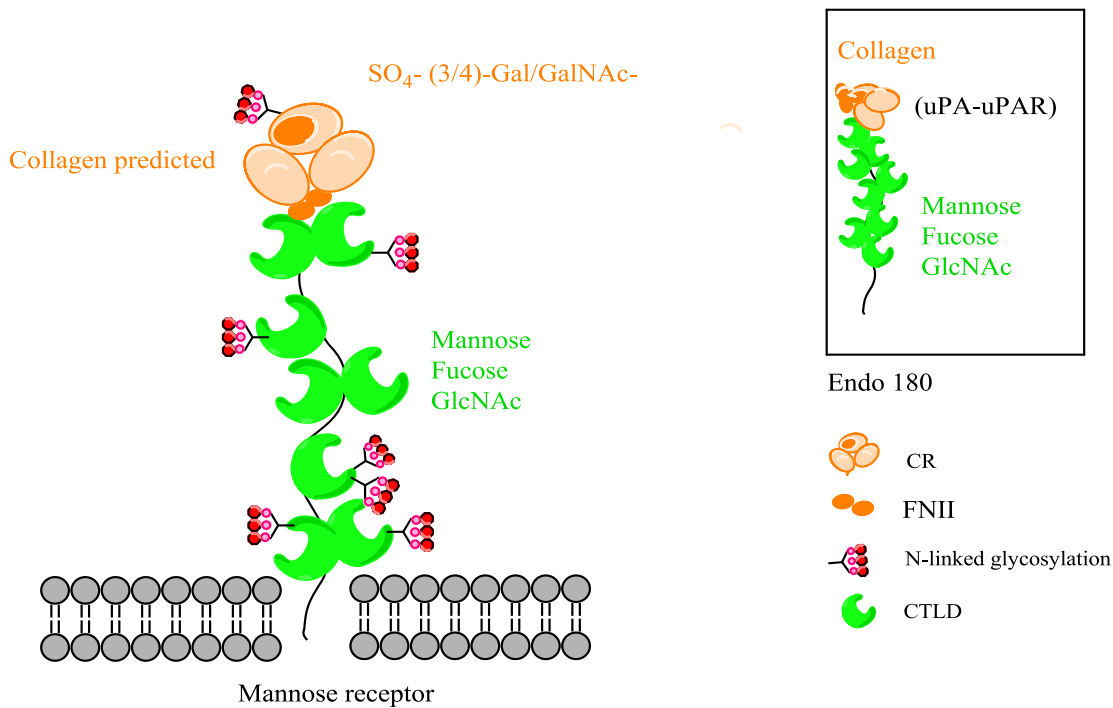
Figure 1.14   Schematic representation of the domain structures in mannose receptor (MR). The structure consists of extended conformation and predicted N-linked glycosylation, indicated by red diamonds, cysteine rich (CR) domain, fibronectin type two repeats (FNII) and multiple C-type lectin like carbohydrate recognition domains (CLTDs), a transmembrane domain and a short cytoplasmic tail. The inset shows the comparison of Endo180 to MR, which the CR domain lack of N-linked glycosylation responsible for lectin activity. Abbreviation: uPA-uPAR; urokinase plasminogen activator-uPA receptor complex. Adapted from (Taylor, Gordon et al. 2005) *Trends in Immunology*. Vol. 26. No.2 February 2005.
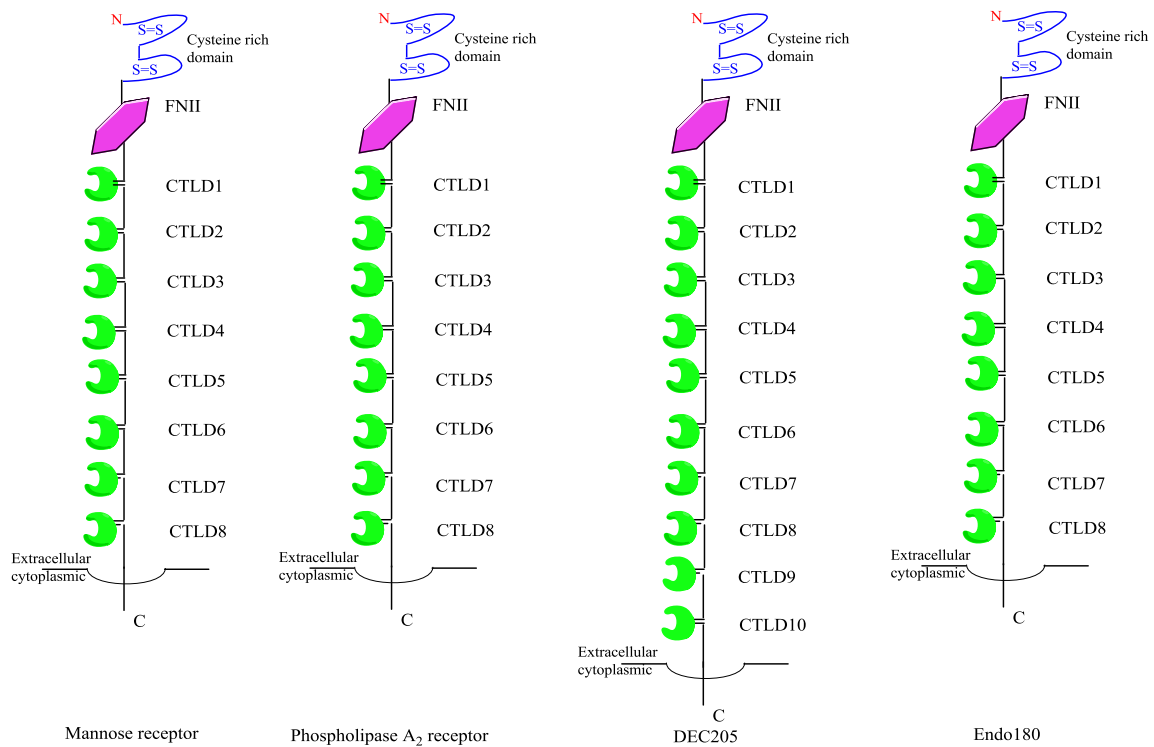
Figure 1.15   Schematic representation of the mannose receptor family showing the domain structure of each family. Adapted from East and Isacke (2002) "The mannose receptor family" *Biochimica et Biophysica Acta*.

1.9.2 The role and function of lectins in skin wound healing.

Much of the study of wound healing has focused on the different regulation of gene expressions, involvement and identification of glycans and lectins. In wound healing, the expression anti inflammatory reaction can be characterized by the increase of MR, CD205, Endo 180 and galectins that are expressed in different phases in the early stage of wound healing and in the resolution phase (Zhang, Tachado et al. 2005; Klima, Lacina et al. 2009; Zhang, Su et al. 2010). These lectins are important for the regulation of myoblast motility, differentiation of fibroblasts into myoblasts, and in the modulation of wound contraction and scarring   (Henderson, Mackinnon et al. 2006; Honardoust, Jiang et al. 2006; Jansen and Pavlath 2006; Klima, Lacina et al. 2009).

The expression of Endo 180 was gradually increased in the area of unwounded epithelium

close to the wound after 1-28 days of wounding (Honardoust, Jiang et al. 2006). The activation and increased expression of Endo 180 in the unwounded area promoted cellular proliferation with increased uPA expression, which is the main source of migrating keratinocytes for reepithelisation in the early phase of wound healing (Honardoust, Jiang et al. 2006). The study also confirmed that the cultured keratinocytes at the edge of the experimental scratch wound showed no difference in the expression of Endo 180, indicating that wounding did not induce Endo 180 expression (Honardoust, Jiang et al. 2006). The presence of growth factors were most likely to upregulate Endo 180 expression in keratinocytes after wounding *in vivo* (Honardoust, Jiang et al. 2006).

In the regulation of wound contraction, Endo 180 may also function as a co-receptor with integrins in myofibroblasts, and facilitate the removal of excess collagen from the ECM which is important to normalize the structure of collagen rich wound connective tissue and to prevent the formation of scar (Honardoust, Jiang et al. 2006).

The identification of the dynamic regulation of lectins in different phases of wound healing, addresses the potential target for the development of a biologically active hydrogel as a wound dressing to aid in wound healing (Markowska, Jefferies et al.). Biologically active carbohydrate ligands can be chemically added to drugs for delivery to specific ligands that would be beneficial for wound healing (Tizard, Carpenter et al. 1989). The specificity of lectins allow scientists to elucidate design features to treat chronic wounds from injuries and diabetic conditions as modulations in materials for wound treatment containing materials that could functionally direct cellular functions and assist speedy recovery.

1.10 The design of the hydrogel.

One of the aims of this research is to make bioactive hydrogels that would improve healing conditions to be used in chronic wound applications. The use of natural and synthetic polymers in the hydrogels is a good approach to tackle problems with wounds, especially when dealing with debridement which require frequent change of dressings. Also, maladies such as diabetes and autoimmune, require biological intervention to stimulate cellular proliferation and differentiation which are vitals in healing progression. Therefore, hydrogels with bioactive properties which can stimulate cell proliferation, migration and differentiation is of great interest in this design. KGM was chosen due to its excellent bioactivities on skin cells, which stimulate fibroblast proliferation and helps to maintain cell viability in stressed condition without media change for 20 days (Shahbuddin, Shahbuddin et al. 2013).

KGM however have weak mechanical properties and breaks easily when immersed in water after a short period due to abundance of hydroxyl groups in its polymeric chain. Improvement of this material was then achieved by crosslinking using cerium (IV) ammonium nitrate (Ce(IV)) as initiator at various concentrations. The use of Ce(IV) in the polymerisation of hydrogel at lower concentration is safe for tissue engineering application (Vickers, McArthur et al. 2008). The mechanism of this approach is shown in Figure 1.16. Lower concentration of Ce(IV) in the hydrogels was not cytotoxic and made good hydrogels which were biologically active with skin cells and able to stimulate cell migration, reepithelisation and healing progression on tissue engineered skin (which will be discussed throughout chapter 4-8). However, these hydrogels were very weak and broke easily after 2-3 days in medium. Although higher concentration of Ce(IV) was able to make mechanically stable hydrogels, it was cytotoxic to skin cells (Shahbuddin, Bullock et al. 2013).
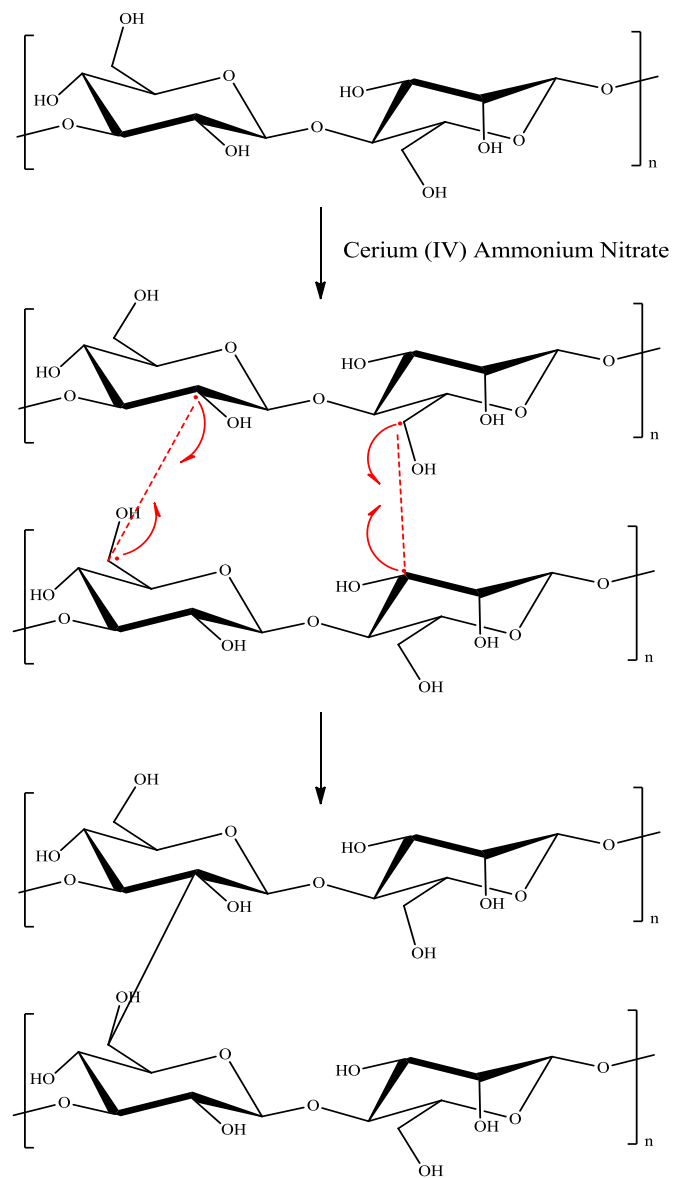
Figure 1.16   Synthesis of KGM hydrogels and the formation of crosslinked KGM initiated by Ce(IV).

In order to improve KGM's mechanophysical properties, synthetic polymers, PEGDA and NVP were introduced in the design. PEGDA was selected due to its amphiphilic nature, biocompatibility and good solubility in both polar and non-polar solvents (i.e. water and many other organic solvents). PEGDA is commercially available by Sigma-Aldrich and polymerized rapidly and easily in the presence of water by free radical polymerisation with ultraviolet light at ambient conditions.

NVP is a hydrophilic, nonionic monomer that is soluble in water, polar and non-polar solvent which easily polymerized thermally and photolytically. The molecular structures of NVP and PEGDA are shown in Figure 1.17. NVP-based materials have been explored for many biomaterials due to its high water uptake and good physical properties. Therefore, it is in our interest to design an interpenetrating network (IPN) of KGM, P(NVP) and PEGDA for wound healing application. Two different type of IPNs were developed, semi IPN and graft-conetwork, where in graph-conetwork, the KGM was crosslinked by Ce(IV) but not in semi IPN. The schematic representations of this design are shown in Figure 1.18-1.22.

The variations of KGM/NVP/PEGDA ratio in the polymerisation mixture influenced the free water content, physicochemistry, and bioactivities on skin cells (Shahbuddin, Bullock et al. 2013). These will be discussed later throughout Chapter 5-8 in this thesis.

Konjac glucomannan

N-vinyl pyrrolidinone

Poly(ethylene glycol) diacrylate
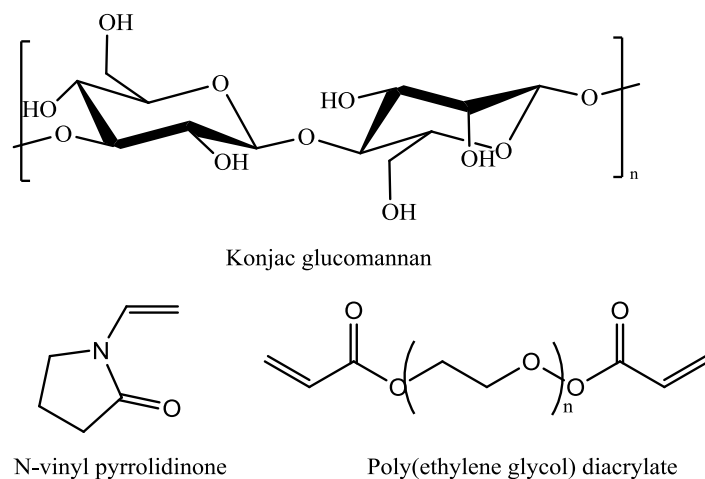
Figure 1.17 Chemical structures for KGM, NVP and PEGDA monomers.
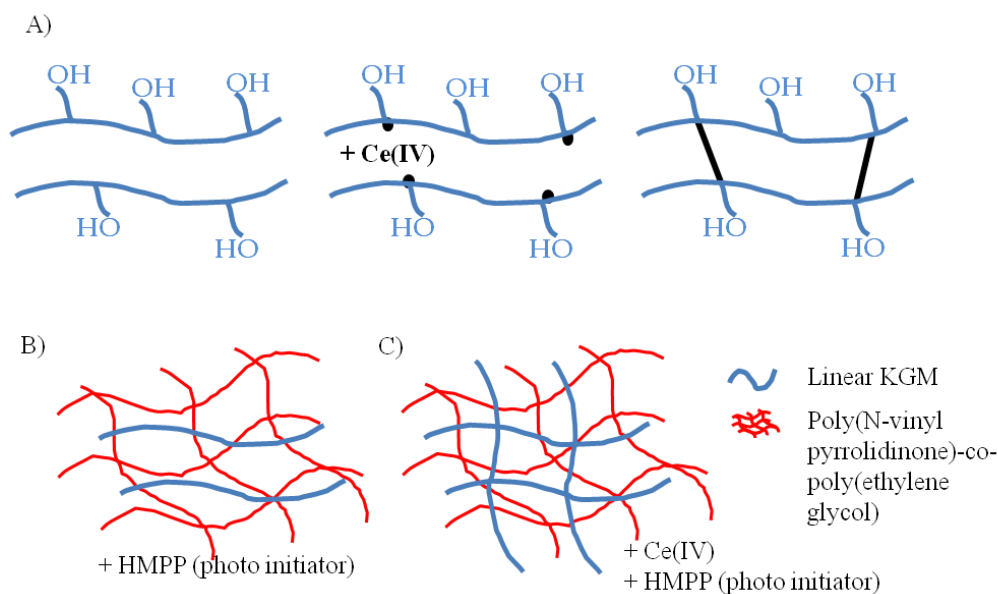
Figure 1.18 Schematic representation of (A) the formation of crosslinks in linear KGM by the addition of Ce(IV) in aqueous solution (B) semi-IPN and (C) graft-conetwork.

Formation of radical
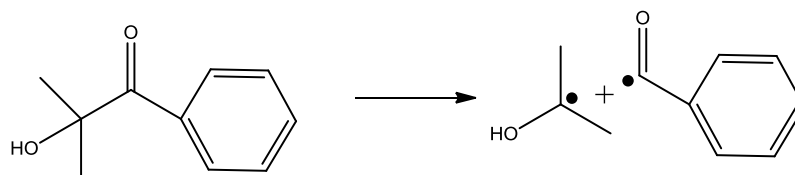
Initiation
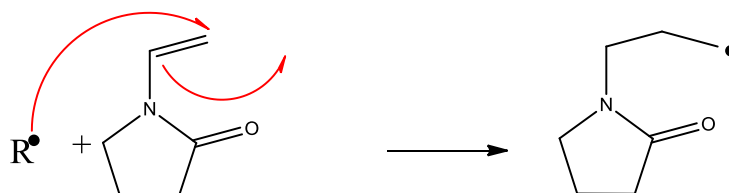
Propagation
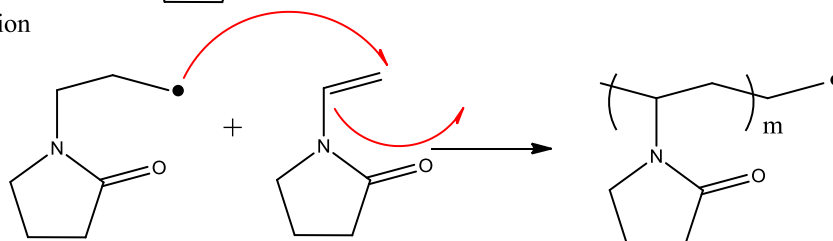
Termination
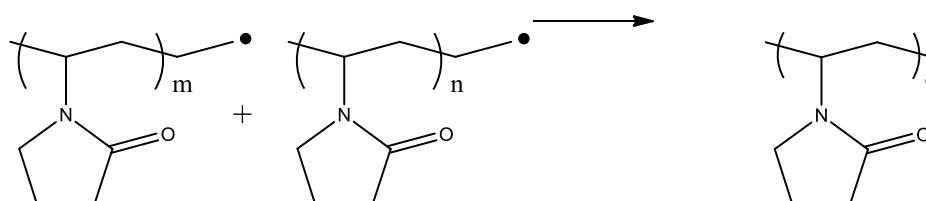
Figure 1.19 Schematic representation of the formation P(NVP) via photopolymerisation using HMPP as initiator.
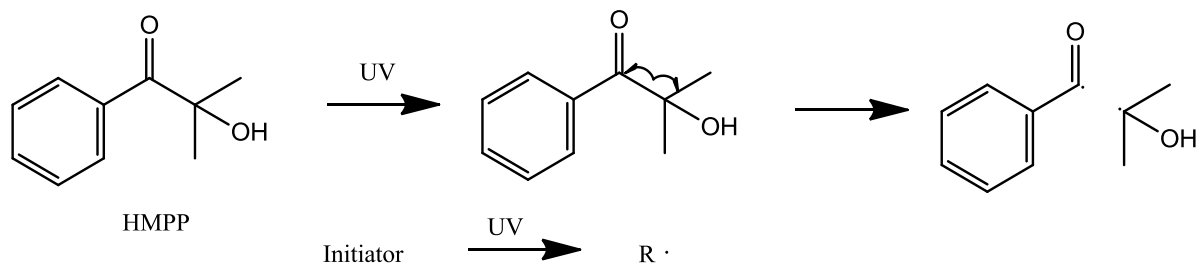
Step 1: The dissociation of the photo initiator by UV exposure
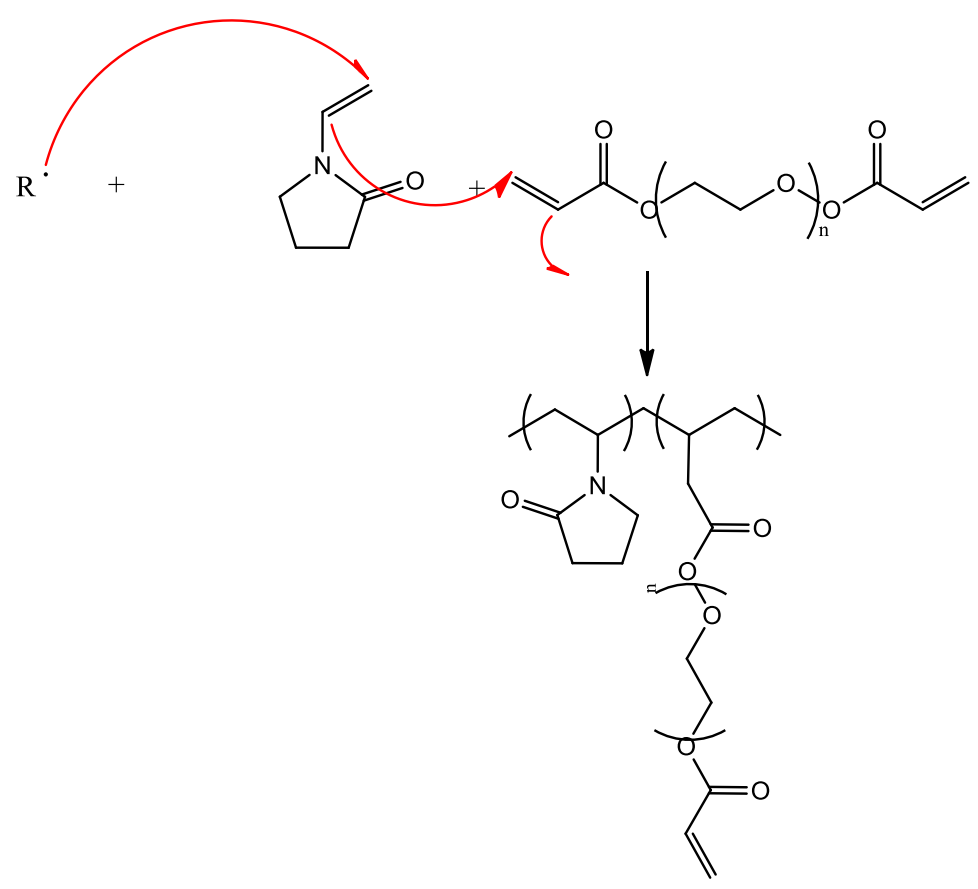
Step 2: Formation of network by PEGDA and NVP monomers

Figure 1.20 Schematic representation of the formation P(NVP-co-PEGDA) copolymers via photopolymerisation using HMPP as initiator.
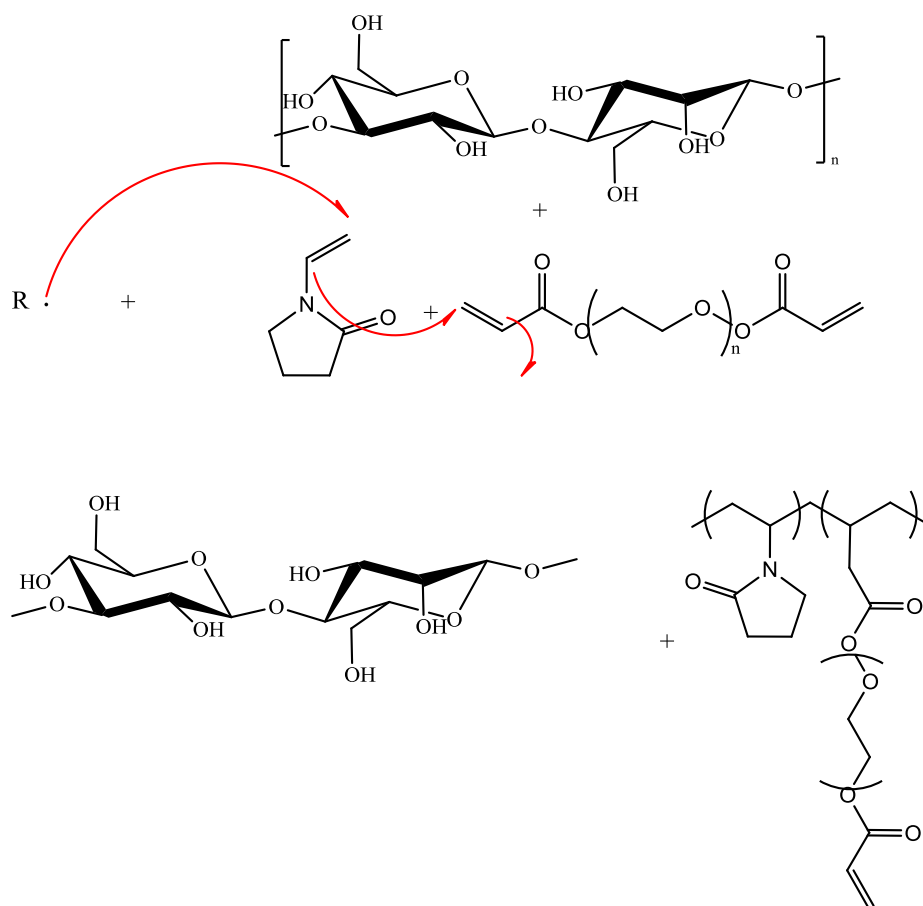
Figure 1.21   Synthesis of semi-IPN of P(NVP-co-PEGDA) with uncrosslinked KGM via photopolymerisation using HMPP as initiator.

.
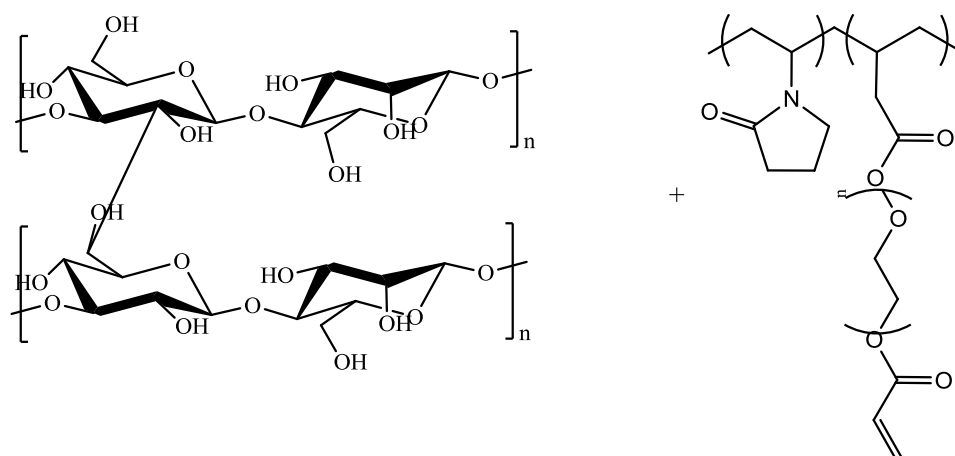
Figure 1.22   Schematic formation of graft-conetwork of P(NVP-co-PEGDA) with crosslinked KGM via photopolymerisation using HMPP and Ce(IV) as initiators.

1.11 Characterizations.

Methods of characterization using spectrometry and thermo analysis are useful to identify the formation of crosslinks inside the crosslinked KGM and IPN of KGM and P(NVP-co-PEGDA). The techniques are important to identify the influence of hydrogel's swelling behavior, crosslinks, chemical confirmations, surface properties and biological activities. Combinational approaches with less invasive technique helps scientists to further understand underlying chemical composition and structure in biological system in cell-cell, cell-material and material-material interaction in endeavor for the best system in tissue engineering. For example, the combination of confocal Raman spectroscopy (CRS) and SEM gives an ultrastructural and chemical analysis in a non-destructive manner at high resolution, as most biomaterials are vulnerable to high temperature (van Apeldoorn, Aksenov et al. 2005).

1.11.1 Gel Permeation Chromatography (GPC).

The molecular weight of a polymer is very important in the synthesis of hydrogels and also in the cell-cell and cell-matrix interactions. GPC also known as size exclusion chromatography (SEC) was used to determine the molecular weight and distribution of KGM and KGM extracts from ethanol, ultrafiltration and enzyme hydrolysation. The method involves the permeation of a polymer solution through a column packed with microporous beads of polystyrene of different sized pore diameters (Odian 2004). The smaller sized polymer molecules will penetrate all the beads in the column due to their smaller hydrodynamic volume while the higher molecular weight polymer with larger size through the beads in the column (Rodriguez 1996). The time for passage of polymer molecules through the column decreases with increasing molecular weight and the molecular weight of a polymer is measured in a function of time using appropriate detectors such as refractive index, viscosity and light scattering (Odian 2004). Calibration of a column with standard polymer samples of

known molecular weight allows determination of molecular weight distribution. The process of GPC is shown in Figure 1.22.

Solvent
flow

(a)   (b)   (c)

✚ Small molecules
⬤ Large molecules
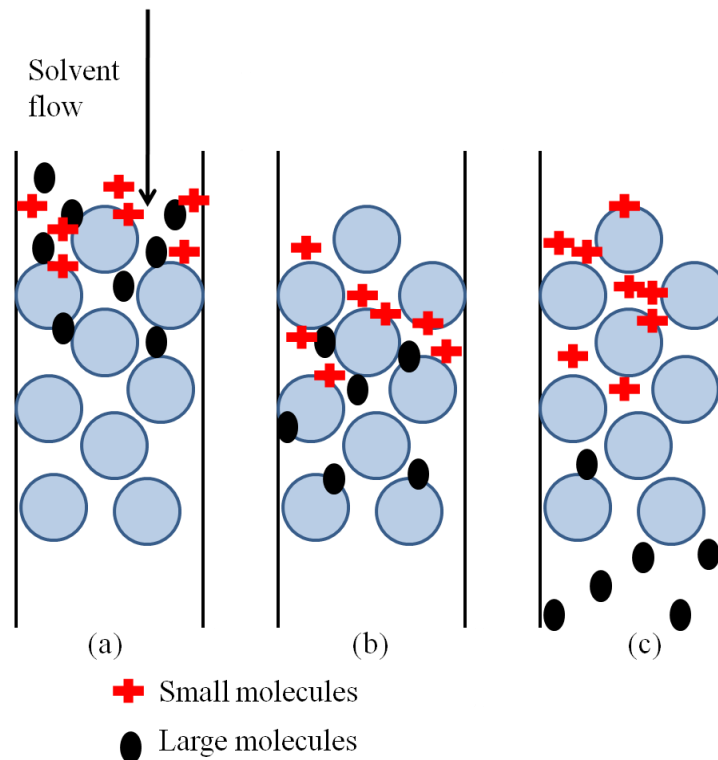
Figure 1.22 Process of GPC (a) sample injection, (b) elution and (c) continued elution. Taken from Principles of Polymer Systems (Rodriguez 1996).

1.11.2 Equilibrium water content (EWC).

The ability of hydrogel to absorb water and maintain hydration are important in the promotion of wound healing and also in controlling permeation of nutrients into cells and diffusion of cellular metabolic waste (Winter 1962). The amount of absorb water in the hydrogel is expressed as EWC which is calculated accordingly to the equation:

$$EWC = \frac{Ws - Wd}{Ws} \times 100$$

Where W_s : the weight of the swollen gel.

   W_d: the weight of the dry gel after swelling.

1.11.3 Fourier Transform Infrared (FTIR).

FTIR is a useful and powerful technique to identify and examine the chemical structure of a substance based on dipole-dipole interactions of molecules that are sensitive to infrared when subjected to infrared. This is because the atoms constituting a molecule are always in constant vibration and the frequency of the vibration are specific to localized bonds (Rodriguez 1996). These chemical bonds usually can be excited and absorb infrared in specific frequencies (Kačuráková and Mathlouthi 1996). The technique is widely used in the investigation of structural arrangement and chemical composition of hydrogels (Mansur, Sadahira et al. 2008). IR spectroscopy is one of the most often used spectroscopy due to its rapid sensitivity and great variety of sampling technique (Kačuráková and Mathlouthi 1996). Most infrared spectrophotometer use a glowing light source that provide light from 2.5 to 15 μm where a wavelength of 2.5 μm correspond to a wave number or frequency of 4000 cm^{-1} and 10 μm is equivalent to 1000 cm^{-1} (Rodriguez 1996).

Sampling preparation of a hydrogel on FTIR may usually be a thin film (of approximately 0.001 m thick and held in a non absorbing cell (often made of NaCl) and mixed with KBr powder or mull with a heavy paraffin oil held between NaCl flats (Rodriguez 1996). Water and alcohol are not used as solvent in this process as they absorb strongly in the infrared region and also may damage the sample (Rodriguez 1996). Attentuated total refraction (ATR) is an IR sampling technique for FTIR which is very simple and provides the best quality data with improvement of sample-to-sample reproducibility and minimizing user-to-user spectral variation without meticulous sample preparation (Kačuráková and Mathlouthi 1996). ATR also enables to detect structural features of hydrogels on a molecular basis (Kačuráková and Mathlouthi 1996).
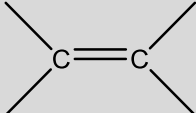
The first study of carbohydrate polymers (cellulose) using IR was first determine by C.Y Liang and R.H. Marchessault (Liang and Marchessault 1959; Liang and Marchessault 1959

(a)). The positions of characteristic infrared bands in FTIR spectra are summarized in Table 1.12.

Table 1.12 Position of Characteristic Infrared Bands in FTIR spectra (Rodriguez 1996).

Group	Frequency range cm^{-1}
OH stretching vibration	
Free OH	3610-3645 (sharp)
Intramolecular hydrogen bonds	3450-3600 (sharp)
Intermolecular hydrogen bonds	3200-3550 (broad)
Chelate compounds	2500-3200 (very broad)
NH stretching vibration	
Free NH	3300-3500
Hydrogen bonded NH	3070-3350
CH stretching vibrations	
$\equiv$C-H	3280-3340
=C-H	3000-3100
C-CH$_3$	2872 ± 10, 2962 ± 10
O-CH$_3$	2815-2832
N-CH$_3$ (aromatic)	2810-2805
N-CH$_3$ (aliphatic)	2780-2805
CH$_2$	2853 ± 10, 2926 ± 10
CH	2880-2900
SH stretching vibrations	
Free SH	2550-2600
C$\equiv$N stretching vibration	
Non conjugated	2240-2260

Conjugated	2215-2240
C≡C stretching vibration	
C≡C (terminal)	2100-2140
C-C≡C-C	2190-2260
C-C≡C-C≡CH	2040-2200
C=O stretching vibration	
Non conjugated	1700-1900
Conjugated	1590-1750
Amides	~1650
C=C stretching vibrations	
Non conjugated	1620-1680
Conjugated	1585-1625
CH bending vibrations	
CH_2	1405-1465
CH_3	1355-1395, 1430-1470
C-O-C vibrations in esters	
Formates	~1175
Acetates	~1240, 1010-1040
Benzoates	~1275
C-OH bending vibrations	
Secondary cyclic alcohols	990-1060
CH out-of-plane bending vibrations in substituted ethylenic systems.	
-CH=CH_2	905-915, 985-995
-CH=CH- (cis)	650-750

-CH=CH- (trans)	960-970
C=CH$_2$	885-895
	790-840

$$ \underset{\diagup}{\overset{\diagdown}{C}} = \underset{\diagdown}{\overset{\diagup}{C}} $$

1.11.4 Scanning Electron Microscopy (SEM).

The information about the samples topography, composition and other properties such as pore sizes,electrical conductivity and characteristic 'network' structure in hydrogels can be examined using SEM (Perkins, Davidson et al. 2006; Freitas, Gaffo et al. 2014). This can be done by analyzing slow secondary electron that generated from inelastic scattering of primary electron beam. The method gives an excellent spatial resolution because the electrons escape from the top of the interaction volume. The advatanges of SEM gives scientists information about the materials and helped them to understand the interactions between the materials and cells.

Many researchers find that SEM is a useful tool for characterization of biomaterials as it can be controlled from about 10-500,000 times. In the study of polycaprolactone (PCL) degradation in vivo after six month scientists found significant changes in materials topography with presence of microcracks and voids on the material's surface(Lam, Hutmacher et al. 2009). This however did not occur for materials that were incubated in physiological condition for the same length of time. This information helped to understand the rate of degradation in both in vitro and in vivo which is vital for the design of biomaterial scaffold for tissue engineering.

Another less invasive and useful method that use a combination approach is focused ion beam (FIB)/SEM (Milani, Drobne et al. 2007). It is a technique that used embedded electron column and ion column in the same specimen chamber to aim at the same point on the

specimen surface. The technique is widely used in semiconductor technology before the application in biological specimens (Milani, Drobne et al. 2007). In this system, the focused ion beam is operated at low beam current to obtain the image while the high beam current used specifically for in situ sputtering, then the secondary electrons that collected from sputtered secondary ions will give the image (Milani, Drobne et al. 2007).

This combination in a microscale is not only in invasive but reveal crutial information about the sample composition (biological) as accurate as 2D histology.

1.11.5 Differential Scanning Calorimetry (DSC).

DSC is thermo analytical technique which can be used to examine polymeric materials by their thermal transition (Rodriguez 1996). Thee subtle changes in structure can be observed when the polymer sample is compared to other material undergoing similar heating process (Rodriguez 1996). This thermoanalytical technique reflects the change in heat capacity of a sample as a function of temperature by measuring the heat flow required to maintain a zero temperature differential between an inert reference material and the polymer sample (Odian 2004) (Figure 1.23).
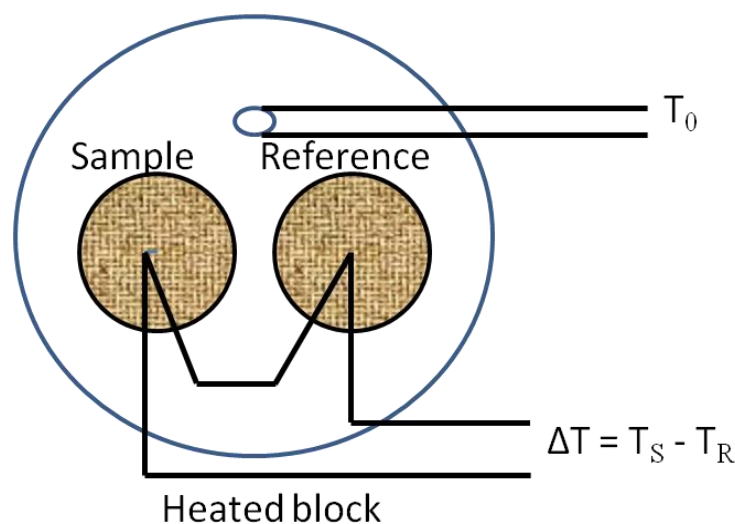
Figure 1.23 Schematic diagram of apparatus for Differential Scanning Calorimetri. Sample and reference materials are contained in a heated block that is programmed so that T_0

ncreases linearly with time (Rodriguez 1996).

DSC is also used to determine the amount of free water inside the hydrogel, as free water do not directly bound by hydrogen bonding. It also has similar transition temperature, enthalpies and DSC curves to pure water (Kim, Lee et al. 2004). The amount of free water inside the hydrogel can be calculated approximately using the amount of melting endothermic heat of fusion for pure water per mg of samples (As is discussed in 5.2.5, Figure 5.12). However, DSC does not uniquely identify the chemical composition of materials but rather suggesting the transition the formation of crosslinks and strong interaction between the polymers. The composition of unknown materials may be completed using FTIR and NMR analysis.

1.11.6 ^{13}C Solid State NMR

High resolution solid state NMR spectroscopy is a useful means to obtain structural information of solid and liquid polymers (Kobayashi, Ando et al. 1995). The basic concept of solid state NMR is characterized by the presence of anisotropic (directionally dependent) interactions. When a compound with hydrogens is placed in a strong magnetic field then irradiated with a radio-frequency signal, an absorption of energy occur at specific frequency as transition between different spin orientation level give rise to interactions between nuclei (Laws, Bitter et al. 2002). Anisotropic interactions have a substantial influence on the behavior of a system of nuclear spin. However, in a classical liquid state NMR experiment, the free movement of atoms in the compound known as Brownian motion leads to an averaging of anisotropic interaction, which sometimes can be neglected on the time scale of the NMR experiment. NMR spectroscopy also can be used for compositional analysis which include the detection of isotactic-atactic ratios, monomer sequence distribution in copolymers and other configurational variations (Rodriguez 1996).

1.12 Aim.

The aim of this project was to explore the actions of konjac glucomannan (KGM) and develop hydrogels from KGM for their actions on skin cells. Initially, investigations of the chemistry and biological properties of 5 different species of *Amorphophallus* with skin cells were conducted then KGM hydrogels were developed. The specific objectives were as follows.

1. Investigation of the biological effects of KGM on skin cells.

1. Investigation of the structure-activity relationship of KGM extracts (i.e. Glc:Man ratio, MW distributions and % GM content) to skin cells.

2. To investigate to what extent the biological activities of KGM on skin cells requires foetal calf serum (FCS).

3. To determine the potential of KGM to support skin cells and ADMSC in nutrient deprived conditions for up to 20 days.

4. To determine the involvement of mannose sensitive receptors or other lectins in the interactions of KGM with skin cells.

2. Investigation of the potential of KGM hydrogels for cell transportation.

1. To investigate the effect of KGM, crosslinked KGM and KGM-Xanthan blend hydrogels on the transportation of fibroblasts up to 18 hours.

3. Development of KGM hydrogels for wound healing.

1. To develop two types of biologically active KGM hydrogels; biodegradable – crosslinked KGM and non-degradable; semi-IPN and graft-conetworks hydrogels.

2. To determine the chemical and physical properties of the hydrogels using scanning electron microscopy (SEM), Fourier Transform infrared spectroscopy (FTIR), differential scanning calorimetry (DSC), equilibrium water content (EWC), ^{13}C solid state NMR and relate these to their biological effect on skin cells.

4. Investigation of the effect of KGM hydrogels on the migration of skin cells in wound scratch assay.

1. To examine the effect of KGM on the proliferation and migration of mitomycin C treated fibroblasts and keratinocytes in a wound scratch assay.

2. To examine the effect of KGM hydrogels on the proliferation and migration of mitomycin C treated fibroblasts and keratinocytes in a wound scratch assay.

5. Investigation of the biological effect of KGM hydrogels on skin cells, TE skin and wound model.

1. To examine the effects of KGM hydrogels on the stimulation of cell proliferation in TE skin.

2. To examine the effect of KGM hydrogels on the reepithelisation of TE skin and healing in a TE wound model.

3. To investigate the effect of KGM hydrogels on the extent of contraction of TE skin .

2. Materials and Method.

2.1 Materials.

Materials were obtained from the following manufacturers: all KGM samples, *A. oncophyllus, A. paeoniifolius, A. prainii* and *A. elegans* were provided by the Institute of Biological Sciences, Faculty of Science, University of Malaya, , except for *A. konjac* Koch which was obtained without any purification (99% GM content) from Health Plus Ltd. London U.K. β-mannanase from *C.japonicus* (EC 3.2.1.78 enzyme activity 5000 U.mg^{-1}) (Megazyme Ltd. Ireland); ethanol (Fisher, U.K.); phosphate-buffered saline (PBS) tablets (Oxoid, Unipath, Hamshire, U.K.); Dulbecco's modified Eagle's medium (DMEM) (ICN Flow, Thame, Oxfordshire, U.K.); glutamine, penicillin and streptomycin and Hank's solution (Gibco Europe, Life Technologies, Paisley, U.K.), fetal calf serum (FCS) (Advanced Protein Products, Brairley Hill, West Midlands, U.K.); Difco trypsin, (Difco Laboratories, Detroit, MI, U.S.A.); isopropanol, (BDH Laboratory Supplies, Lutterworth, Leicestershire, U.K.); 3-[4,5-dimethylthiazol-2-yl]-2,5 diphenyltetrazolium bromide-thiazolyl blue (MTT), cholera toxin, epidermal growth factor (EGF), adenine, insulin, sodium chloride, transferrin, triiodothryonine, 0.02 % ethylenediamine tetraacetic acid (EDTA) in PBS, Trypsin/EDTA (0.05% w/v trypsin/ 0.02% w/v EDTA), 4',6-Diamindino-2-phenylidole (DAPI) and Trypan blue (Sigma, Poole, Dorset, U.K.). 3.7% of formaldehyde, SYTO9 (Molecular Probes, U.S.), Propidium Iodide (PI) (Invitrogen, U.K.). No. 22 and 15a scalpel blade (Swann-Morton, Sheffield, U.K.), Neubauer haemocytometer (Weber Scientific International, U.K.), stainless steel rings and grids (Department of Medical Physics at the Royal Hallamshire Hospital, Sheffield, UK), ThinCert™ cell culture inserts (Greiner, U.K.), plasticware for cell culture (Costar, U.K.) and Class II laminar flow hood (Walker Safety Cabinets, U.K.).

2.2 Separation of high molecular weight and low molecular weight components of KGM (*A. konjac* Koch) using ultrafiltration, ethanol extraction and enzyme treatment.

2.2.1 Separation of high molecular weight and low molecular weight components of KGM (*A. konjac* Koch) using ultrafiltration.

1 g of KGM was added to 2 L of distilled water in a 2000 mL beaker and filtered through a 30,000 $g.mol^{-1}$ cut-off filter (Whatman, UK) using an ultrafiltration device (Millipore 3000) under vacuum pressure and nitrogen gas to allow the low molecular weight component to pass through. Both HMW and LMW KGM recovered from this process were lyophilized and the molecular weight distribution obtained using Gel Permeation Chromatography (GPC) as per section 2.3.

2.2.2 Separation of high molecular weight and low molecular weight components of KGM (*A. konjac* Koch) using ethanol extraction.

1 g KGM was dissolved in 100 mL of ethanol in a 250 mL beaker for two hrs then filtered twice (11 nm pore size, Whatman, UK). KGM recovered from this process was lyophilised and then analysed for molecular weight using GPC.

2.2.3 Enzymatic digestion of KGM (*A. konjac* Koch) .

Materials

Enzymes β-Mannanase (*C. japonicus*), PBS, and Bovine Serum Albumin (Sigma). β-D-mannanase is a recombinant enzyme from endo and exo acting *Cellvibro japonicus*, purchased from Megazymes, Ireland. *C. japonicus* is a saprophytic soil bacterium that cleaves plant cell walls to make energy. There are at least three types of β-mannanase genes in *C.japonicus* (Hogg et al., 2003). The specificity of this enzyme is 417 $U.mg^{-1}$ on carob galactomannan (5000 $U.mL^{-1}$). One unit of mannanase activity is defined as the amount of enzyme required to release one μmol of mannose reducing sugar equivalent per minute from carob galactomannan in sodium phosphate buffer (100 mM) in pH 7. The buffer for β-Mannanase (*C. japonicus*) was PBS with BSA (0.5 mg per each mL of PBS).

Method

Hydrolysis with β-mannanase from *C.japonicus* (Megazyme, EC 3.2.1.78) was carried out on 1.5 g of KGM in 250 mL of buffer, pH 7 at room temperature (or -5°C) for between 10 min to 5 hrs. A range of concentrations of β-mannanase (0.1, 1, 10, 100 and 500 $U.mL^{-1}$) was added to obtain a series of KGM with different molecular weight distributions. After hydrolysis, the solutions were boiled for ten min to denature the enzyme, lyophilised and stored at 4°C in a fridge. Molecular weight distributions were obtained using GPC. We then confirmed the stimulatory activity on fibroblast proliferation of the KGM heated at 100°C using cell culture to ensure that the boiling procedure did not change the biological activity.

2.3 Analysis of KGM (*A. konjac* Koch) molecular weights using Gel Permeation Chromatography (GPC).

The average molecular weights of KGM were determined by Aqueous RI-GPC (Agilent Technology, USA) (Figure 2.1) using HMW Aqueous TSK 4 Viscotech column (950 mm) at 1 mL.min^{-1} flow rate on an aqueous GPC. 2 mg of KGM or KGM extracts were dissolved in 2 mL of 0.1 M NaNO$_3$/NaH$_2$PO$_4$ buffer and filtered through 0.4 µm pore filter (Whatman, UK) pore filter before injecting into the column. Results were analysed with Cirrus™ GPC/Multidetector software, Version 3 (Varian, Inc. USA).

Figure 2.1 Photomicrograph of an aqueous-IR GPC from Agilent Technology.

2.3.1 Calibration of GPC

Calibration was done using poly(ethylene glycol)/poly (ethylene oxide) (PEG/PEO) standards. The raw data obtained was further analysed using cirrus GPC online software.

Gel Permeation Chromatography calibration was conducted using poly(ethylene glycol)/poly (ethylene oxide) (PEG/PEO) from Agilent Technologies. Three different calibrants namely,

red, yellow and green were used in this method with each containing a mixture of four narrow polydispersity polyethylene (glycol/oxide) standards (Table 2.1). The M_n values and mass contained in the vial. The retention time of the polymeric samples were recorded and plotted against the molecular weight of standard calibrants (Figure 2.2).

Table 2.1 Calibrants used in the calibration of GPC.

Vial	M_n (g/mol)
Red	1,258,000
	116,300
	12,140
	615
Yellow	909,500
	62,100
	3930
	194
Green	442,800
	23,520
	1,500
	106
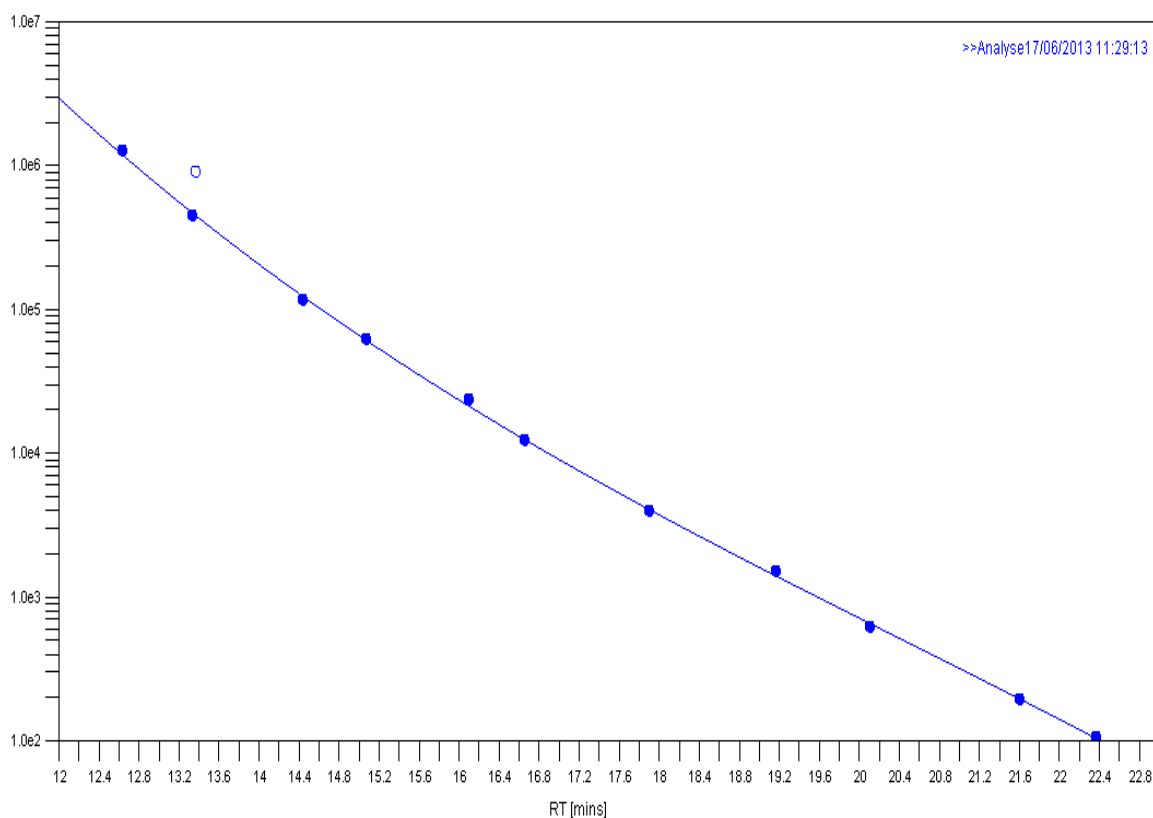
Figure 2.2 The calibration curve to describe the relationship between retention time (RT) and molecular weight.

2.4. Cell culture.

2.4.1 Medium preparation.

All procedures were done at room temperature and in sterile condition in a Class II laminar flow hood.

Adenine

0.5 g of Adenine powder was mixed thoroughly in 20 mL of distilled water with 1 M HCl titrated slowly in a drop wise manner to solubilize the powder. Then distilled water was added to make a 80 mL volume. The solution was then filtered, then aliquoted into 2 mL aliquots before being stored in a -5 $^{\circ}$C. 2 mL of this was used in 500 mL of medium making a final concentration of 1.85×10^{-4} M.

Cholera toxin

100 mg of cholera toxin was dissolved in 118 mL of distilled water to make a stock solution and stored at 4 ^{o}C. 0.2 µL of this solution was added to 20 mL of medium containing serum to form a base stock of 8.47 pg.mL^{-1} and then stored at 4 ^{o}C. 500 µL of this was used in 500 mL medium to make 10^{-10} M concentration.

Endothelial Growth Factor (EGF)

10 mg of EGF was dissolved in 100 mL of 10% Green's then aliquoted into 50 µL aliquots and stored in -5 ^{o}C. 50 µL of this was used in 500 mL medium to make a final concentration of 10 ng.mL^{-1}.

Hydrocortisone

0.5 g of hydrocortisone was added into 2 mL of 100% ethanol and mixed thoroughly. Then the solution was added into 18 mL of PBS to form a base stock solution. 80 µL of this was used in 500 mL medium to make a final concentration of 0.4 µg.mL^{-1}.

Insulin

0.02 g of insulin was dissolved in 2 mL of 0.01 M HCl and mixed thoroughly. Then, the solution was added into 18 mL of distilled water, filter sterilized and stored at 4 ^{o}C. 500 µL of this was used in 500 mL medium to make a concentration of 0.5 mg.mL^{-1}.

3, 3' Triiodo-L-Thryronine (T$_3$)

13.6 mg of 3, 3' Triiodo-L-Thryronine (T$_3$) sodium salt was dissolved in minimum amount of 0.02 M NaOH and the volume was made up to 100 mL of distilled water. The solution was then filtered and aliquoted into 200 µL aliquots and stored at -5 ^{o}C. T$_3$ aliquots were used to make up T/T stock which was used to make Green's medium.

T/T Apotransferrin

100 mg of Transferrin was dissolved in 12 mL of distilled water. Then 200 µL of T$_3$ stock was added into the solution and distilled water was added to make up 20 mL solution. The

solution was then filtered and aliquot into 500 µL and stored at -5 °C. 500 µL of this was used in 500 mL medium to make a final concentration of 5 µg.mL^{-1}.

2.4.2 Fibroblast and adipose derived stem cell (ADMSC) culture medium (10% DMEM).

438.75 mL of DMEM high glucose (with 4500 mg.L^{-1} glucose and pyruvate) was supplemented with 50 mL FCS, 5 mL of 2×10^{-3} M L-glutamine, 1.25 mL of 0.625 µl.L^{-1} amphotericin B, and 5 mL 100 I.U.mL^{-1} penicillin and of 100 µg.mL^{-1} streptomycin to make a total volume of 500 mL. The medium was stored in a refrigerator at 4 °C for a maximum of 4 weeks. 3 mL of medium was placed in a 5 mL bijou and incubated at 37 °C for at least 24 hrs prior to use as a sterility check.

2.4.3 Serum free and 2% FCS supplemented fibroblasts culture medium.

478.75 mL of DMEM high glucose (with 4500 mg.L^{-1} glucose and pyruvate) was supplemented with 10 mL FCS (10% w/v), 5 mL of 2×10^{-3} M L-glutamine (100 µg.ml^{-1}), 1.25 mL of amphotericin B (0.625 µl.L^{-1}), and 5 mL penicillin (100 I.U.mL^{-1}) and of streptomycin (100 µg.mL^{-1}) to make a total volume of 500 mL. For serum free, FCS was replaced with DMEM. The medium was stored in a refrigerator at 4 °C for a maximum of 4 weeks. 3 mL of medium was placed in a 5 mL bijou and incubated at 37 °C for at least 24 hrs prior to use as a sterility check

2.4.4 Keratinocyte culture medium (Green's medium with 10% FCS).

330 mL of DMEM high glucose and 108 mL of Ham's F12 medium in a 3:1 ratio were supplemented with 50 mL FCS, 500 µL of human recombinant EGF (10 ng.mL^{-1}), 80 µL of hydrocortisone (0.4 µg.mL^{-1}), 500 µL of cholera toxin (10^{-10} M), 2 mL of adenine (1.8×10^{-4}), 500 µL of insulin (5 mg.mL^{-1}), 500 µL of mixture of apo-transferrin (5 µg.ml^{-1}) and 3,3,5-tri-idothyronine (2×10^{-7} M), 1.25 µL of amphotericin B (0.625 µg.ml^{-1}), 5 mL of penicillin (100

I.U.ml^{-1}) and streptomycin (100 µg.ml^{-1}) to make a total volume of 500 mL. The medium was stored in a refrigerator at 4 ^{o}C for a maximum of 4 weeks. 3 mL of medium was placed in a 5 mL bijou and incubated at 37 ^{o}C for at least 24 hrs prior to use as a sterility check.

2.4.5 3T3 culture medium.

438.75 mL of DMEM high glucose (with 4500 mg.L^{-1} glucose and pyruvate) was supplemented with 10 mL New Born Calf Serum (NBCS) (10% w/v), 5 mL of 2 x 10^{-3} M L-glutamine (100 µg.ml^{-1}), 1.25 mL of amphotericin B (0.625 µl.L^{-1}), and 5 mL penicillin (100 I.U.mL^{-1}) and of streptomycin (100 µg.mL^{-1}) to make a total volume of 500 mL. The medium was stored in a refrigerator at 4 ^{o}C for a maximum of 4 weeks. 3 mL of medium was placed in a 5 mL bijou and incubated at 37 ^{o}C for at least 24 hrs prior to use as a sterility check.

2.5 Isolation and culture of keratinocytes, fibroblasts, and adipose derived stem cells (ADMSC) from skin.

Human keratinocytes and fibroblasts were isolated from skin removed during abdominoplasty or breast reduction elective surgeries in the Department of Plastic Surgery, Northern General Hospital, Sheffield with fully informed patient consent for the use of skin for experimental research. All tissue was banked and used on an anonymous basis under the Human Tissue Authority Research Tissue Bank Licence number 12179. Human dermal adipose collected at the same time in these samples was also used to isolate ADMSC

2.5.1 Isolation and culture of keratinocyte.

0.1% w/v Difco Trypsin in PBS was prepared by adding 0.5 g of Difco-Trypsin powder, 0.5 g phenol red and 0.5 g D-glucose into 500 mL of PBS. Then, the pH of the solution was adjusted to 7 using 2 M NaOH using a pH meter, 20 µm pore filter sterilized and put into 10

mL aliquots then stored at $-5\ ^{o}C$ for future use in this procedure. Primary keratinocytes were extracted from skin following incubation with 10 mL of prepared Difco-Trypsin (0.1%) overnight at $4\ ^{o}C$. 5 mL of FCS was added to neutralize the trypsin followed by separation of epidermis from the dermis. The underside of the epidermis and top of the dermis were gently scraped into Green's medium to retrieve keratinocytes and the resulting cell suspension were transferred into a 25 mL universal and centrifuged at 180 g for 5 min. The pellet was resuspended in Green's media and the cells were counted before transfer to a T75 flask that was previously seeded with $5x10^5$ i3T3. The cells were incubated at $37\ ^{o}C$, in a 5 % CO_2 in a humidified atmosphere. The medium was changed at every 2-3 days and keratinocytes were passaged at 70-80 % confluency. Only passages 1-2 were used for experiments.

2.5.2 Isolation and culture of fibroblast from skin.

0.05 % Collagenase was prepared by dissolving Collagenase A powder in DMEM, filter sterilizing, supplementing with FCS 10% v/v and aliquoting into 10 ml aliquots stored at -20 ^{o}C. Primary fibroblasts were isolated from skin by mincing the dermal region of the skin into small pieces, followed by digestion with 10 mL of collagenase A (0.05 %) in DMEM overnight at $37\ ^{o}C$ with 5 % CO_2. The cell suspension was then centrifuged at 400 g for 10 min and resuspended in 10% DMEM. These cells were then seeded into T25 flasks and incubated at $37\ ^{o}C$ with 5% CO_2. The medium was changed every 2 days and the cells were passaged as needed, fibroblasts between passage 4 and 9 were used in the experiments.

2.5.3 Isolation and culture of human adipose stem cell (ADMSC) from full thickness skin.

Human subcutaneous fat was selected as the source of ADMSCs. Tissue was obtained from discarded skin from elective breast reduction or abdominoplasty surgery after fully informed consent from Sheffield Teaching Hospitals trust and handled on an anonymous basis under a

research tissue bank licence (number 08/H1308/39) under the Human Tissue Authority.

Samples were sectioned with a scalpel in Petri dishes, with 10 mL of PBS and 10 mL penicillin (100 units.mL^{-1}) and streptomycin (100 μg.mL^{-1}).Samples were mechanically minced with a scalpel, and the pieces were collected in 50 mL tubes. Tissue was washed with 15-20 mL PBS before centrifugation at 330 g for 5 min. The pelleted tissue was transferred to a new 50 mL tube. Hank's solution (Gibco Europe, Life Technologies, Paisley, U.K.) containing 0.1% collagenase type A (Roche Diagnostics GmbH, Mannheim, Germany), 0.1 % albumin bovine fetal (BSA) (Sigma-Aldrich, Dorset, UK) and 1% antibiotic (penicillin/ streptomycin) was added to the tissue and incubated at 37 ^{o}C for 30 min with periodical shaking to aid chemical disaggregation. Digested tissues were centrifuged at 330 g for 5 min. The floating fractions consisting of adipocytes were discarded and the pellets representing the stromal vascular fraction (SVF) were resuspended in 10 % DMEM. Cells were centrifuged at 330 g for 5 min, and the pellets re-suspended in 10% DMEM before seeding into one T25 flask. Cells were maintained at 37°C and 5% CO_2.

After 24 hrs, non-adherent cells were discarded by removing the culture medium, and washing with PBS. Regular visual inspections were undertaken to observe cell morphology and exclude infection. During the culture period, growth medium was changed three times a week. After one week, ADMSCs reached 80%-90% confluence following which cells were subcultured using 5 mL Trypsin/EDTA (Sigma-Aldrich, Dorset, UK) per T25. 100,000 cells were seeded in each T75 flask, depending on the requirements. Cells between passages 4 and 7 were used in experiments.

2.6 Subculture of cells.

2.6.1 Keratinocyte subculture.

There are two steps process involved in keratinocyte subculture; removal of feeder layer using 0.002% (w/v) EDTA in PBS and detachment of keratinocytes using 2.5 mL of trypsin/EDTA. First, the medium was removed and washed with 10 mL of PBS to remove any remaining of FCS. Then, 5 mL of 0.002% (w/v) EDTA in PBS was added to the flask and incubated for 20 min for the detachment of i3T3 cells. Cell detachment was monitored by microscope every 5 min until i3T3 detachment was completed. The cell suspension was removed from the flask and the flask washed with PBS. 5 mL of Trypsin/EDTA was added to the flask and incubated at 37^oC for 5 to 10 min. Again, cell detachment was observed under the microscope at every 5 min. 10 mL of 10% Green's media was added to the flask to neutralize the trypsin and the cell suspension transferred to a universal and centrifuged at 330 g for 5 min. The pellet of cells was re-suspended in 10% Greens media and sub-cultured into new flasks pre-seeded with i3T3s. Keratinocyte at passages 1-2 were used for all experiments.

2.6.2 Fibroblast subculture.

Flasks containing fibroblasts were washed twice with PBS. 5 mL Trypsin/EDTA was added into the flask and incubated at 37^oC for 5 min for cell detachment. Cell detachment was confirmed by viewing under the microscope. 10 mL DMEM was added and the cells suspension transferred to a universal and centrifuged at 330 g for 5 min. The pellet was re-suspended in a known volume of DMEM and a cell count was performed before any experimentation. Fibroblasts at passages 5-9 were used for all experiments.

2.7 Preparation of irradiated 3T3.

Irradiated 3T3 (i3T3) murine fibroblasts were used as a feeder layer during keratinocyte culture. Unirradiated 3T3 (passage 14 stored in 10% DMSO in FCS in a liquid nitrogen Dewar at -196°C) were used in the production of i3T3. First, a cryovial of 3T3 passage 14 was thawed and the cells expanded in culture using standard fibroblast sub-culture protocol into 10 flasks and then subcultured again for a seeding density of 30×10^7 cells in a 10 layer CellStack™. After a week, the cells at approximate 80% confluency were subcultured, resuspended and centrifuged at 300 g for 5 min. The cells were re-suspended in 20 mL of culture medium and irradiated at a dose of 60 Gy using a Cs 137 source at the Department of Cancer Studies, Medical School, University of Sheffield. Post irradiation, the cells were suspended in a culture medium, centrifuged at 300 g, and counted. A concentration of 4×10^6 cells per mL in 10% DMSO in FCS was prepared and transferred into cryovials and frozen down accordingly to method 2.9.1.

2.8 Cell count and viability assessment.

Cell count and viability assessments were performed using trypan blue exclusion method (Hunt 1987). A 50 μl sample of cell suspension in a known volume of cell medium was added to another 50 μl of trypan blue solution (0.4% in PBS) in a 2 mL Eppendorf tube. Using a 20 μl pipette, 10 μl of the mixed solution was then transferred under a glass coverslip pressed onto a Neubauer haemacytometer. The distinction of viable and non-viable cells was observed under a light microscope where the non-viable cells will appear blue. Viable cells were counted and the concentration of viable cells in the suspension was calculated.

2.9 Cell cryopreservation.

Materials

Cellstar Cryovials were obtained from Greiner Bio-one, Stonehouse, Gloucestershire, England. Initial freezing of cells was carried out using a Nalgene^{TM} Cryofreezing container purchased from Nalgene Co., Rochester, New York.

2.9.1 Method of cryopreservation.

The detachment of cells from tissue culture plastic was described in the section (2.3). The suspended cells were then centrifuged at 330 g for 5 min and then re-suspended in 10% DMSO in FCS. A cell count was performed prior to that in order to obtain of 4×10^6 cells per mL and transferred to cryovials. The cryovials were placed in a Nalgene Freezing Container with isopropanol to control the decrement of temperature to -1^oC per minute and then placed into a -80^oC freezer overnight. The frozen cryovials were then transferred to a liquid nitrogen Dewar at -196^oC.

2.9.2 Thawing of cryopreserved cells.

Cryovials were removed from Dewar and thawed in a water bath at 37^oC for a few min. 10 mL of pre-warmed cell culture medium was added to a universal and cells from the cryovials added to it. The cell suspension was centrifuged at 330 g for 5 min. The supernatant was discarded and the cell pellet was suspended in a known volume of cell culture medium. Cell counts and viability assessment were performed before seeding the cells in flasks.

2.10 Mono- and co-culture of fibroblasts and keratinocytes on tissue culture plastic for the biological effects of KGM.

Materials

Modifications and extraction of KGM (*A. konjac* Koch) using ethanol and enzyme were

conducted as per section 2.2. Fibroblast culture medium with 0, 2 and 10% v/v FCS were made accordingly to section 2.4.1 and keratinocyte culture medium with 10% FCS was made accordingly to section 2.4.3.

2.10.1 The effect of serum and KGM on human fibroblasts.

$2x10^4$ fibroblasts in 1 mL of 0, 2 and 10% FCS medium were placed in a 12 well plates and incubated at 37 ^{o}C, 5% CO_2 for 24h. Then, the medium culture was removed and 1 mL of 10 mg.mL^{-1} of KGM of different species in 10% DMEM was added to each well. In all cases the cells were then cultured for 1, 3 and 5 days and measurements of cell viability were undertaken using the MTT assay.

2.10.2 The effect of KGM and fractionated KGM on human fibroblasts.

$2x10^4$ fibroblasts in 1 mL of medium were placed in a 12 well plate and incubated at 37°C, 5% CO_2 for 24 h. Then, the culture medium was removed and 1 mL of 10 mg.mL^{-1} of KGM or KGM of different molecular weight fractions obtained by ethanol extractions, ultrafiltration or enzyme hydrolysis in 10% DMEM was added into the well. In all cases the cells were then cultured for 1, 3, and 5 days and measurements of cell viability were undertaken using the MTT assay.

2.10.3 The effect of KGM and fractionated KGM on human keratinocytes.

$4x10^4$ keratinocytes (co-cultured with $2x10^4$ i3T3 in 1 mL of 10 % Green) were placed in a 12 well plate and incubated at 37°C, 5% CO_2 for 24 h. Then, the culture medium was removed and 1 mL of 10 mg.mL^{-1} of KGM or KGM of different molecular weight fractions obtained by ethanol extractions, ultrafiltration or enzyme hydrolysis in 10% Green's medium was added into the well. In all cases the cells were then cultured for 1, 3 and 5 days and measurements of cell viability were undertaken using the MTT assay. The effect of KGM on the rate of keratinocyte proliferation was expressed as a percentage of the control

proliferation.

2.10.4 The ability of KGM (*A. konjac* Koch) on supporting keratinocyte, fibroblast and ADMSC metabolic activity in unchanged media for 20 days.

$2x10^4$ fibroblasts and $2x10^4$ ADMSC in 1 mL of 10 % DMEM were cultured separately in 12 well plates and incubated at 37°C, 5% CO_2 for 24 hrs before adding 15 mg of KGM powder to half of the wells. Then all cells were maintained for 20 days without changing the media. For keratinocytes, $2x10^4$ i3T3 with $4x10^4$ keratinocytes in 1 mL of 10% Greens were cultured in 12 well plates and incubated at 37°C, 5% CO_2 for 48 hrs. The culture medium was then removed and 1 mL of 1 mg.mL^{-1} of KGM powder was added to wells. Then, the culture condition was maintained for 20 days without changing the medium. Cell viabilities for the control and the KGM treated cells were assessed at days 1, 5, 10 and 20 using a MTT assay.

2.11 Semi quantification of the presence of MR on fibroblasts and keratinocytes using Con-FITC staining.

$2x10^4$ fibroblasts in 1 mL of 10 % DMEM or $5x10^4$ keratinocytes (co-cultured with $2x10^4$ i3T3 in 1 mL of 10% Green) were placed in a 12 well plates respectively and incubated at 37°C, 5% CO_2 for 76 hrs. The culture medium was removed and 1 mL of a fresh medium containing D-mannose (1, 10 and 20 mg.mL^{-1}) was added into the well for 60 min. After removal of the medium containing D-mannose, the cells were then washed gently twice with PBS. 1 mL of 3.7% Formaldehyde was added for 30 min at 4°C. The cells were washed again with PBS. Then 1 mL of (10 μg.mL^{-1}) of Con A-FITC and 1 μg.mL^{-1} of DAPI were added to the cultures for 60 min in an incubator at 37°C. The cells were washed twice using a PBS to remove the unbound Con A–FITC. The cells were imaged using a fluorescence microscope (Axon Instruments ImageXpress (Axoncorp, USA)) at excitation and emission wavelengths

for DAPI and Con A–FITC of 340 and 488 nm and 545 and 610 nm respectively.

2.12 The blocking of MR on fibroblasts and keratinocyte using D-mannose.

2×10^4 fibroblasts in 1 mL of 10% DMEM and 5×10^4 keratinocytes (co-cultured with 2×10^4 i3T3 in 1 mL of 10% Green's) were placed in 12 well plates respectively and incubated at 37°C, 5% CO_2 for 24hrs. The culture medium was then changed and 1 mL of fresh medium containing D-mannose (1, 10 and 20 mg.mL^{-1}) was added into the wells for 60 min. Then the medium containing D-mannose was removed and 1 mL of fresh medium, containing 10 mg.mL^{-1} of KGM was added to each well. Cell viability was then measured for days 1, 3, and 5 using an MTT assay.

2.13 Investigation of the effect of concanavalin A and the interaction with KGM on fibroblasts.

2×10^4 fibroblasts in 1 mL of 10% DMEM were cultured in 12 well plates and incubated at 37°C, 5% CO_2 for 24 h. The culture medium was then changed and 1 mL of PBS containing Con A (10, 50 and 100 µg.mL^{-1}) was added for 30 min. After removal of the PBS containing Con A, 1 mL of fresh medium containing 10 mg.mL^{-1} of KGM in 10% DMEM was added to each well. Cell viability was then measured for days 1, 3 and 5 using a MTT assay.

To investigate the interaction of Con A with KGM, 2×10^4 fibroblasts in 1 mL of 10% DMEM were cultured in 12 well plates and incubated at 37°C, 5% CO_2 for 72 h. The culture medium was then changed and 1 mL of fresh medium containing 10 mg.mL^{-1} KGM was added into the well and placed in an incubator for 1 hr. Then, 1 mL of 100 µg.mL^{-1} Con A-FITC in PBS was added into the culture medium and placed in an incubator for another 30 min. The medium was then removed and the cells were washed twice using a PBS to remove the KGM bound Con A–FITC. The cells were imaged using a fluorescence microscope (Axon Instruments ImageXpress (Axoncorp, USA)) at excitation and emission wavelengths for

DAPI and Con A–FITC of 340 and 488 nm and 545 and 610 nm respectively.

2.14 Measurement of cell viability and proliferation assay.

2.14.1 MTT assay
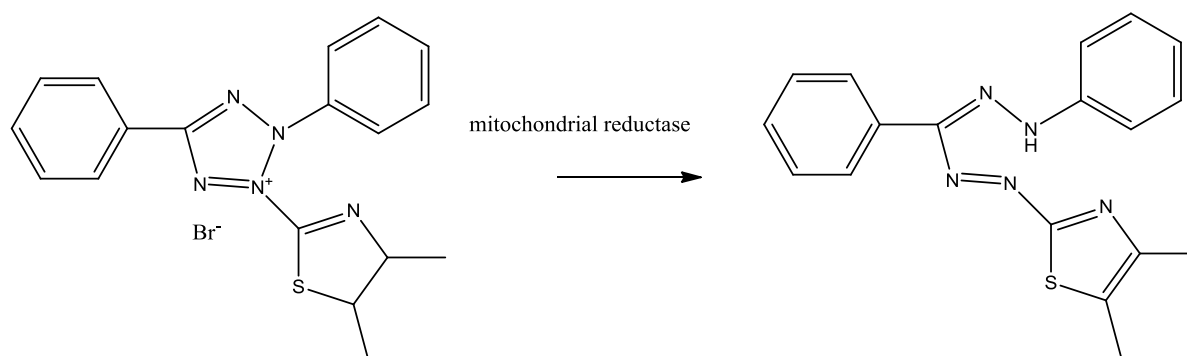
Figure 2.3   Reduction of MTT by mitochondrial dehydrogenase.

3-(4,5-Dimethylthiazol-2-yl)-2,5-diphenyltetrazolium   bromide   or   MTT   assay   is   a

colourimetric indicator of cell number or viability by means of mitochondrial dehydrogenase

activity according to method of Nik and Otto (Nik and Otto 1990). The cells were gently

washed with PBS and 1.0 mL of MTT solution was added per well. Then the plates were

incubated with for 40 min at 37°C, 5% CO_2 in a humidified atmosphere. During this time,

mitochondrial dehydrogenase activity will reduce MTT into an insoluble purple-coloured

formazan product that can be eluted using acidified isopropanol, made of 0.125 μL1 M HCl

in 100 mL of isopropanol. The reduction of MTT by mitochondrial dehydrogenase is shown

in Figure 2.3. After 40 min, the MTT solution was subsequently removed and 200 μl of

acidified isopropanol was used to elute the formazan product from the cells. 200 μl of the

isopropanol was then transferred into a 96 well plate and the optical density at 540 nm (and

reference at 630 nm) was read in a Dynex Technologies MRXII microplate reader attached to

a PC running Revelation 2.0 software.

2.14.2 AlamarBlue™ assay
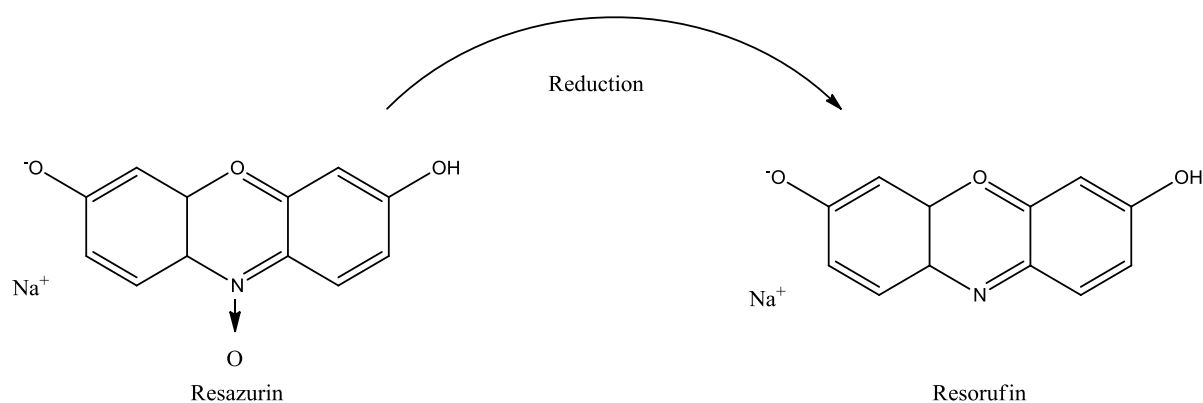
Figure 2.4   Reduction of Resazurin by mitochondrial dehydrogenase.

AlamarBlue™ assay is a colourimetric growth indicator based on detection of metabolic activity. The redox indicator in the solution changes colour from blue to red in response to chemical reduction of alamar blue into purple by the mitochondrial dehydrogenase activity in cell nuclei. The chemical reaction of this reduction process is shown in Figure 2.4. The changes in the colour which indicate the number of cells or cell viability was then measured using a plate reader. To measure the cell viability, first the samples were washed with PBS and an AlamarBlue® assay performed by adding 5 mL of AlamarBlue® (diluted 1:10 in PBS) (AbD Serotec, Kiddlington, UK) and incubated for 60 min. All cultures were kept in identical conditions of 5% CO_2, 37°C, and assayed at the same time point. Absorbance at 570 nm was then measured in a colourimetric plate reader (Bio-TEK, NorthStar Scientific LTD, Leeds, UK) to obtain baseline values of cell attachment. Samples were then washed with PBS and returned to culture conditions. AlamarBlue® assay was repeated after 7 and 14 days of culture.

2.14.3 Picogreen assay.

Picogreen™ a fluorescent nucleic acid stain was used for the quantification of total cellular dsDNA (double strainds DNA). The method used in this study was conducted according to

Ahn *et. al.,* 1996 (Ahn, Costa et al. 1996).

All media was removed and cells were washed twice with PBS. Then 200 μL of 10% digesting buffer was added and cells were frozen at -80 ^{o}C and then thawed in a dry incubator for three cycles to break the cell membranes and extract the DNA. The cells were then scraped off and centrifuged at (~1700 g) for 10 min to collect the DNA from the supernatant. 100 μL of the supernatant was added to 100 μL of Picogreen (1:200) and mixed well. 100 μL of this solution was then transferred to a fluorescence plate reader (Biotex instruments, Inc., USA) and samples excited at 340 nm with an emission wavelength at 488 nm. A quantitative estimation of the cell number was obtained by calibrating this reading against a known number of cells using this method.

2.14.4 Phalloidin-TRITC and DAPI staining.

$5x10^4$ keratinocytes (co-cultured with $2x10^4$ i3T3 in 1 mL of 10% Green) and $2x10^4$ fibroblasts were cultured for 24 hr in a 12 well plate respectively. The medium was then removed and the cells were washed with PBS twice. The cells were then fixed with 3.7% formaldehyde for 1 hr in 4°C. The formaldehyde was then removed and the cells were then washed twice with PBS. 1 mL of Phalloidin-TRITC (1 μg.mL^{-1}) and DAPI (1 μg.mL^{-1}) in PBS were added to each sample and incubated for 1 hr in an incubator at 37°C with 5% CO_2. The medium was then removed and washed twice with PBS then, the two-colour fluorescence assay was observed using an a fluorescence microscope (Axon Instruments ImageXpress (Axoncorp, USA)) The excitation and emission wavelengths were 480 and 500 nm for Phalloidin-TRICT and 340 and 488 for DAPI.

2.14.5 Cell viability assessment using Live/Dead assay.

$5x10^4$ keratinocytes (co-cultured with $2x10^4$ i3T3 in 1 mL of 10% Green) and $2x10^4$ fibroblasts were cultured for 24 hr in a 12 well plate respectively. The medium was then

removed and then 1 mL of KGM (1, 5 or 10 mg.mL^{-1}) was added to the cultures. After 3 days, the medium was removed and the cells were washed with PBS twice. 1 mL of SYTO9 (1 uμg.mL^{-1}) and PI (1 μg.mL^{-1}) were added to each sample and incubated for 1 hr in an incubator at 37°C with 5% CO_2. The medium was then removed and washed twice with PBS then, the two-colour fluorescence assay was observed using an a fluorescence microscope (Axon Instruments ImageXpress (Axoncorp, USA)) The excitation wavelengths were 480 nm for PI and 545 nm for SYTO9. The optimal emission wavelengths were 500 and 610 nm respectively.

2.15 The effect of KGM, xanthan and KGM-xanthan blend on the transportation of fibroblasts.

2.15.1 Synthesis and preparation of KGM, xanthan and KGM-xanthan blend hydrogels

The hydrogels were prepared by adding 30 mg of KGM or xanthan powder in 1 mL of free DMEM in a 12 well plate, respectively. Then, the mixture is left to settle and gel for 30 min. For KGM and xanthan blend, 30 mg of 1:1 ratio of KGM and xanthan mixture was used.

2.15.2 The effect of KGM, xanthan and KGM-xanthan blend for the transportation of fibroblasts.

1×10^5 fibroblasts in 1 mL of 10% DMEM were cultured in two 12 well plate and incubated at 37°C, 5% CO_2 for 24 hr. Then, the hydrogels made previously in a 12 well plate were transferred into a 12 well plate and placed in direct contact with the cells. The control well plate was placed in an incubator (37°C, 5% CO_2) while the other well plate was placed on a laboratory bench (at room temperature) and subjected to mechanical stress from a rocking shaker at 4 rpm up to 24 hours.   Cell viability was then measured after 12, 18 and 24 hours

using a MTT assay.

2.16 Synthesis and characterization of KGM hydrogels.

Materials

The monomer N-vinyl-2-pyrrolidone (NVP, ≥99%, Aldrich) was purified by distillation at reduced pressure and stored at 4^oC until use. Konjac glucomannan (KGM 97%, Health Plus Ltd) was used as supplied. The crosslinker, poly(ethylene glycol) diacrylate (PEGDA) and the initiators, 2-hydroxy-2-methylpropiophenone (HMPP, 97%) and Cerium Ammonium Nitrate (Ce(IV)), Sodium Chloride (NaCl), Hydrochloric acid (HCl), 3-(4,5-dimethylthiazolyl)-2-5-diphenyltetrazolium bromide (MTT), isopropanol and Toluidine Blue. All chemicals were supplied by Sigma Aldrich, Poole, U.K. and used as supplied. 3.7% of formaldehyde, SYTO9 (Molecular Probes, U.S.), Propidium Iodide (PI) (Invitrogen, U.K.).

2.16.1 KGM polymerisation using Ce(IV) ammonium nitrate.

KGM hydrogel was prepared by free radical polymerisation using Ce(IV) as initiator. Two set of hydrogels were made by either varying concentration of KGM (1, 1.5, 2 and 2.5 (w/v) %) with 0.01 (w/v) % Ce(IV) as constant or varying concentrations of Ce(IV) ($5x10^{-4}$, $1x10^{-3}$, $1.5x10^{-3}$, $3x10^{-3}$ and $6x10^{-3}$ (w/v) %) with 1.0 % KGM as constant. KGM was dissolved in 160 mL dH_2O and stirred vigorously for 30 min at room temperature to form a uniform solution. Degassing with nitrogen gas was conducted prior reaction with Ce(IV) to remove oxygen and to improve the mixing. Then the amount of Ce(IV) was added to the solution and mixed thoroughly. The solution was poured onto a Petri dish (140x20 mm) covered with PTFE film and left to evaporate at room temperature for 2-4 days.

2.16.2 UV Polymerisation.

2.16.2.1 Purification of NVP monomers.
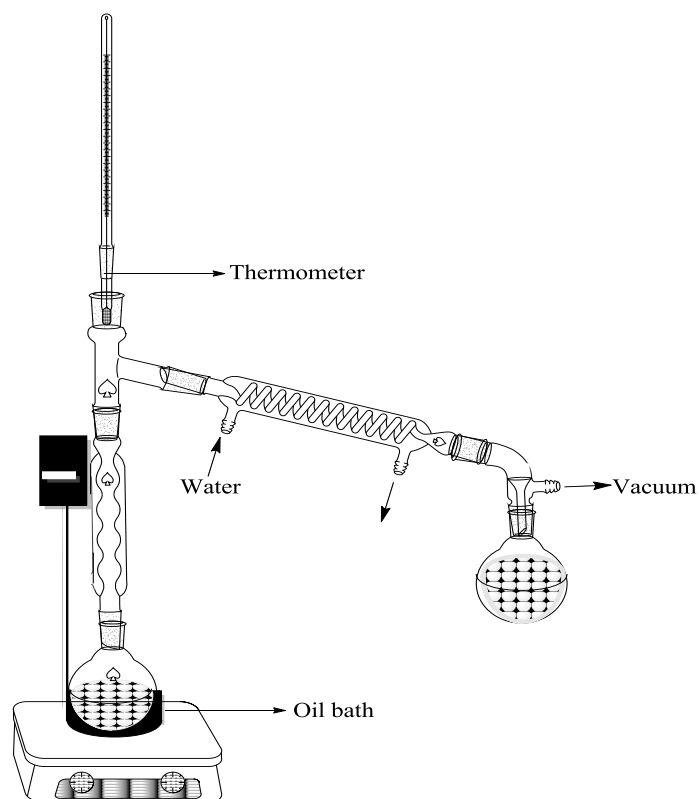
Figure 2.5 Experimental set up for the distillation of NVP monomers for purification.

Purification of NVP liquid mixure as supplied by Sigma-Aldrich was conducted by continous fractional distillation at $180^{o}C$ (in oil bath) at reduced pressure in a fume hood at Department of Chemistry, University of Sheffield (Figure 2.5). It was necessary to monitor the temperature at the thermometer attached to distilled tube to not exceeding $120^{o}C$, which is the flash point for NVP. The distilled tube was kept insulated using cotton and then wrapped with aluminium foil to allow evaporation of NVP monomers. The monomers was then collected at the end of the procedure in a round bottom flask and kept in refrigerator at $-4^{o}C$ for the use in the future.

2.16.2.2 Semi-IPN of KGM and P(NVP-co-PEGDA).

Figure 2.6 Experimental set up for the polymerisation of semi-IPN and graph conetwork (A) Dymax UV curing system, (B) mould for polymerisation and (C) example of the polymerised hydrogel.

The experimental set up for the polymerisation of semi IPN and graft conetwork is shown in Figure 2.6. Semi-IPN was prepared by free radical polymerisation using 2% (w/v) 2-hydroxy-2-methylpropiophenone (HMPP) as initiator in PEGDA solution. 25 mL dH$_2$O was added into a 100 mL beaker and 10 g of NVP was mixed thoroughly for 30 min. Then (14, 24 and 35 (w/v) %) KGM were added into the solution and stirred well for another 30 min. 2 g of PEGDA with 2 (w/v) % HMPP was then added into the solution and stirred well for another 30 min. Using a syringe, the solution of approximate 10 mL was then injected into a pre-

made mold of dimensions 7.5x7.5 cm^2 with a thickness of 250 μm, consisting of a quartz plate covered with PTFE film. Then the solution was covered with another quartz plate and then placed horizontally into a UV curing machine using Bluewave 200^{TM} Version 3 (Dymax Corp, U.K) attached with 400 watt mercury bulb (Dymax PN 36970). The irradiation process was conducted for 6 min, with 3 min on each side alternately. The hydrogel produced was removed from the mold and placed in 70% ethanol and rocked gently for 3 days to remove unreacted monomers. The ethanol was changed daily before washing twice in PBS. The hydrogels were then stored in PBS.

2.16.2.3 UV Polymerisation: Graft conetwork of KGM and P(NVP-co-PEGDA).

Graft conetwork of KGM was prepared by free radical polymerisation using 2 (w/v)% 2-hydroxy-2-methylpropiophenone (HMPP) in PEGDA solution and Ce(IV) as initiators. 25 mL dH$_2$O was added into a 100 mL beaker and 10 g of NVP was mixed thoroughly for 30 min. Then (14, 24 and 35 (w/v) %) KGM were added into the solution and stirred well for another 30 min. 2 mL of PEGDA with 2% (w/v) HMPP was then added into the solution and stirred well for another 30 min. Then (0.5 or 1 (w/v) %) Ce(IV) was added into the solution and mixed for 1 hr. Using a syringe, the solution of approximate 10 mL was then injected into a pre-made mold of dimensions 7.5x7.5 cm^2 with a thickness of 250 μm, consisting of a quartz plate covered with PTFE film. Then the solution was covered with another quartz plate and then placed horizontally into a UV curing machine using Bluewave 200^{TM} Version 3 (Dymax Corp, U.K) attached with 400 watt mercury bulb (Dymax PN 36970). The irradiation process was conducted for 6 min, with 3 min on each side alternately. The hydrogel produced was removed from the mold and placed in 70% ethanol and rocked gently for 3 days to wash unreacted monomers. The ethanol was changed daily before washing twice in PBS. The hydrogels were then stored in PBS.

2.16.3 Indirect contact of KGM hydrogels with human primary fibroblasts and keratinocytes.

1 mL of $2x10^4$ cells.mL^{-1} cells in 10% DMEM or $4x10^4$ keratinocytes (co-cultured with $2x10^4$ i3T3 in 1 mL of 10% Green were seeded into a 12 well plate and left to attach overnight. 0.79 cm^2 hydrogel was placed in inside the well and cell proliferation was measured after 1, 3 and 5 days using MTT assays1 (Figure 2.7A).

2.16.4 Direct contact of KGM hydrogels with human primary fibroblasts and keratinocytes.

1 mL of $2x10^4$ cells.mL^{-1} fibroblasts in 10% DMEM or $4x10^4$ keratinocytes (co-cultured with $2x10^4$ i3T3 in 1 mL of 10% Green were seeded into a 12 well plate and left to attach overnight. 0.79 cm^2 hydrogel was placed in a Thin Cert (0.4 µm) with 500 µl fresh medium and an additional 500 µl fresh medium was added into the well. Cell proliferation was measured after 3 days of incubation at 37^oC, 5% CO_2 using MTT assays (Figure 2.7B).
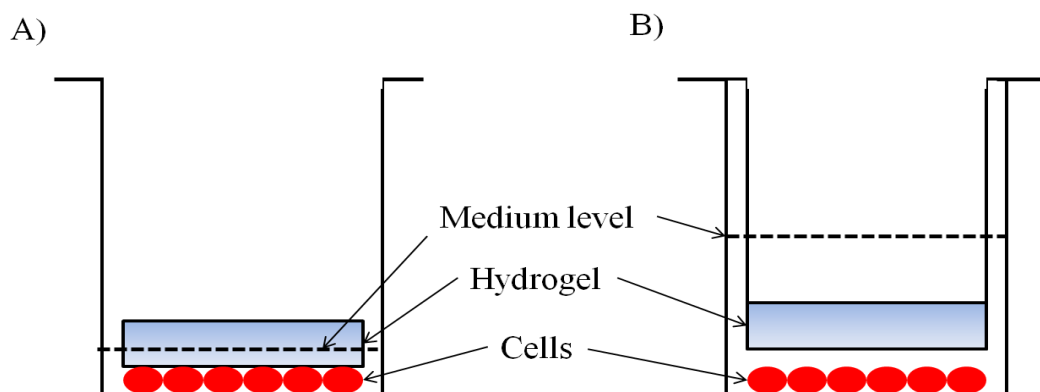
Figure 2.7   Diagram showing schematic for (A) direct and (B) indirect contact of hydrogel with cells.

2.16.5 Live/Dead staining of human primary fibroblasts and keratinocytes.

$2x10^4$ fibroblasts in 10% DMEM or $4x10^4$ keratinocytes (co-cultured with $2x10^4$ i3T3 in 1 mL of 10% Green were cultured for 24 hr in 12 well plate respectively then 0.79 cm^2 KGM film with increasing concentrations of Ce(IV) was added into the well plate. After 3 days, the medium was removed and the cells were washed with PBS twice. 1 mL of SYTO9 (1 µg.mL^{-1}) and PI (1 µg.mL^{-1}) were added to each sample and incubated for 1 hr in an incubator at 37^oC. The medium was then removed and washed twice with PBS then, the two-colour fluorescence assay was observed using an a fluorescence microscope (Axon Instruments ImageXpress (Axoncorp, USA). The excitation wavelengths were 480 nm for PI and 545 nm for SYTO9. The optimal emission wavelengths were 500 and 610 nm respectively.

2.16.6 Differential Scanning Calorimetri (DSC).

The glass transition of the dried synthesized hydrogel was measured using DSC (Perkin Elmer DSC Pyris-1) (Massachusetts, U.S.A) (Figure 2.8). The hydrogels, with sample size approximately 4.5 ± 0.5 mg were measured over and placed in an aluminium pan in the cell of the DSC unit and an empty pan was used as the inert control. The crucibles were then closed by pressing aluminium cap, which was pierced by a needle on the top for degassing. Nitrogen was used as the purge gas. DSC was performed from -60 and 360^oC at a heating rate of 1^oC per minute. The computer software (Perkin Elmer) for the apparatus plotted and analysed the thermal analysis curves and the area values of endo and exothermic heat was recorded in the unit of (mJ).

Figure 2.8 Photomicrograph of Perkin Elmer DSC

Pyris I.

2.16.7 Measurement of free water content in hydrated KGM hydrogel using DSC.

The amount of free water content in hydrated hydrogels were measured using DSC (Perkin Elmer DSC Pyris-1) (Massachusetts, U.S.A) (Figure 2.8). The hydrogels were soaked in dH$_2$O overnight prior analyses. The hydrated hydrogels, with sample size approximately 4.5 ± 0.5 mg were measured over and placed in an aluminium pan in the cell of the DSC unit and an empty pan was used as the inert control. The crucibles were then closed by pressing aluminium cap, which was pierced by a needle on the top for degassing. Nitrogen was used as the purge gas. DSC was performed from -60 and 60°C at a heating rate of 1°C per minute. The computer software (Perkin Elmer) for the apparatus plotted and analysed the thermal analysis curves and the values of endothermic heat were normalized to sample weight and presented in units of (mJ.mg^{-1}). The amount of energy released was subjected to the amount of free water inside the hydrogel.

2.16.8 Equilibrium Water Content (EWC).

Circular discs were cut from a sheet of dry hydrogel. Then the discs were put in 12 well plate with 3 mL of dH$_2$O to swell for 48 hrs. The swollen disc was then weighed and any excess water was removed gently by a paper towel. The polymer was then placed in a vacuum oven at 50°C over a 24 hr period. The weight of the dried polymer disc was then recorded every two hrs until the weight remained constant.

$$\text{EWC (\%)} = \frac{W_w - W_d}{W_w} \text{ x } 100$$

Where W_w = wet weight and W_d = dry weight

2.16.9 ^{13}C solid state NMR Spectroscopy.

^{13}C solid state NMR spectroscopy analysis was done by Dr. David Apperley at the University of Durham EPSRC solid state NMR service. A Varian Unity Inova Spectrometer VNMRS 400 with a 7.5 mm MAS probe was used with reference to neat tetramethylsilane. The measurement on crosspolarisation was carried out at 1.00 ms contact time, 53.2 kHz TPPM decoupling, 6800 Hz spinning rate, 0.010 s Gaussian broadening with FT size 16384 in ambient temperature. Approximately 500 mg of hydrogel was sent to the University of Durham by first class post. The samples were lightly ground in a mortar and pestle prior to analysis.

2.16.10 Measurement of KGM content in the hydrogels.

Quantification of the amount of KGM inside the hydrogels was determined by toluidine blue staining as described (Smith, Mallia et al. 1980) with some modifications. A disc of hydrogel with a diameter of 7 mm was cut in half and was stained by incubating the hydrogel in a 24 well plate with 1 mL of 0.01% toluidine blue in aqueous 0.01N HCl/0.2 wt % NaCl overnight on a rocking shaker at room temperature. Then, the hydrogel was rinsed twice with dH$_2$O and left overnight in dH$_2$O to remove excess toluidine blue. The hydrated sample was then transferred into a new 24 well plate with 1 mL of Cellosolve™ (2-ethoxy ethanol) added into the well and left for 2 days to dissolve and elute the bound blue dye. 100 μL of the dye solution was transferred into a 96 well plate and the absorption was measured at 562 nm.

2.16.11 Fourier Transform Infrared (FTIR).

Figure 2.9 FTIR spectrometer (Spectrum 100, Perkin Elmer, USA) on single reflection ATR.

The surface chemistry of the hydrogels were analysed on the FTIR (Spectrum 100, Perkin Elmer, USA) using a universal diamond (Figure 2.9). The hydrogels were cut into 0.79 cm^2, having a thickness of about 1-5 mm. The crystal area was cleaned using DCM (dichloromethane) (CH_2Cl_2) and the background was collected. The hydrogel was then placed onto the small crystal area and the pressure arm was positioned over the crystal and pressure of about 70-80% was applied until the strongest spectral bond showed intensity beyond 70% T. The spectra in the range of 4000 to 750 cm^{-1} at 2 cm^{-1} resolution and averaging 300 number of scan were collected using Spectrum ^{TM} FTIR software. Then, the top plate was cleaned for the use of other samples.

2.16.12 Scanning Electron Microscopy

SEM was utilized to characterize the morphologies of P(NVP-co-PEGDA) and KGM hydrogels' surface and cross section. For surface analysis, the hydrogel was cut into 1 cm^2, sputter coated with gold (Cressington 108, Cressington, U.K.) and imaged using SEM

(Philip XL-20 SEM). For cross section analysis, the squared hydrogel was cut vertically at the center, and sputter coated with gold (Cressington 108, Cressington, U.K.). This was then imaged using the same SEM model. Magnification of 250-1000x were utilized to observe the morphological differences between the hydrogels.

2.17 The effect of fibronectin and i3T3 on the attachment of keratinocytes and fibroblasts on full IPN hydrogels.

Keratinocyte attachment was investigated on 3 different surfaces, TCP (control), on KGM coated TCP and on full IPN hydrogel (24% (w/v) KGM with 1.0% (w/v) Ce(IV)). 5 mg.mL^{-1} KGM in free medium was used to coat the TCP surface and left to dry in a fume hood for 24-48 hrs. Then, each surface was either coated with 5 µg.mL^{-1} fibronectin or seeded with $2x10^4$ i3T3 as feeder layer or both or neither coated with fibronectin and feeder layer. The coating or feeder layer was left to settle for overnight before $1x10^5$ keratinocytes (co-cultured with $5x10^4$ i3T3 in 1 mL of 10% Green were seeded onto the surface. Keratinocyte proliferation was measured after 3 days using MTT assay.

As for fibroblasts, $1x10^5$ cells in 1 mL 10 % DMEM were used in this experiment.

2.18 The effect of KGM and KGM hydrogels on tissue engineered skin models.

2.18.1 Preparation of tissue engineered skin models.

All procedures were performed in sterile condition in a class II culture hood. The skin was obtained aseptically from operation theatre in approximately 0.6 mm thickness.

2.18.2 De-epidermisation of donor skin.

The split thickness skin graft was removed from its container and cut into a sheet of appropriate size before it was transferred into a 100 mL sterile plastic container containing sterile 1 M sodium chloride solution. The skin was then incubated at 37°C for 24 hrs to separate the dermis from the epidermis. Usually after 24 hrs there will be a visible separation of epidermis from the dermis and this was removed by gentle scraping the epidermis with a blunt ended spatula. The de-epidermised dermis was then washed twice with PBS and then transferred into a 100 mL sterile plastic container containing 10% Green's medium and incubated at 37°C for a minimum of 48 hrs. This is to ensure that any remaining of sodium chloride was washed out, to saturate the DED with culture medium, and also to check the for presence of infection in the DED by observation of any changes in the colour of the medium. For each and every experiment, DED from one single patient was used to reduce inter patient variation in skin characteristics. The DED was cut into squares with dimensions of approximately 2.0x2.0 cm^2.

2.18.3 Production of tissue-engineered skin skin models.

Following de-epidermisation, the DED was cut with a scalpel into squares of approximately 2.0x2.0 cm^2 and placed into a six well plate with the papillary dermis facing upwards. A

chamfered metal ring with internal diameter of 1 cm was placed in the centre of each piece of DED and was pressed down gently to create a water seal tight to prevent leakage of the cell suspension.

Then 3×10^5 keratinocytes in 300 µl 10% Greens and 1×10^5 fibroblasts in 200 µl 10% Green's were seeded into the centre of the ring. An amount of Green's medium was then added outside the ring. This was incubated for 48 hrs at 37^oC in a humidified 5% CO^2 incubator. Seeding rings were removed and a sterile stainless steel grid was introduced underneath the composite in each well to achieve air liquid interface (ALI). Fresh 10% Green's medium or Green's medium supplemented with KGM at different concentrations was placed into each well. The skin models were then cultured at 37^oC in a humidified 5% CO^2 atmosphere for 14 days.

A cartoon illustrating the experimental set up for a seeded composite at an ALI is shown in figure 2.10 below.
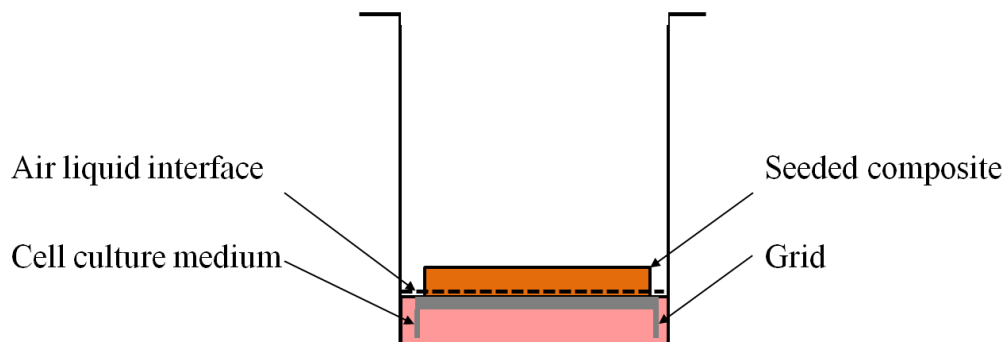
Figure 2.10 Diagram showing schematic for the culture of tissue engineered skin composite at an air liquid interface.

2.18.4 The effect of KGM on tissue engineered skin models.

Material

KGM solution KGM powder was dissolved in 10% Green's to produce stock concentrations of 1 and 5 mg.mL^{-1}. This solution was made fresh for each experiment.

Method

To examine the effect of KGM on the contraction and re-epithelisation of the skin composite, the composites were prepared as per section 2.15.3 and left in ALI condition overnight before adding medium with concentrations of KGM (1 and 5 mg.mL^{-1}) into the culture. The composites were photographed every 2-3 days for image analysis. After 14 days the composites were fixed in formalin, and wax embedded in paraffin wax before being stained with H&E for further observation on the tissue architecture and reepithelisation of the composites.

2.18.5 The effect of KGM hydrogel on tissue engineered skin models.

Material

KGM hydrogels were synthesized as per section 2.161-2.16-3. The materials were washed with 70% IMS, PBS and rinsed with 10% Green's prior putting in adjacent to the composites.

Method

To examine the effect of KGM on the contraction and reepithelisation of the skin composite, the composites were prepared as per section 2.15.3 and left in ALI condition for overnight before putting the hydrogel on the top of the composite. The composites were photographed for every 2-3 days for image analysis and after 7, 14 and 21 days, the composite viability was measured using AlamarBlue™. Then the composites were fixed in formalin, and wax embedded in paraffin wax, before being stained with H&E for further observation on the tissue architecture and reepithelisation of the composites.

2.18.5 Assessment of composite contraction by digital photography and image analysis.

The composites were photographed using a Fuji digital camera. For each picture, the 6-well plate was placed alongside a scale bar to allow calibration of the captured image in order to accurately measure the area of the composites. The procedure was performed inside a

laminar flow hood to maintain sterility. All images were imported into ImageJ software (NIH, Maryland. USA). The scale bar in each photograph was used to calibrate the image, a mouse was used freehand to trace the margin of the composites and the software used to calculate the area. The area of the composite on day 0 (when it was raised to an air-liquid interface) was designated 100 % and all changes in area were expressed relative to this initial measurement.

2.18.6 Haematoxylin and Eosin staining.

The stain was used to show the cellular architecture and interactions within the skin composites as haematoxylin stains cell nuclei purple or blue while eosin stains proteins and other basic structures of dermis pink.

Sections were dewaxed slides in xylene for three min. Then the slide was incubated in ethanol, 100% for 2 min, 70% for 1 minute, then dH_2O for 1.5 min. The slide was then stained with haematoxylin for 3 min before rinsing in tap water for 4 minutes. The slides were then stained with Eosin for 5 min before washing in dH_2O for 30 seconds. The slide was then dehydrated through ascending grades of ethanol, 70% for 2 min, and 100% for 1 minute before being placed into xylene for 1 minute. Each slide was then mounted with DPX mountant (Fisher Chemicals, U.K.) and covered with a cover slip.

2.18.7 Assessment of epidermal thickness by digital photography and image analysis.

The H&E stained composites were photographed using an electron microscope with MoticTek software. All images were imported into ImageJ software and calibrated with known distance to make a scale bar in each photograph. A mouse was used freehand to trace the margin of the basal membrane and epidermal layer and then the software was used to calculate the area of this plot relative to the calibration derived from the scale. Average

thickness of basal membrane and epidermal layer was calculated by dividing each area with the length of respective area.

2.19 The effect of KGM hydrogels on a wound of skin model.

Material

KGM hydrogels as per section 2.4.1 and 2.4.3. The materials were washed with 70% IMS, PBS and rinsed with 10% Green's prior putting in adjacent to the composites.

2.19.1 Production of wound on a tissue engineered skin model.

Tissue engineered composite was produced accordingly to 2.15.3 and left at ALI for 5 days. The composite was then transferred into a petri dish and a 6 mm incision of was made on the composite using a Swann-Morton blade No. 15a. Then, 20 μL of human thrombin (25 I.U.) was added into 250 μL of 6 mg.mL^{-1} fibrinogen in PBS to make a fibrin glue to be applied in the cavity to create the environment that is similar to wound. The fibrin glue was applied on the backside of the composite and left for 10 min for the glue to set, this ensured that the cavity was sealed. The composite was then transferred back onto the grid and left to settle for overnight before KGM hydrogel was applied onto the surface.

2.19.2 The effect of KGM hydrogels on a wounded skin model.

The effect of KGM hydrogels on a wounded skin model was conducted following 2.15.3 and 2.16.2 procedures. The hydrogels in PBS were washed subsequently in 70% IMS, PBS and culture medium before were cut into 0.79 cm^2 and placed on the top of the composites. The viability of TE composites was measured using Alamar blue™ and then processed on a tissue processor for histology accordingly to procedures 2.13.2 and 2.15.7.

2.20 Cell migration assay.

2.20.1 The effect of mitomycin C (MMC) on fibroblasts and keratinocytes.

1 mL of 1x10^5 fibroblasts was cultured in a 12 well plate for overnight and treated with 300 mL concentrations of mitomycin C in PBS (1, 10 and 100 μg.mL^{-1}) for 30 min before washed with PBS and reincubated with fresh medium. Cell viability was measured using MTT assay after 1, 3 and 5 days.

As for keratinocytes, 1 mL of 5x10^4 i3T3 and 1x10^5 keratinocytes was cultured in a 12 well plate for overnight and treated with 300 mL concentrations of MMC in PBS (1, 10 and 100 μg.mL^{-1}) for 30 min. The medium was then removed and washed with PBS. 1 mL of fresh medium was added into the culture and then incubated at 37°C with 5% CO_2.Cell viability was measured using MTT assay after 1, 3 and 5 days.

2.20.2 Migration of fibroblasts and keratinocytes.

Cell migration was detected by scratch wound healing assay. 1 mL of 1x10^5 fibroblasts or 1 mL of 1x10^5 keratinocytes co-cultured with 1 mL of 5x10^4 i3T3 was cultured in 12 well plate till confluent for 48 hrs and the scratch wound was introduced using a 1000 μL pipette tip. The culture was then washed three times with PBS to remove cell debris and treated with 300 mL of 10 μg.mL^{-1} of mitomycin C in PBS for 30 min for fibroblasts and 60 min for keratinocytes. The medium was then removed and washed with PBS. 1 mL of fresh medium was added into the culture and then incubated at 37°C with 5% CO_2. 3 independent repeats were captured at 0, 24 and 48 hrs time points during cell migration by Olympus microscope camera. The area of cell migration into wound site was quantified using ImageJ and presented as relative migration cells compared with the 0 hr. The magnification of each picture was 20 x.

$$\text{(\% Area of Relative migration cells)} = (\frac{(Area\ of\ 0hr - Area\ of\ 5hr)}{Area\ of\ 0hr} x\ 100)$$

2.20.3 The effect of KGM on the migration of fibroblasts and keratinocytes

Cell culture for each fibroblasts and keratinocytes were prepared accordingly to 2.17.2. 5×10^4 fibroblasts in 1 mL of 10% DMEM or 1×10^5 keratinocytes (co-cultured with 5×10^4 i3T3 in 1 mL of 10% Green were used in this experiment. The cells were left to attach for two days and form a confluent monolayer on the well plate. The culture medium was then removed and 1 mL of concentrations of KGM (1, 5 and 10 mg.mL^{-1}) in culture medium was added into the well. The cell migration at every 0, 8, 12 and 24 hrs were then observed using Olympus microscope camera and analysed using an ImageJ software.

2.20.4 The effect of KGM hydrogels on the migration of fibroblasts and keratinocytes.

Cell culture for each fibroblasts and keratinocytes were prepared accordingly to 2.17.2. 5×10^4 fibroblasts in 1 mL of 10% DMEM or 1×10^5 keratinocytes (co-cultured with 5×10^4 i3T3 in 1 mL of 10% Green were used in this experiment. The cells were left to attach for two days and form a confluent monolayer on the well plate. The culture medium was then removed and 1 mL of fresh medium was added into the well. Then, 0.79 cm^2 of washed hydrogel was put in the middle of scratch area. The cell migration at every 0, 8, 12 and 24 hr were then observed using Olympus microscope camera and analysed using an ImageJ software.

2.20.5 Live/Dead staining on the effect of KGM hydrogels on cell migration.

Following 2.17.4, Live/Dead staining of migrated cells in adjacent with KGM hydrogels was conducted. The hydrogel and cell medium were first removed from the wellplate and washed with PBS twice. Then, 1 mL of SYTO9 (1 $\mu g.mL^{-1}$) and PI (1 $\mu g.mL^{-1}$) were added to each sample and incubated for 1 hr in an incubator at 37^oC with 5% CO_2. The medium was then removed and washed with PBS twice. The Live/Dead stained cells were observed using an Axon Instrument (Biotex instruments, Inc., USA) accordingly to 2.13.4.

2.21 Statistical Analysis.

Quantitative data (e.g. MTT optical density readings) were analysed using Minitab (MiniTab Inc. USA) and Microsoft Excel (Microsoft Corporation) to obtain means and standard deviation (SD), n = number of independent experiments each with three replicates. Student's t-test was performed to determine statistical significance, indicated in the corresponding figures or tables by: ns (not significant; $p \geq 0.05$), * (significant; $p < 0.05$), ** (highly significant; $p < 0.01$) and *** (extremely significant; $p < 0.001$).

Chapter 3. Investigation of KGM biological effect on skin cells.

3.1 Introduction.

Polysaccharides form glycosidic structure of cell wall which are recognizable by cell surface receptors (Alonso-Sande, Teijeiro-Osorio et al. 2009; Farris, Schaich et al. 2009). Biologically active polysaccharides with the ability to ignite cellular responses in skin could be skin protective agent and useful for wound healing application (Ruszova, Pavek et al. 2008).

Glycosylated glucomannan (GM) and glucans are important constituents of plant and bacterial cell walls which not only function to retain the cell structure but also are involved in cellular recognition by cell surface receptors such as the mannose receptor (MR), toll like receptors 2, 4 (TLR2, TLR4) and soluble mannose binding lectin (MBL) when in contact with mammalian cells (Gow, van de Veerdonk et al. 2012). The recognition of specific types of sugar such as fucose, mannose, glucose, N-acetylglucosamine and heparin is specific to the type of lectin (Tizard, Carpenter et al. 1989; Lis and Sharon 1998). Lectin involved in many biological functions such as immune responses, cellular recognition, migration and metabolism (Lis and Sharon 1998; Dam and Brewer 2010).

Konjac glucomannan (KGM) is a natural polysaccharide of β(1-4)-D—glucomannopyranosyl backbone of D-mannose and D-glucose derived from the tuber of *Amorphophallus konjac* C. Koch which belongs to the Araceae family. It is used in Asia as a food, a traditional medicine, for pharmaceuticals, biomaterials and in the chemical industries due to its low cost, high viscosity, excellent film forming ability, biocompatibility and biodegradability. (Alonso-Sande, Teijeiro-Osorio et al. 2009).

The ratio of mannose to glucose in KGM is approximately 1.6:1 (Kato and Matsuda 1969). The ratio of mannose:glucose is one of the factors that affect the biological activities of GM

(Huang, Takahashi et al. 2002; Leung, Liu et al. 2004). Other factors are the structure, degree of branching, molecular weight, solubility, solution conformation and ionic charges (Bohn and BeMiller 1995; Kulicke, Lettau et al. 1997).

KGM with different molecular weight distributions have shown potential for the applications in drug delivery systems (Chen, Liu et al. 2005; Wen, Wang et al. 2008; Gupta, Gupta et al. 2009) and wound healing treatment (Zhang H 2007). Hydrolysed KGM has also shown good results in the treatment of *acne vulgaris* (Al-Ghazzewi and Tester 2010) and atopic dermatitis in mice (Onishi, Kawamoto et al. 2007).

Human dermal fibroblasts and keratinocytes are reported to express Mannose Receptors (MRs) which recognize carbohydrate expression on the surface of microorganisms (Szolnoky, Bata-Csorgo et al. 2001; Wollenberg, Mommaas et al. 2002; Hespanhol, Soeiro et al. 2005) and that this expression is dependent in the presence of 10% FCS. In the presence of FCS the expression was significantly increased about two fold (Honardoust, Jiang et al. 2006). MRs have been implicated in many cellular responses including innate immunity response (Taylor, Gordon et al. 2005), regulation of myoblasts motility and muscle growth (Jansen and Pavlath 2006), clearance of glycoconjugates (Lee, Evers et al. 2002), wound healing (Honardoust, Jiang et al. 2006) and host defence from pathogens (Hespanhol, Soeiro et al. 2005). In wound healing, MR plays a role in re-epithelization and connective tissue remodelling (Honardoust, Jiang et al. 2006).

MR expression is spatiotemporarily increased in the migrating and remodelling stages of wound healing (Honardoust, Jiang et al. 2006; Zhang, Su et al. 2010). This process is regulated by cell-extracellular matrix interactions and orchestrated by the release and activation of growth factors and cytokines at the wound site (Honardoust, Jiang et al. 2006). MRs are required for the degradation of ECM and cell migration, and also to activate and

liberate growth factors from the matrix (Blasi and Carmeliet 2002; Jansen and Pavlath 2006). GM active components in Aloe Vera have also been reported to exhibit wound healing properties interacting via MR (Choi and Chung 2003).

Following the literature on MR, investigation of their role in the stimulation and inhibition of fibroblast and keratinocyte proliferation was conducted. MR can be blocked D-mannose (Szolnoky, Bata-Csorgo et al. 2001; Hespanhol, Soeiro et al. 2005) and semi quantification of MR on cell surface was measured using Con A-FITC staining. The knowledge of MR involvement in KGM biological effect on fibroblasts and keratinocytes proliferation would be useful for the development of KGM hydrogel for wound healing.

Investigation on the ability of KGM to support cells (fibroblasts, keratinocytes and adipose derived stem cells) in unchanged culture mediums for up to 3 weeks following reports on the ability of mannose rich lectin was conducted following literature on FRIL from hyacinth bean (*Dolichos lab lab*) helped to preserve human cord blood progenitor cells in suspension culture for up to 1 month without media changes (Colucci, Moore et al. 1999) and stem cells up to 2 weeks in culture (Kollet, Moore et al. 2000).

3.2. Results.

3.2.1 The effects of   KGM from different species of *Amorphophallus*   on fibroblast proliferation-relationship to glucomannan content.

Table 3.1 shows the percentage of GM found in 5 species of *Amorphophallus* and the Glu:Man ratio. The *A. konjac* Koch had the highest GM content with a 2:1 Glu:Man ratio with 97% of glucomannan content followed by *A. oncophyllus, A. paeoniifolius, A. prainii* and *A. elegans. A. konjac* Koch*, A. oncophyllus* and *A. elegans* were found to have a higher mannose content compared to glucose.

The effect of preparations of commercially available *A.konjac* Koch and laboratory prepared preparations of *A. oncophyllus*, *A. paeoniifolius, A. prainii* and *A. elegans* on fibroblast proliferation is shown in Figure 3.1. This effect was found to be dependent on KGM species and also concentration. *A. konjac* Koch, *A. oncophyllus* and *A. paeoniifolius,* with 50% or more percentage of GM stimulated fibroblast proliferation after 3 and 5 days in culture while *A. prainii* and *A. elegans* inhibited fibroblast proliferation. 10 mg.mL^{-1} *A. konjac* Koch had the highest stimulation on fibroblast proliferation at day 3 and 5 compared to similar concentrations of *A. oncophyllus* and *A. paeoniifolius.* In contrast, *A. prainii* and *A. elegans* inhibited fibroblast proliferation at all concentrations by days 3 and 5 compared to control cells.

Table 3.1 Comparison of the mannose and glucose content of KGM extracted from five different species of *Amorphophallus,* result courtesy from Ms. Dahlia Shahbuddin. (Shahbuddin, Shahbuddin et al. 2013).

Species	Man:Glc ratio	GM(%)
A. konjac Koch	2.2:1	97
A. oncophyllus	2.5:1	57.28
A. paeoniifolius	0.8:1	49.82
A. prainii	0.18:1	29.86
A. elegans	235:1	16.78
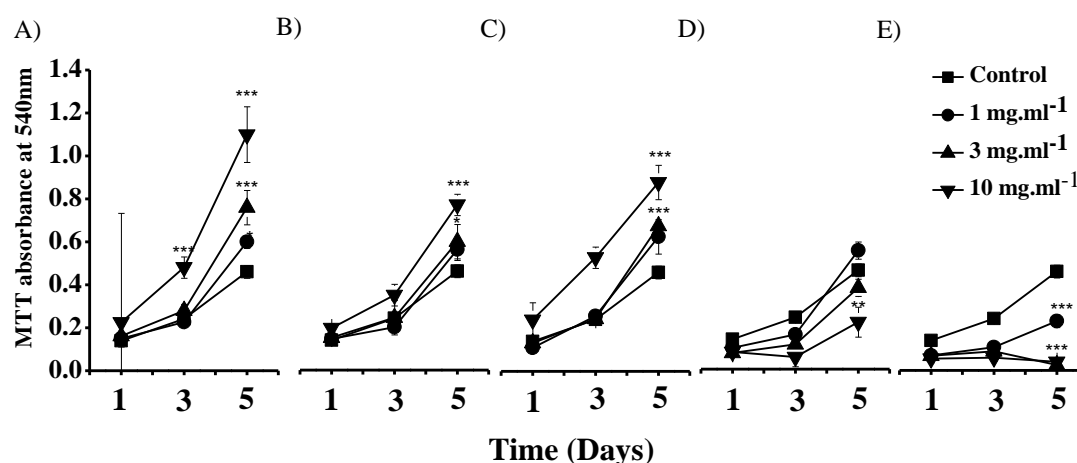
Figure 3.1 Comparison of the effect of KGM extracted from five different species of *Amorphophallus* on fibroblast metabolic activity. 2×10^4 fibroblasts were cultured in 1 mL of 10% DMEM in 12 well plate for 24 hr. Cells were then cultured in 10% FCS supplemented with various concentrations of KGM for 1, 3 and 5 days (A) *A.konjac* Koch, (B) *A.oncophyllus*, (C) *A.paeoniifolius*, (D) *A.praiini* and (E) *A.elegans*. Cell proliferation was assessed using MTT assay. Results shown are means ± SD, (n=3), ***p<0.001 highly significant, **p<0.01 very significant and *p<0.05 significant compared to control.

3.2.2 The effect of KGM from different species on fibroblasts is dependent on serum.

The dependency of the presence of serum on KGM's stimulation on fibroblast proliferation was examined by varying the concentration of FCS 0-10% in culture medium. Then, 10 mg.mL^{-1} of KGM in designated culture medium was added into the culture and cell proliferation was measured using MTT assay after 5 days. Figure 3.2A shows the effect of the KGM extract in varying serum concentrations of 0, 2 and 10%. The cell proliferation was extremely low in 0% FCS but addition of KGM (*A. konjac* Koch) and *A. oncophyllus* increased fibroblast proliferation by a factor of 5 fold compared to control and other species of KGM. Fibroblasts proliferation was increased to 17 fold and 15 fold in 2% FCS and 35 and 30 fold in 10% FCS by addition of KGM (*A. konjac* Koch) and *A. oncophyllus* respectively when compared to control with 0% FCS .

In 0% FCS, the other 3 KGM extracts from *A. paeonifolius, A. prainii* and *A. elegans* did not increase proliferation. However, an increase in fibroblast proliferation was observed with increasing FCS, although species other than *A. konjac* Koch and *A. oncophyllus* were unable to stimulate fibroblast proliferation compared to control. In 10% FCS, *A. elegans* inhibited fibroblast proliferation while the other two species *A.paeonifolius* and *A.prainii* did not.
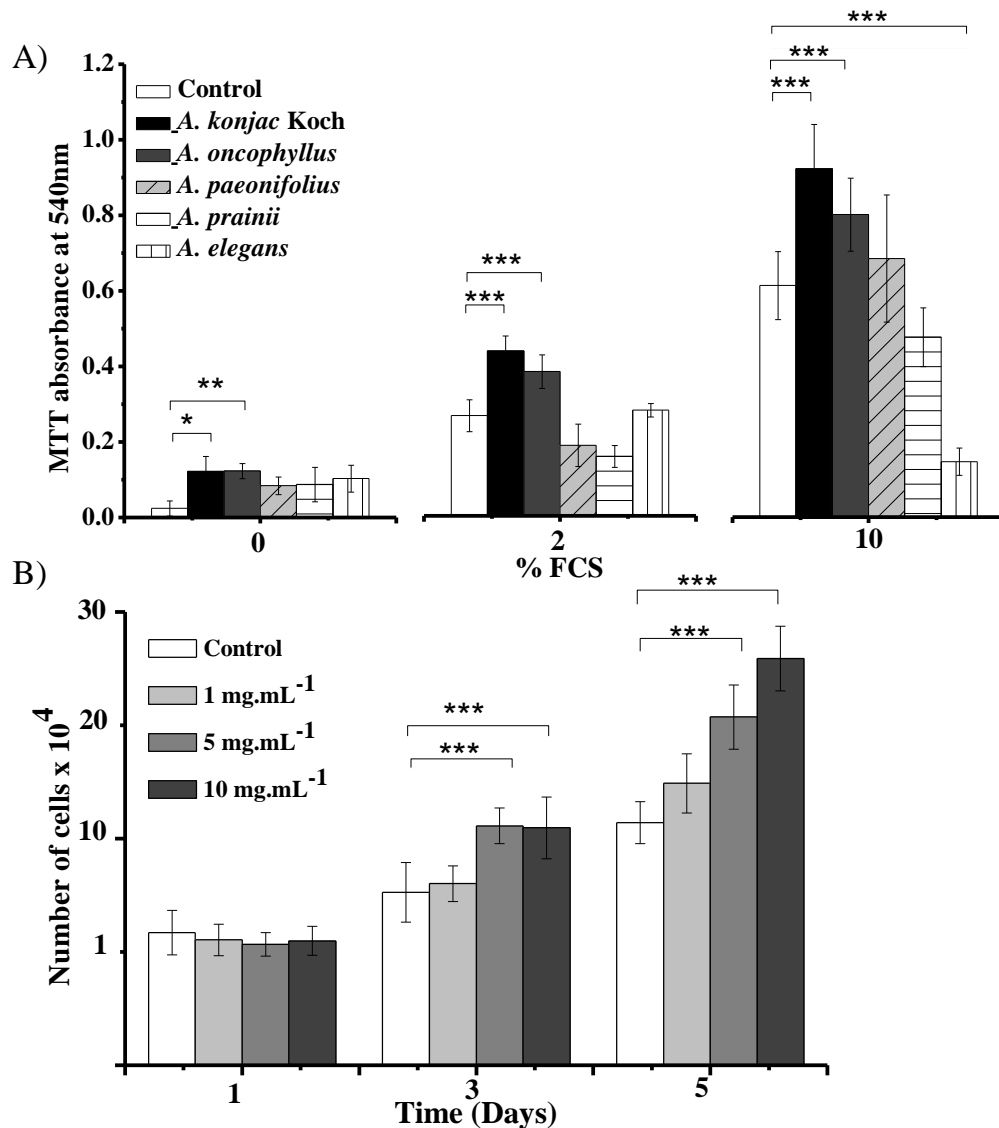
Figure 3.2 (A) Investigation of the serum dependency of the stimulatory effect of KGM on fibroblast metabolic proliferation mg.mL^{-1} extracted from 5 species, *A.konjac* Koch, *A.oncophyllus, A.paeonifolius, A.prainii* and *A.elegans*. Cell proliferation was measured using MTT assay (n=2). (B) Measurement of the DNA content of fibroblasts by the effect of KGM (*A.konjac* Koch) on proliferation using PicoGreen™. DNA content of known cell number was calibrated with PicoGreen. 2×10^4 fibroblasts were cultured in 1 mL of 10% DMEM supplemented with various concentrations of KGM for 1, 3 and 5 days. Results shown are means ±SD, (n=2), ***p<0.001 highly significant compared to control cells.

3.2.3 The effect of KGM on the proliferation of fibroblasts

The measurement of fibroblast cell number was quantified using a fluorochrome, PicoGreen™ assay for total cellular DNA. The total cellular DNA was then calibrated against known number of cells. The primary aim of this study was to confirm that the increase of cell number was parallel to the increase in metabolic activity as measured with MTT (Figure 3.2 B). The figure shows a significant increase in cell number in the culture with 5 and 10 mg.mL^{-1} KGM after 3 and 5 days. After 5 days, the cell number increased more than two fold compared to control cells as is shown in Figure 3.3.
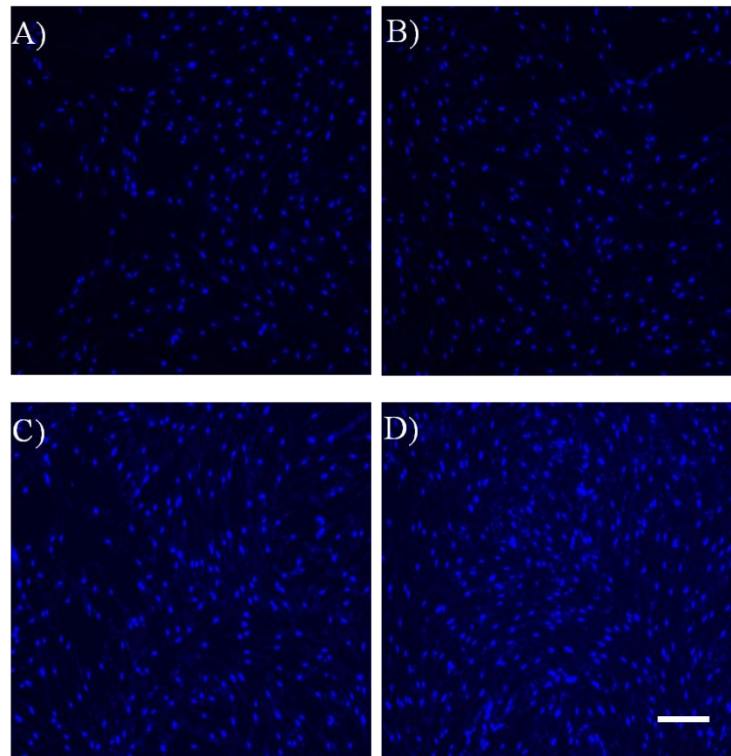
Figure 3.3 Micrographs showing the increase number of cells with increase concentration of KGM (*A. konjac* Koch) of nuclei stained fibroblasts with DAPI on (A) control no KGM, (B) 1 mg, (C) 5 mg and (D) 10 mg at day 3. Initially 2×10^4 cells were cultured in 10% DMEM. (Scale bar: 100 μm).

3.2.4 The effect of KGM on keratinocytes.

We then measured the biological activity of KGM (from *A. konjac* Koch) on keratinocyte proliferation using MTT assay and found that KGM inhibited keratinocyte proliferation more than 50% after 5 days. The rate of proliferation was dropped with 5 and 10 mg.mL^{-1} KGM compared to controls after 3 days and the effect was clearly marked after 5 days (Figure 3.4). We then further investigated the viability of keratinocytes cultured with KGM using Live/Dead assay and Figure 3.4B) shows that the presence of 1, 5 and 10 mg.mL^{-1} KGM killed the cells in dose dependent manner where the highest concentration of KGM had the most dead cells.

3.2.5 KGM supports fibroblast and ADMSC but not keratinocyte viability in unchanged media for up to 20 days.

The ability of KGM (from *A. konjac* Koch) to support skin cells and ADMSC was then examined in unchanged media conditions for up to 20 days to mimic the deprivation of nutrient condition (Figure 3.5). Typically, medium need to be changed at every 3-4 days to be able to supply ample nutrients to the increased number of cells. We include ADMSC in this study following the literatures on the ability of mannose rich lectin to support progenitor and stem cells in unchanged medium for 4 weeks.

After 20 days in culture, the viability of control cells was decreased compared to day 5 and 9, suggesting the nutrient deprivation had cause the cells to lower its metabolism. Further study showed that the addition of 15 mg.mL^{-1} native KGM helped to maintain fibroblast viability with 3-5 fold greater compared to control cells throughout 3 weeks of culture (Figure 3.5A). Figure 3.6 shows there were no differences in the morphology of fibroblasts after 5 and 20 days in nutrient deprived culture with and without KGM.

The effect was investigated with the same cell density cultured until confluence for 9 days

(Figure 3.5B). 15 mg.mL^{-1} KGM was then added into the culture for a further period of 11 days and measured the cell metabolic activities. A similar result as in Figure 3.5A where the presence of KGM significantly increased the viability of fibroblasts compared to control cells.

The addition of 1 mg.mL^{-1} KGM in keratinocyte culture medium of nutrient deprived condition showed similarity as was seen with KGM inhibitory effect on keratinocyte proliferation in normal culture medium (Figure 3.5C). There were differences in the morphology of keratinocytes with evidence of cell damage after 20 days in culture with KGM. There was also fewer number of keratinocytes cultured with KGM after 5 days in culture as shown in Figure 3.7. However, in contrast KGM was found to significantly support ADMSC in culture without media changes for 3 weeks (Figure 3.5D).
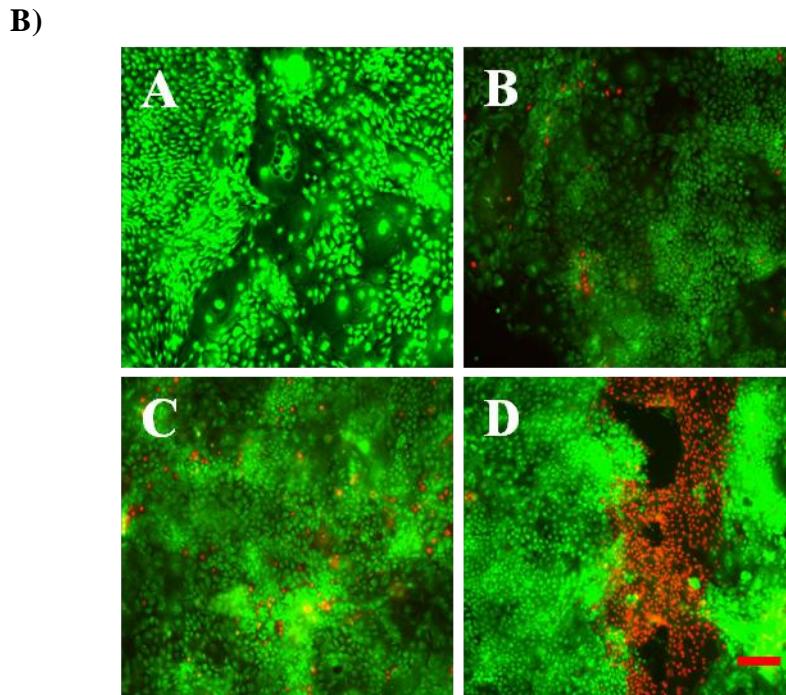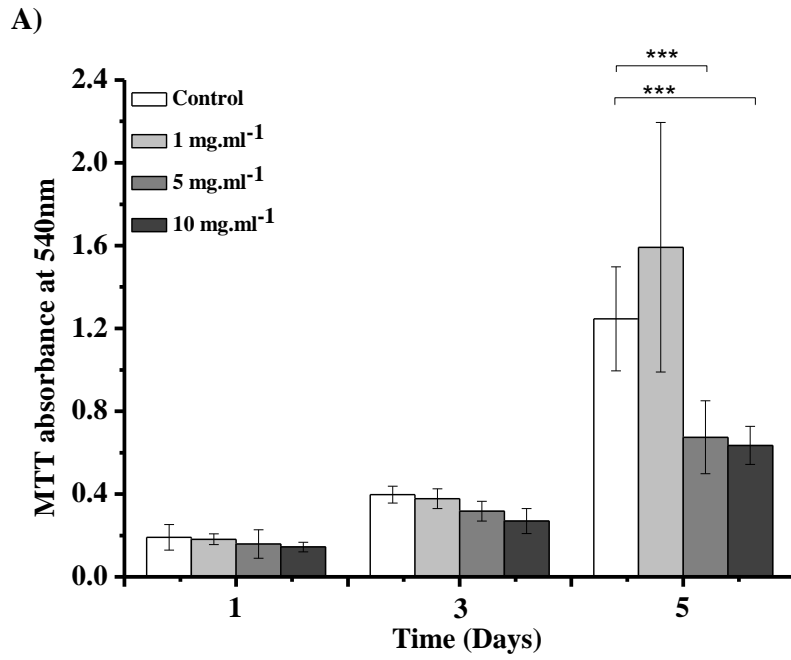
Figure 3.4 Effect of KGM (*A.konjac* Koch) on human keratinocyte proliferation assessed by MTT assay. 2×10^5 keratinocytes were co-cultured with 2×10^5 i3T3 for two days in 1 mL of 10% Green's medium, then treated with KGM for 1, 3 and 5 days. Results shown are mean ±SD, (n=3), ***P<0.001 highly significant, **P<0.01 very significant and *P<0.05 significant in comparison to control. The bottom panel shows the viability of cells stained with live/dead stain where (A) are control cells and (B), (C) and (D) are cells cultured for 5 days in the presence of 1, 5 and 10 mg.ml^{-1} KGM respectively. (Scale bar: 100 μm).
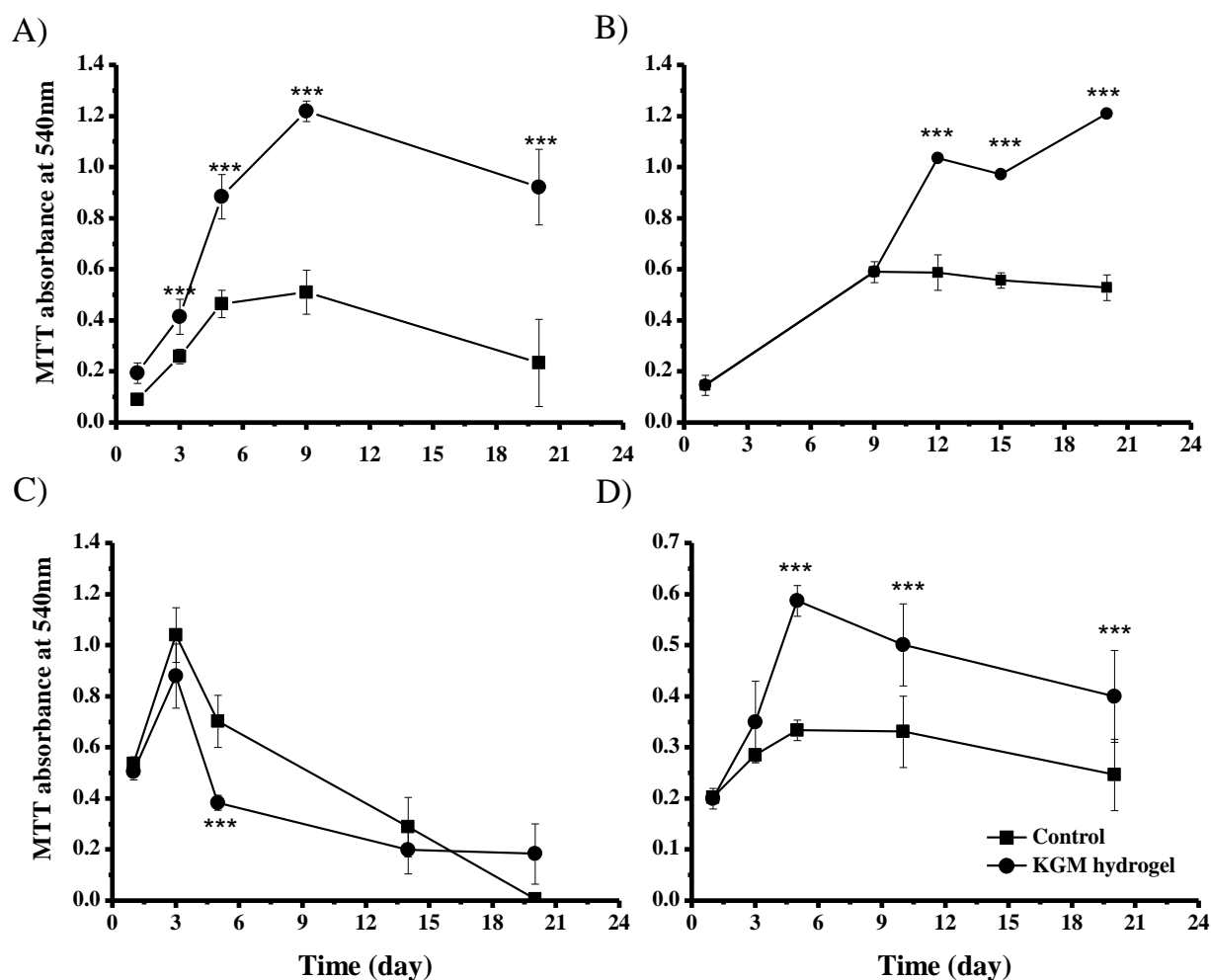
Figure 3.5 (A, C-D) Investigation of the ability of KGM (*A. konjac* Koch) to support the metabolic activity of (A) fibroblasts, (C) keratinocytes and (D) ADMSC under conditions of media starvation. $2x10^4$ fibroblasts were seeded in 1 mL of 10% DMEM or $2x10^5$ keratinocytes were co-cultured with $2x10^5$ i3T3 for two days in 1 mL of 10% Green's medium or $5x10^4$ ADMSC were seeded in 1 mL of 10% DMEM, then supplemented with 15 mg of KGM, and not changed for 20 days. Metabolic activity was assessed at 1, 3, 5, 9 and 20 days via MTT assay. (B) Investigation of KGM to increase fibroblast metabolic activity, not proliferation. $2x10^4$ fibroblasts were seeded in 1 mL of 10% DMEM and left until they reached confluency at day 9. Then, at day 9, 15 mg KGM was added into the media and cell viability was assessed at day 12, 15 and 20 using MTT assay. ■ control, ● - fibroblasts + 15 mg.mL^{-1} KGM (*A. Konjac* Koch*)*. Results shown are means ±SD, (A, C and D) (n=3) and (B) (n=1) ***p<0.001 highly significant, **p<0.01 very significant and *p<0.05 significant in comparison to control.

Day

5   **20**
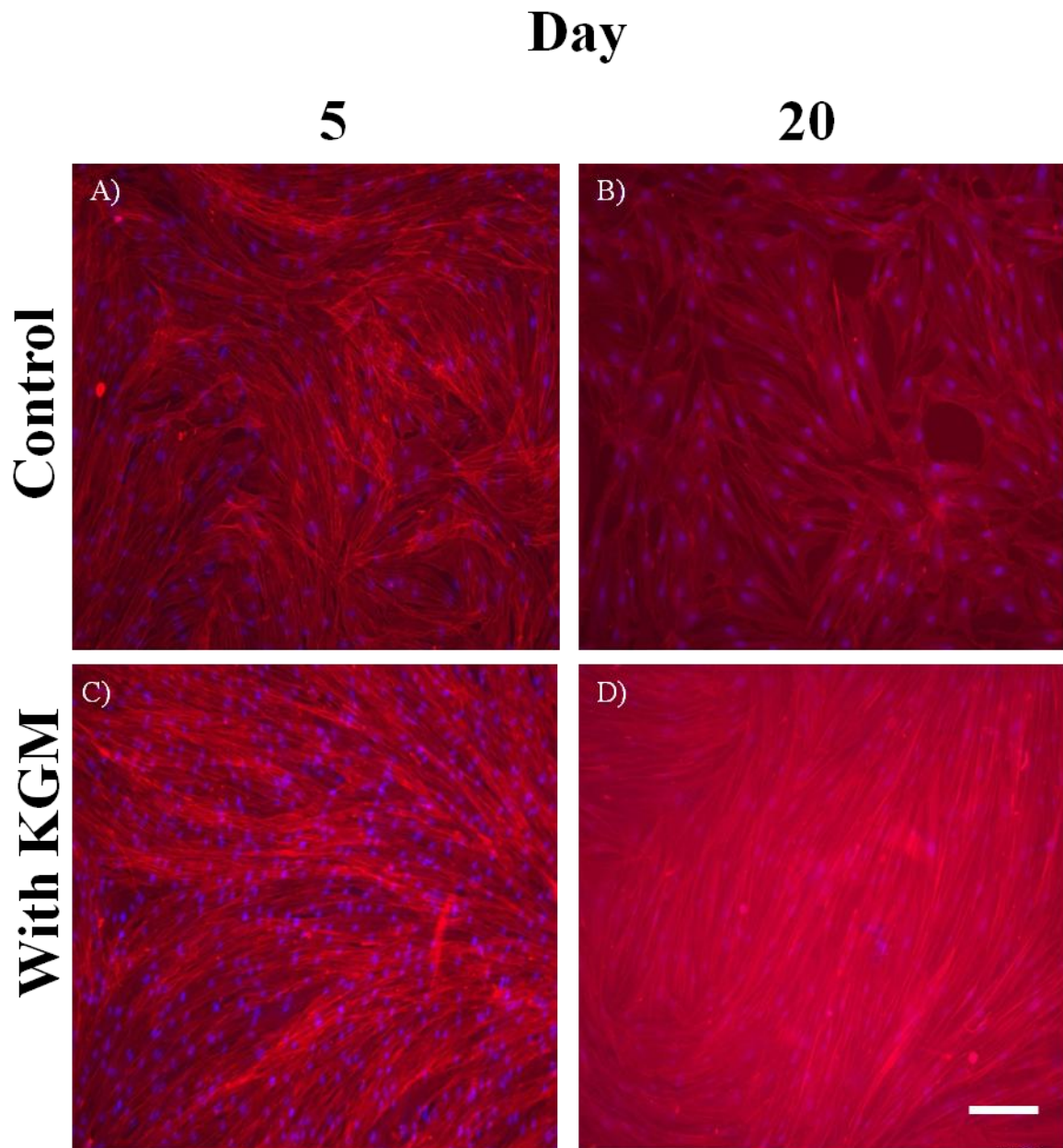
Figure 3.6   Morphology of fibroblast cultured deliberately in unchanged media up to 20 days. (A-B) Control (without KGM) and (C-D) with KGM. Cell's cytoskeleton was stained with phalloidin-TRITC (red) and nuclei with DAPI (blue). (Scale bar: 100μm).

Day

5   **20**
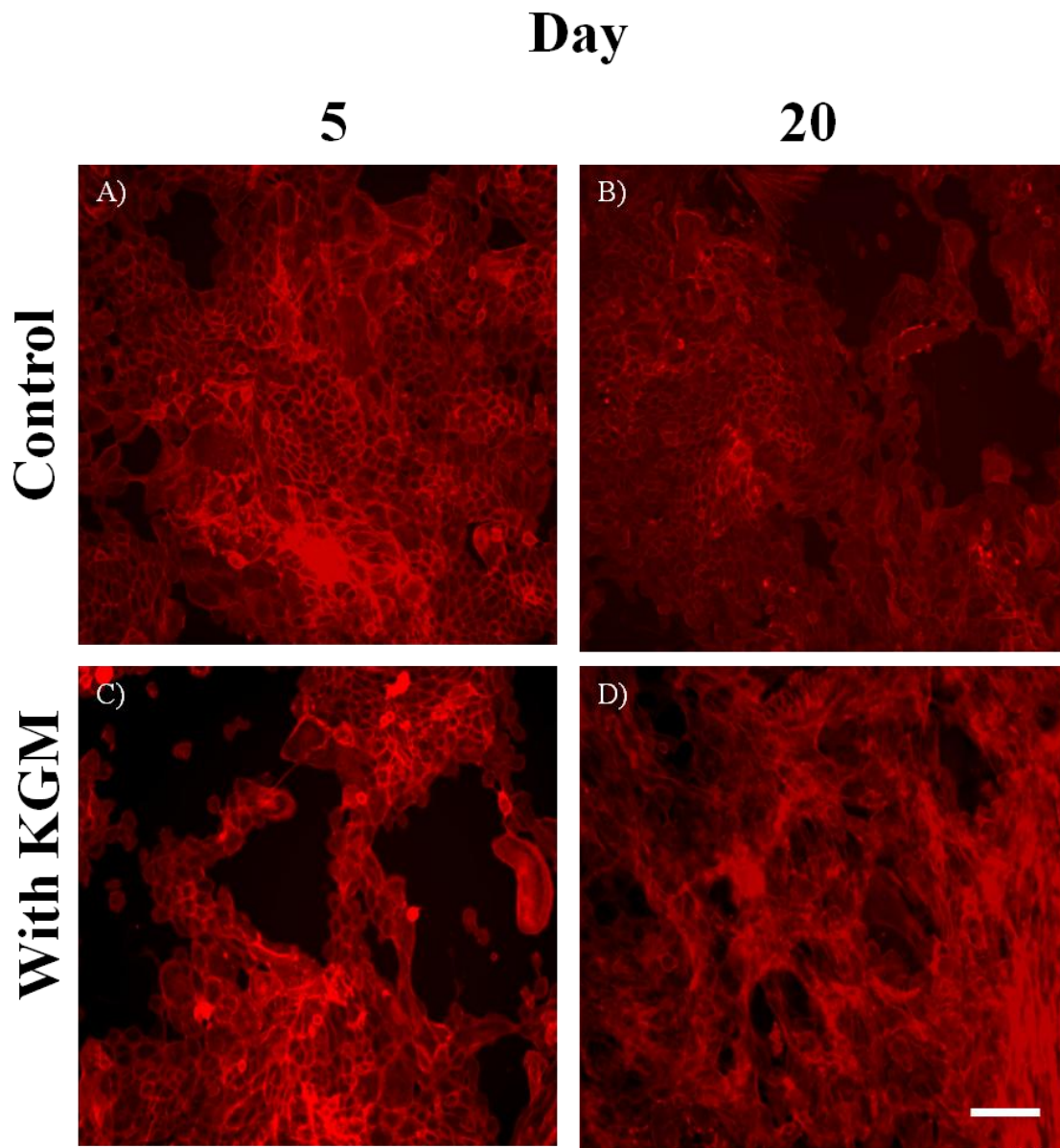
Figure 3.7   Morphology of keratinocyte cultured deliberately in unchanged media up to 20 days. (A-B) Control (without KGM) and (C-D) with KGM. Cell's cytoskeleton was stained with phalloidin-TRITC (red) and nuclei with DAPI (blue). (Scale bar: 100μm).

3.2.6 Determination of KGM molecular weights by enzymatic hydrolysation using β-mannanase and extraction using ethanol and ultrafiltration.

Enzymatic hydrolysation of KGM's long polymeric chains by β-mannanase enables scientists to synthesize low molecular weight chain of KGMs in a highly selective and precise manner. In this study, β-mannanase from *C.japonicus* was used to cleave KGM's high molecular β(1-4) glycosidic chains and the enzymatic activity was stopped by heat inactivation at 100°C for 10 minutes.

The molecular weight and the effect of heat inactivation on KGM (*A. konjac* Koch) molecular weight distribution and biological activity was then examined and shown in Figure 3.8 and 3.9. The heat treatment changed KGM's average molecular weight and polydispersity compared to untreated KGM (Table 3.2) but latter experiment showed that this did not affect its biological activity on the stimulation of fibroblast proliferation (Figure 3.11D).

Attempts to produce low molecular weight of KGM were conducted using 100 and 500 U.mg^{-1} β-mannanase at both room temperature and 60°C. We started the enzymatic treatment using 500 U at both 60°C and room temperature and gradually decreased the amount of enzyme and time in order to produce higher molecular weight. We found that the use of 100 and 500 U enzyme in conditions 60°C and room temperature completely hydrolysed the KGM and did not give any differences in term of molecular weight distribution and polydispersity which are shown in Figure 3.10. The profile for GPC chromatograms of these KGM is shown in Table 3.3.

Attempts to produce molecular weight in the range of 100000–500000 g.mol^{-1} were conducted using low concentration of enzyme at 0.1, 1 and 10 U at 5°C and room temperature. Hydrolysation in 5°C temperature was chosen to decrease β-mannanase activity

in order to obtain the highest molecular distribution range that would be beneficial for fibroblast proliferation. Enzyme concentrations of 0.1–1 U.mg^{-1} in room temperature and 5°C produced KGM molecular weight in the range of 95,000–160,000 g.mol^{-1}. KGM hydrolysed with 0.1 U.mg^{-1} enzyme at 5°C gave higher molecular weight of 160,000 g.mol^{-1} compared to those prepared with 0.1–1 U.mg^{-1} of enzyme hydrolysed KGM at room temperature. The profile of GPC chromatograms for these hydrolysed KGM are shown in Table 3.4. We then examined the biological effect of these hydrolysed KGM on fibroblasts (Figure 3. 11D).

Table 3.2 Molecular weight data of non-treated (*A. konjac* Koch) KGM and after treatment with 100°C for 10 minutes measured by GPC.

	Sample	Time	Condition	Molecular weight (Mn)	Polydispersity
A	KGM (*A. konjac* Koch)	-	-	1500000 (±500000)	2.5
				16000(±5000)	1.02
				8000 (±500)	1.04
				2000(±400)	1.07
B	KGM (*A. konjac* Koch)	10 min	Heated at 100°C	500000 (±100000)	1.64
			To denature enzyme	7000 (±1000)	1.12
				1200 (±500)	1.21
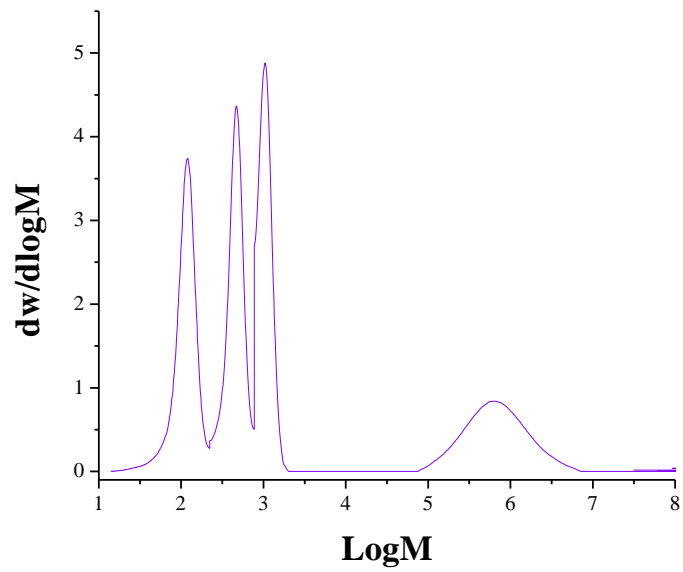
Figure 3.8   The GPC profiles of KGM (*A. konjac* Koch) without heat treatment for 10 minutes.
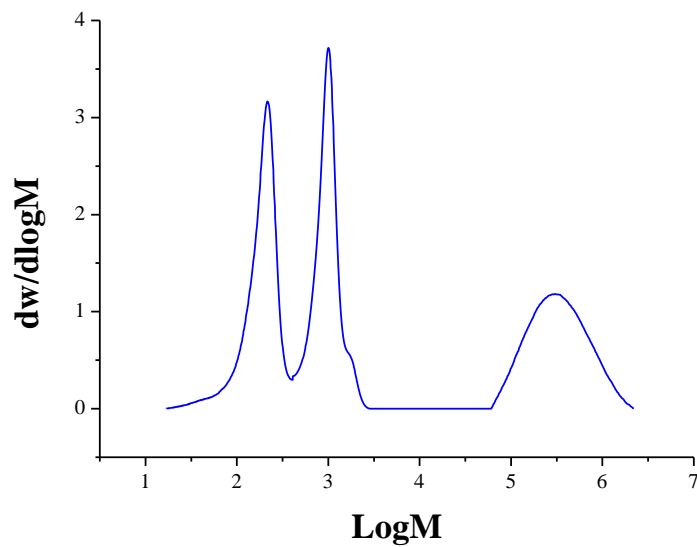
Figure 3.9   The GPC profile of KGM (*A. konjac* Koch) which was heated with 100$^{\mathrm{o}}$C for 10 minutes for enzyme inactivation to observe if the heating process broke the polymeric chain and changed the molecular weight distribution.
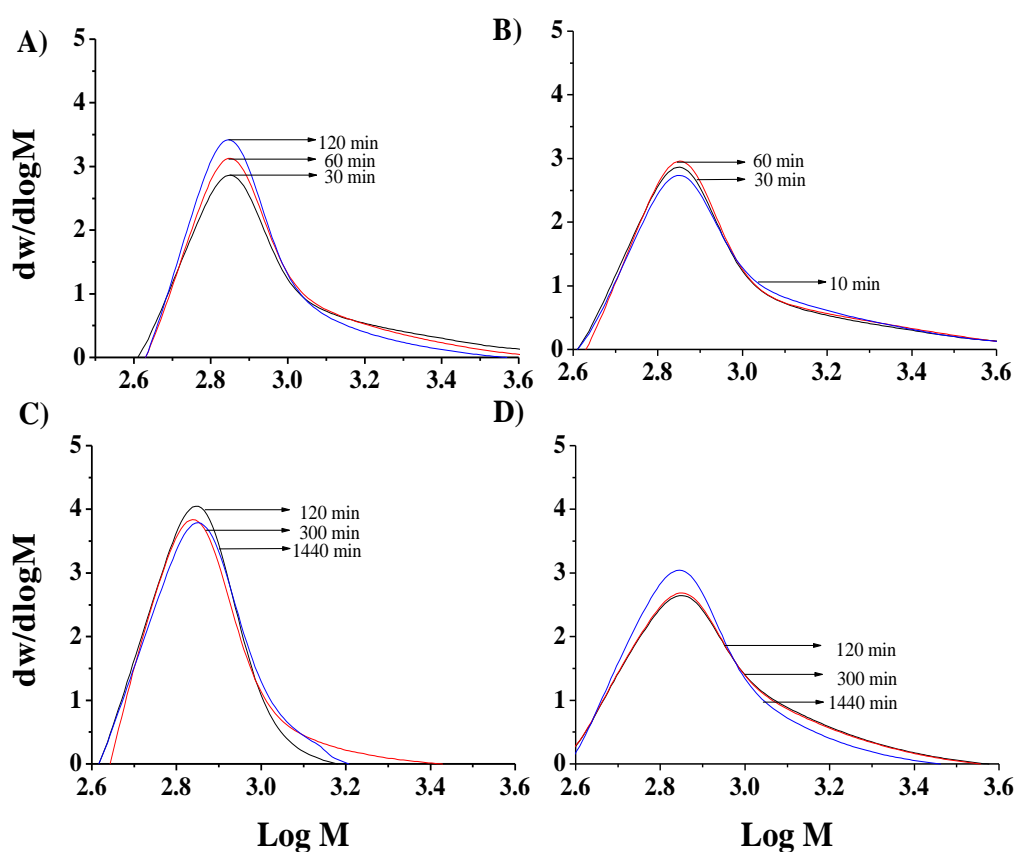
Figure 3.10 The GPC profiles of hydrolysed KGM (*A. konjac* Koch) by β-mannanase at different concentrations A-B) 100 U.mg^{-1} at 60°C and room temperature and C-D) 500 U.mg^{-1} at 60°C and room temperature.

Attempts to produce KGM with different molecular weight using ethanol extraction and ultrafiltration were conducted and the molecular weights obtained from these processes were summarized in Table 3.5 and 3.6. 400,000 g.mol^{-1} and 1000 g.mol^{-1} was obtained for HMW KGM and LMW KGM from ultrafiltration, respectively. 2000 g.mol^{-1} LMW KGM was obtained from ethanol extraction. The extracts biological activity was then examined in cell culture with human dermal fibroblasts and is shown in Figure 3.11B.

Table 3.3   Molecular weight data for GPC chromatograms on the effect of β-mannanase hydrolysed KGM (*A. konjac* Koch) at different concentrations 100 and 500 U.mg^{-1} at room temperature and 60°C at different time of hydrolysation as shown in Figure 3.8.

	Concentration of β- mannanase (u.mL^{-1})	Time of hydrolysation	Condition	Molecular weight (Mn)	Polydispersity
A	100	30 min	60°C	800 (±100)	1.33
		60 min		700 (±100)	1.20
		120 min		700 (±100)	1.10
B	100	10 min	Room temperature	800 (±100)	1.43
		30 min		800 (±100)	1.27
		60 min		800 (±100)	1.35
C	500	120 min	60°C	700 (±100)	1.10
		300 min		700 (±100)	1.08
		1440 min		700 (±100)	1.06
D	500	120 min	Room temperature	700 (±100)	1.10
		300 min		700 (±100)	1.10
		1440 min		700 (±100)	1.02

Table 3.4   Molecular weight data on the effect of β-mannanase hydrolysed KGM (*A. konjac* Koch) at different concentrations 0.1, 1 and 10 U.mg^{-1} at room temperature and 5°C for 10 minutes.

	Concentration of β- mannanase (u.mL^{-1})	Time of hydrolysation	Condition	Molecular weight (Mn)	Polydispersity
A	0.1	10 min	Room temperature	120000 (±50000) 500 (±100)	2.89 1.04
B	0.1	10 min	5°C	150000 (5000) 70000 (±1000)	2.88 4.91
C	1	10 min	Room temperature	90000 (±1000) 600 (±100)	1.43 1.02
D	10	10 min	Room temperature	700 (±100)	1.02

Table 3.5   Molecular weight data of the effect of KGM (*A. konjac* Koch) extracts following treatment with ethanol.

	Fractions of KGM	Time	Condition	Molecular weight (Mn)	Polydispersity
A	HMW+LMW		Room Temperature	500000 (±50000) 700 (±100)	1.64 1.12
B	LMW	-	Room Temperature	1000 (±500) 563 (±100)	1.69 1.08
C	HMW	-	Room temperature	400000 (±50000) 600 (±100)	2.28 1.05

Table 3.6   Molecular weight data of KGM (*A. konjac* Koch) extracts following treatment with ultrafiltration.

	Fractions of KGM	Time	Condition	Molecular weight (Mn)	Polydispersity
A	HMW	-	Room Temperature	300000 (±50000) 900 (±100)	1.62 1.10
B	LMW	-	Room Temperature	1100 (±100) 500 (±100)	1.05 1.05

3.2.7 The effect of different MW extracts of KGM (*A. konjac* Koch) on fibroblast proliferation.

The relationship between the distribution of molecular weight and the biological activity of the extracts on fibroblast proliferation following KGM treatment of ethanol, ultrafiltration and enzyme was then investigated using MTT assay. Figure 3.11 shows that the treatment (b) ultrafiltration, (c) ethanol and (d) β-mannanase significantly reduced KGM biological activity compared to (a) non-modified KGM. HMW components from ultrafiltration and ethanol extraction were found to retain some stimulatory activity on fibroblast proliferation (+ 144%) after 5 days when compared to non-modified KGM (+ 244%) (compared to controls in the absence of any KGM). However, LMW KGM from ultrafiltration did not significantly affect the rate of proliferation when compared to control cells after 5 days while ethanol extraction reduced fibroblast proliferation after 3 and 5 days by approximately -25% compared to non-modified KGM.

Figure 3.12 summarises the effect of a range of concentration of β-mannanase hydrolysed KGM at room temperature and 5°C. The biological activities of 0.1 U.mL^{-1} β-mannanase hydrolysed KGM at room temperature or at 5°C for 10 minutes showed no stimulation or inhibition on fibroblast proliferation. The ability to stimulate fibroblast proliferation was completely lost following the treatment with 10 and 100 U.mL^{-1} enzyme for 10 min on KGM.

We then examined the effect of ethanol extracted HMW and LMW KGM on keratinocyte proliferation and found that the inhibitory effect was dependent on the molecular weight of KGM (Figure 3.13)

The relationship between KGM and molecular weight following treatment with ethanol, ultrafiltration and enzymes on fibroblast and keratinocyte proliferation after 5 days are summarized in Figure 3.14. It was found that the effect of KGM on both fibroblasts and

keratinocytes was clearly dependent on the molecular weight of the fractionated material – non modified KGM molecular weight component of around $1x10^6$ g.mol^{-1} stimulated fibroblast proliferation (by + 240%) but was very inhibitory to keratinocytes proliferation (-60%). The HMW components (of approximately $5x10^5$ g.mol^{-1}) shown some stimulatory activity on fibroblast proliferation (+ 144%) while inhibit keratinocyte proliferation (by -50%).

It was observed that molecular weight >100,000 g.mol^{-1} retained the biological activity of KGM stimulating fibroblast proliferation. Low molecular weights KGM (~2000-10,000 g.mol^{-1}) from ethanol extraction and enzymatic had no effect on the cells but (<1000 g.mol^{-1}) was inhibitory to cells.

Table 3.7 The relationship between the distribution of KGM (*A. konjac* Koch*)* molecular weight and ability to stimulate fibroblasts proliferation at day 5 as measured with MTT assay. Cells from passage 5-9 were used (seeded at 2×10^4 cells.mL^{-1}) in 10% DMEM. (n=3), +++ highly significant, ++ very significant and + significant in comparison to control.

KGM treatment	Effect on fibroblasts
KGM (non modified)	+++
Heat treated KGM	+++
0.1 U.mg^{-1} β-mannanase treated KGM (at 5˚C) (10 min)	-
0.1 U.mg^{-1} β-mannanase treated KGM (10 min)	-
1 U.mg^{-1} β-mannanase treated KGM (10 min)	-
10 U.mg^{-1} β-mannanase treated KGM (10 min)	-
100 U.mg^{-1} β-mannanase treated KGM (1 hour)	-
Ethanol extracted HMW	++
Ethanol extracted LMW	-
Ethanol treated KGM	++
Ultrafiltration extracted HMW	++
Ultrafiltration extracted LMW	-
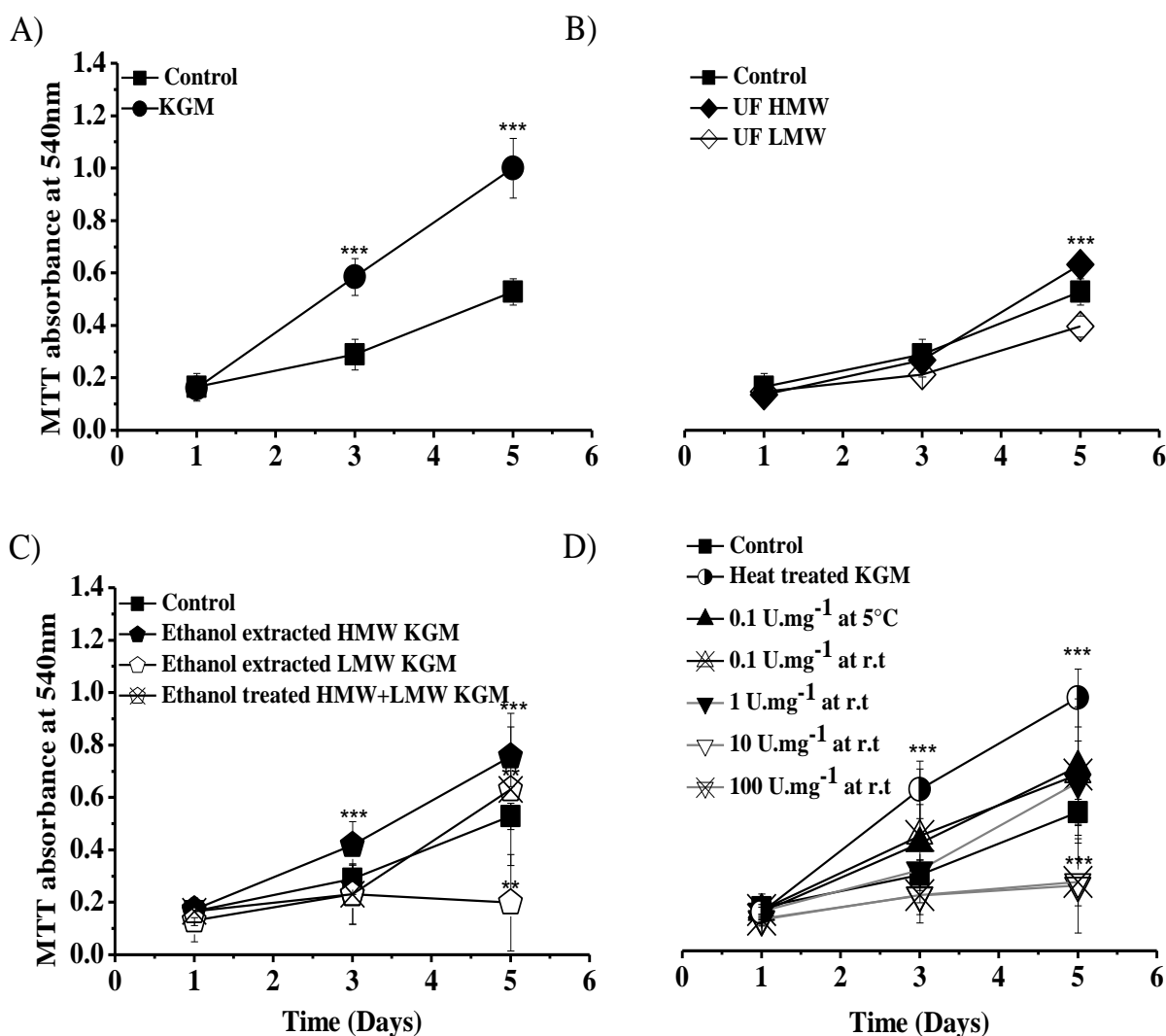
Figure 3.11 The effect of extracts of KGM (*A. konjac* Koch) on fibroblast proliferation. 2×10^4 fibroblasts were seeded in 1 mL of 10% DMEM containing 10 mg.mL^{-1} KGM extracts. Metabolic activity was measured after 1, 3 and 5 days of incubation using MTT assay. (A) non-modified KGM extract, (B) high molecular weight and low molecular weight ultra-filtration extracts, (C) ethanol extracted KGM further divided into high molecular weight and low molecular weight extracts and a combined extract of low molecular weight and high molecular weight KGM. (D) shows the effects of enzyme treatment with β-mannanase at a range of concentrations and temperatures on KGM activity. Results shown are mean ±SD, (n=4), ***p<0.001 highly significant compared to control.
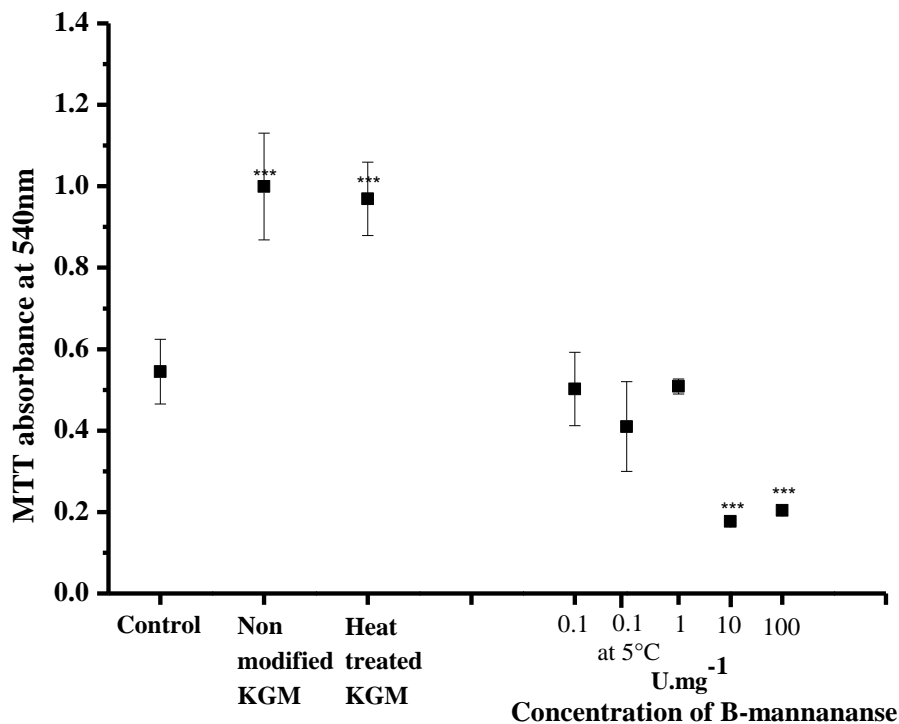
Figure 3.12 The effect of β-mannanase treatment at different concentrations for 10min, except for 100 U.mg^{-1} (1 hr) on KGM (*A. konjac* Koch) on the stimulation of fibroblast rate of proliferation at day 5 measured as measured by MTT assay. Result shows that KGM treated with enzyme at lowest concentration of 0.1 U.mg^{-1} completely lost its biological activity and concentration more than 10 U.mg^{-1} hydrolysed KGM became inhibitory to the cells. The biological activity on KGM hydrolysed with 0.1 U.mg^{-1} at room temperature and 5° C did not have any effect on fibroblast proliferation. The ability of heat treated KGM on fibroblast proliferation did not shown any difference to non modified KGM. mean ±SD, (n=2), ***P<0.001 highly significant, **P<0.01 very significant and *P<0.05 significant in comparison to control.

3.2.8 The effect of different molecular weight extracts of KGM (*A. konjac* Koch) on keratinocyte proliferation.

The effect of HMW and LMW KGM extract following treatment with ethanol on keratinocyte proliferation was measured using MTT assay and shown in Figure 3.13. We found ethanol treatment reduced KGM inhibition on keratinocyte proliferation and that this effect is clearly dependent on molecular weight of KGM. The LMW KGM had the least inhibition (-25%) while the HMW KGM had an almost equivalent effect to KGM.

Figure 3.14 shows the relationship between the distribution of KGM (*A. konjac* Koch) molecular weight and ability to stimulate fibroblasts and keratinocyte proliferation at day 5
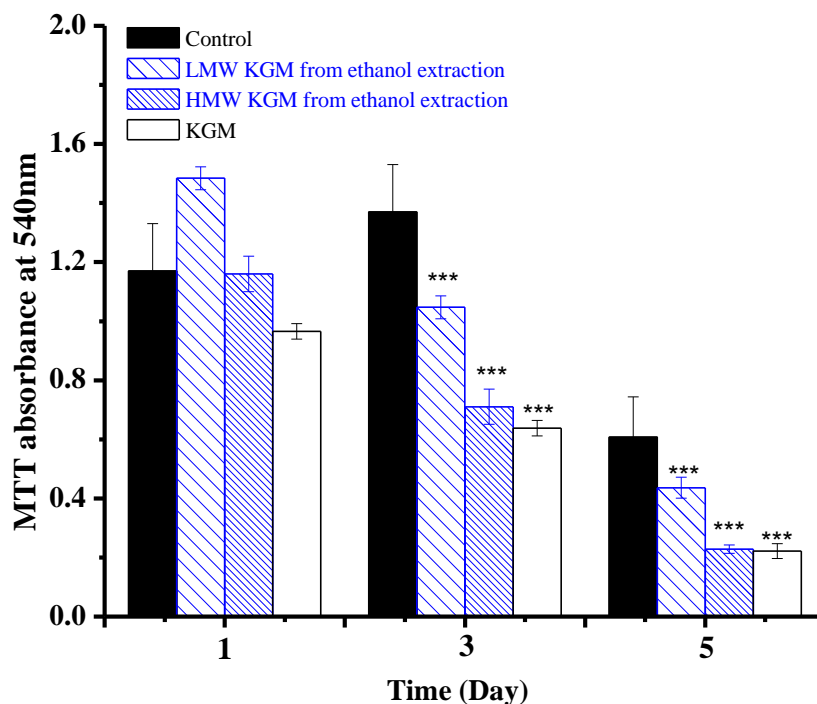
Figure 3.13 The effect of extracts of KGM (*A. konjac* Koch) on keratinocyte proliferation. 4×10^4 keratinocytes were co-cultured with 2×10^4 i3T3 in 1mL of 10% Greens containing 10 mg.mL^{-1} KGM extracts. Metabolic activity was measured after 1, 3 and 5 days of incubation using MTT assay. (Results shown are mean ±SD, (n=2), ***p<0.001 highly significant compared to control).
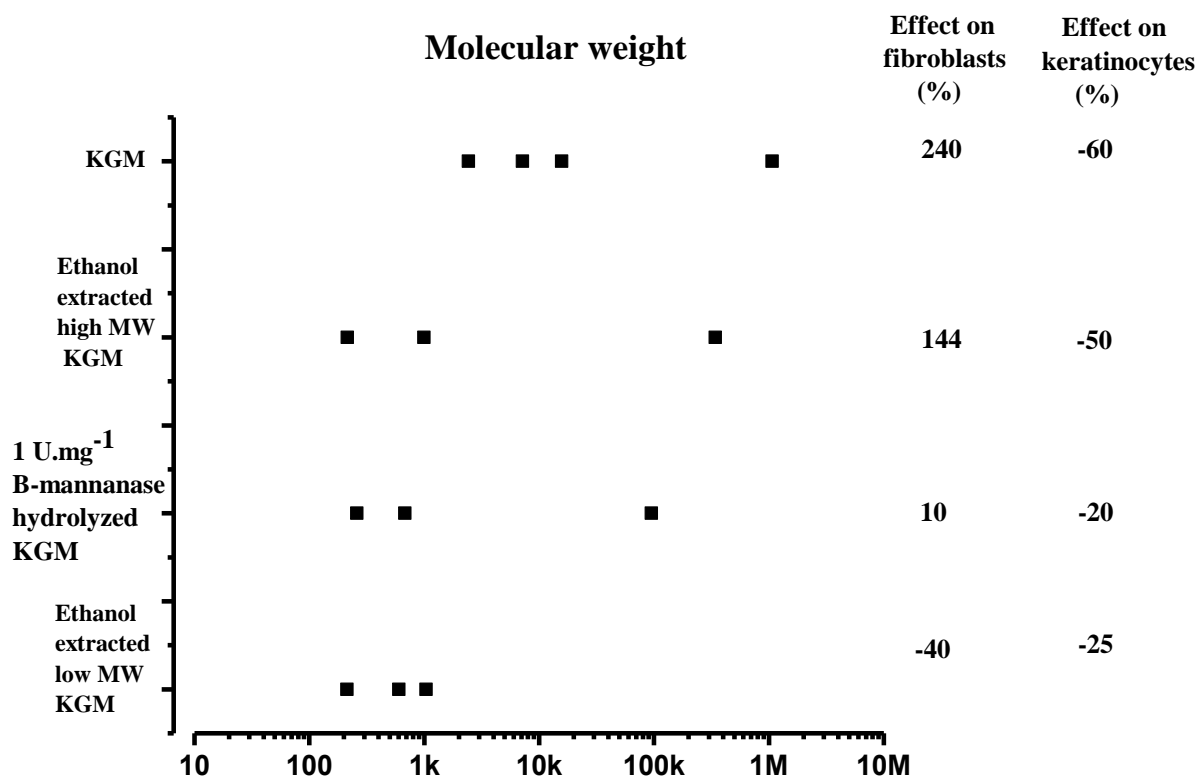
Figure 3.14 The relationship between the distribution of KGM (*A. konjac* Koch) molecular weight and ability to stimulate fibroblasts and keratinocyte proliferation at day 5 as measured with MTT assay. Result shows that KGM was very stimulatory to fibroblast proliferation but inhibitory to keratinocyte proliferation, and these effects were influenced by higher molecular weight. 2×10^4 fibroblasts were cultured in 1 mL of 10% DMEM for 1 day and 2×10^4 keratinocytes were co-cultured with 2×10^4 i3T3 for two days in 1 mL of 10% Green's medium. Then, 10 mg.mL^{-1} of KGM extract was added into the medium.

3.2.9 Blocking of MR on fibroblasts and keratinocytes by D-mannose.

In this study, investigation on the involvement of MR on KGM biological activities on fibroblasts and keratinocyte proliferation was conducted using a simple sugar, D-mannose to block mannose sensitive receptors. The effect on KGM's biological activity on both cells were measured using the MTT assay. Figure 3.15 shows the addition of increasing concentrations of D-mannose from 1 to 20 mg.mL^{-1} in fibroblast culture did not affect fibroblast proliferation nor inhibit KGM stimulation on fibroblast proliferation, clearly indicating that MR is not involved in this response. On the other hand, Figure 3.16 shows that increasing concentrations of D-mannose from 1 to 10 mg.mL^{-1} inhibited keratinoycte proliferation and also inhibit KGM inhibition of keratinocyte proliferation, suggesting the involvement of MR with the cell type.

Semi quantification of the presence of MR on fibroblasts and keratinocytes was measured using Con A – FITC staining (Figure 3.17). Con A is known to bind onto glycosylated feature of cell surface which contains lectins and MR that this binding can be blocked using mannose. The technique provides a semi-quantitative assessment of the MR density on the cells. From this study, we found that concentration of > 10 mg.ml^{-1} mannose completely blocked Con A – FITC adhesion onto fibroblasts as for keratinocytes > 40 mg.mL^{-1} mannose was required. These results suggest that keratinocytes have a higher density of MR compared to fibroblasts where a higher concentration of mannose was required to block the binding of Con A.
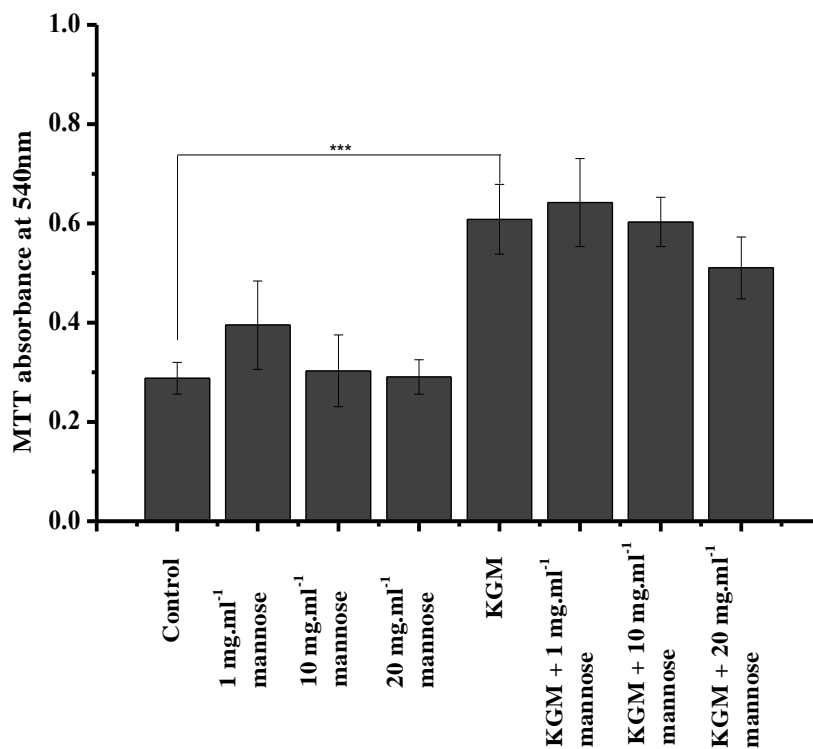
Figure 3.15 The effect of concentrations of D-mannose (1–20 mg.mL^{-1}) and competition with KGM on fibroblast proliferation. $2x10^4$ fibroblasts were cultured in 1 mL of 10% DMEM in a 12 well plate before being supplemented with medium containing mannose or mannose with an extract of KGM (from *A.konjac* Koch) at 10 mg.mL^{-1}. Results shown are mean ±SD, (n=3), ***p<0.001 highly significant, **p<0.01 very significant in comparison to control.
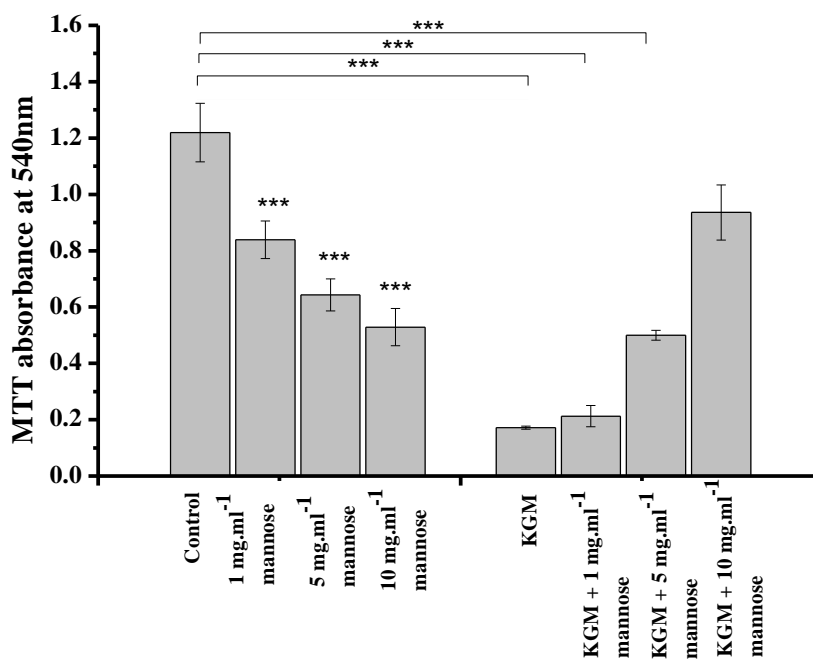
Figure 3.16   The effect of concentrations of D-mannose (1–10 mg.mL^{-1}) and competition with KGM on keratinocyte proliferation. $2x10^4$ keratinocytes were co-cultured with $2x10^4$ i3T3 for two days in 1 mL of 10% Green's medium in a 12 well plate before being supplemented with medium containing mannose or mannose with an extract of KGM (from *A.konjac* Koch) at 10 mg.mL $^{-1}$. Results shown are mean ±SD, (n=3), ***p<0.001 highly significant, **p<0.01 very significant in comparison to control.
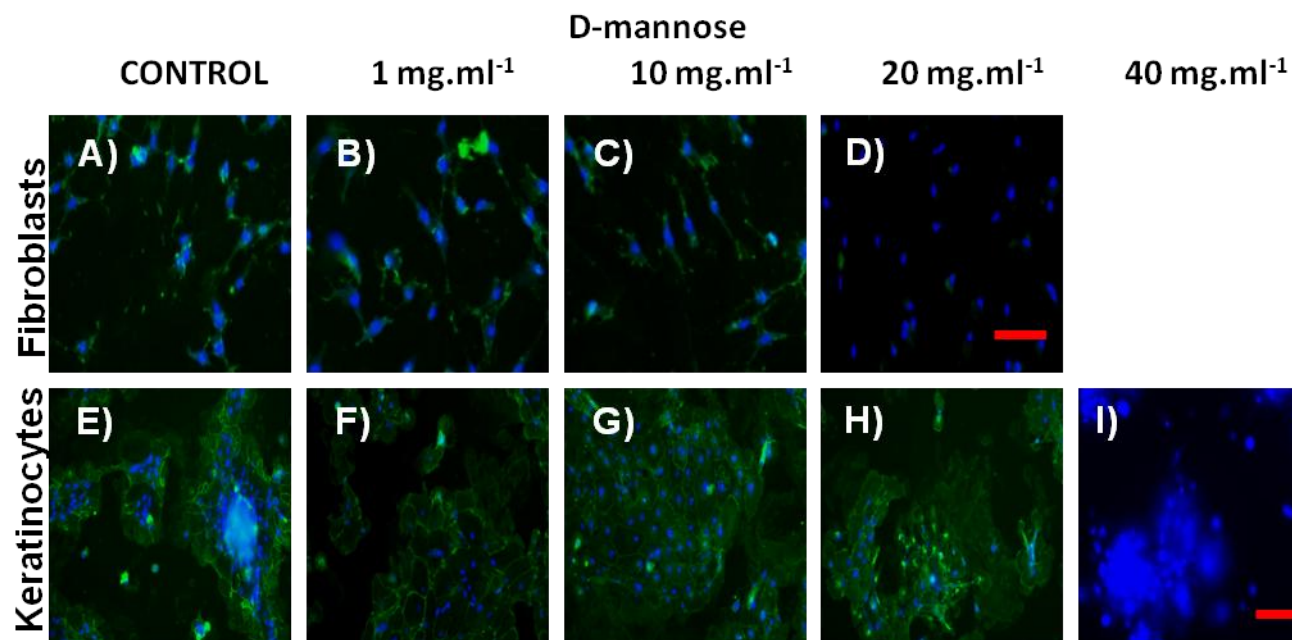
Figure 3.17 Binding of Con A-FITC (green) to fibroblasts and keratinocytes in the presence of D-mannose, cell nuclei are labelled with DAPI (blue). (A-D) 2×10^4 fibroblasts (seeded in 1 mL of 10% DMEM) or (E-H) 4×10^4 keratinocytes (co-cultured with 2×10^4 i3T3 in 1 mL of 10% Green) were cultured for 3 days then amount of D-mannose was added into the culture to block mannose sensitive receptors (MR). After an hour, the unbounded mannose was washed and Con A-FITC was added into the culture. Con A binds to glycosylated surface of the cells that consist of different type of lectins, where semi quantification of MR was conducted by observation of unbounded Con A on the cell surface which was blocked by D-mannose. Photographs show dose dependent inhibition of Con A binding to fibroblasts. In keratinocytes, this inhibition was only seen at 40 mg.mL^{-1}. (Scale bar: 300 μm).

3.2.10 Investigation of the effect of Concanavalin A and its interaction with KGM on fibroblast culture.

Investigation of the effect of concentrations of Con A (10-100 $\mu g.mL^{-1}$) on fibroblast culture found no significant differences in fibroblast proliferation with all concentrations of Con A (Figure 3.18A). However, 10-100 $\mu g.mL^{-1}$ Con A significantly inhibited KGM stimulatory effect on fibroblast proliferation, where 10 $\mu g.mL^{-1}$ Con A reduced KGM stimulatory effect of fibroblast proliferation by more than 50% (Figure 3.18B). This result suggests that other lectins than MR was responsible for the stimulation of proliferation by KGM, presumably because the binding of KGM onto lectins preventing it from adhere onto the cell surface.

The hypothesis of KGM binding onto Con A-FITC, by culturing fibroblasts with 1, 5 and 10 $mg.mL^{-1}$ KGM before adding 100 $\mu g.mL^{-1}$ Con A into the culture for 30 minutes, according to method 2.13. The cells were then washed twice with PBS to remove KGM and possibly Con A bound to KGM from the culture. Visualization of Con A-FITC binding onto cell surface was observed using a fluorescence microscope (Axon Instrument) and shown in Figure 3.19.

The cells cultured with 5 and 10 $mg.mL^{-1}$ KGM (Figure 3.19 H and K) did not show any Con A-FITC binding compared to control cells and the cells cultured with 1 $mg.mL^{-1}$ KGM. We assumed that the addition of 1 $mg.mL^{-1}$ KGM did not effectively cover the cell surface due to insignificant effect on the inhibition of keratinocyte proliferation, shown previously thus leaving larger surface area for Con A-FITC to adhere. The cells which were supplemented with 5 and 10 $mg.mL^{-1}$ KGM had most of its glycosylated surface covered with KGM, thus leaving Con A–FITC to bind onto the KGM, not the cell surface. Hence, the washing procedure with PBS to remove KGM clearly removed Con A-FITC which bound to KGM.

A)

B)
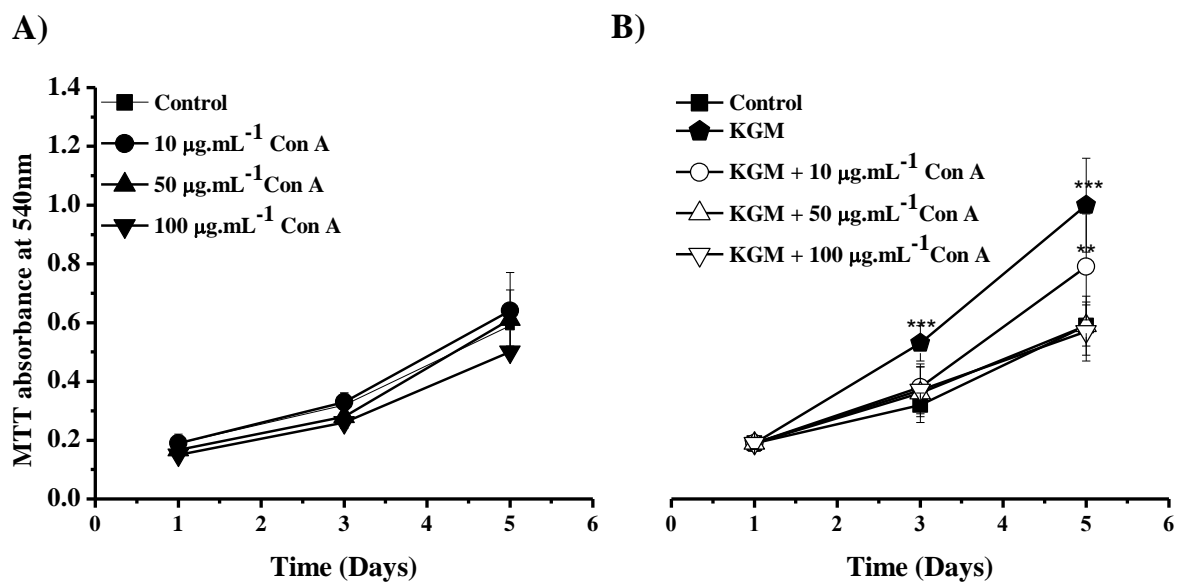
Figure 3.18   (A) Effect of Con A on fibroblast proliferation and (B) inhibition of the effect of KGM on fibroblast proliferation by Con A after 1, 3 and 5 of culture. Results shown are mean ±SD, (n=3), ***p<0.001 highly significant, **p<0.01 very significant in comparison to control.
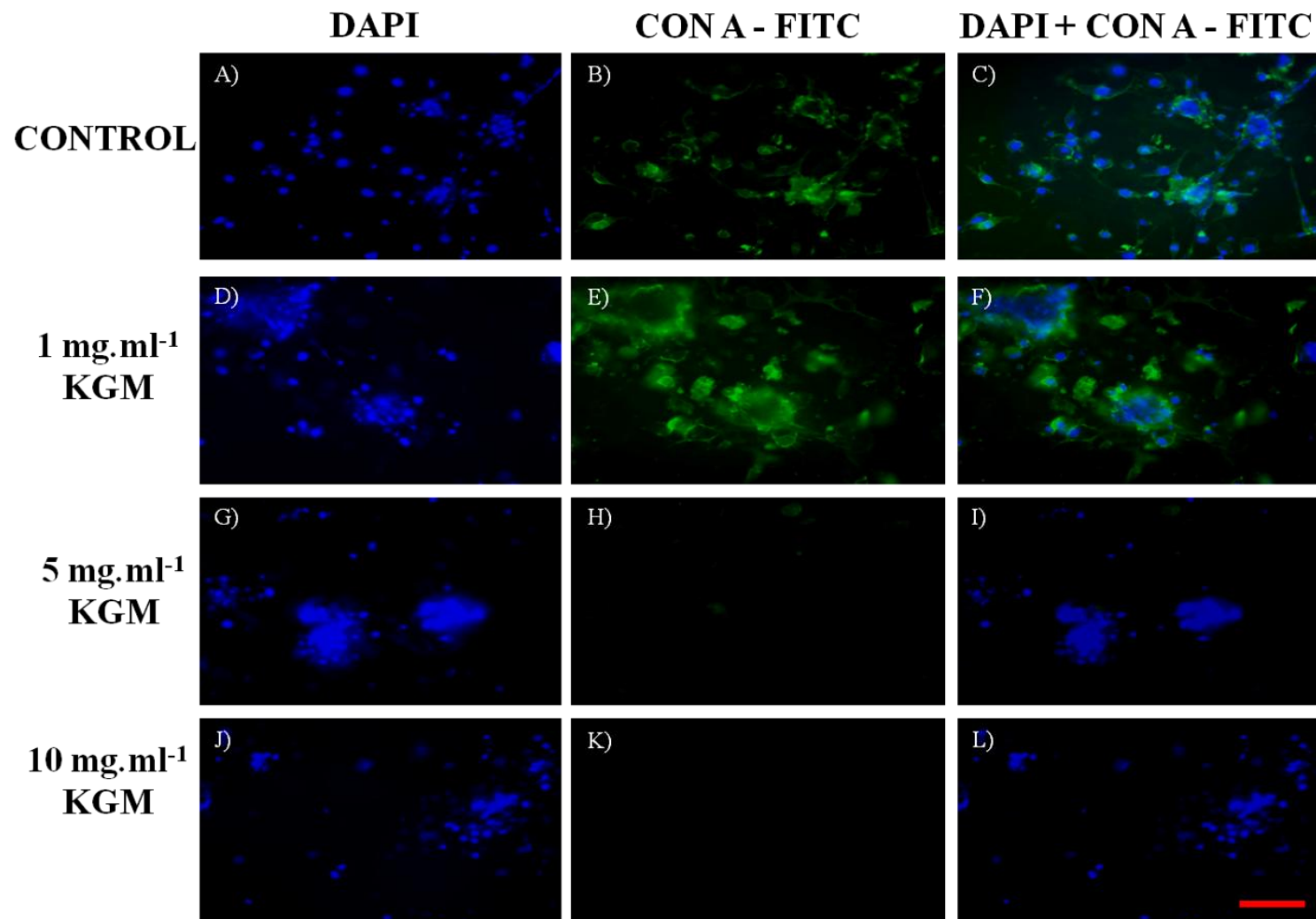
**Figure 3.19**   Con A binding onto keratinocyte surface was blocked by 5 and 10 mg.ml^{-1} KGM, suggesting that Con A binds to KGM. (Scale bar: 100 μm).

3.3 Discussion.

The first part of this chapter discussed the relationship between the species of KGM, Man:Glc ratio, glucomannan content, distribution of molecular weight , treatments with ethanol, ultrafiltration and enzyme on the biological activities of skin cells. The species with more than 50% glucomannan content (*A. konjac* Koch, *A. oncophyllus* and *A. paeonifolius*) stimulated fibroblast viability, whereas *A. prainii* and *A. elegans* did not. KGM with the higher mannose to glucose ratio was very stimulatory to fibroblast proliferation (*A. konjac* Koch with 2.2:1 and *A. oncophyllus* with 2.5:1) and inhibitory to fibroblast proliferation (*A. elegans* 235:1). These results suggest that the variability in the biological response to the KGM species may be related to the content of GM and Glu:Man ratio.

KGM treatment with ethanol, ultrafiltration and hydrolytic enzyme affected KGM's molecular weight and biological activities on fibroblasts and keratinocytesHigh molecular weight KGM (>100,000) stimulated fibroblast and inhibited keratinocyte proliferation. These effects also were susceptible to enzyme degradation with β-mannanase and ethanol extraction where the ability of KGM to stimulate fibroblast or inhibit keratinocyte proliferation decreased with a decrease in molecular weight. Ethanol extracted HMW KGM stimulated fibroblast proliferation at 144% compared to non-modified KGM while ethanol extracted HMW inhibit keratinocyte proliferation at -50% compared to non-modified KGM at -60%. The results were consistent with the relationship of *Aloe vera* molecular weight fractions with higher content of mannose ability to stimulate the proliferation of murine T-cell (Leung, Liu et al. 2004). KGM's structure-activity relationship was also found to be similar to that of (1-3)-β-glucan, where molecular weights higher than 550,000 g.mol^{-1} showed the highest immunopotentiating activity, while fractions from the same source with molecular weights of 5000-10000 showed no activity. (Kojima, Tabata et al. 1986; Gomaa, Kraus et al. 1992; Bohn and BeMiller 1995; Kulicke, Lettau et al. 1997).   However, (1-3)-β-glucan with an

average molecular weight of less than 20,000 g.mol^{-1} with a degree of branching (DB) of <0.25 has anti-tumor activity which may suggest the influence of DB and molecular weight with its biological activity (Blaschek, Kasbauer et al. 1992; Gomaa, Kraus et al. 1992). In glycoprotein synthesis, it has been proposed that the introduction of low molecular weights of KGM may act as alternate substrates for Golgi enzymes, which affects the synthesis of glycoproteins (Varki A, R et al. 1999).

KGM components of (1-4)-β-D-Glc and (1-4)-β-D-Man were reported to have a few short side chains which may contain galactose residues and exhibit some degree of acetylation which depends on the plant species (Stephen 1983; Cescutti, Campa et al. 2002). Glucomannan which is an active component of KGM and also found in structural cell wall of yeast and bacteria was reportedly beneficial for medical purposes such as photoprotective effect in UVB irradiated human keratinocytes and *in vivo* model of UV induced erythemia formation in human volunteers (Ruszova, Pavek et al. 2008), inhibition of the growth of *Candida albicans* in the presence of the presence of *Lactobacillus* and *Lactococcus* species (Sutherland, Tester et al. 2008), wound healing (Leung, Liu et al. 2004) and in the treatment of diabetes to increase insulin sensitivity (Vuksan, Sievenpiper et al. 2000; Vuksan, Sievenpiper et al. 2001). The structure-activity relationship of glucomannan is found to be similar to β(1-4) glucan immunostimulatory and biological activities which dependent on the molecular weight, irrespective of the chemical structure of the sugar (Kojima, Tabata et al. 1986; Gomaa, Kraus et al. 1992; Bohn and BeMiller 1995; Kulicke, Lettau et al. 1997)

The second part of this chapter discussed the effect of FCS on KGM's ability to stimulate fibroblast proliferation. The results showed that KGM was able to stimulate fibroblast proliferation in the absence and presence of 2 and 10% of FCS. However, this effect was more evident with 10% FCS (with more than 35 fold) compared to in 2 and 0% FCS, (17 and 5 fold) respectively. Although KGM was able to stimulate cell proliferation in the absence of

FCS compared to control, the cell population was too low compared to those cultured with 2 and 10% FCS. This effect could relate to the expression of MRs in keratinocytes and fibroblasts, which were dependent on the concentration of FCS. The expression of MR in skin fibroblasts and keratinocytes were increased to about two fold in the presence of 10% FCS when compared to 1% FCS (Wollenberg, Mommaas et al. 2002). The expression of MRs in cells *in vivo* and *in vitro* also can be modulated by a number of agents such as pathogens (Astarie-Dequeker, N'Diaye et al. 1999), vitamin D_3 (Clohisy, Bar-Shavit et al. 1987) dexamethasone (Mokoena and Gordon 1985) and interleukin 4 (Stein, Keshav et al. 1992) and FCS (Wollenberg, Mommaas et al. 2002). FCS is a rich source of platelet mitogens - it contains growth factors and essential chemicals for various cell functions such as growth and differentiation, in which explained its effect on KGM's stimulation of fibroblast proliferation.

The involvement of lectins in the interaction of KGM with fibroblasts and keratinocytes was investigated and discussed in this chapter. Mannose receptors (MRs) are involved in many cellular responses such as the host defense from pathogens (Hespanhol, Soeiro et al. 2005), regulation of innate immunity (Taylor, Gordon et al. 2005), regulation of myoblasts motility and muscle growth (Jansen and Pavlath 2006), clearance of glycoconjugates (Lee, Evers et al. 2002), and wound healing (Honardoust, Jiang et al. 2006). In wound healing, MRs plays a role in re-epithelization and connective tissue remodeling (Honardoust, Jiang et al. 2006). The expression of MRs was reported on both human dermal fibroblasts and keratinocytes (Wollenberg, Mommaas et al. 2002; Hespanhol, Soeiro et al. 2005; Shahbuddin, Shahbuddin et al. 2013). .

The mechanism of KGM's biological effect on fibroblast and keratinocyte metabolic activity was investigated using Con A, a plant lectin which specifically binds to glycosylated surfaces containing different type of receptors, such as galectin, MRs and Dectin on cell membrane (Goldstein, Hollerman et al. 1965; Becker, Reeke et al. 1976; Moore, Fuchs et al. 2000) and

using D-mannose, as inhibitor to mannose specific receptor (Hespanhol, Soeiro et al. 2005).

The visualization of mannose specific receptors on keratinocyte and fibroblast's surfaces were conducted using Con A-FITC where D-mannose was used to semi quantify the presence of lectins on the cell surface by specifically block the binding of Con A-FITC onto mannose specific receptors. (Labsky, Dvorankova et al. 2003). It was found that fibroblasts had less mannose specific receptors compared to keratinocytes where D-mannose of >20 mg.mL^{-1} was required to completely block Con A-FITC adhesion, whereas keratinocytes required more than 40 mg.mL^{-1} (Shahbuddin, Shahbuddin et al. 2013).

In separate experiment, D-mannose at 1-20 mg.mL^{-1} did not affect fibroblast proliferation or KGM's stimulation of fibroblast proliferation. However, Con A culture with fibroblasts did not affect fibroblast proliferation but significantly inhibited KGM's stimulation of fibroblast proliferation. The result suggests the involvement of other lectins which are not specific to mannose but responsible for KGM's stimulation on fibroblast proliferation. The exact mode of action in this interaction is still unclear because Con A also bound onto KGM, which may have prevented it from interacting with cells.

The supplementation of D- mannose in keratinocyte cultures effectively inhibited keratinocyte proliferation and the effects of KGM on keratinocyte proliferation in a dose dependent manner, suggesting the involvement of MR in KGM's biological effect on keratinocyte but not fibroblasts.

Although it is not possible to identify with confidence the exact mechanism of action of the KGM high molecular weight fractions, the evidence shows that the stimulation of fibroblast proliferation by KGM involves Con A receptors whereas in the case of keratinocytes, mannose specific receptors were responsible for KGM inhibition of the proliferation.

The reports of mannose rich lectins having the ability to preserve human cord blood progenitor cells in suspension cultures for up to one month without media change (Colucci,

Moore et al. 1999) and stem cells for up to 2 weeks in culture (Kollet, Moore et al. 2000) and the the very recent report on the use of plant polysaccharides in cell encapsulation for the short term storage of stem cells for the use in cell therapy (Bo Chen, Bernice Wright et al. 2012) were the motivation behind the study of KGM's ability to support skin cells and ADMSC in nutrient deprived condition in this chapter.

The preservation of cells' metabolism in stressed conditions by lectins was mediated by preventing cellular proliferation and differentiation through interaction with a tyrosine kinase receptor, (Flt3^{+}) which is central to regulation of stem cells (Moore, Fuchs et al. 1997).

In this study, the presence of KGM in the culture medium of fibroblasts and ADMSC (but not of keratinocytes) maintained a high level of metabolic activity in unchanged media conditions for up to 20 days. The presence of KGM in the medium enabled fibroblasts and ADMSC to maintain a high level of metabolic activity in starved media conditions, where normally there was a decrease in metabolic activity in the absence of KGM after 10 days. This may be due to the increasing presence of metabolic waste in the medium and also the lack of the essential amino acid glutamine (normally provided in the media every few days). A dosage of 15 mg.mL^{-1} was chosen for prolonged culture of fibroblasts and ADMSC as the previous study of KGM at 10 mg.mL^{-1} showed the highest stimulation of fibroblasts proliferation for up to 5 days. Accordingly it was decided that it would be interesting to see the effect of the additional 5 mg.ml^{-1} on sustaining cell viability in 20 days of unchanged medium.

The result shows KGM's great potential in assisting cell transportation and long term preservation by stimulation of cell proliferation and maintaining cell viability in a nutrient deprived condition (Shahbuddin, Shahbuddin et al. 2013). Polysaccharide based hydrogels have gained significant interest as carriers and substrate to assist cell transportation compared to conventional cryopreservation method which is very challenging, expensive and risk of

detrimental effect from DMSO (Volden, Haugen et al. 1980; Cao, Li et al. 2007). It is also biocompatible, cheap and relatively easy to use on cells. Recent studies had shown that alginate, marine polysaccharide of mannuronic and guluronic acids supports corneal epithelial cells (Wright, Cave et al. 2012), hMSC and mESC preservations with similar level of cell viability, expression of stem cell markers, proliferation rates and morphology as equivalent to the stored cells in the incubator. (Chen, Zhang et al. 2009).

3.4 Conclusions.

In conclusion, the data in this chapter show that plant derived KGM (*A. konjac* Koch) has significant stimulatory effects on fibroblast proliferation and viability under conditions of media starvation for up to 20 days but not on keratinocytes. KGM's effect with fibroblasts in deprived medium condition was also observed with ADMSC. These results suggest that KGM has potentials for wound healing applications and also for the transportation of cells.

Chapter 4. Development of biodegradable hydrogels from KGM for wound healing.

4.1 Introduction.

Biodegradable hydrogels from synthetic or natural materials can be specifically tailored to obtain suitable characteristics for biomedical purposes such as implant devices and sutures. Commonly used synthetic biodegradable polymers are polyester based Poly(lactic acid) (PLA) and poly(glycolic acid) (PGA) (Lee, Cobain et al. 2007). However, these polymers have drawbacks in that their degradation products may produce high local acidity which may damage adjacent cells and thus become toxic to cells (Drury and Mooney 2003).

Biodegradable polymers can be specifically tailored to obtain suitable characteristics for biomedical purposes such as implant devices and sutures. Some of the commonly used biodegradable polymers are natural polysaccharides, or synthetic polymers like Poly(lactic acid) (PLA) and poly(glycolic acid) (PGA) (Hoffman 2002). Polysaccharides are of considerable interest due to their unique chemical and mechanical properties, biocompatibility and biological activities interacting via specific carbohydrate-protein interactions (Xiao, Liu et al. 2001; Lu, Zhang et al. 2004; Farris, Schaich et al. 2009). Their biodegradability is also predictable and controllable due to the presence of OH- groups at the backbone which will degrade via hydrolysis (Hoffman 2002; Zhang, Xie et al. 2005).

Degradation is deterioration of materials can be described by chemical and physical degradation (Kolybaba 2003). There are two types of degradation: chemical and physical degradation. Chemical degradation happens when the chemical structure of a material collapses and starts to disintegrate into smaller fractions via enzymatic cleavage or hydrolysation cleavage while physical degradation can occur through surface or bulk erosion (Kohn 2004). The degradation can also occur from the action of microorganisms such as

bacteria and fungi etc. (Kolybaba 2003). Biodegradation is an important factor for a polymer to be used in biomedical application, especially as drug delivery vehicles and implants, as the accumulation of the residues post degradation can cause undesired side effects. The degradation of synthetic polymers can be promoted by incorporation of biodegradable linkages such as natural polymers from polysaccharides and polypeptides. Polysaccharides such as cellulose, dextran, hyaluronic acid, chitosan and chitin have been employed for polymers due to their characteristics which are relatively low immunogenicity, ease of functionalization and degradation by enzymes present in the body (Mi, Shyu et al. 2003; Peattie, Nayate et al. 2004; Alonso-Sande, Teijeiro-Osorio et al. 2009). In the development of biodegradable hydrogels for wound healing, the choice of polymers and the type of polymerisation are very important to avoid cytotoxicity and immunogenicity effects when in contact with biological cells. There are four types of terms used to describe the disintegration of materials over time: biodegradation, bioerosion, bioabsorbtion, and bioresorption (Kohn 2004).

This chapter describes the development of biodegradable hydrogels that would be able to deliver KGM onto a wound site to help to improve healing progression without the need for frequent dressing changes. Previous chapters have shown that KGM's biological activities are very stimulatory to fibroblast proliferation and inhibitory to keratinocyte proliferation, which would benefit the healing process and at the same time possibly reduce the rate of contraction in wound healing.

KGM was successfully synthesized using cerium ammonium nitrate (Ce (IV)) via free radical polymerisation in aqueous solution. The use of Ce(IV) in polymerisation of polysaccharide is not new and has long been used to initiate graft polymerisation of numerous monomers onto assorted substrates, including grafting of synthetic polymer onto natural polysaccharide e.g polyacrylamide onto guar gum (Thimma, Reddy et al. 2003). Ce(IV) also does not possess

any cytotoxicity when adjacent to skin cells at low concentrations and is used extensively in burn treatments as an antiseptic (Ross, Phipps et al. 1993; Jakupec, Unfried et al. 2005).

The polymerisation of konjac glucomannan using Ce(IV) proceeds through chain transfer polymerisation, creating crosslinks among initiated sites on the glucomannan structure. This grafting has been shown to be dependent upon the concentration of the initiator and also the concentration of the substrate.

In order to obtain more stable and controlled degradation, the concentrations of KGM and Ce(IV) were increased in two sets of polymers with increasing concentrations of Ce(IV) (where the amount of KGM was kept constant) and increasing concentrations of KGM (where the amount of (Ce(IV)) was kept constant). The degradation and integrity of each polymer in water up to 96 hr was then observed and recorded. Later in this chapter, the effect of increasing concentrations of Ce(IV) and KGM in indirect and direct contact with skin cells after 1, 3 and 5 days were measured using the MTT assay, which was used to measure cell viability.

The characterizations of the crosslinked KGM were conducted using Differential Scanning Calorimetry (DSC) and Fourier Transform Infrared (FTIR) to measure the changes in KGM's conformation with increasing concentrations of Ce(IV) by studying the hydrogel's phase separation, T_g and formation of crosslinks. DSC measurements are effective measurements to study the strength and synergistic interaction of crosslinked KGM initiated by the ceric while FTIR provides information on the changes of chemical conformations in the crosslinked KGM by means of dipole interactions.

4.2 Results.

4.2.1 Synthesis and Characterizations of KGM hydrogel using Fourier Transform Infra red (FTIR).

Table 4.1 The chemical compositions of crosslinked KGM with increasing concentrations of Ce(IV) and KGM.

Hydrogel	KGM (%)	Ce(IV) (%)	P(NVP) (%)	PEGDA wt 2% HMPP
Crosslinked KGM (Increasing concentrations of Ce(IV))	1	0.001	-	-
	1	0.0015	-	-
	1	0.003	-	-
	1	0.006	-	-
Crosslinked KGM (Increasing concentrations of KGM)	0.5	0.001	-	-
	1	0.001	-	-
	1.25	0.001	-	-
	1.5	0.001	-	-

The biodegradable KGM hydrogels were successfully synthesised in aqueous solution at room temperature using Ce(IV) as initiator by either varying the concentration of KGM or the concentration of Ce(IV). All hydrogels were then characterized using FTIR and DSC and their biological effects on skin cells were investigated using the MTT assay.

Fourier Transform Infrared (FTIR) is a useful tool in the investigation of molecular structure of polymers by the measurement of the changes in the dipole moment of vibrating molecules when exposed to IR (Griffiths and De Haseth 2007). FTIR recorded the changes in the confirmation of chemical structures which are sensitive to environmental changes (Griffiths and De Haseth 2007). The most frequently used IR spectral region in carbohydrate analysis for glucose and mannose is the anomeric region at 950-700 cm^{-1} (Mathlouthi and Koenig 1986) where the α and β conformers of glucose, galactose and mannose can be distinguished using the 2α and 2β bands at 870-840 cm^{-1} and 890 cm^{-1} , respectively (Mathlouthi and Koenig 1986).

In this study, molecular analysis with FTIR technique with attenuated total reflectance (ATR) was used to detect structural features on crosslinked KGM. The objective in this study was to determine glucomannan conformation and spectral features in crosslinked KGM. The FTIR spectra of KGM and crosslinked KGM hydrogels with increasing concentrations of Ce(IV) is shown at Figure 4.2. All hydrogels exhibited qualitatively similar spectra as previously reported (Xiao, Gao et al. 2000; Yu, Huang et al. 2006; Chua, Chan et al. 2012) with broad bands stretching from 3000-3500 cm^{-1}, which was assigned to the OH group (Mathlouthi and Koenig 1986; Kačuráková, Capek et al. 2000; Xiao, Gao et al. 2000; Xiao, Liu et al. 2001; Li, Qi et al. 2009), peaks at 1150 cm^{-1} and 1030 cm^{-1} assigned for C-O-C stretching modes from ether groups in the pyranose ring (Chua, Chan et al. 2012) and peaks attributed to β-glucosidic and β-mannosidic linkages at 870 cm^{-1} and 800 cm^{-1} (Mathlouthi and Koenig 1986; Hua, Zhang et al. 2004; Widjanarko, Nugroho et al. 2011). The methyl group that attached to –OH group which peaked at 2922 cm^{-1} and the peaks at 1300-1000 cm^{-1} assigned to the stretching vibrations of –CH- and the peaks 1730 cm^{-1} assigned for C=O were also observed in all samples (Mathlouthi and Koenig 1986; Jacon, Rao et al. 1993; Xiao, Liu et al. 2001). The spectra in the range of 1700-700 cm^{-1} show major distinctions between the

crosslinked hydrogels with diminishing peaks observed with increasing concentrations of Ce(IV). The region of 1640cm^{-1} which is marked by blue lines in the Figure 4.2 show the existence of β-1,4 linked glucose in glucomannan (Widjanarko, Nugroho et al. 2011). (Figure 4.3). β C1-O-C4 stretching modes between 1200-900 cm^{-1} were observed at 1150 cm^{-1} and 1050 cm^{-1} in our hydrogels. The increasing concentration of Ce(IV), formed greater crosslinking in the glucomannan chain resulted in the absorption of OH^{-} peak in the region of 3700-3000 cm^{-1} and also the absorption of the acetyl band in the region 3000-2700 cm^{-1}. The result also suggests that increasing concentrations of Ce(IV) created strong intermolecular interaction which later supported the DSC results where increasing concentrations of Ce(IV) increased the thermal stability of the crosslinked KGM.
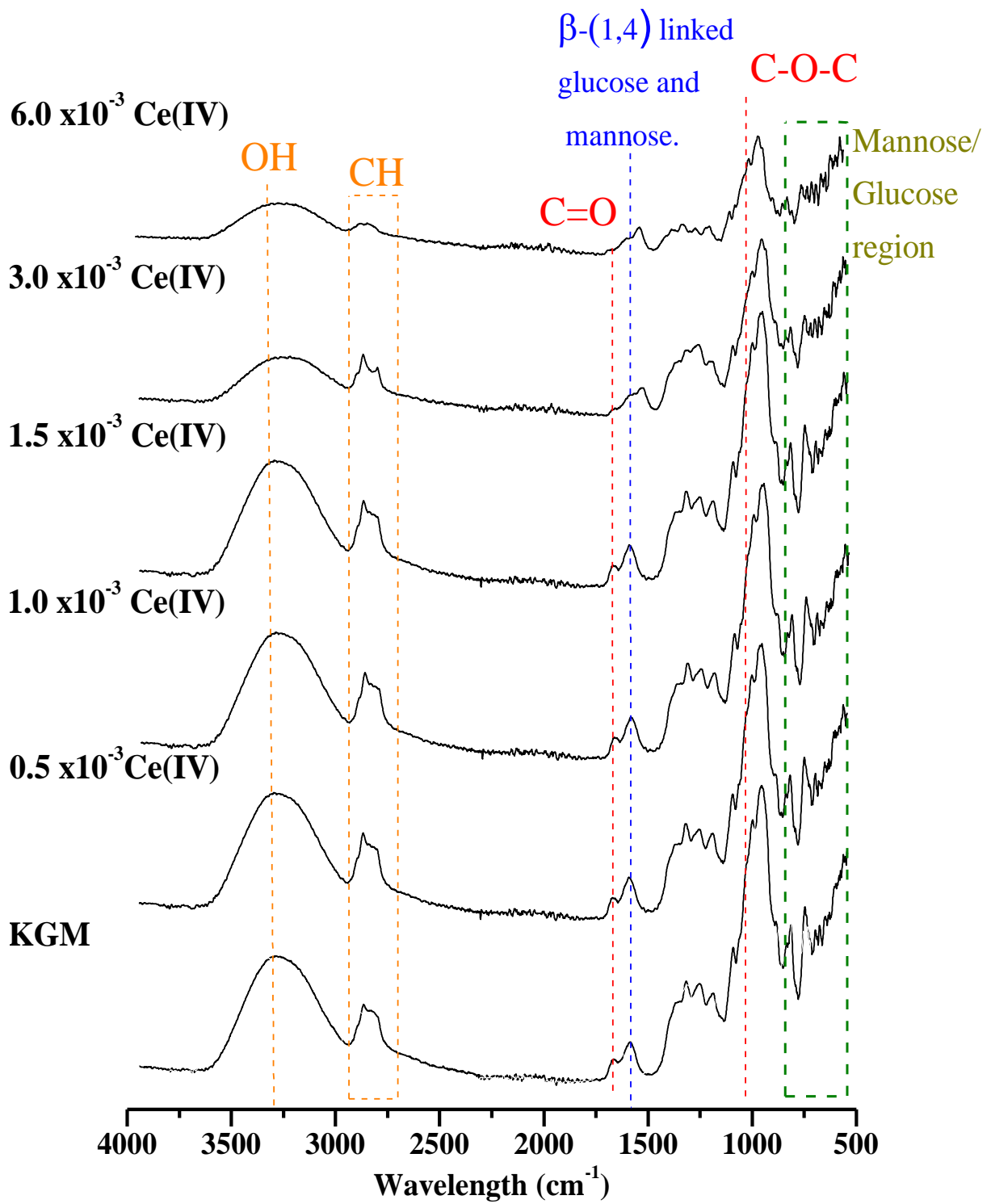
Figure 4.1 Comparison of FTIR spectra range from 4000-500 cm^{-1} of KGM hydrogels with increasing concentrations of Ce(IV).
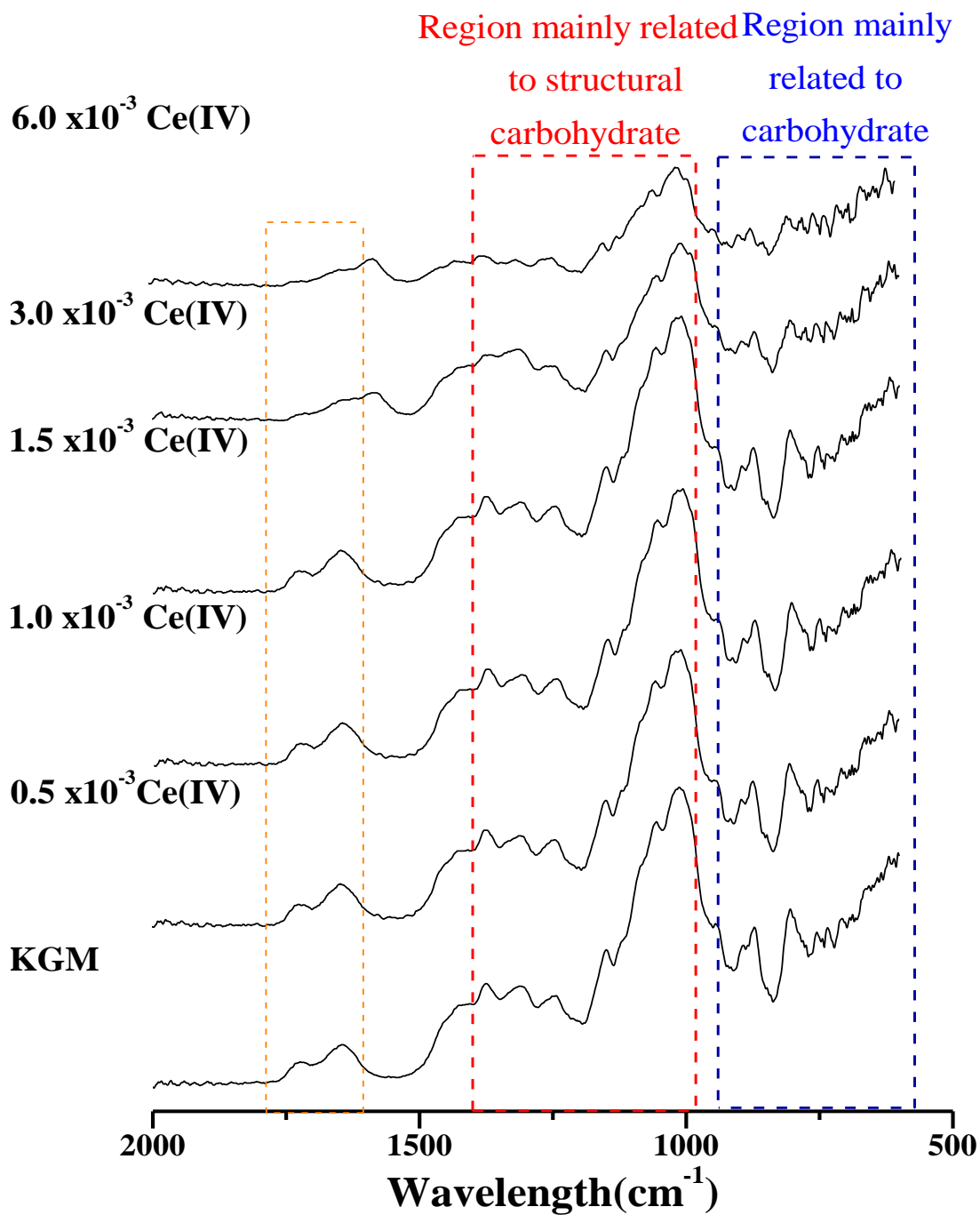
Figure 4.2 FTIR spectra range from 2000-500 cm^{-1} show differences in relative intensities of the bands, diminished peaks and shifting peaks on KGM hydrogels with increasing concentrations of Ce(IV).

Table 4.2 Summary of the details of the FTIR spectra of the crosslinked KGM hydrogels with increasing concentrations of Ce(IV).

Peak (cm^{-1})	Assignments	KGM	Reference
3397	-OH-	√	(Li, Qi et al. 2009; Xu, Luo et al. 2009; Widjanarko, Nugroho et al. 2011; Chua, Chan et al. 2012)
2953	-CH$_2$- in C-CH$_3$	√	(Xiao, Liu et al. 2001; Widjanarko, Nugroho et al. 2011; Chua, Chan et al. 2012)
1730	C=O	√	(Jacon, Rao et al. 1993; Xiao, Liu et al. 2001; Chen, Liu et al. 2005; Moshaverinia, Roohpour et al. 2009)
1640	β-1,4 linked glucose in glucomannan		(Černáa, Barros et al. 2003; Li, Qi et al. 2009; Xu, Luo et al. 2009; Widjanarko, Nugroho et al. 2011)
1372	-CH$_2$-	√	(Mathlouthi and Koenig 1986; Száraz and Forsling 2000; Pandey and Pitman 2003; Vaaler 2008; Widjanarko, Nugroho et al. 2011)
1375	-CH$_2$-	√	(Widjanarko, Nugroho et al. 2011; Chua, Chan et al. 2012)
1244	C-O-C stretch	√	(Černáa, Barros et al. 2003; Widjanarko, Nugroho et al. 2011)
1150	C-O-C	√	(Kačuráková, Capek et al. 2000; Kačurákováa and Wilson 2001; Widjanarko, Nugroho et al. 2011; Chua, Chan et al. 2012)
1050	C-O (on KGM)	√	(Xu, Luo et al. 2009)
941			(Kačuráková, Capek et al. 2000)
891	-CH- in glucose		(Kačurákováa and Wilson 2001)

872	-CH- in mannose	√	(Mathlouthi and Koenig 1986; Kačuráková, Capek et al. 2000; Hua, Zhang et al. 2004; Xu, Luo et al. 2009; Widjanarko, Nugroho et al. 2011; Chua, Chan et al. 2012)
808	-CH- in mannose	√	(Hua, Zhang et al. 2004; Xu, Luo et al. 2009; Widjanarko, Nugroho et al. 2011; Chua, Chan et al. 2012)
745	-CH- in mannose	√	(Higa, Rogero et al. 1999; Hua, Zhang et al. 2004; Widjanarko, Nugroho et al. 2011)

4.2.2 Characterization of crosslinked KGM hydrogels using Differential Scanning Calorimetry (DSC).

The thermal stability and miscibility of the crosslinked KGM with increasing concentrations of Ce(IV) were investigated by means of endothermic peaks in DSC thermograms. DSC is a thermoanalytical technique which is used to examine polymeric materials to determine the phase thermal transition of a polymer. The observed thermal transitions will be unique to different polymer compositions which can be utilized for comparison with other polymers. Although the thermal transition does not uniquely identify the chemical composition in the polymer, FTIR was used to complete the analysis of the synthesized polymers.

The DSC thermograms of the crosslinked KGM hydrogels with increasing concentrations of Ce(IV) are shown in Figure 4.3. All hydrogels were subjected to -60 to 360°C heating at 10.0^{o}C per min in nitrogen atmosphere. The KGM without Ce(IV) showed a sole endothermic curve stretching from 113 to 190°C with T_g at 126°C while the addition of 1×10^{-3}% (w/v) Ce(IV) gave a broader curve stretching between 80 and 190°C, with T_g at 118°C. The T_g tend to shift to a 20-30°C higher temperature with increasing Ce(IV) concentrations. This suggested the existence of an intermolecular hydrogen bonding effect in the linear KGM. The endothermic peak area of the hydrogels with $0-1 \times 10^{-3}$% (w/v) Ce(IV) increased

gradually from 6307 to 7987 mJ, although the peak temperature was slightly dropped from 127 to 118°C. Then the peak temperature was increased to 145°C with the 1.5x10^{-3} % (w/v) Ce(IV). However, the endothermic peak area for this hydrogel was smaller than the hydrogel with 1x10^{-3} % (w/v) Ce(IV) hydrogel with 3466 mJ. The hydrogels with 3.0-6x10^{-3} % (w/v) Ce(IV) had both endothermic (T$_g$) and exothermic peaks in their thermograms. The endothermic peaks (T$_g$) for both hydrogels were 165 and 176°C, respectively while the exothermic peaks were 185 and 217°C, respectively. The endothermic areas for both hydrogels were 14083 and 11958 mJ, respectively, which were almost three times larger than the hydrogel with 1.5x10^{-3} % (w/v) Ce(IV). The increase of the area of endothermic peaks in the hydrogels with increasing concentrations of Ce(IV) may suggest the increase formation of crosslinks. The presence of exothermic peaks in both hydrogels with 3.0-6x10^{-3} % (w/v) Ce(IV) may due to the greater amount crosslinks inside the network which required enormous amount of heat in the rearrangement and reorganization of the molecules in the polymeric network. This could also due to the presence of high concentrations of Ce(IV) that formed radicals in the polymer which was not removed from the hydrogel. The area of exothermic peak in the hydrogel with 6x10^{-3} % (w/v) Ce(IV) were larger than the hydrogel with 3x10^{-3} % (w/v) Ce(IV) with 4572 and 2887 mJ, respectively. The summary of the thermograms of the hydrogels with increasing concentrations of Ce(IV) is shown in Table 4.3.

	Concentration of Ce(IV)	Onset (^{o}C)	Peak Temperature (^{o}C)	Area (mJ)
1	0	113	127	6302
2	1.0x10^{-3}	81	118	7987
3	1.5x10^{-3}	107	145	3466
4	3.0x10^{-3}	139	165	14083
		183	185	2887
5	6.0x10^{-3}	168	176	11958
		209	217	4572

Table 4.3 Summary of the details of the DSC thermograms of the crosslinked KGM hydrogels with increasing concentrations of Ce(IV).
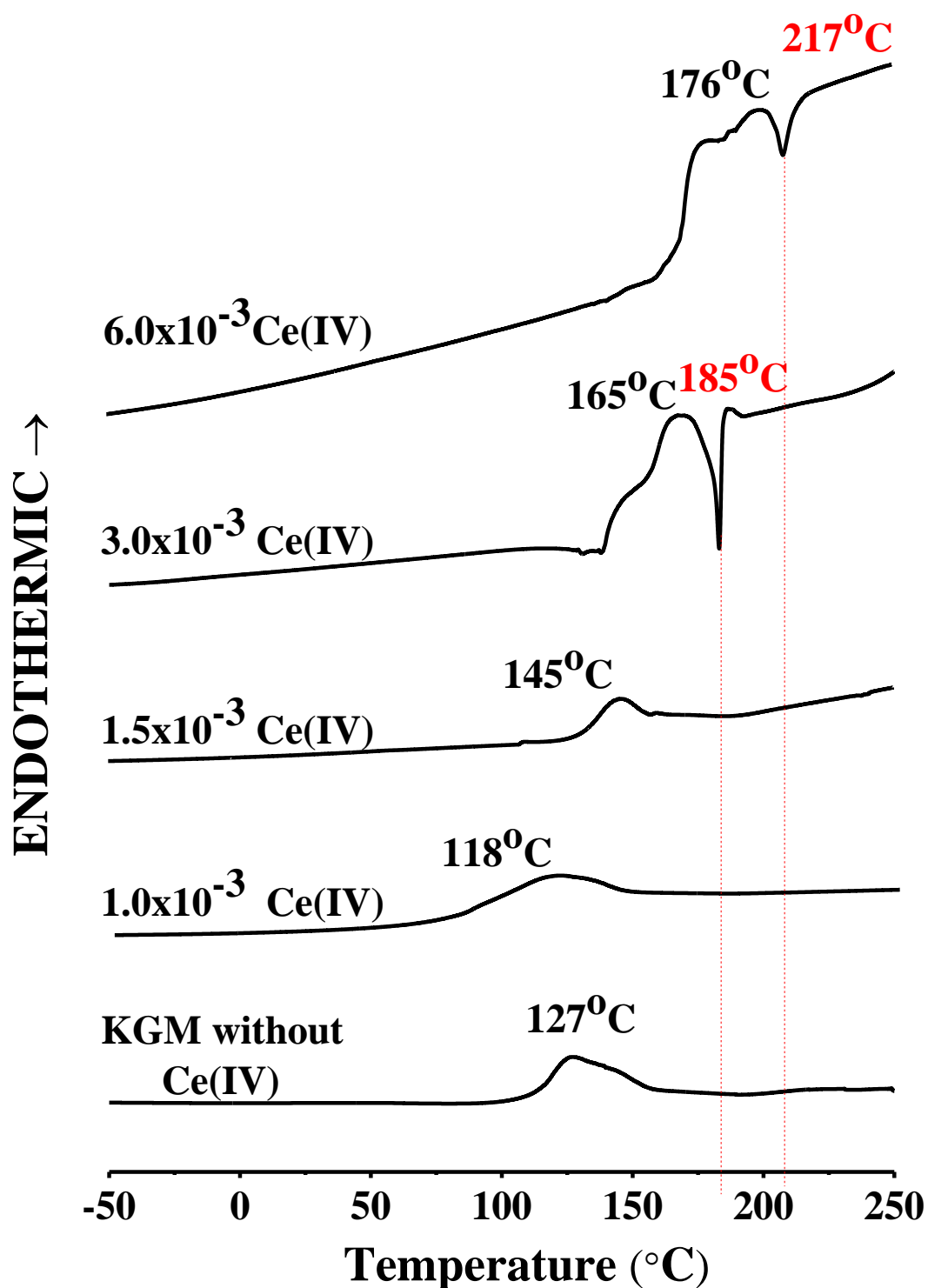

Figure 4.3 Comparisons of DSC thermograms of the crosslinked KGM hydrogels with increasing concentrations of Ce(IV) subjected to heating from -60 to 260°C at 10°C per min in nitrogen atmosphere. The endothermic peaks for the hydrogels increased with the

increasing Ce(IV) concentrations. Label temperatures for the hydrogel's endothermic peaks are in black and exothermic peaks are in red.

4.2.3 Cytocompatibility of the crosslinked KGM hydrogel with increasing concentrations of Ce(IV).

4.2.3.1 The effect of hydrogels in indirect contact with keratinocytes and fibroblasts

Biocompatibility of KGM hydrogels with increasing concentrations of Ce(IV) was examined by placing the hydrogels in indirect contact with fibroblasts and keratinocytes, then cell proliferation was measured after 3 days using MTT assay (Figure 4.4 A and B). The results show that indirect contact of the KGM hydrogels with the cells had no effect on the proliferation of both keratinocytes or fibroblasts.

4.2.3.2 The effect of hydrogels in direct contact with keratinocytes and fibroblasts

Investigation of the cytocompatibility of KGM hydrogels with increasing concentrations of Ce(IV) was conducted in direct contact with keratinocytes and fibroblasts where the cell proliferation was measured using MTT assay after 1, 3 and 5 days.

The result in Figure 4.5 show the effect of the KGM hydrogels with increasing concentration of Ce(IV) in direct contact with keratinocytes and fibroblasts (A and B, respectively). All hydrogels were very inhibitory to keratinocyte viability but selectively inhibited fibroblasts viability in a concentration dependent manner. Only the concentration of $1 \times 10^{-3}\%$ (w/v) Ce(IV) significantly stimulated fibroblast viability. The Live/Dead staining micrographs of fibroblasts and keratinocytes are shown in Figure 4.6 and 4.7, respectively. Figure 4.6 shows the absence of dead cells in the culture of fibroblasts when the hydrogels were placed in

direct contact with the cells. The decrease in the number of fibroblasts with increasing concentrations of Ce(IV) was also observed. The low number of fibroblasts was consistent with the MTT assay result shown in Figure 4.5A. On the contrary, Figure 4.7 shows the presence of dead cells and reduced number of keratinocytes in the culture with increasing concentrations of Ce(IV). The observation was consistent with the MTT result shown in Figure 4.5B

4.2.4 The effect of increasing concentrations of KGM in the crosslinked hydrogels on fibroblasts and keratinocytes.

Investigations on the effects of KGM hydrogels on fibroblast and keratinocyte cytocompatibility and bioactivity were conducted by placing cells in direct contact with the hydrogel with increasing concentrations KGM. 1×10^{-3}% (w/v) Ce(IV) was used in this formulation. Studies were conducted by placing the hydrogels directly on the cultures of fibroblasts and keratinocytes and then, cell viability was measured after 1, 3 and 5 days using the MTT assay Figure 4.8 (A and B). The concentrations of KGM at 0.5-1.25% (w/v) significantly stimulated fibroblast viability, while 1.5% (w/v) KGM did not. Although the effect was shown to be dependent on the concentration of KGM, the inability of 1.5% (w/v) KGM to stimulate fibroblast viability was perhaps related to the changes in physico-chemistry of the hydrogel from rapid absorption of the medium inside the culture wells.

Hydrogels with increasing concentrations of KGM in direct contact with keratinocytes significantly inhibited cell proliferation after 1 to 5 days (Figure 4.8B) which was also similar to the result in Figure 4.5B.

A)

B)

Figure 4.4 Indirect contact with crosslinked KGM hydrogel with increasing concentration of Ce(IV) with 1% KGM (w/v) with (A) fibroblasts and (B) keratinocytes measured after 3 days by MTT assay. 1 mL of 2×10^4 fibroblasts were cultured in 10% DMEM or 1 mL of 2×10^4 keratinocytes co-cultured with 2×10^4 i3T3 in 10% Greens' in 12 well plate for overnight. Then, 0.79 cm^2 hydrogel was put in direct contact with the cells, respectively. Results shown are means ± SD, (n=3). ***p<0.001 highly significant, **p<0.01 very significant and *p<0.05 significant compared to control.

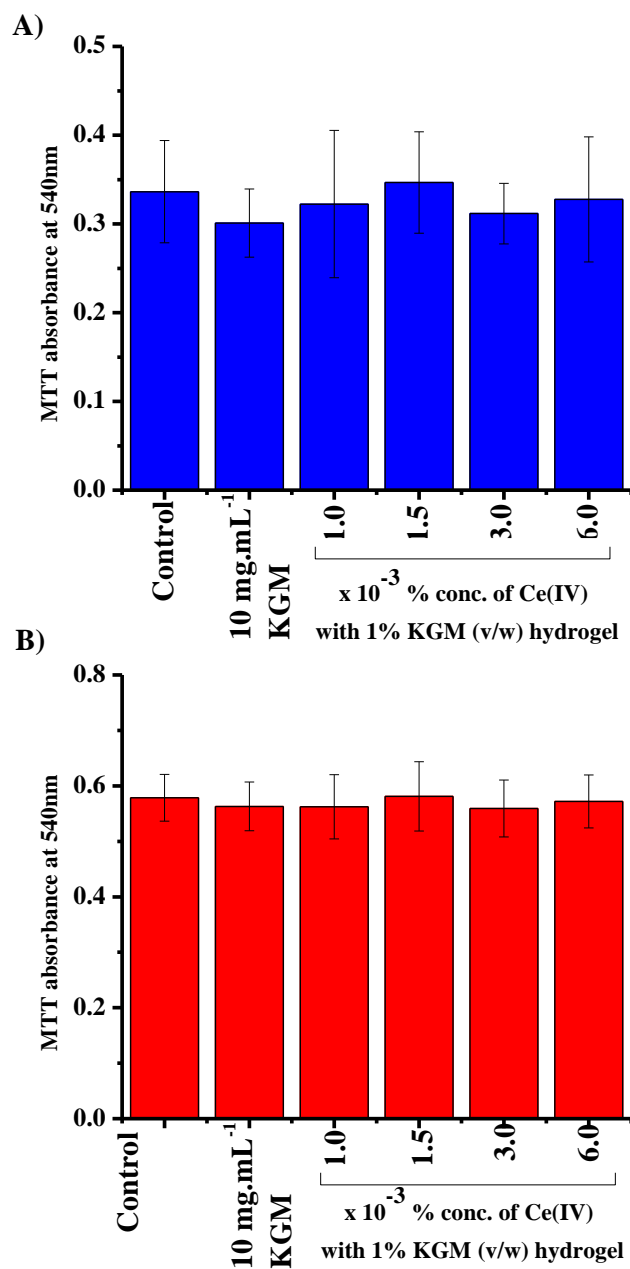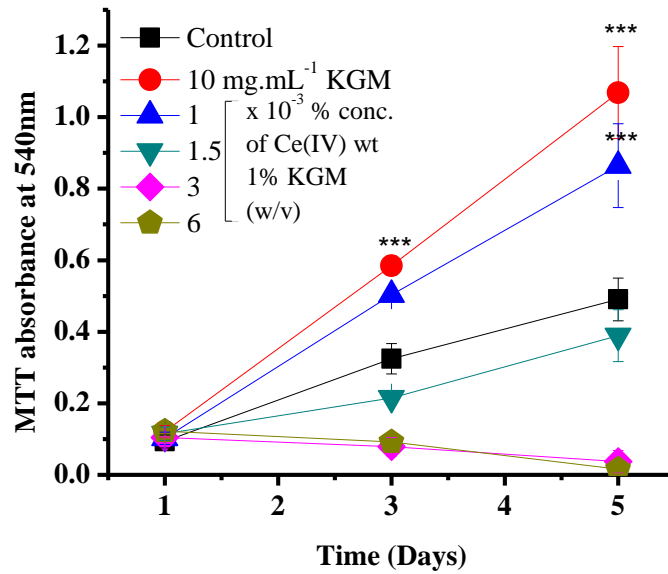**Figure 4.5** The effect of direct contact with KGM hydrogels with increasing concentration of Ce(IV) with 1% KGM (w/v) hydrogels with (A) fibroblasts and (B) keratinocytes measured after 1, 3 and 5 days using MTT assay. 1 mL of 2×10^4 fibroblasts were cultured in 10% DMEM or 1 mL of 2×10^4 keratinocytes co-cultured with 2×10^4 i3T3 in 10% Greens' in 12 well plate for overnight. Then, 0.79 cm^2 hydrogel was put in direct contact with the cells, respectively. Results shown are means $\pm$ SD, (n=3). ***p<0.001 highly significant, **p<0.01 very significant and *p<0.05 significant compared to control.
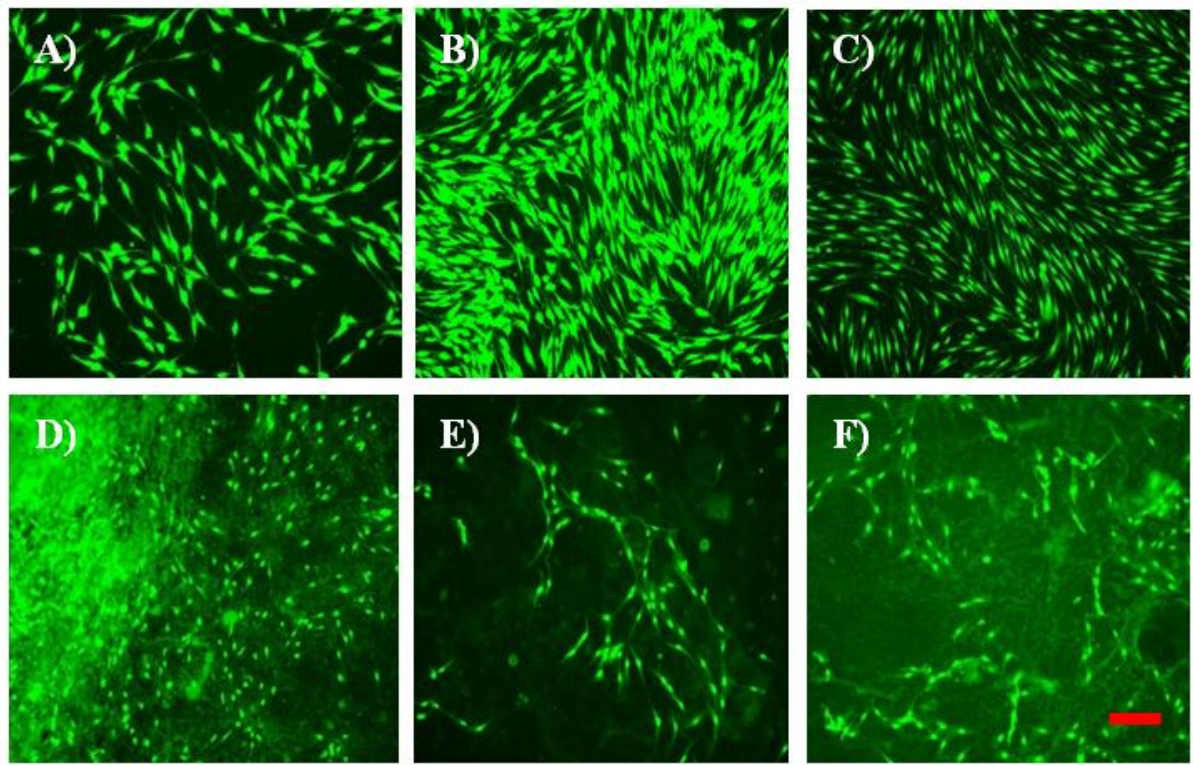
Figure 4.6 Live and dead stained fibroblasts with Syto9 and PI cultured in direct contact with KGM hydrogel observed after 5 days of culture A) control, B) KGM , C) 1×10^{-3} D) 1.5×10^{-3}, E) 3×10^{-3} and F) 6×10^{-3} % (w/v) of Ce (IV). 1 mL of 2×10^{4} cells were cultured in 10% DMEM in 12 well plate. (Scale bar: 100 μm).
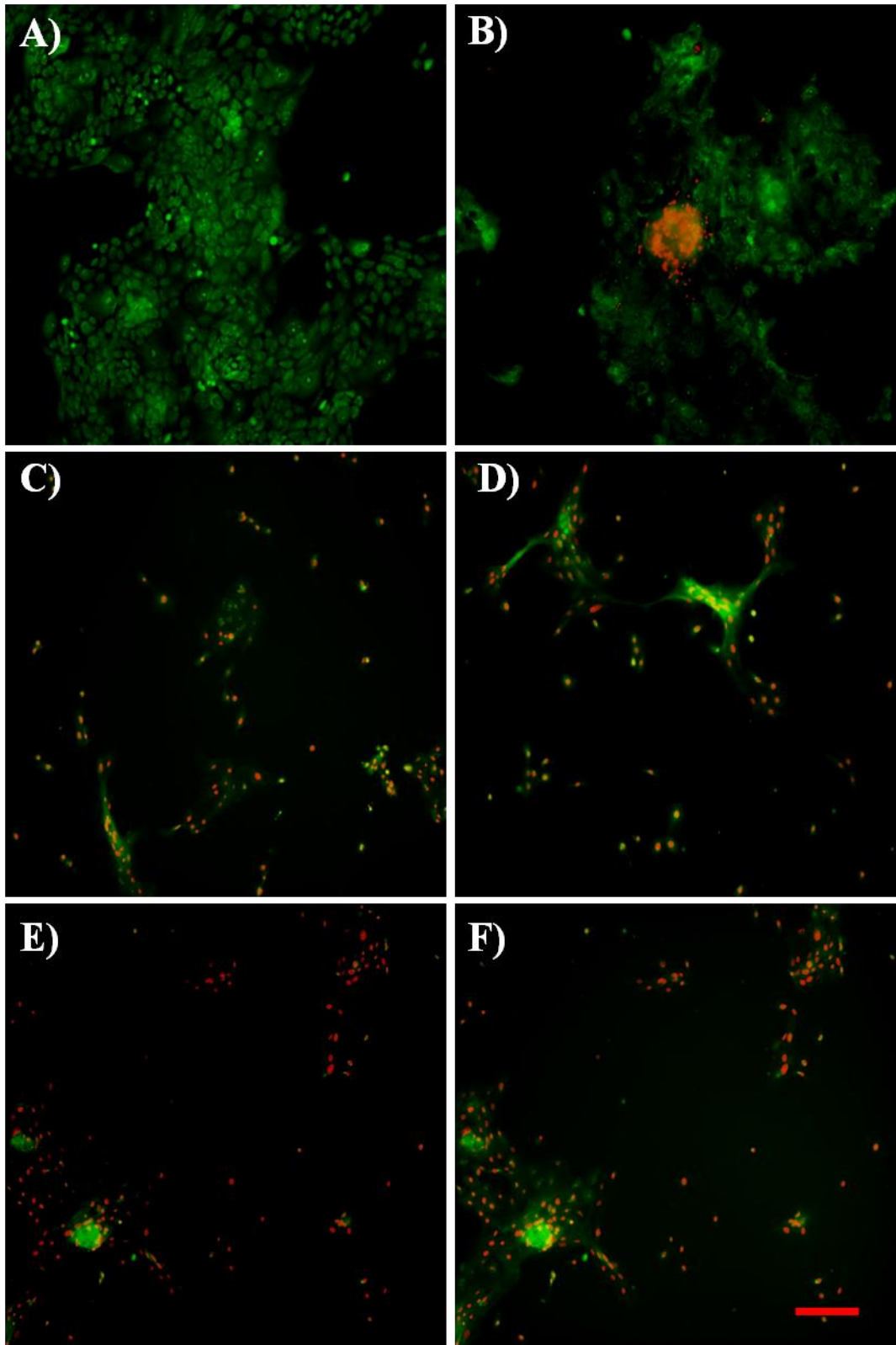
Figure 4.7 Live and dead stained keratinocytes with (Syto9 and PI) cultured in direct contact with KGM hydrogels observed after 3 days of culture (A) control, (B) KGM, (C) $1\text{x}10^{-3}$ (D) $1.5 \text{ x}10^{-3}$, (E) $3\text{x}10^{-3}$ and (F) $6\text{x}10^{-3}$ % (w/v) of Ce(IV). 1 mL of $2\text{x}10^{4}$ keratinocytes co-cultured with $2\text{x}10^{4}$ i3T3 in 10% Green's in 12 well plate. (Scale bar: 100

μm).
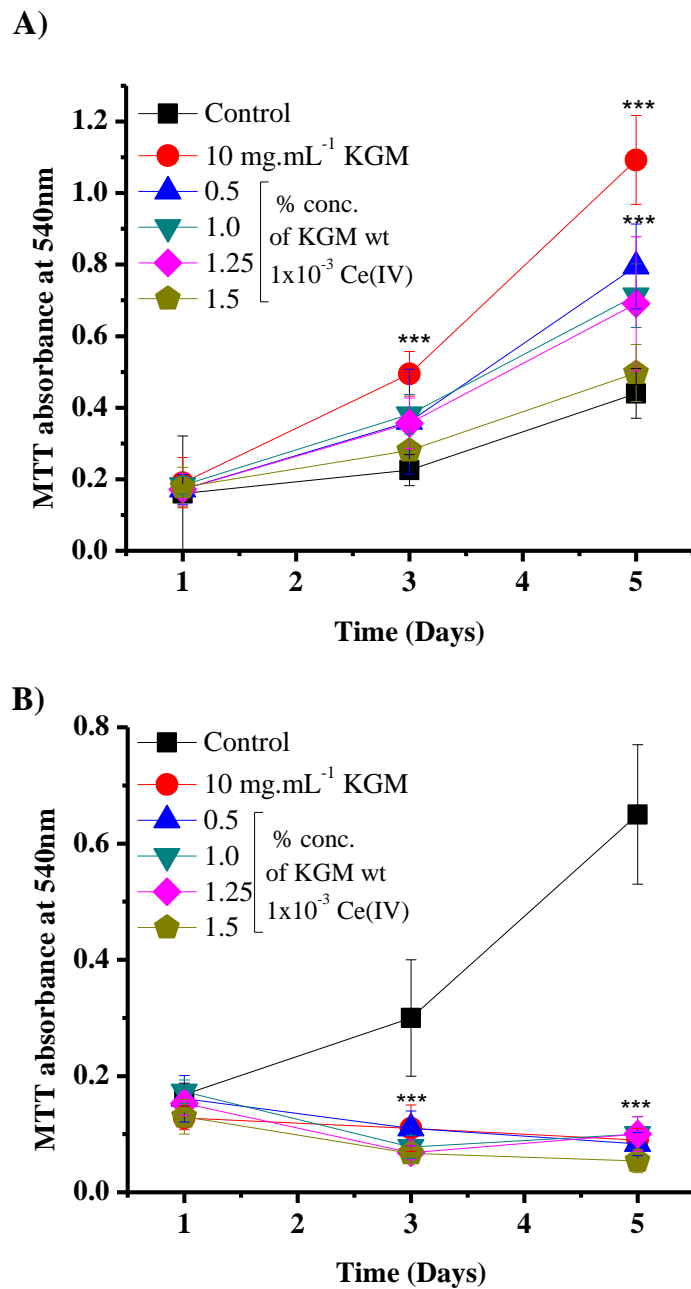
Figure 4.8 The effect of KGM hydrogels with increasing concentrations of KGM with 1×10^{-3} % (w/v) Ce(IV) in direct contact with A) fibroblasts and B) keratinocytes measured after 1, 3 and 5 days using MTT assay. 1 mL of 2×10^4 fibroblasts were cultured in 10% DMEM or 1 mL of 2×10^4 keratinocytes co-cultured with 2×10^4 i3T3 in 10% Greens' in 12 well plate for overnight. Then, 0.79 cm^2 hydrogel was put in direct contact with the cells, respectively. Results shown are means ± SD, (n=2). ***p<0.001 highly significant, **p<0.01

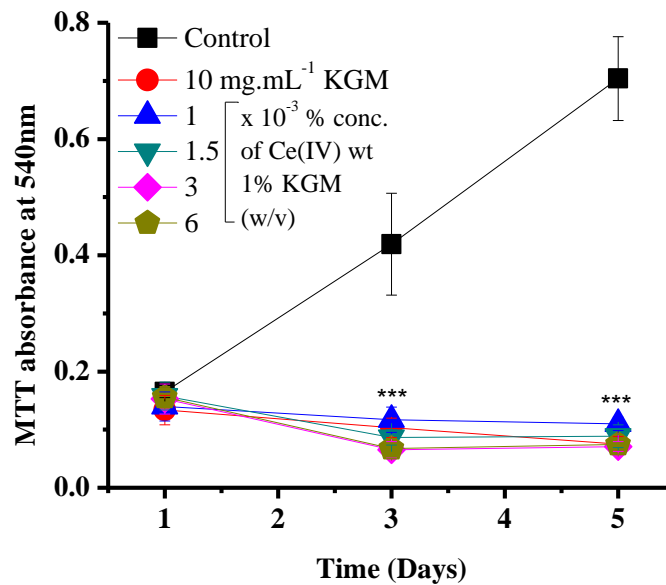very significant and *p<0.05 significant compared to control.

4.2.5 The degradation of KGM hydrogels with increasing concentrations of Ce(IV) and KGM.

4.2.5.1 The degradation of crosslinked KGM hydrogels with increasing concentrations of Ce(IV).

The physical integrity of KGM hydrogels with increasing concentrations of Ce(IV) was observed over 0-96 hr (Figure 4.9). The hydrogels were opaque and very brittle, and those with higher concentrations of Ce(IV) appeared slightly yellowish due to the presence of ceric iron compared to lower Ce(IV) concentrated hydrogels. It was observed that 1% (w/v) KGM hydrogels with lower concentrations of Ce(IV) $(1-1.5 \times 10^{-3}\%$ (w/v)) degraded faster than those with higher concentrations $(3-6 \times 10^{-3}\%$ (w/v)) Ce(IV) hydrogels which took more than 48 hr to begin degrading. At 96 hr, the hydrogels with $(1-1.5 \times 10^{-3}\%$ (w/v)) Ce(IV) completely dissolved in water but the hydrogels with $(3-6 \times 10^{-3}\%$ (w/v)) Ce(IV) appeared very soft and fragile. The observations on the hydrogel's physical integrities are summarized in Table 4.3.

4.2.5.2 The degradation of crosslinked KGM hydrogels with increasing concentrations of KGM.

The degradation of crosslinked KGM hydrogels with increasing concentration of KGM was then observed in aqueous solution after 0-96 hr (Figure 4.10). It was observed that the hydrogels with higher concentrations of KGM (1.25-1.5% (w/v)) started to break up faster compared to hydrogels with lower concentration (0.5-1% (w/v)), suggesting that hydrogels with higher concentrations of KGM, hence with greater amount of OH groups have a greater capacity to absorb more water and higher degree of hydrolysis. In this case, the hydrogel with

higher concentration of KGM showed faster disintegration from the inside (bulk degradation). This involves dissolution and degradation of surface layers and also involve with the leaching of unbound or loosely bound components or an uptake of fluids into the hydrogel. The observations on the integrity of the hydrogels are summarized in Table 4.4.

Table 4.3 Qualitative observations of the degradation of crosslinked KGM hydrogels with increasing concentrations of Ce(IV) in aqueous solution after 24, 48 and 96 hr in 12 well plates.

% Concentration of Ce (x 10^{-3}) (w/v)	Time (hr)				
	0	12	24	48	96
1	Solid	Solid	Start to break	60-70% dissolved	Dissolved
1.5	Solid	Solid	Start to break	60-70% dissolved	Dissolved
3	Solid	Solid	Solid	Start to break	Start to break
6	Solid	Solid	Solid	Solid	Start to break

Table 4.4 Qualitative observations of the degradation of crosslinked KGM hydrogels with increasing concentrations of KGM in aqueous solution after 24, 48 and 96 hr in 12 well plates.

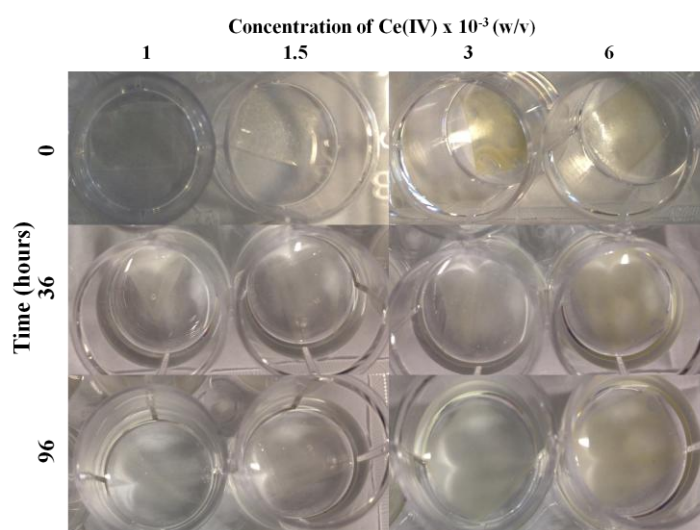| % Concentration of KGM	Time (hr)				
	0	12	24	48	96
0.5	Solid	Solid	Start to break	60-70% dissolved	Dissolved
1	Solid	Solid	Start to break	60-70% dissolved	Dissolved
1.25	Solid	Start to break	Dissolved	Dissolved	Dissolved
1.5	Solid	Start to break	Dissolved	Dissolved	Dissolved

Figure 4.9　　Images of the degradation of KGM hydrogels with increasing concentrations of Ce(IV) in aqueous solution (0 to 96 hr).
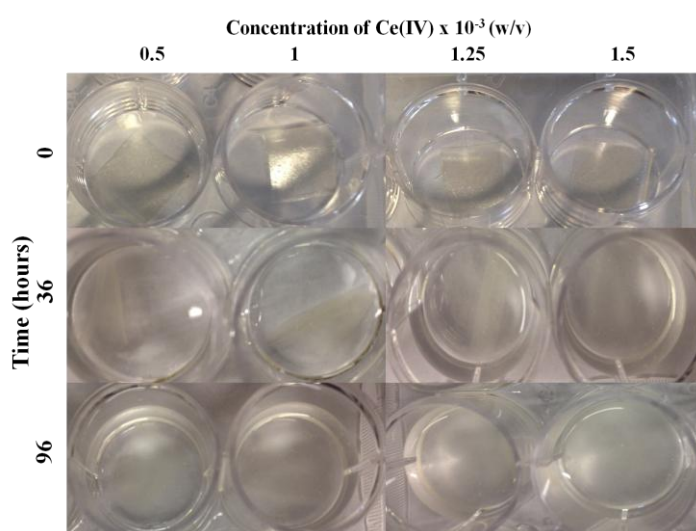

Figure 4.10　　Images of the breakdown of KGM hydrogels with increasing concentrations of KGM in aqueous solution (0 to 96 hr).

4.3 Discussion.

Biodegradable KGM hydrogels were successfully synthesized in aqueous conditions using Ce(IV) and KGM at various concentrations. Ce(IV) was used to initiate the hydrogen on the alpha position of hydroxyl group on KGM to form crosslinks and then the concentration of the initiator was increased to create more crosslinking that would improve the hydrogel's mechanical and physical properties by strengthening the hydrogel. Hydrogels with higher concentrations of Ce(IV) were able to sustain their shape for more than 96 hr compared to other hydrogels with lower concentrations. For further experiments, 1×10^{-3}% (w/v) Ce(IV) was chosen in the formulation of hydrogels with increasing concentrations of KGM. The hydrogels with higher KGM concentrations (1.25-1.5% (w/v)) degraded faster compared to those with lower concentrations of KGM, indicating that higher concentrations of KGM with more hydroxyl groups were able to absorb more water inside the hydrogel, which then broke the bulk formation from the inside from hydrolysis.

Biocompatibility is an essential issue for biomaterials. It is important to ensure that the hydrogels will not provoke any inflammatory response while their degradation products must be safe to cells. Initially, the effect of hydrogels in indirect contact with skin cells were examined in order to investigate any release of potential toxic products that might be harmful to cells. Indirect contact studies showed that increasing concentrations of Ce(IV) and KGM in crosslinked hydrogels did not stimulate or adversely inhibit the viability of fibroblasts and keratinocytes after 3 days.

The direct contact study of hydrogels with increasing concentrations of Ce(IV) with skin cells showed that all hydrogels inhibited keratinocytes whereas only those with concentrations of $3 \text{-} 6 \times 10^{-3}$% (w/v) Ce(IV) were inhibitory to fibroblasts (Figure 4.4). There are two reasons that may contribute to the inhibition of keratinocyte proliferation, i) the expansion and the

breaking of the hydrogel that exposed a larger area of KGM onto the cell surface and ii) the presence of Ce(IV) in the hydrogel. The crosslinked KGM hydrogel with $1x10^{-3}$% (w/v) Ce(IV) stimulated fibroblast viability after 3 and 5 days almost as equivalent to 10 mg.mL^{-1} KGM. The Ce(IV) concentration was then used in the formulation of crosslinked hydrogel with increasing concentrations of KGM.

Next, the effect of hydrogels with increasing concentrations of KGM in direct contact with skin cells showed that hydrogels with 0.5-1.25% (w/v) KGM stimulated fibroblast viability while 1.5% (w/v) KGM did not. On the other hand, all hydrogels with 0.5-1.5% (w/v) KGM inhibited keratinocyte viability which was consistent with KGM's effects on keratinocyte viability (Shahbuddin, Shahbuddin et al. 2013). The inability of crosslinked hydrogels with 1.5% (w/v) KGM to stimulate fibroblast viability may be attributed to the alteration in KGM hydrogel's physico-chemistry from rapid absorption of the medium in the culture well that possibly affects the interaction of cells with materials. From these results, it was observed that 1% (w/v) KGM with $1x10^{-3}$% (w/v) Ce(IV) achieved optimum conditions to stimulate fibroblast proliferation compared to other formulations.

The next part in this chapter discusses the characterization of the crosslinked hydrogels with increasing concentrations of Ce(IV) using DSC and FTIR. The DSC thermograms of crosslinked KGM with increasing concentration of Ce(IV) show the trend of increasing of temperature of the endothermic peaks from 80 to 217°C and the increase of the endothermal and exothermal energies (Figure 4.3). The hydrogels with $3x10^{-3}$% and $6x10^{-3}$% (w/v) Ce(IV) had two distinct peaks of endo and exothermic, which were not observed in the hydrogels with lower Ce(IV) concentrations. The exothermic peaks were due to the increase in the crosslinking in the hydrogels which absorbed more energy in order to immobilize and break KGM polymeric chains. It also presumed that unremoved high concentrations of Ce(IV) in the hydrogels contributed to the factor.

The FTIR spectra of crosslinked KGM hydrogels with increasing concentrations of Ce(IV) showed the presence of β-1,4 linked glucosidic and β-1,4 linked mannosidic linkages at 1027-1244 cm^{-1} (Figure 4.4) which were seen between 1200-900 cm^{-1} in xylans, chitin, carrageenan and cellulose (Černáa, Barros et al. 2003). The spectra in the region 1200-700 cm^{-1} also give information about the conformational changes and structures between the hydrogels whereas diminishing spectra bands and differences in relative intensities of the bands at 1700-1500 cm^{-1}, 1300-1100 cm^{-1} and 900-700 cm^{-1} were likely due to significant steric reaarangement and interactions in C-OH due to crosslinking (Nikonenko, Buslov et al. 2005).

4.4 Conclusions.

In conclusion, biodegradable, crosslinked KGM hydrogels were successfully synthesized in aqueous medium using Ce(IV) as an initiator and at room temperature. The synthesis and characterization of the hydrogels with increasing concentrations of KGM or Ce(IV) were defined. The results showed that although increasing concentrations of Ce(IV) were able to sustain the hydrogel's physical integrity for more than 96 hr, and very inhibitory to both skin cells. The exact mechanism of the hydrogel's biological activities on skin cells is unknown, but is likely to be related to the effect of native KGM (*A. konjac* Koch) as mentioned in the previous chapter. The biodegradibilityof the hydrogels and their ability to stimulate fibroblast viability are very appealing for applications in wound healing.

Chapter 5. Synthesis and preparation of KGM and poly(N-vinyl pyrrolidinone) bipolymer semi interpenetrating network (IPN) and graft-conetwork.

5.1 Introduction.

The aim of the study was to develop a non-biodegradable interpenetrating network (IPN) and graft-conetwork of KGM for the treatment of cutaneous wounds as crosslinked KGM was only able to maintain for 2-4 days before fully disintegrated. The ability to swell in a controlled swelling ability is important in the removal of exudate while simultaneously keeping moist environment to the wound site (Queen, Evans et al. 1987). Copolymerisation of KGM with either synthetic or natural polymers not only help to sustain the hydrogel from breaking apart too easily or rapidly, but also aiding to create a suitable microenvironment for the wound to heal quickly (Shevchenko, James et al. 2010). A stable material will also ease the handling by the practitioners and also improve material's flexibility to adhere onto the wound site without breaking (Shevchenko, James et al. 2010).

The copolymerisation of KGM with other synthetic or natural polymers is a challenge due to KGM's rapid gelation in water and insolubility in other solvents due to the presence of acetyl groups at every 13 or 19 molecular units on the KGM backbone (Maeda, Shimahara et al. 1980). Improvements of KGM solubility by chemical and physical modification such as methylation, enzymatic hydrolysation and irradiation are likely to affect KGM's molecular weight and biological activity as was reported in Chapter 3 which may not be suitable for the purpose in the development of biologically active hydrogel for wound healing.

In this chapter, methods of the development non-biodegradable interpenetrating network (IPN) and graft-conetwork of KGM were reported. Two sets of hydrogels, semi-IPN and graft-conetwork were made of copolymerisation of poly(N-vinyl pyrrolidinone) (P(NVP))

and Poly(ethyle glycol diacrylate) (PEGDA) with KGM using HMPP (and Ce(IV)) as initiator and cured in an UV oven. To the best of my knowledge, this is the first study ever conducted using these chemical formulations.

IPN is a blend of two or more polymers by physical entanglement where each individual network may be formed simultaneously or sequentially. (Peppas, Bures et al. 2000; Farris, Schaich et al. 2009). Semi-IPN are formed when only one polymer in the system is crosslinked while full IPN are formed when crosslinking occurs between two or more interpenetrating polymer networks (Hoffman 2002). Graft polymer is a combination of two different set of system that is either crosslinked hydrophilic polymers or hydrophobic surfaces with a second hydrophilic polymer covalently attached (Rimmer 2011) while conetwork is composed of segments that are covalently attached to each other where the most important key aspect is the co-continuous nature of the morphology (Rimmer 2011). The scheme in Figure 1.21-1.22 (in Chapter 1) illustrate the formation of semi-IPN and graft-conetwork prepared via UV photocrosslinking under rapid free radical polymerisation.

In this study, P(NVP) was selected due to its homopolymer solubility in water and also its wide application in wound dressings and biomedical applications (Razzak, Darwis et al. 2001; Moshaverinia, Roohpour et al. 2009). P(NVP) can be conjugated to a number of drugs and polymers for pharmaceutical application (Rimmer 2011) and previous work from Rimmer group demonstrated the biocompatibility of P(NVP) copolymerized with EDGMA and DEGBAC in both direct and indirect contact with fibroblasts (Smith, Rimmer et al. 2006). This study also showed that while fibroblasts did not attach to this hydrogel, the presence of P(NVP) adjacent to the cells significantly increased fibroblast viability (Smith, Rimmer et al. 2006).

Polyethylene glycol diacrylate (PEGDA) is a Poly(ethylene glycol) (PEG) based polymer and

have been used in myriad biological applications such as scaffold in tissue engineering, medical devices and wound dressings (Higa, Rogero et al. 1999; Imaz and Forcada 2008). It is favorable due to its negligible toxicity and limited immunological reaction (Bae, Gemeinhart et al. 2010).

The incorporation of, P(NVP) and PEGDA with KGM was selected to further enhance the crosslinked KGM hydrogels physical stability by photopolymerisation which would be useful for wound healing application (Drury and Mooney 2003; Lee, Cobain et al. 2007). In considering hydrogels as wound dressings, it is necessary to investigate the hydrogels in indirect and in direct contact with skin cells. The cells are not required to grow on the hydrogels rather than having the cells in close proximity with the hydrogels. The most important criteria for wound dressings would be biocompatibility and do not illicit serious immunological response when placed on the defect site of human's body. The use of P(NVP) as vitreous substitute had shown that the materials were injectable, had optimal optical properties and did not stimulate excessive immune response (Vijayasekaran, Chirila et al. 1996). *In vitro* cytotoxicity test showed that P(NVP) based hydrogels crosslinked with diethylene glycol dimethacrylate (DEGDMA) significantly increase fibroblast viability in both, presence and absence of serum conditions (Hong, Chirila et al. 1997), which supported the finding by Smith et. al (2007). The same result also was observed in P(NVP) based chitosan who showed dual properties of supporting epithelial cell (SiHa) growth and selectively inhibited fibroblast (NIH3T3) growth and attachment on to the hydrogel (Risbud, Hardikar et al. 2000).

Further in this chapter, characterizations of different chemical and physical properties of the synthesized semi-IPN and graft-conetwork hydrogels were conducted, and the relationship between the changes in the hydrogel's chemical compositions, physical properties (EWC) and free water content with its biological activities on skin cells were also investigated. The

water loving property is an important feature for hydrogels, especially for the treatment of wound (Winter 1962). Hydrogel's hydrophilicity is defined by equilibrium water content (EWC) which is the measurement of the amount of water that a hydrogel able to absorb. Although, there are several disadvantages of high hydrophilicity such as poor mechanical property, and inhibition of cell attachment and biological activities (Jhon and Andrade 1973; Blokzijl and Engberts 1993; Cauich-Rodriguez, Deb et al. 1996), it is important to note that water plays significant role in cellular interactions and promotion of wound healing (Jhon and Andrade 1973).

The interaction of water with carbohydrate containing hydrogel plays essential role in both protein-protein and protein-carbohydrate interactions by mediation of hydrogen-bonding interactions between protein and carbohydrate. (Bundle and Young 1992; Holgersson, Gustafsson et al. 2005; Snyder, Mecinović et al. 2011). Water is the main component of polysaccharide based hydrogels with more than 90% of their weight when in their swollen state and the involvement of water in the binding interactions of protein and polysaccharides is an important part in these key interactions (Lemieux 1993).

There are three types of water inside a hydrogel matrix: i) free water, the water in the outermost layer which can be easily removed under temperate conditions as it does not take part in hydrogen bonds with polymer molecules, ii) bound water, which is bound directly to the polymer chains via hydrophilic groups or hydrogen bonds, becoming an integral to the hydrogel structure, and iii) semi bound water, which is intermediate between bound and free water (Kim, Lee et al. 2004) . The influence of water in cellular and protein interaction by carbohydrate moieties can be driven either by hydrophobic stacking between the carbohydrate and protein (Bundle and Young 1992) or the degree of swelling capacity (Peppas, Bures et al. 2000).

The structure and properties of the hydrogels were studied in detail by scanning electron

microscopy (SEM), Fourier Transform infrared spectroscopy (FTIR), differential scanning calorimetric (DSC), equilibrium water content (EWC), ^{13}C NMR, toluidine blue staining and biological studies were conducted using skin cells, fibroblasts and keratinocytes. ^{13}C NMR and FTIR were used to determine the changes in the chemical structure of linear KGM when incorporated with P(NVP-co-PEGDA). Calorimetric assement of the state of water in the hydrogel and its relationship with the changes in the chemistry and biological activities were also reported in this chapter.

5.2 Results.

5.2.1 The synthesis and characterizations of semi-IPN and graft-conetwork.

In these experiments semi IPNs and graft-conetworks composed of cross-linked KGM and P(NVP-co-PEGDA) were prepared. In a graft-conetwork, first KGM was cross-linked with Ce(IV) in the presence of NVP and PEGDA monomers. Then in a second step, the NVP and PEGDA were further photopolymerized. In this system, crosslinking and grafting of the KGM occurred in the first step then the photopolymerisation was used to complete the polymerisation of NVP and PEGDA. For semi IPNs the Ce(IV) was omitted so that the KGM was not cross-linked. The formulation data for each semi-IPN and graft-conetwork is provided in Table 5.1.

Table 5.1 The chemical compositions in P(NVP-co-PEGDA), semi-IPN and graft-conetwork hydrogels.

Hydrogel	KGM (%)	Ce(IV) (%)	P(NVP) (%)	PEGDA wt 2% HMPP
Semi-IPN	14	-	40	8
	24	-	40	8
	35	-	40	8

	14	0.5	40	8
Graft-conetwork	14	1	40	8
	24	0.5	40	8
	24	1	40	8

5.2.2 Observation on the hydrogels' morphologies and surfaces using scanning electron microscopy (SEM).

Characteristic morphology of dried P(NVP-co-PEGDA) samples caused by the presence of KGM was observed by SEM. All hydrogels were opaque and possessed no particular texture or porousity on the surface (Figure 5.7). This due to the samples preparation in moulds with the polymerizing mixtures pressed against poly(ethylene terephthalate) sheet. The SEM of the hydrogels, P(NVP-co-PEGDA), 1% crosslinked KGM with $1x10^{-3}$ % (w/v) Ce(IV), semi-IPNs and graft-conetworks with different concentrations of KGM and Ce(IV) was conducted at magnification 200-500x. The introduction of KGM into P(NVP-co-PEGDA) as semi IPN and graph-conetwork, grossly separated the hydrogels into two phase structure, where the outer surface of the hydrogels were smooth while the KGM was in the inside. Further examination on the hydrogel's cross section (the hydrogels were cut vertically from the centre) showed sponge-like morphologies with porous that were typical of reaction by induced phase separation (Figure 5.8).

The mechanism to explain the formation of this morphologies and the related studies on their effect to physicochemical properties (EWC, free water content, FTIR, DSC and ^{13}C Solid State NMR) are interesting and will be discussed in Section 5.3.

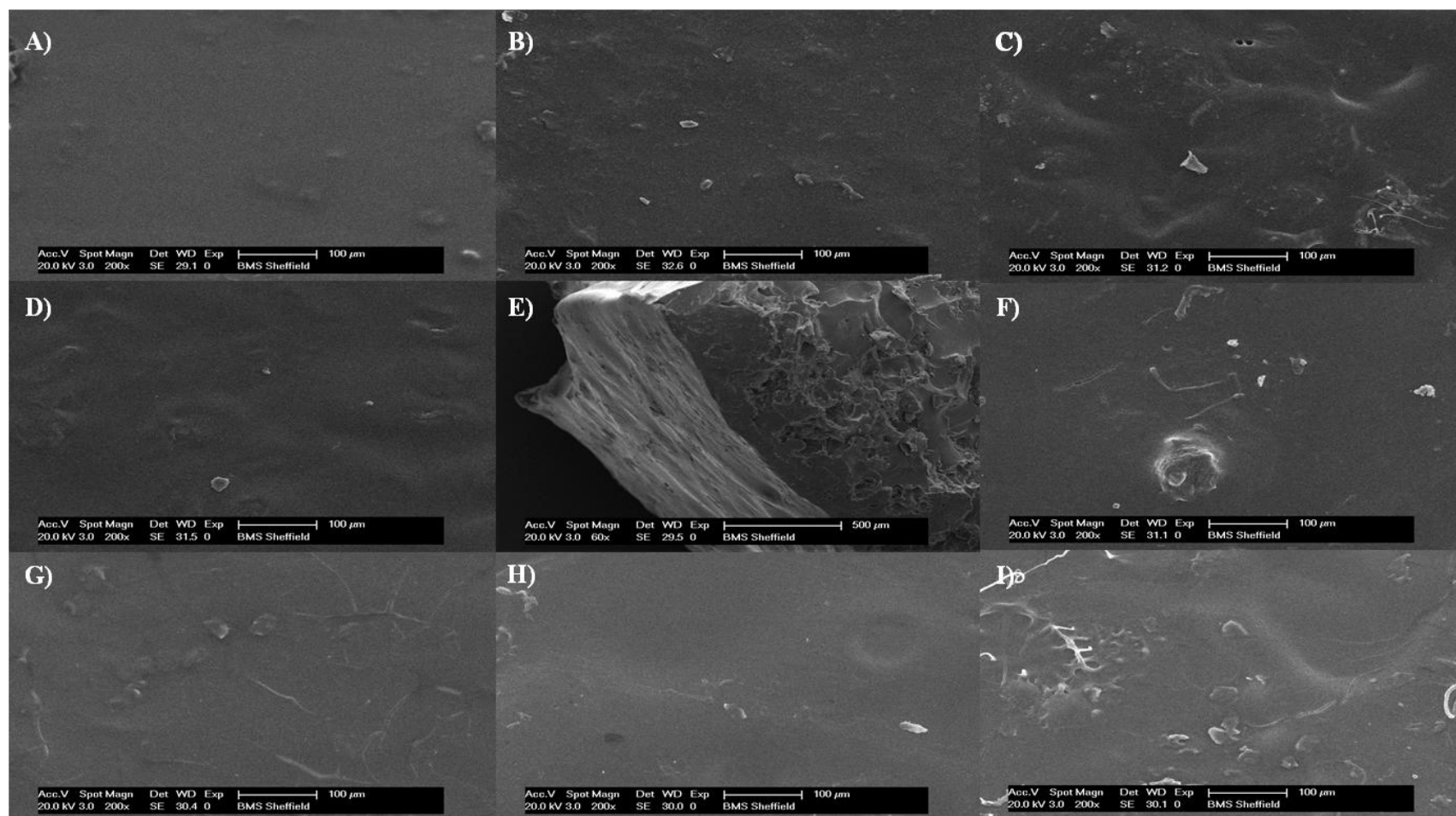**Figure 5.7**   The morphologies of the surface of (A) P(NVP-co-PEGDA), (B) crosslinked 1% (w/v) KGM with 1x10-3% (w/v) Ce(IV), (C-E) Semi-IPN of 14, 24 and 35% (w/v) of KGM , (F-G) Graft-conetwork of 14% (w/v) of KGM wt 0.5 and 1% (w/v) of Ce(IV) respectively and (H-I) Graft-conetwork of 24% (w/v) of KGM wt 0.5 and 1% (w/v) Ce(IV) respectively observed using SEM.

Figure 5.8 The morphologies of the cross sections of (A) P(NVP-co-PEGDA), (B) crosslinked 1% (w/v) KGM with 1×10^{-3}% (w/v) Ce(IV), (C-E) Semi-IPN of 14, 24 and 35% (w/v) of KGM , (F-G) Graft-conetwork of 14% (w/v) of KGM wt 0.5 and 1% (w/v) of Ce(IV) respectively and (H-I) Graft-conetwork of 24% (w/v) of KGM wt 0.5 and 1% (w/v) Ce(IV) respectively.

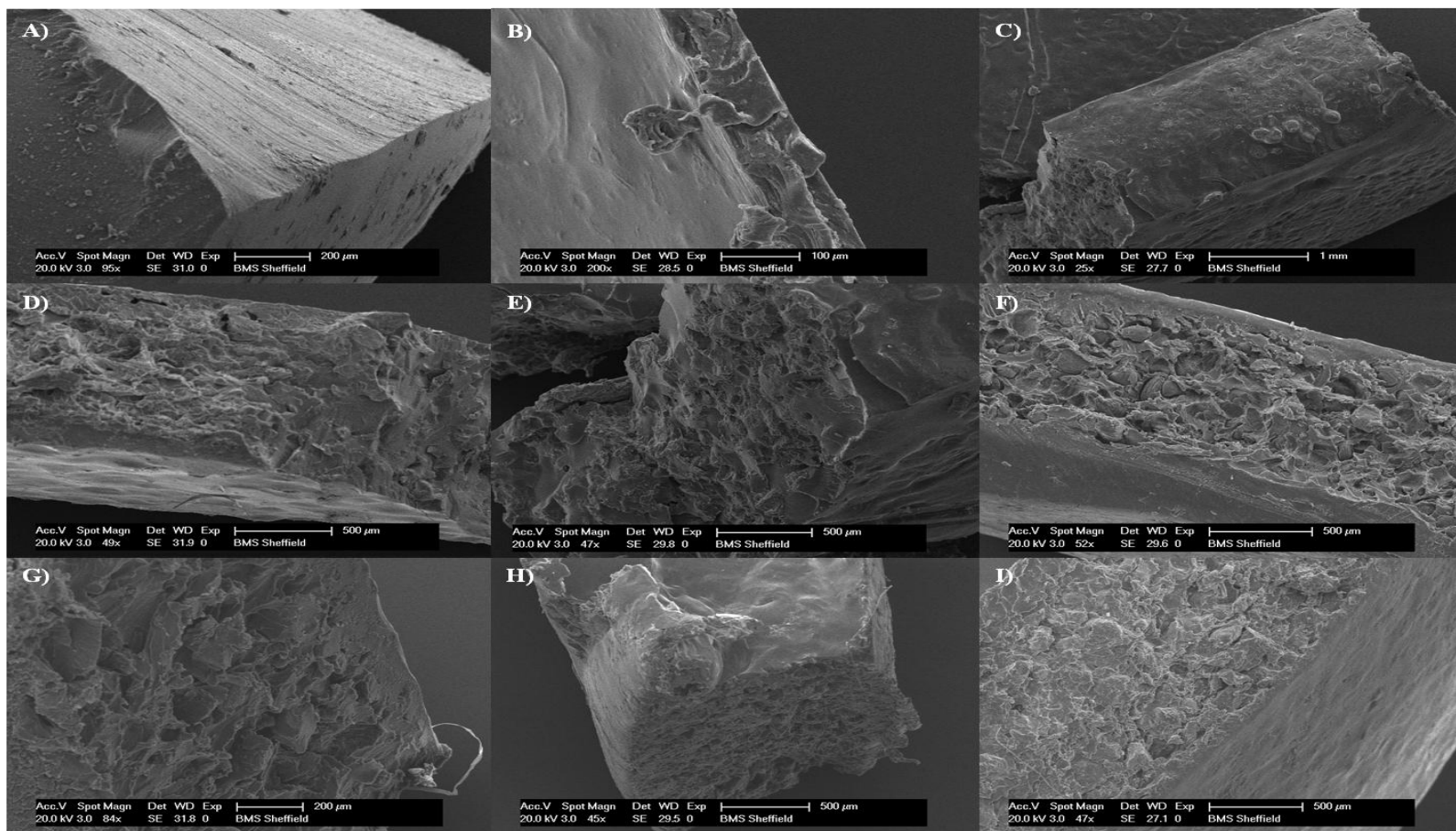## 5.2.3 Characterizations of semi-IPN and graft-conetwork hydrogels using FTIR.

P(NVP) has been investigated in polymerisation with some hydroxyl containing polymers such as PVA (Mumtaz, Labrugère § et al. 2009), cellulose (Sadeghi and Yarahmadi 2011) and PMMA (Dai, Sun et al. 2012), where hydroxyl bonding appears to be a major factor in inducing miscibility. This part of the thesis examined the molecular interactions of KGM, P(NVP-co-PEGDA), semi-IPN and graft-conetwork via FTIR-ATR. All hydrogels displayed the presence of hydroxyl (-OH) groups which gave broad band between 3500-3000 cm^{-1} and characteristic peak of –CH group attached to the hydroxyl group at 2920 cm^{-1} (Xiao, Liu et al. 2001; Widjanarko, Nugroho et al. 2011). FTIR can be used to monitor the conversion of the C=C bonds in NVP and PEGDA during crosslinking (Száraz and Forsling 2000).

The assignment peaks observed in P(NVP-co-PEGDA) spectrum are as follow; C=O at 1702 cm^{-1}, C=C at 1666 cm^{-1}, CN at 1290 cm^{-1}, C=C bending at 985 and 851 cm^{-1} in PEGDA. On the other hand, the assignment peaks for specific groups in KGM spectrum are 3397 cm^{-1} (OH), 2953 cm^{-1} (CH), 1702 cm^{-1} (C=O), 1375 cm^{-1} (C-H), 1150 cm^{-1} (C-O), 1050 cm^{-1} (C-O-C), 900-700 cm^{-1} (CH in mannose/glucose). The spectra for both semi-IPN and graft-conetwork displayed almost all assignment peaks observed in P(NVP-co-PEGDA) and KGM, except at 1666 cm^{-1} which was absorbed into broader peak of 1703 cm^{-1} assigned to (C=O), suggesting polymerisation of NVP and PEGDA monomers. The peaks 2159 and 2028 cm^{-1} which assigned to C≡C stretching vibrations were observed in graft conetwork hydrogels but not semi-IPN, suggesting the addition of Ce(IV) in the formulation may form more grafting in the network. The peak at 1703 cm^{-1} was low in KGM compared to P(NVP), indicating of more C=O acetyl group in P(NVP) (Chen, Liu et al. 2005).

The molecular structures of KGM in the hydrogels was confirmed by the peaks at 900-700 cm^{-1}, which were specifically assigned to mannose and glucose and at 1670 cm^{-1} which confirms the β-(1,4) glycosidic chain in glucomannan (Mathlouthi and Koenig 1986; Hua, Zhang et al. 2004; Widjanarko, Nugroho et al. 2011). Further, the presence of β-1,4 linked glucosidic and β-1,4 linked mannosidic linkages in KGM and KGM hydrogels were observed at 1027-1244 cm^{-1} which specifically assigned to C-O-C stretch vibration and also C-O (Hua, Zhang et al. 2004; Widjanarko, Nugroho et al. 2011). The peak 1375 cm^{-1} which assigned to CH deformation of cellulose was also detected in KGM spectra. The references for each assignment peak are summarized in Table 5.2.
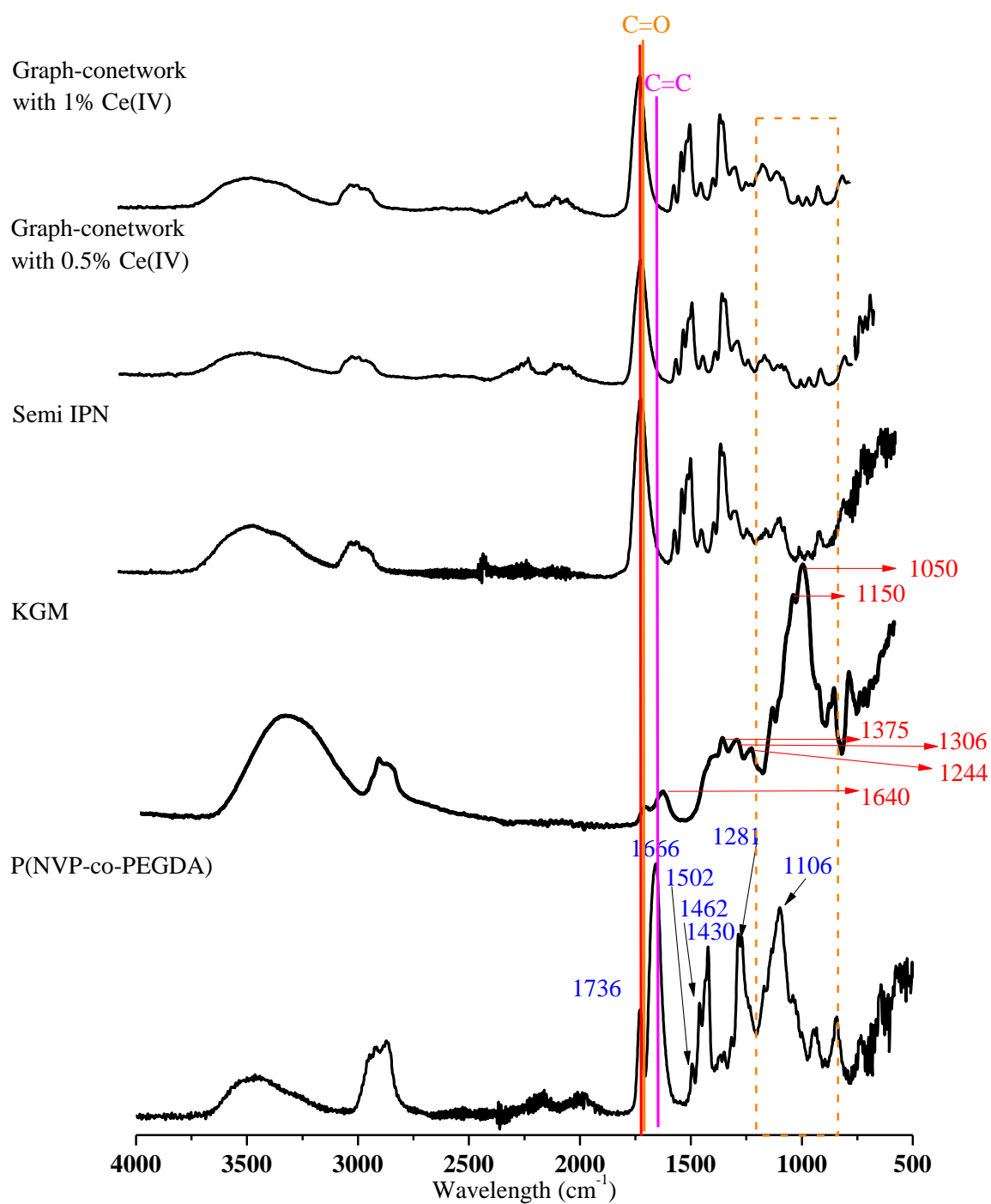
Figure 5.9 Comparison of the FTIR spectra between semi-IPN and graph-conetwork hydrogels shows the broadening of peak at 1666 cm^{-1} to 1736 cm^{-1}, to indicate crosslinking of NVP and PEGDA during polymerisation.
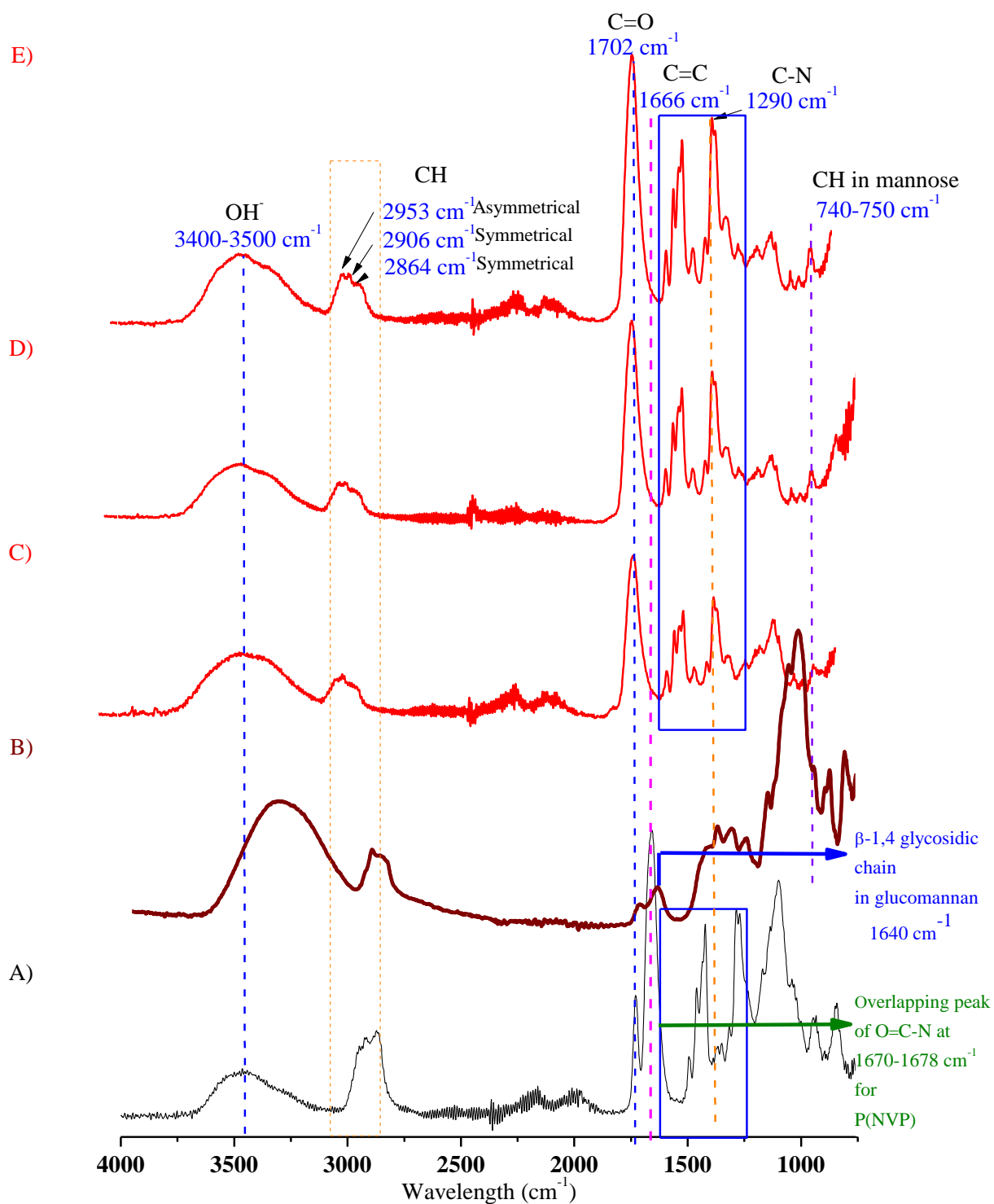
Figure 5.10 Comparison of FTIR spectra for (A) P(NVP-co-PEGDA), (B) KGM and (C-E) semi-IPN with 35, 24 and 14% (w/v) KGM. The blue box at semi-IPN hydrogel spectra labeled to show the similaries with the peaks observed in P(NVP-co-PEGDA).

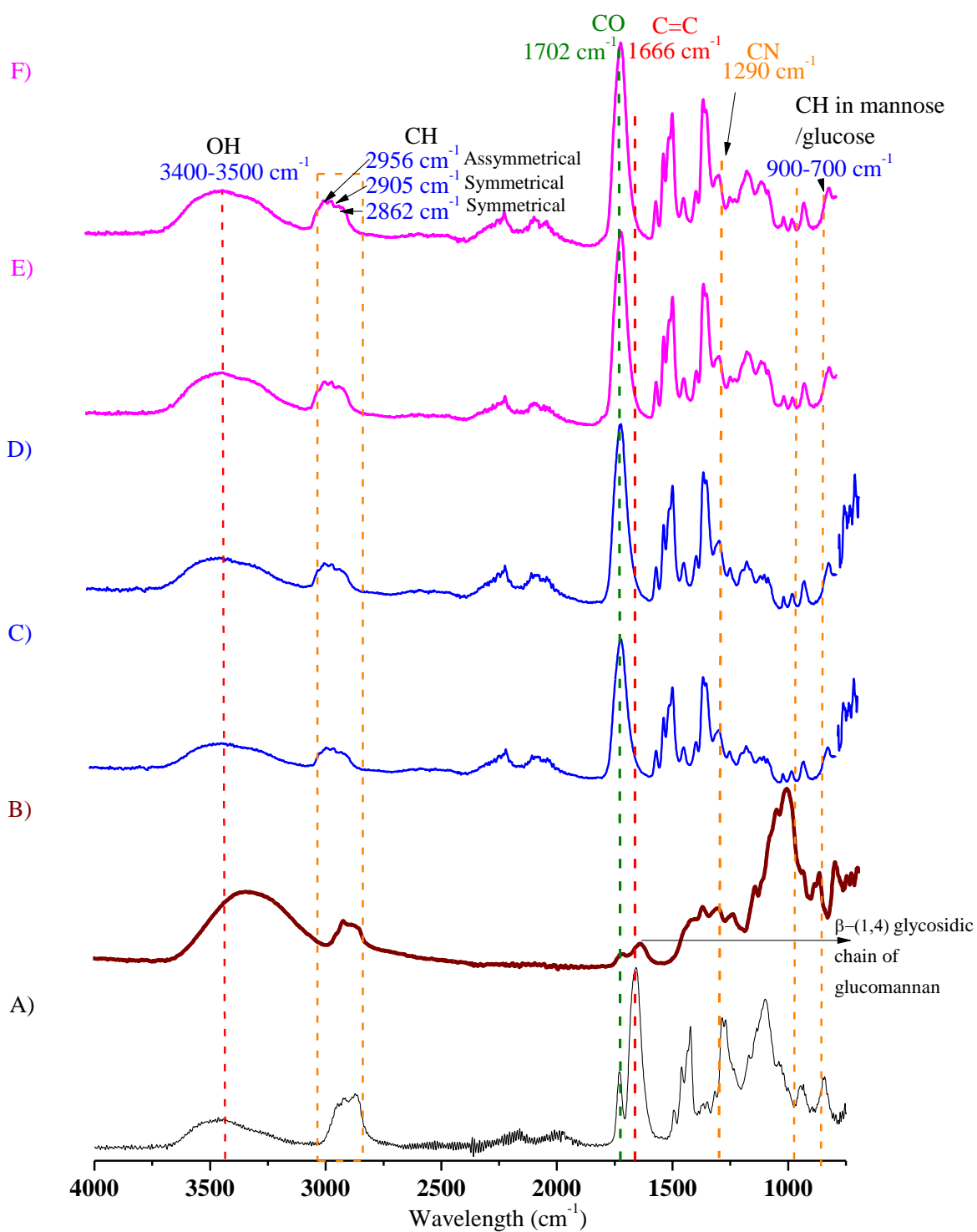**Figure 5.11** Comparison of FTIR spectra for (A) P(NVP-co-PEGDA), (B) KGM and (C-D) graft-conetworks with 14% KGM wt 0.5 or 1% Ce(IV) respectively and (E-F) graft-conetworks with 24% KGM wt 0.5 or 1% Ce(IV) respectively.

Table 5.2   Summary of the absorption regions and assignments for KGM, P(NVP-co-PEGDA), semi-IPN and graft-conetwork hydrogels with KGM.

Peak (cm^{-1})	Assignments	P(NVP-co-PEGDA)	KGM	Semi-IPN	Graft-conetwork	Reference
3397	-OH-	√	√	√	√	(Mathlouthi and Koenig 1986; Kačuráková and Mathlouthi 1996; Li, Qi et al. 2009; Xu, Luo et al. 2009; Widjanarko, Nugroho et al. 2011)
2953	-CH$_2$- in C-CH$_3$	√	√	√	√	(Mathlouthi and Koenig 1986; Kačuráková and Mathlouthi 1996; Xiao, Liu et al. 2001; Widjanarko, Nugroho et al. 2011)
2159	C-C≡C-C				√	(Masaidova, Yakunina et al. 1966; Garbuz, Zhbankov et al. 1973; Rodriguez 1996)
2028	C-C≡C-C≡CH				√	(Masaidova, Yakunina et al. 1966; Garbuz, Zhbankov et al. 1973; Rodriguez 1996)
1700-1710	C=O	√	√			(Mathlouthi and Koenig 1986; Kačuráková and Mathlouthi 1996; Xiao, Liu et al. 2001; Chen, Liu et al. 2005; Son,

						Kim et al. 2007; Moshaverinia, Roohpour et al. 2009; Chao, Su et al. 2013)
1666	O=C-N (Amide I)	√				(Száraz and Forsling 2000; Son, Kim et al. 2007; Chao, Su et al. 2013)
1640	β 1,4 linked glucose in glucomannan		√			(Černáa, Barros et al. 2003; Li, Qi et al. 2009; Xu, Luo et al. 2009; Widjanarko, Nugroho et al. 2011)
1640	B-(1,4) Glycosidic linkage in glucomannan		√	√	√	(Mathlouthi and Koenig 1986; Kačuráková and Mathlouthi 1996; Widjanarko, Nugroho et al. 2011)
1375	-CH$_2$-		√	√	√	(Mathlouthi and Koenig 1986; Száraz and Forsling 2000; Pandey and Pitman 2003; Vaaler 2008; Widjanarko, Nugroho et al. 2011)
1270-1290	Pyrolidone	√		√	√	(Száraz and Forsling 2000; Son, Kim et al. 2007)
1244	C-O-C stretch	√	√	√	√	(Xu, Luo et al. 2009; Chao, Su et al. 2013)
1150	-CH$_2$-	√	√	√	√	(Guo, Huang et al. 1996; Xiao, Liu et al. 2001)

1050	C-O	√	√	√	√	(Widjanarko, Nugroho et al. 2011; Chao, Su et al. 2013)
1013	C-O (on KGM)		√	√	√	(Mathlouthi and Koenig 1986; Xu, Luo et al. 2009)
985	=C-H (PEGDA)	√		√	√	(Száraz and Forsling 2000; Chao, Su et al. 2013)
875	-CH- in mannose		√	√	√	(Mathlouthi and Koenig 1986; Hua, Zhang et al. 2004; Xu, Luo et al. 2009; Widjanarko, Nugroho et al. 2011)
851	=C-H (PEGDA)	√		√	√	(Száraz and Forsling 2000; Chao, Su et al. 2013)
808	-CH- in mannose		√			(Hua, Zhang et al. 2004; Xu, Luo et al. 2009; Widjanarko, Nugroho et al. 2011)
745	-CH- in mannose		√			(Mathlouthi and Koenig 1986; Hua, Zhang et al. 2004; Widjanarko, Nugroho et al. 2011)

5.2.4 Characterization of semi IPN and graft conetwork using DSC.

Calorimetric analyses for semi-IPN and graft-conetwork was done using DSC and carried out over the full range of studied compositions. The hydrogels in dry condition were subjected to heating process between -60 to 360°C at a heating rate of 10°C per minute in a nitrogen atmosphere. The details of the thermograms in Figure 5.11 are shown in Table 5.3. From the thermograms, it was clear that the hydrogel's endothermic peak temperature increased with increasing KGM and Ce(IV) concentrations, reflecting the increase of phase separation. The thermograms also provided information on thermal transitions and morphological changes from semi-IPN and graft-conetwork, where semi-IPN is usually depicted by the formation of two or more peaks while graft-conetwork usually have a single peak. The result in Figure 5.10 suggested that all hydrogels displayed a complex, microphase separation behavior. It was also observed that the glass transition temperature (T_g) depends on the concentrations of KGM and the presence of Ce(IV). The higher concentration of KGM led to a denser KGM morphology in the hydrogel while the presence of Ce(IV) promoted crosslinking of KGM in the IPN. These support the argument that higher crosslinking and hard segment polymers with a denser and random morphologies give higher heat transition compared to linear polymers (Lee, Chun et al. 2001). Three peaks were observed for P(NVP-co-PEGDA) at 143, 148 and 153°C, depicting the presence of different compounds in the copolymer. The shape of the peak for semi-IPN with 24% (w/v) KGM was similar to P(NVP-co-PEGDA) with shoulder peak at 143°C and a narrow peak at 153°C. The increasing concentrations of KGM and the addition of Ce(IV) in graft-conetwork significantly increase the T_g of the hydrogels. T_g value for semi-IPN with 35% (w/v) KGM was higher compared to semi-IPN with 14 and 24% (w/v) indicated the existence of stronger interactions in the system and the shifting of phase transition with increasing concentration of KGM. The similar trend was also observed in graft-conetwork with 14 and 24% (w/v) KGM. From the

thermograms in Figure 5.10 it was shown that only semi-IPN with 35% (w/v) KGM and graft-conetwork with 14% (w/v) KGM and 1% (w/v) Ce(IV) displayed a distinct peak that would be indicative for graft-conetwork. The endothermic peaks for both graft-conetwork with 24% (w/v) KGM initiated using 0.5 and 1% (w/v) Ce(IV) appeared to be very broad and showed sign of degradation with exothermic peaks at around $290^{o}C$ as was seen with crosslinked KGM with higher concentrations of Ce(IV) which was mentioned in the previous chapter. The broad peak and higher T_g were concluded to be induced by the formation of crosslinks in KGM and its interaction with P(NVP-co-PEGDA). The endothermic peaks for graft-conetwork of 14% (w/v) KGM with 1% Ce(IV) and graft-conetwork of 24% (w/v) KGM with 0.5 and 1% (w/v) Ce(IV) displayed complex mixture of copolymerisation with the appearance of shoulder on the broad peaks. Exothermic peak was observed in both graft-conetwork of 24% (w/v) KGM with 0.5 and 1% (w/v) Ce(IV). The endothermic and exothermic peaks for both graft-conetwork hydrogels of 24% (w/v) KGM with 0.5 and 1% (w/v) Ce(IV) appeared to be in the same range with T_g around 151 and $142^{o}C$ and exothermic peaks at about 310 and $318^{o}C$, respectively.

Table 5.4 Summary of the DSC thermograms and characteristic peak termperature in all semi-IPN and graft-conetwork hydrogel samples.

|	Hydrogel	No. of Peak	Type of peak	Onset (^{o}C)	Peak Temperature (^{o}C)	Area (mJ)
1	KGM	1	Endothermic	113	127	6302
2	P(NVP-co-PEGDA)	3	Endothermic	103.5	143 148 153	1639
3	Semi-IPN (14% KGM)	1	Endothermic	103	127	3374
4	Semi-IPN (24% KGM)	2	Endothermic	117	128 153	581 11007
5	Semi-IPN (35% KGM)	1	Endothermic	143	152	5232
6	Graft-conetwork (14% KGM, 0.5% Ce(IV))	2	Endothermic Endothermic	109 155	132 159	1484 732
7	Graft-conetwork (14% KGM, 1% Ce(IV))	1	Endothermic	133	141	1468
8	Graft-conetwork (24% KGM, 0.5% Ce(IV))	2	Endothermic Exothermic	128 276	151 310	16258 1192
9	Graft-conetwork (24% KGM, 1% Ce(IV))	2	Endothermic Exothermic	68 287	142 318	94534 2472
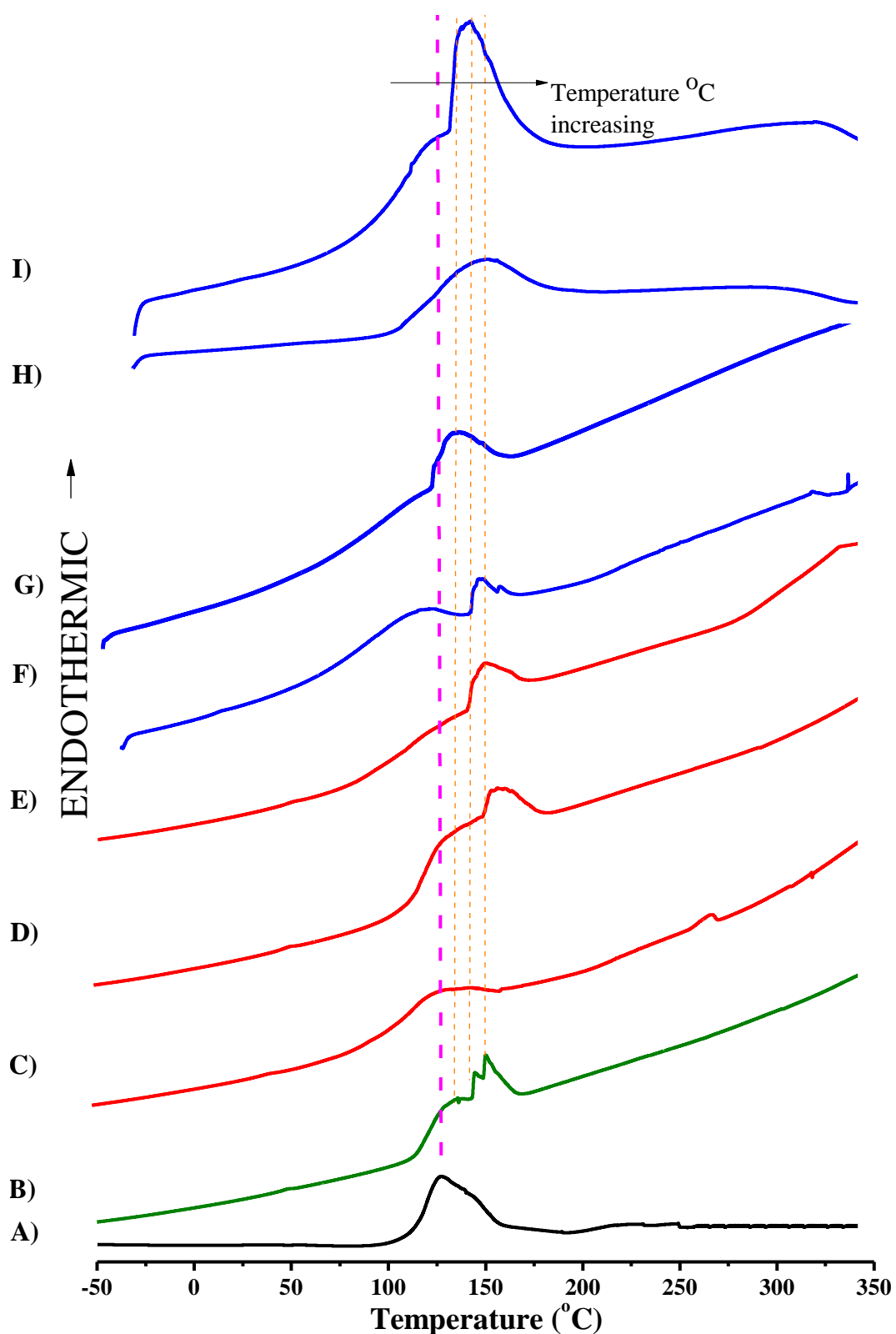
Figure 5.11 DSC Thermograms of dried hydrogels of (A) KGM, (B) P(NVP-co-PEGDA), (C-E) Semi-IPN with 14, 24 and 35% (w/v) KGM, respectively and (F-I) Graft conetwork with 14 and 24% (w/v) KGM and 0.5 and 1% Ce(IV) respectively. The dash line in purple is to show the endothermic peak of KGM and the lines in orange are for P(NVP-co-PEGDA) peaks.

5.2.5 Equilibrium Water Content (EWC) and free-bound water measured using DSC.

The EWC was higher for semi-IPN with (85-93%) compared to graft-conetwork hydrogels with (80-85%). It was observed that increasing concentrations of KGM in semi-IPN (14, 25 and 35% (w/v)) gave inverse relationship with the EWC in the range from 93-85%. The decrease in the EWC of semi-IPN with 35% (w/v) KGM was mainly caused by the compact and denser structure of KGM in the hydrogel. The addition and increasing concentration of Ce(IV) to form KGM crosslinking in P(NVP-co-PEGDA) network for graft-conetwork decreased hydrogel's ability to absorb more water. A trend of 1-3% decrease in the EWC of graft-conetwork with 0.5 and 1% (w/v) Ce(IV) was measured for both 14 and 24% (w/v) KGM (Figure 5.12). It was then observed that the crosslinking and morphology of KGM in the hydrogel played significant roles in the EWC.

Further experiment was then conducted to relate the link between EWC and free water content inside the hydrogel by quantifying the amount of free water inside the hydrogel. This was estimated relatively using DSC which measures the amount of energy required to release free water from the hydrogel when the sample was heated from -60 to 60°C in hydrated condition. Initially, the samples were allowed to hydrate for 24 h and then estimation of 8-12 mg of the hydrogels were sealed in an aluminium pan. The samples were then cooled to -60°C and subsequently heated to 60°C at a rate of 10°C per min. The free water T_m for semi IPNs were almost equivalent to KGM with temperature ranging from 5.2 to 6.4^{o}C while graft conetworks and P(NVP-co-PEGDA) ranged from 1.8 to 2.7^{o}C. The relationship between the energy required to release the amount of water per mg of sample and EWC is summarized in Figure 5.14.
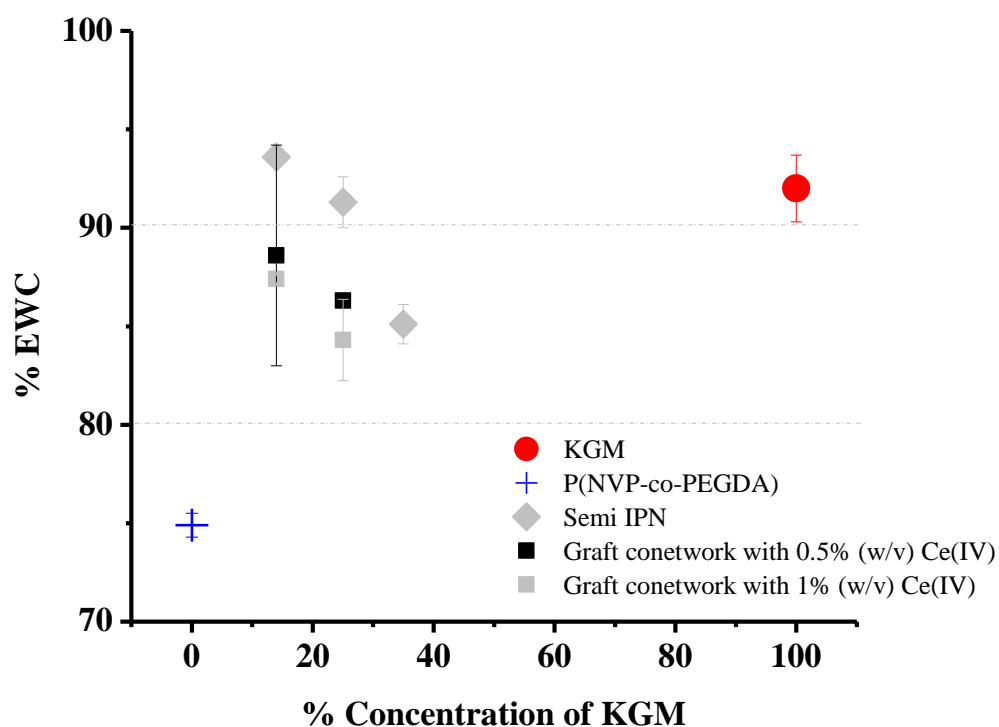
Figure 5.12 The EWC of semi and full IPN hydrogels shows that semi-IPN had higher EWC compared to graft-conetworks. Higher concentration of Ce(IV) in graft-conetworks had lower EWC compared to with hydrogel with 0.5% Ce(IV). ● represents KGM, + represents P(NVP-co-PEGDA) while ◊ represents semi-IPN and □ represents graft-conetworks (where ■ : graft-conetworks with 0.5% (w/v) Ce(IV) and ■ : graft-conetworks with 1% (w/v) Ce(IV).
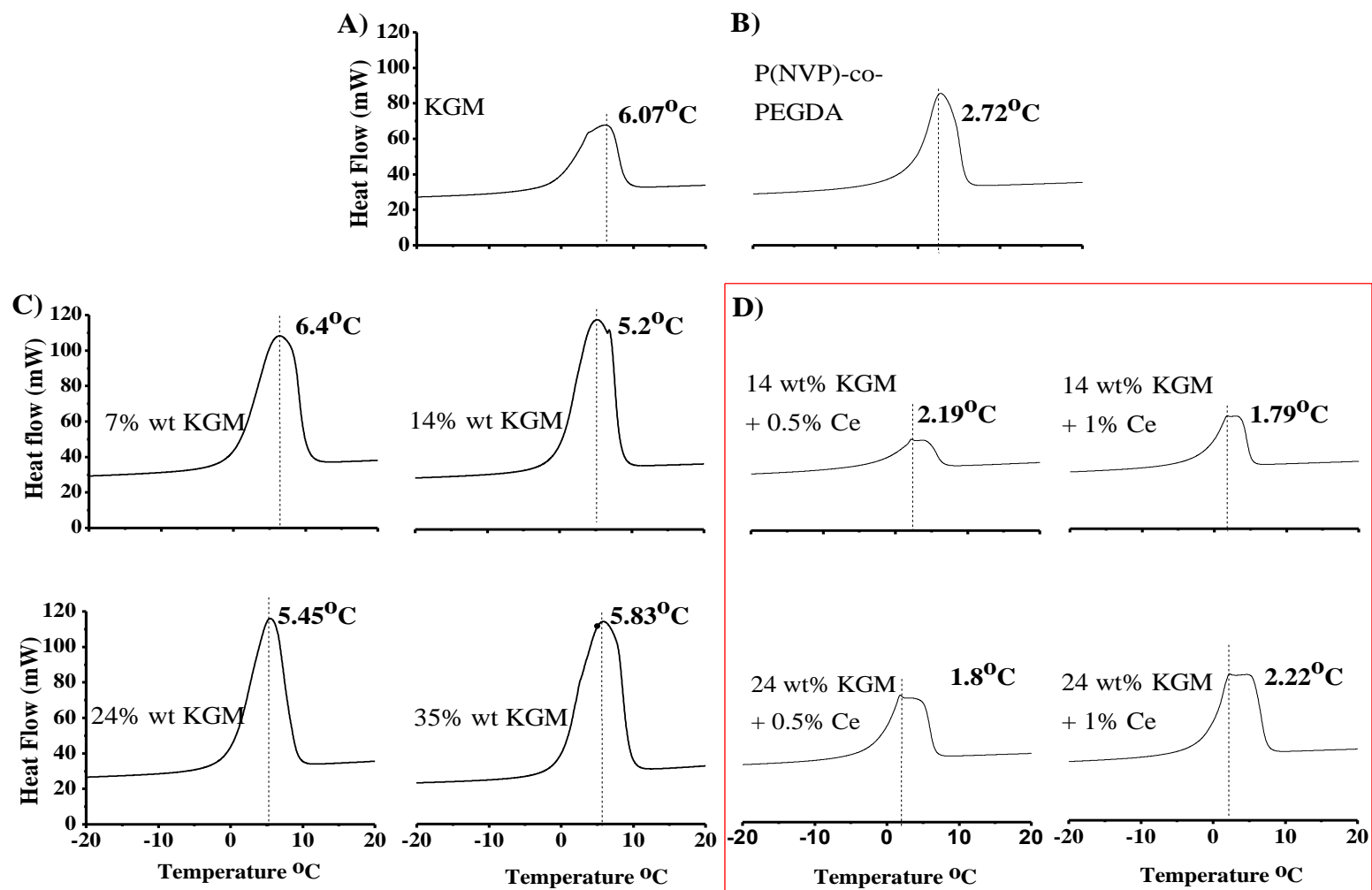
.

Figure 5.13 Thermograms of hydrated (A) KGM, (B) P(NVP-co-PEGDA), (C) semi IPNs and (D) graft-conetworks showing different thermal characteristics when the samples were heated from -60°C to 60°C. The temperature and area of endothermic heat required to release the free water for semi IPNs were higher than graft-conetworks indicating that semi-IPN had more free water content.
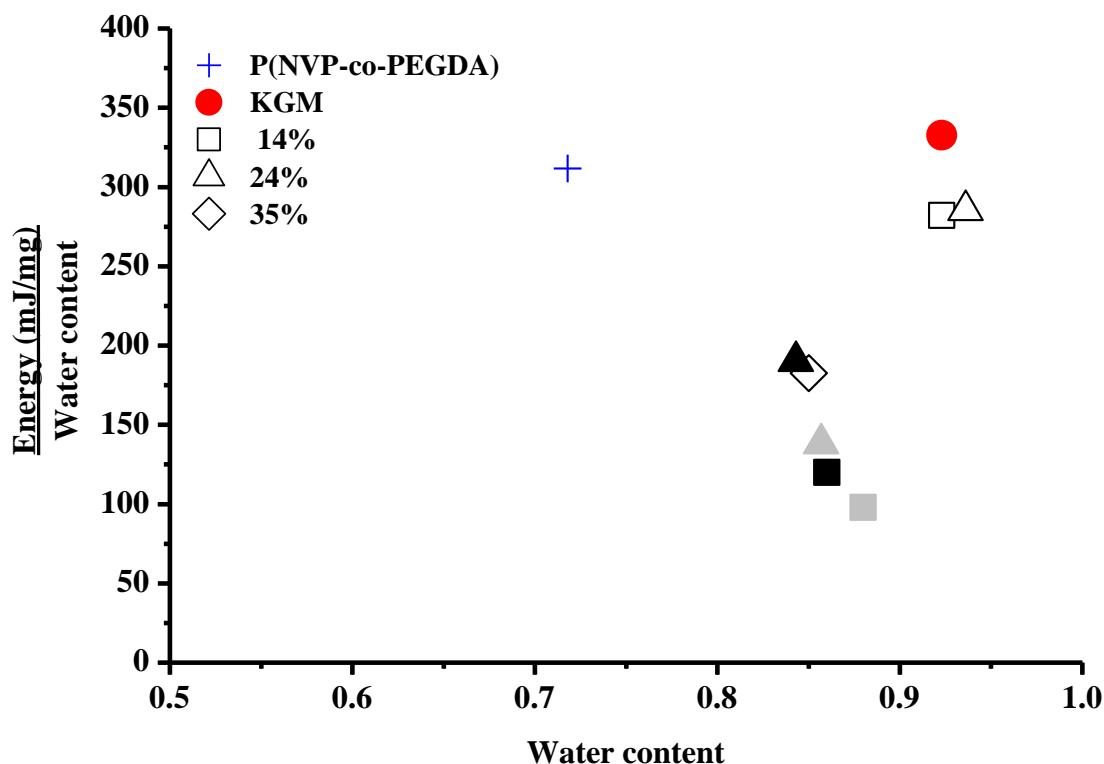
Figure 5.14 Summary of the results in Figure 5.12 and 5.13 which represents the relationship between free water inside the hydrogels measured by the amount of energy required to release the water from the hydrogel measured by DSC and the water content inside the hydrogel. The result shows that semi-IPN had higher free water content and EWC which equivalent to KGM compared to graft-conetworks   and P(NVP-co-PEGDA). ● represents KGM in solution, + represents P(NVP-co-PEGDA) while combinations of KGM in hydrogels are shown as open symbol for semi-IPN (, □ : 14%, Δ : 24% and ◊ 35% (w/v) KGM and grey symbols indicate graft-conetwork with 0.5% Ce(IV) (where ■ ; 14 % and ▲ : 24% (w/v) KGM) and filled symbols indicate graft-conetwork with 1.0% Ce(IV) (where ■ : 14% and ▲ 24% (w/v) KGM).

5.2.6 Characterisation of hydrogels using ^{13}C Solid State NMR Spectroscopy.

Figure 5.15 (A-F) show the spectra of ^{13}C Solid State NMR for all of our synthesized hydrogels. The broad peak of 110 ppm which was observed in Figure 5.14A was absent in P(NVP-co-PEGDA) (Figure 5.14B) indicating the full crosslinking of the vinyl groups.

The peaks at 62, 75 and 102 ppm correspond to C6, C3 and C1 positions of KGM respectively. Signal at 102.5 ppm was identified as cellulostic confirmations of mannosyl and glucosyl units, which signifies the anomeric resonance from the KGM (Whitney, Brigham et al. 1998) and this were found in the crosslinked KGM and in all samples of semi IPNs and graft-conetworks . This broad resonance of crosslinked KGM peaks were due to the presence of a range of conformational changes at C2, C3, C4, C5 and C6 (Gidley, McArthur et al. 1991).

The corresponding C1 confirmation of P(NVP-co-PEGDA) peak at 71 ppm was observed in all samples of the semi IPNs and graft-conetwork. We observed the changes in the intensity at 62, 71, 75 and 102 ppm, suggesting the changes in the chemistry of the KGM and P(NVP-co-PEGDA) by addition of Ce(IV).

C6 and C6' methylene carbons gave rise to a peak that was almost resolved around 60 ppm and this was easily deconvoluted from the peak around 75 ppm. This methylene carbon could then be compared with the methylene on the NVP residues at P5 (approx. 19 ppm) to provide a reasonable estimate of the compositions of the graft-conetworks and the semi-IPNs.

Table 5.5 provides the data showing the relative fractions of NVP (or P(NVP) residues) and glucose/mannose units in the feed and the polymerised materials, extracted from ^{13}C solid state NMR results. It also show that semi IPNs contained more % network composition of (KGM/NVP) than graft conetwork hydrogels, and there was no difference in the % network

composition of graph-conetwork hydrogels with 0.5 and 1% (w/v) Ce(IV), with 24% (w/v) KGM. However for graft-conetwork of 14% (w/v) KGM, difference was observed at 0.5 and 1% (w/v) Ce(IV), with 69 and 62 % respectively. From this result, it can be concluded that moderate conversions of NVP and PEGDA produced materials that contained a larger proportion of KGM than in the feed.

Table 5.5 Molar compositions expressed as percent KGM relative to NVP in the monomer feeds and polymerised networks.

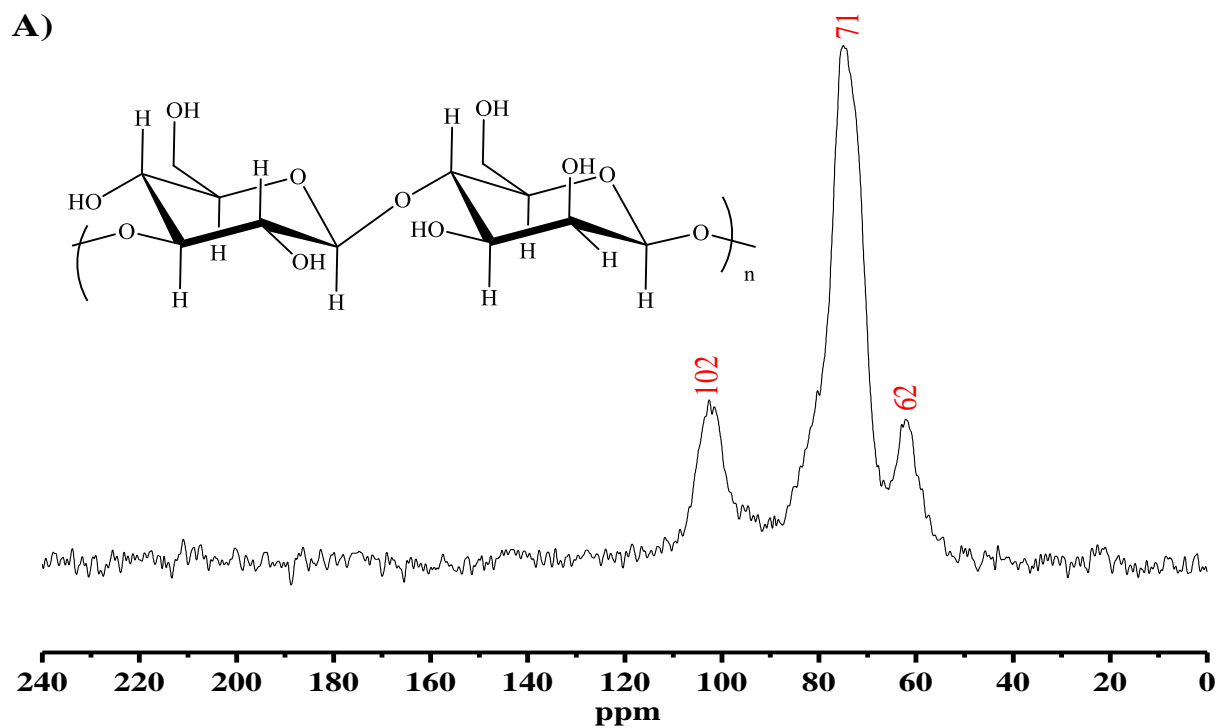|	[Ce]	%Mol. feed [KGM]/NVP	%Network composition [KGM]/NVP
Conetwork 24% KGM	1.0	29.1	50
Conetwork 24% KGM	0.5	29.1	50
Conetwork 14% KGM	1.0	19.3	69
Conetwork 14% KGM	0.5	19.3	62
Semi-IPN 24% KGM	0	29.1	74
Semi-IPN 14% KGM	0	19.3	55

A)

Figure 5.15A Solid State ^{13}C-NMR spectrum of crosslinked KGM
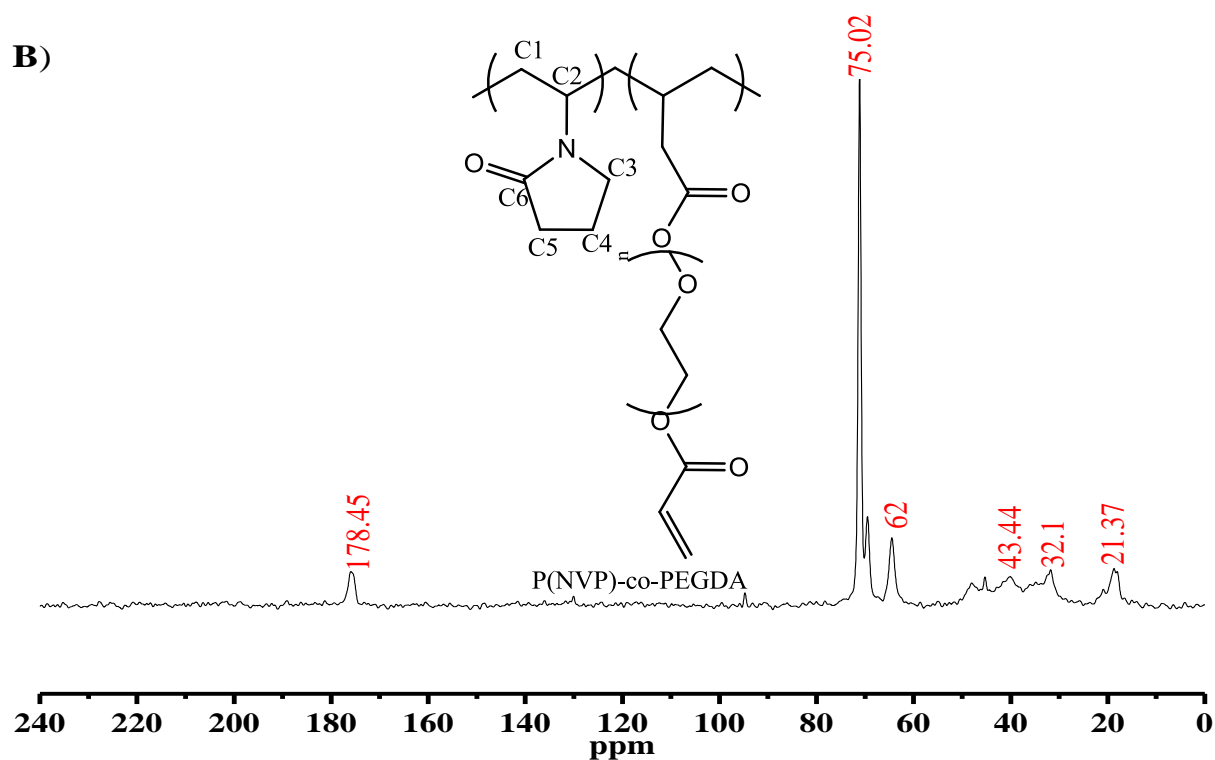
B)

Figure 5.15B Solid State ^{13}C-NMR spectrum of P(NVP-co-PEGDA).

C)
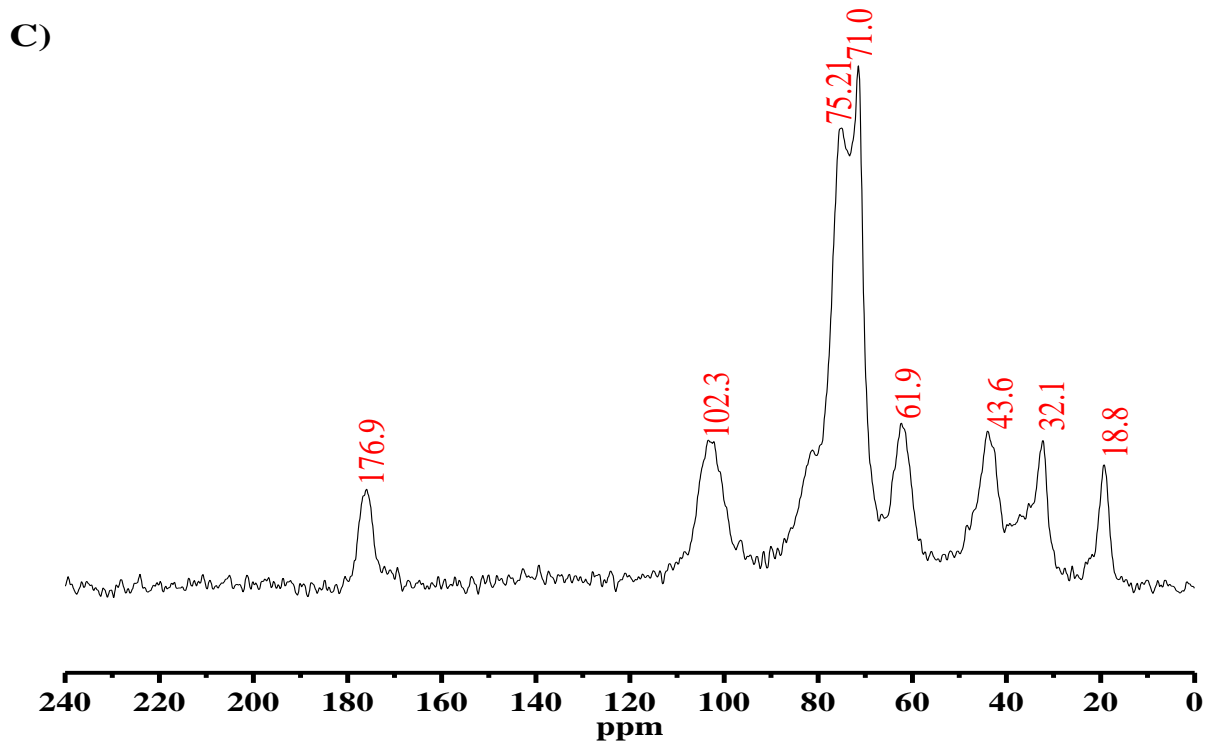
Figure 5.15C Solid State ^{13}C-NMR spectrum of semi-IPN of 14% (w/v) KGM

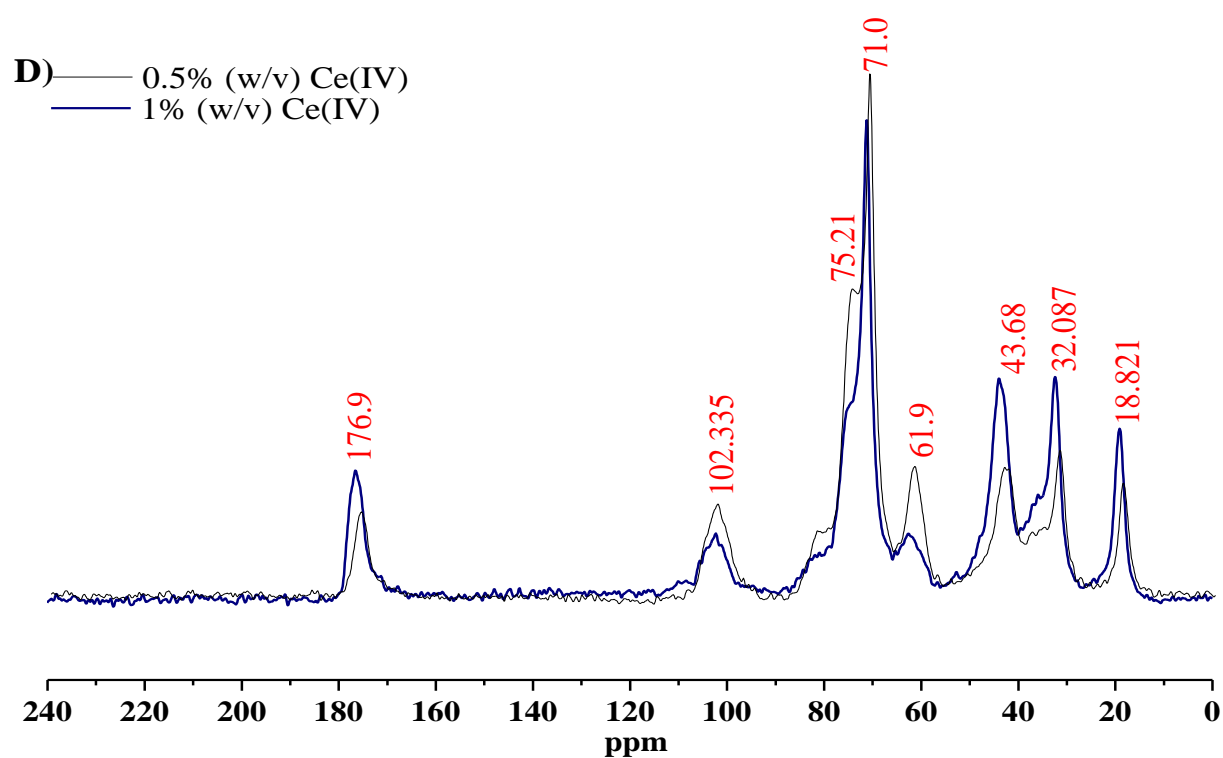**D)** ——— 0.5% (w/v) Ce(IV)
——— 1% (w/v) Ce(IV)

Figure 5.15D Solid State ^{13}C-NMR spectra of graft-conetwork of 14% (w/v) KGM with 0.5 and 1% (w/v) Ce(IV).
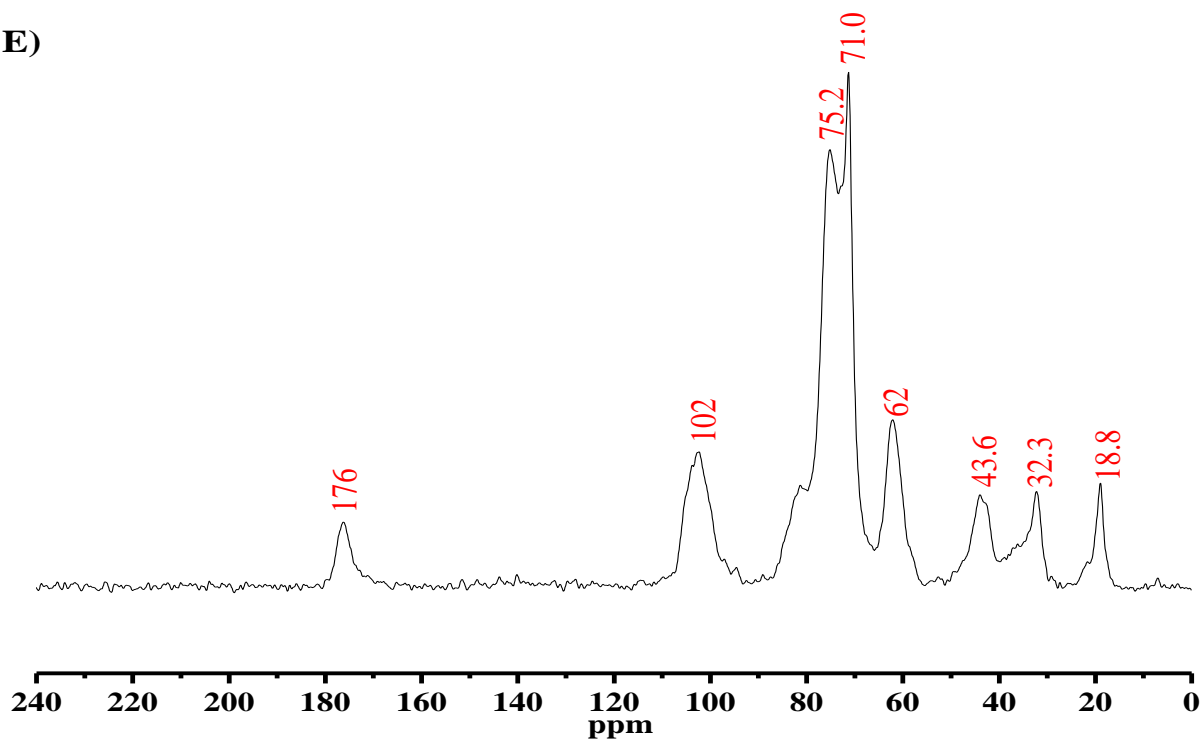
E)

Figure 5.15E Solid State ^{13}C-NMR spectrum of semi-IPN of 24% (w/v) KGM

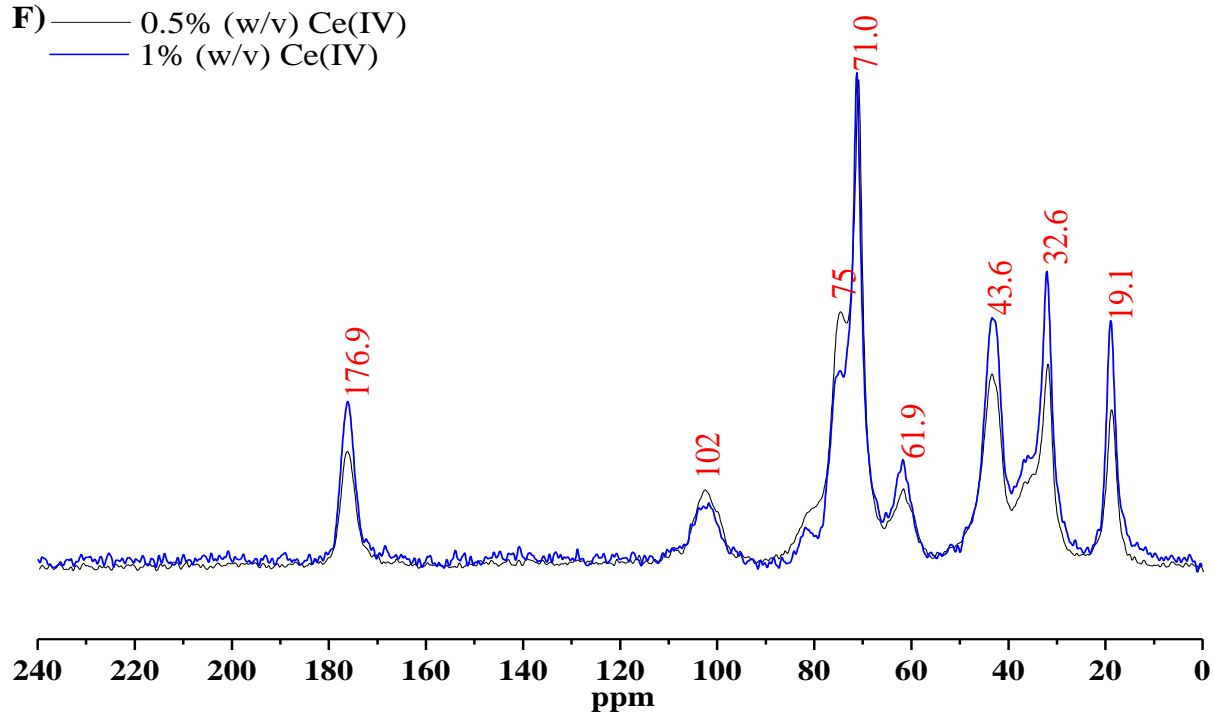**F)** ——— 0.5% (w/v) Ce(IV)
——— 1% (w/v) Ce(IV)

Figure 5.15F Solid State ^{13}C-NMR spectra of graft-conetwork of 24% (w/v) KGM with 0.5 and 1% (w/v) Ce(IV).

5.2.7 The measurement of KGM content in the hydrogel.

The measurement of KGM content inside the hydrogels was done using toluidine blue assay, which specifically stains heavily glycosylated structures such as heparin. Heparin is highly sulfated glycosaminoglycans (GAG). It stains nucleic acid blue and polysaccharide purple. In this experiment, the Toluidine blue was used to indicate the presence of KGM inside the hydrogel. The changes in the coloration of Toluidine blue of all samples are shown in Figure 5.16. The measurement of extracted Toluidine blue from the hydrogels is shown in Figure 5.17. The semi IPNs with 35% (w/v) KGM had the highest content of KGM compared to the other hydrogels with 14 and 24% (w/v) KGM. Comparison of semi-IPN and graft-conetwork with 14 and 24 % (w/v) KGM showed a significant difference in the content of KGM. Similar results were also observed with 0.5 and 1% (w/v) Ce(IV) in the graft-conetwork of 14% (w/v) KGM. Higher KGM content was observed in the graft-conetwork of 14% (w/v) KGM with 0.5% (w/v) Ce(IV) compared to graft-conetwork with the same KGM concentration with 1% (w/v) Ce(IV), suggesting a change in the chemistry of KGM – resulting in less absorbance of toluidine blue.
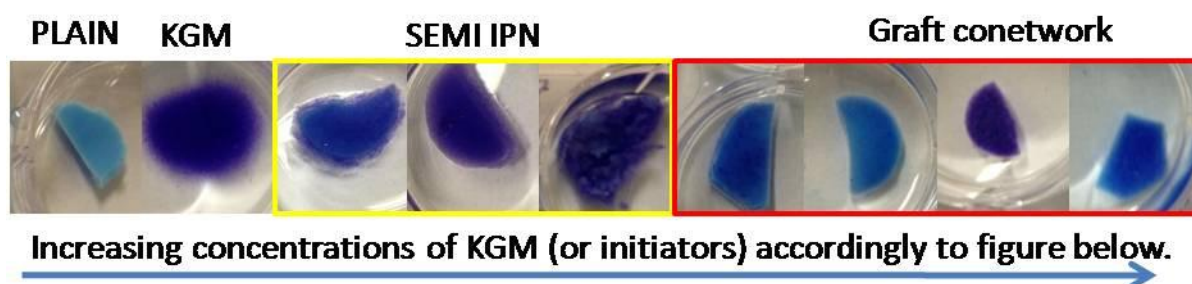

Figure 5.16   The changes in the color of Toluidine blue from light blue to purple or dark blue to indicate the presence of KGM in the hydrogels. The sequence of the hydrogels are as follows; P(NVP-co-PEGDA) (without KGM), KGM (50 mg.mL^{-1}), semi-IPN 14, 24 and 35% KGM (w/v) and graft-conetworks 14% KGM (w/v) with 0.5 and 1% Ce(IV) (w/v) and 24% KGM with 0.5 and 1% Ce(IV) (w/v).
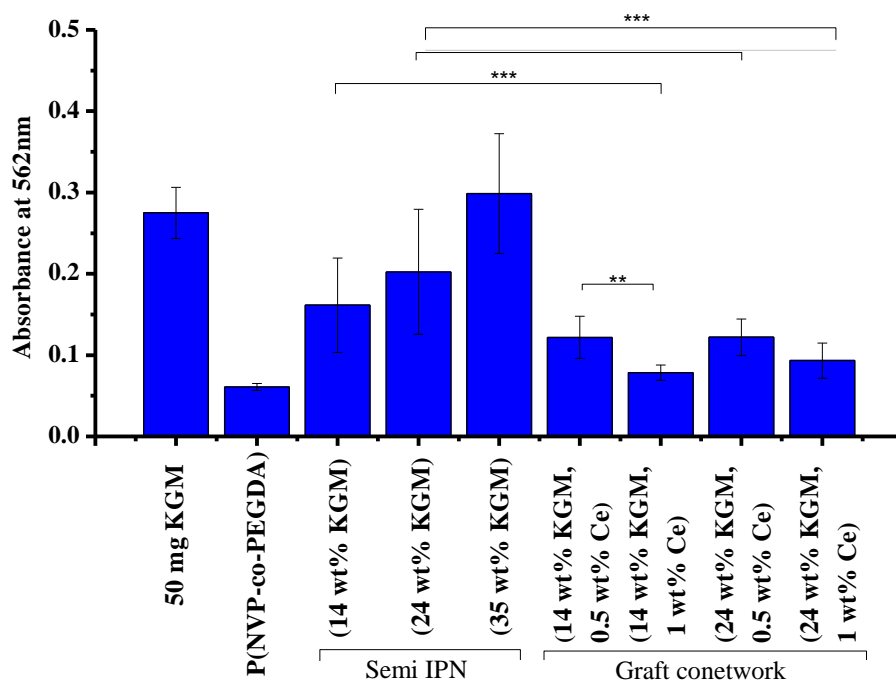
Figure 5.17 The measurement of KGM content in semi-IPN and graft-conetwork using Toluidine blue staining. Results shown are mean $\pm$SD, (n=2), ***P<0.001 highly significant, **P<0.01 very significant and *P<0.05 significant in comparison to control.

5.2.8 Cytocompatibility study and the effect of the hydrogels on human primary fibroblasts.

Cytocompatibility of semi-IPN and graft-conetwork with increasing concentrations of KGM was conducted in indirect contact with human primary fibroblasts and the cell viability after 5 days was measured using MTT assay (Figure 5.18). All samples showed no reduction in cell viability when compared to control, suggesting that both semi-IPN and graft-conetwork hydrogels were cytocompatible. The effect of direct contact of semi-IPN and graft-conetwork hydrogels with fibroblasts after 1, 3 and 5 days in culture is shown in Figure 5.19. It was found that direct contact of semi-IPN with fibroblasts did not stimulate cell viability but

direct contact of graft-conetwork with fibroblasts was able to stimulate cell viability significantly.
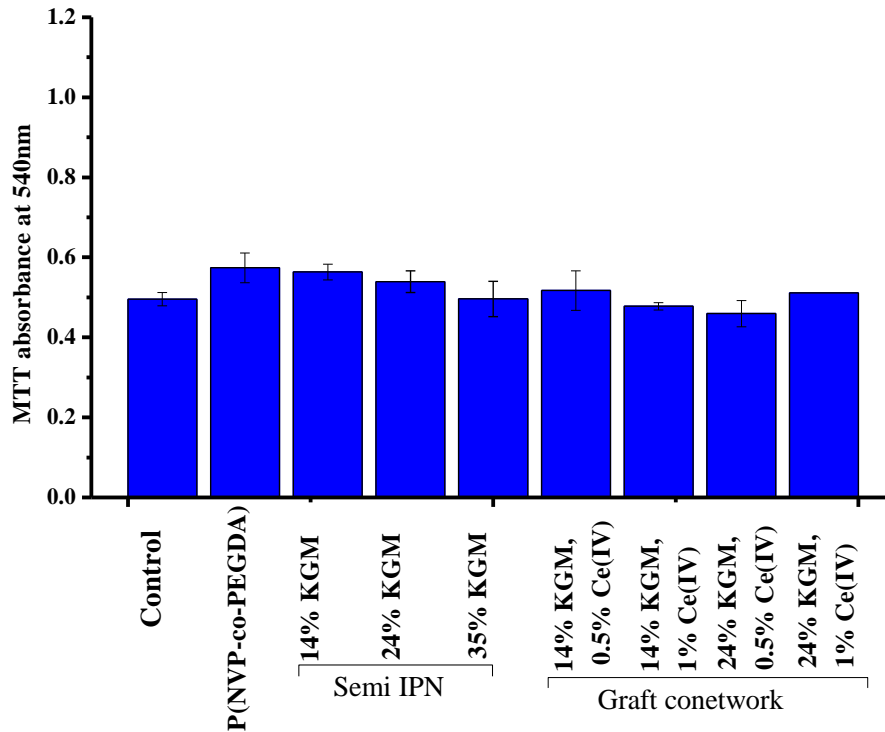
Figure 5.18 The effect of semi-IPN and graft-conetwork hydrogels with increasing concentrations of KGM and Ce(IV) in indirect contact with human primary fibroblasts after 5 days measured by MTT assay. 2×10^4 fibroblasts were cultured in 1 mL of DMEM with 10% FCS supplemented with various concentrations of KGM for 1, 3, and 5 days. The results were compared to control cells without KGM. Results shown are mean $\pm$SD, (n=2) ***p<0.001 highly significant compared to control cells.
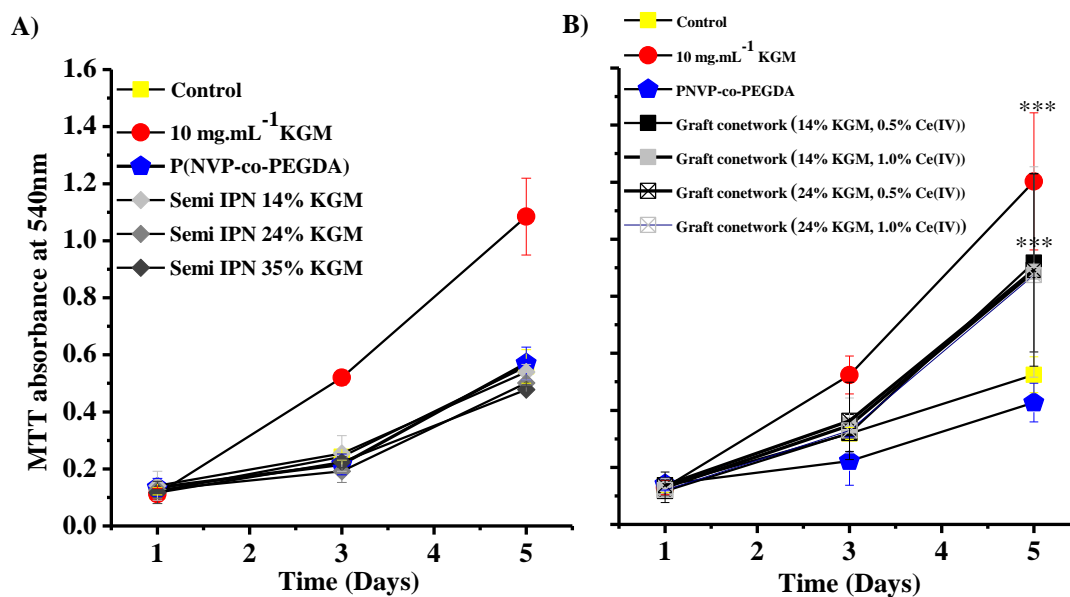
Figure 5.19   The effect of direct contact of A) semi-IPN and B) graft-conetwork hydrogels with increasing concentrations of KGM and Ce(IV) on the viability of human primary fibroblasts measured after 1, 3 and 5 days using MTT assay. $2x10^4$ fibroblasts were cultured in 1 mL of DMEM with 10% The results were compared to control cells without KGM. Results shown are mean $\pm$SD, (n=2), ***p<0.001 highly significant compared to control cells.

5.2.9 Attachment of human dermal keratinocytes on graft-conetwork hydrogel (24 % (w/v) KGM with 1.0 % (w/v) Ce(IV).

Keratinocytes attachment on graft-conetworks and dependency on fibronectin and i3T3 was investigated. Three different surfaces were used in this experiment; TCP, TCP coated with KGM and graft-conetwork of (24% (w/v) KGM, 1.0% Ce(IV) (w/v). The number of cell attached on these surfaces was measured using MTT assay (Figure 5.20).

The result shows few viable keratinocytes cultured on the KGM coated surface and on the hydrogel. It also found that fibronectin did not enhance keratinocyte attachment on the TCP, KGM coated surface and graft-conetwork (Figure 5.21 A-C). The presence of i3T3 was important for successful culture on the graft-conetworks hydrogel (in Figure 5.21C, more

keratinocyte attachment was seen on the hydrogel when the cells were cultured with i3T3 compared to without i3T3 cells).
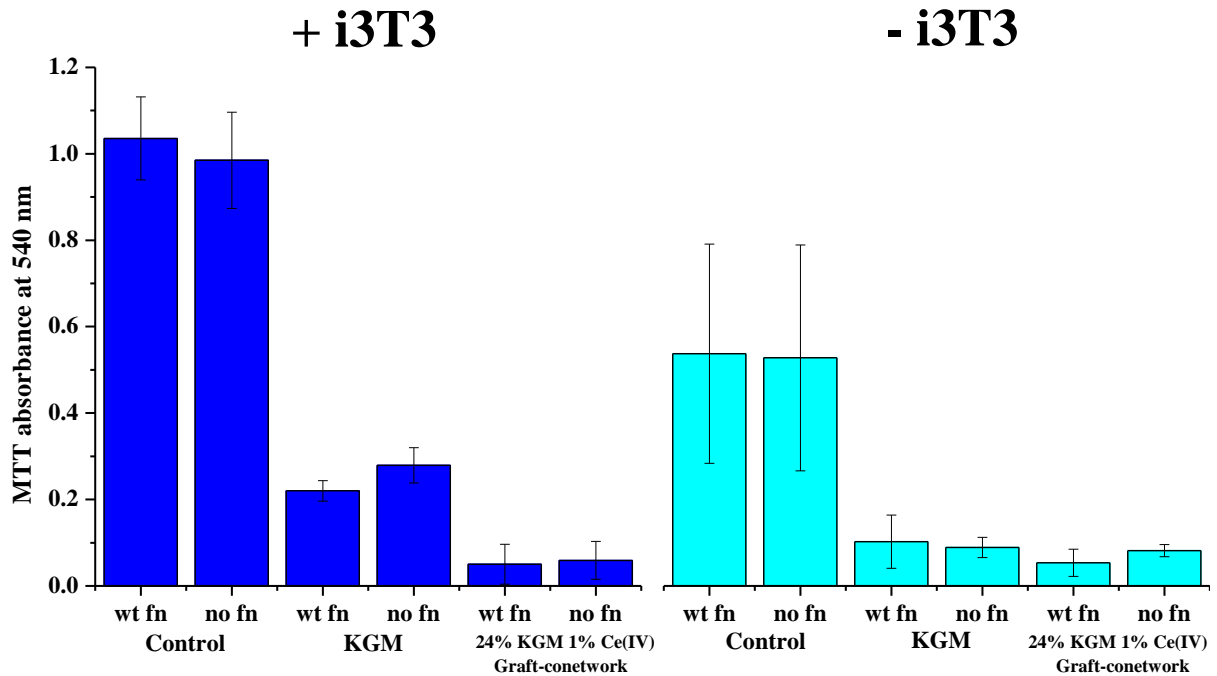
Figure 5.20   Measurement of keratinocyte viability cultured on TCP (control), KGM coated TCP and on graft-conetwork with and without i3T3 and fibronectin respectively. 1×10^5 keratinocytes were co-cultured with 2×10^4 i3T3 on different surfacesin 1 mL of 10% Green's medium. Assessment of keratinocyte proliferation was conducted by MTT assay. Results shown are mean $\pm$SD, (n=2), ***P<0.001 highly significant, **P<0.01 very significant and *P<0.05 significant in comparison to control.

Figure 5.21A Micrographs of the morphology of human keratinocytes in Green's media containing 10% FCS after 3 days of culture. Cells were cultured on tissue culture plastic in the presence and absence of i3T3 without fibronectin (A and C) and with fibronectin (B and D), respectively. (Scale bar: 100μm).

Figure 5.21B Micrographs of the morphology of human keratinocytes in Green's media containing 10% FCS after 3 days of culture. Cells were cultured on tissue culture plastic coated with 5 mg.mL^{-1} KGM in the presence and absence of i3T3 without fibronectin (A and C) and with fibronectin (B and D), respectively. (Scale bar: 100μm).
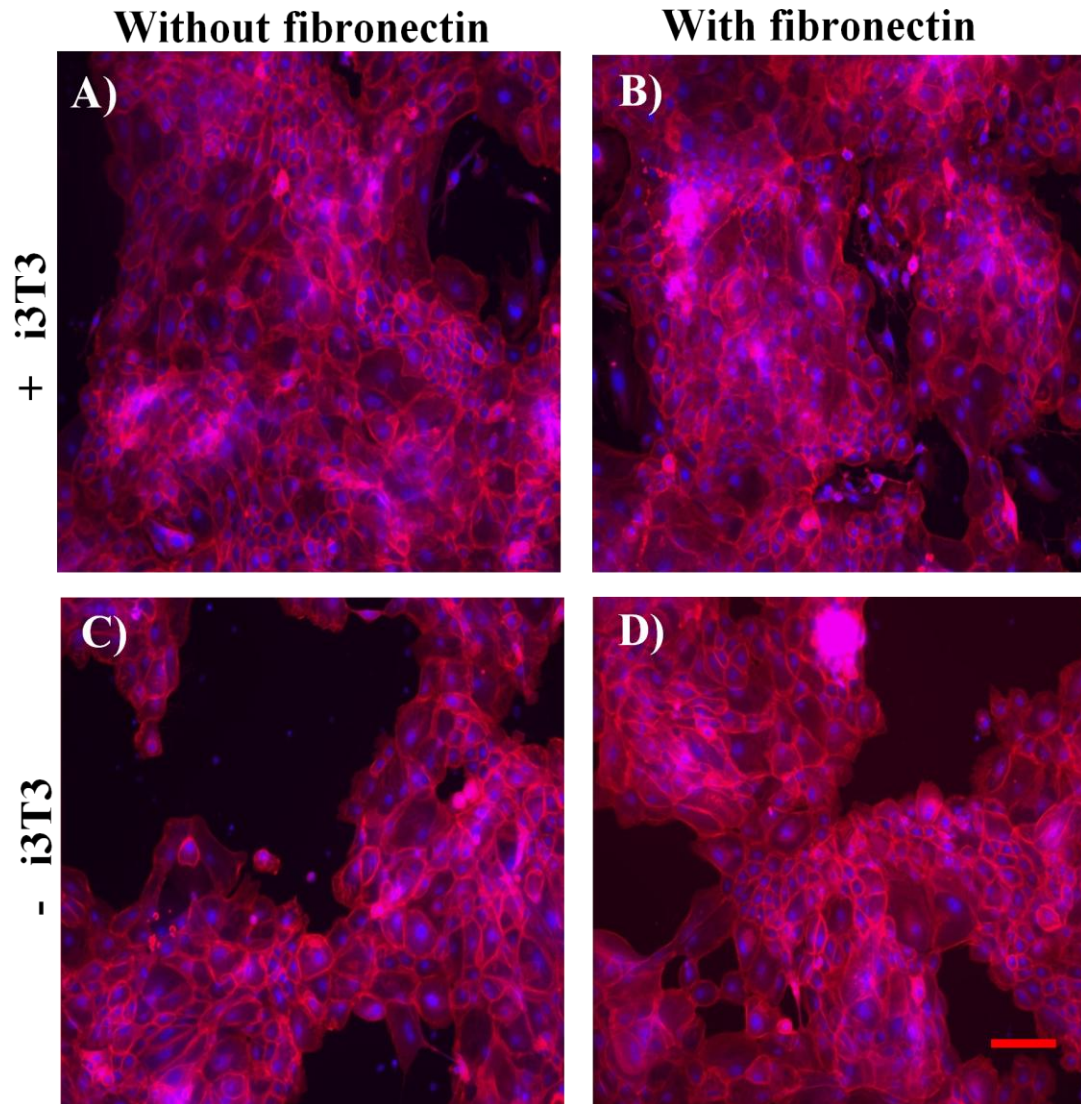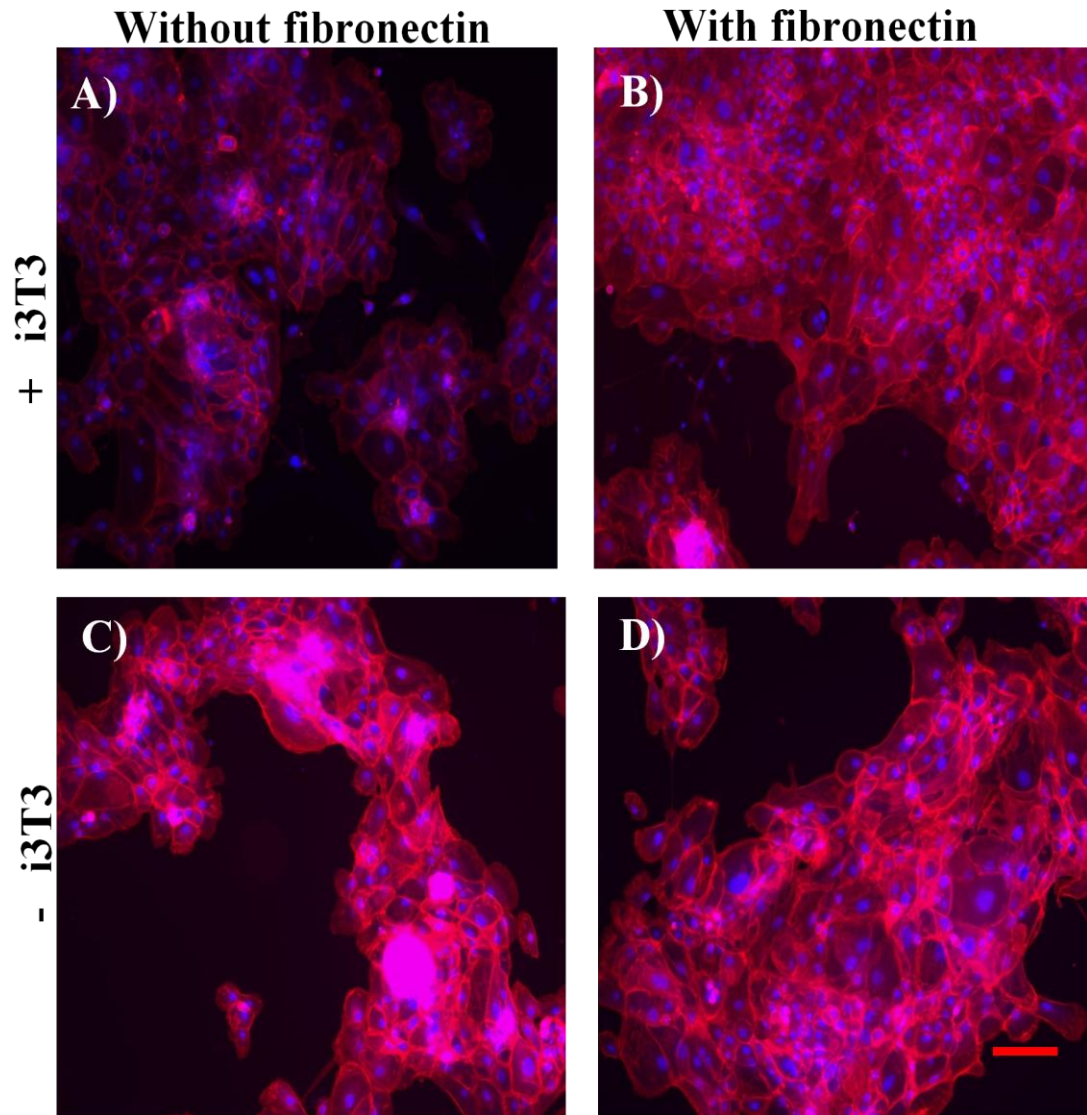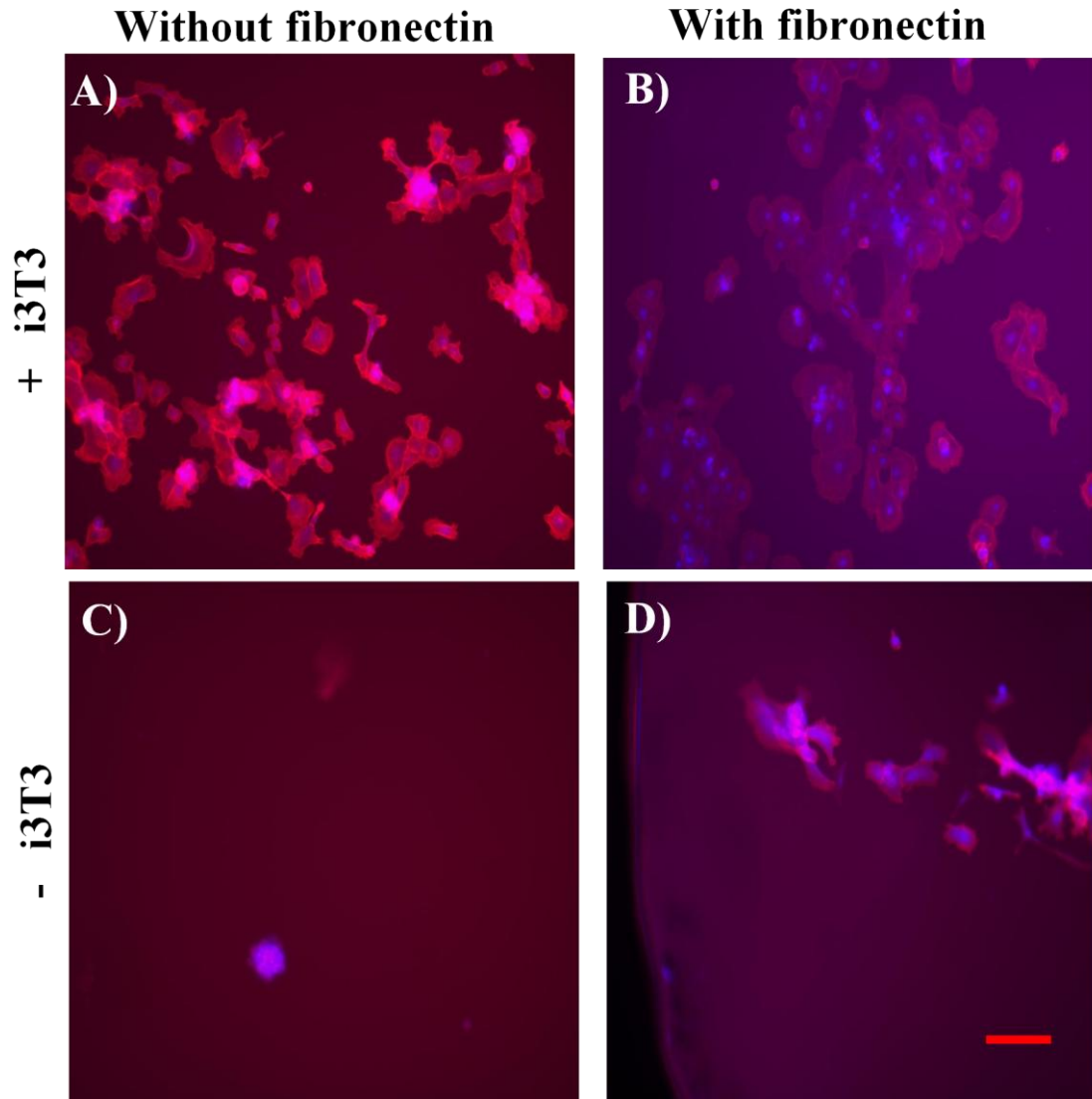
Figure 5.21C Micrographs of the morphology of human keratinocytes in Green's media containing 10% FCS after 3 days of culture. Cells were cultured on a graft-conetwork of 24% (w/v) KGM with 1.0% (w/v) Ce(IV) in the presence and absence of i3T3 without fibronectin (A and C) and with fibronectin (B and D), respectively. (Scale bar: 100 μm).

5.2.10 Attachment of human dermal fibroblasts on a graft-conetwork of (24% (w/v) KGM with 1% (w/v) Ce(IV).

Human dermal fibroblasts were seeded on different surfaces A) TCP, B) P(NVP-co-PEGDA) and C) graft-conetwork of 24 % (w/v) KGM with 1% (w/v) Ce(IV) as shown in Figure 5.22and 5.23.   Fibroblasts did not attach on the plain hydrogel but a small degree of fibroblast attachment was observed on the graft-conetwork, but the population was insignificant. Fibroblast attachment on the hydrogels was observed using Axon Instrument and SEM. Figure 5.21 (B) shows that fibroblasts did not attach on P(NVP-co-PEGDA) whereas the presence of attached cells was observed on graft-conetwork hydrogels (Figure 5.21 (C). However, observation the attachment of fibroblasts onto the hydrogel using SEM shows that the number of cell attached on the hydrogel surface was too low when compared to control (TCP) (Figure 5.22).
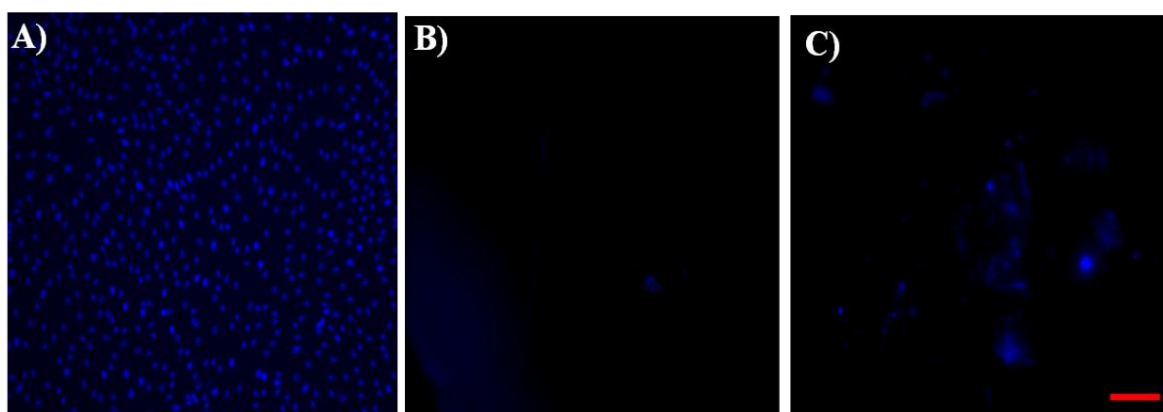
Figure 5.22 Micrographs of the growth and morphology of DAPI stained human dermal fibroblasts stained with after 5 days in culture using Axon Instrument. Cells were cultured on (A) TCP, (B) P(NVP-co-PEGDA) and (C) Graft-conetwork of 24% (w/v) KGM 1% (w/v) Ce(IV). (Scale bar: 100 µm).
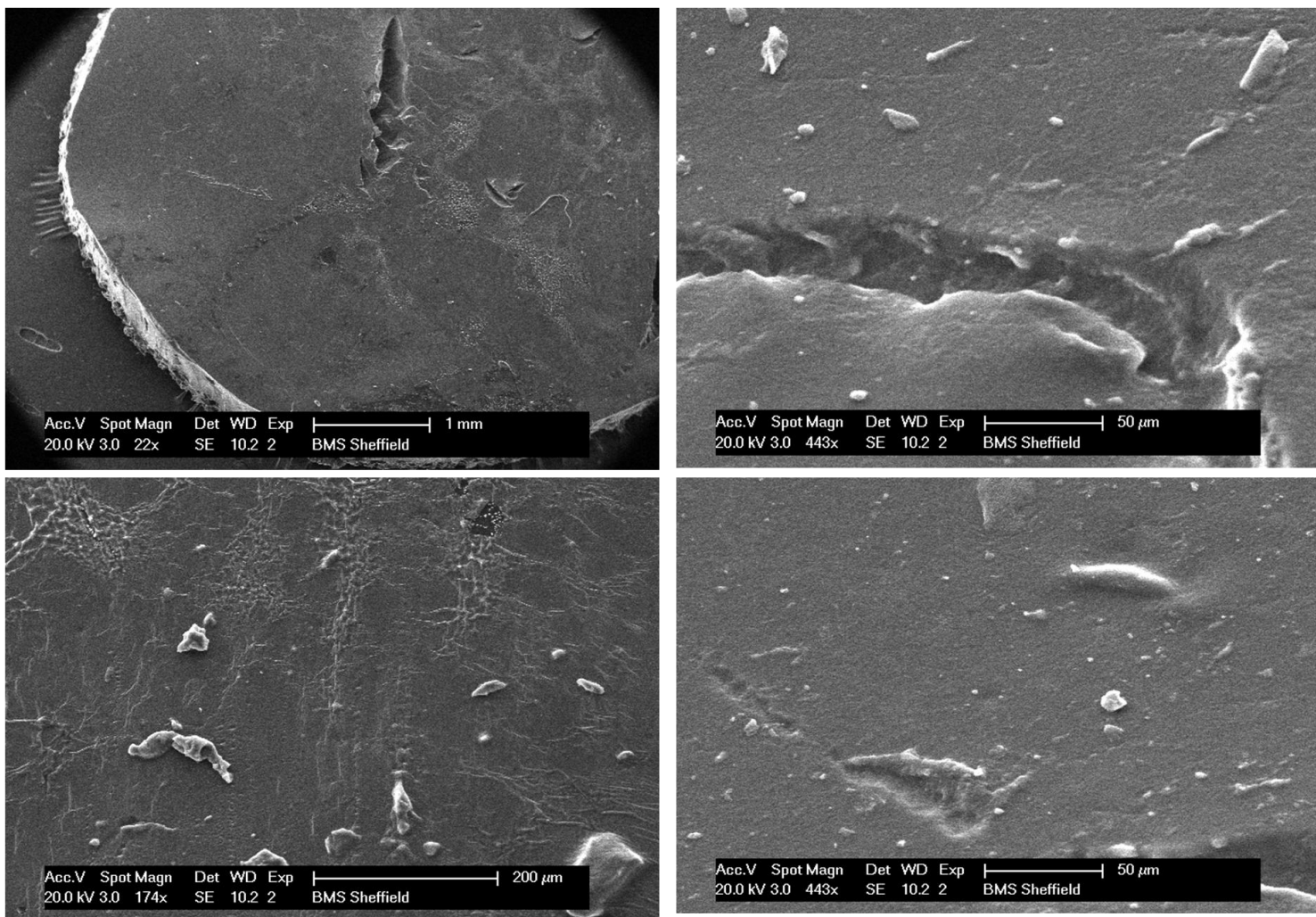
Figure 5.23 SEM micrographs of the growth and morphology of human dermal fibroblasts on graft-conetwork of 24% (w/v) KGM with 1% (w/v) Ce(IV) hydrogel.

227

5.3 Discussion.

The non-biodegradable, semi-IPN and graft-conetwork hydrogels were produced by photopolymerisation using HMPP as photoinitiator where Ce(IV) was added to create a graft-conetwork to initiate crosslinking of the KGM. Alteration of the chemical composition, initiators and the concentration of KGM, in the hydrogels changed the physical, mechanical and biological properties of the hydrogel. Both of the synthesized semi-IPN and graft-conetwork hydrogels were biocompatible, but only graft-conetwork was able to stimulate fibroblast proliferation. The mechanism of this interaction and cell behavior is not fully understood, but from this study, clues were directed to the differences in the chemistry, EWC, bound water and the content of KGM in the hydrogel.

The confirmation of the hydrogels' chemical structure measured using FTIR spectroscopy, where the presence of -1,4 linked glucosidic and β-1,4 linked mannosidic linkages in crosslinked KGM were observed at 1027-1244 cm^{-1} and also detected in both semi-IPN and graft-conetwork (Hua, Zhang et al. 2004; Widjanarko, Nugroho et al. 2011). In semi and graft-conetworks the shifting of peaks 1666 to 1720 cm^{-2} assigned to C=O acetyl group and 1030 to 1095 cm^{-1} assigned to C-O and C-N group, respectively suggest the formation of crosslinks in KGM and P(NVP-co-PEGDA) to form an IPN (Guo, Huang et al. 1996; Lewandowska 2011). The peak at 1727 cm^{-1} was low in KGM compared to P(NVP), suggesting of more C=O acetyl group in P(NVP) (Chen, Liu et al. 2005) while the mannose group which appeared at 808 and 745 cm^{-1} in crosslinked KGM were shifted to 875 cm^{-1} in semi-IPN and graft-conetwork hydrogels (Hua, Zhang et al. 2004; Xu, Luo et al. 2009; Widjanarko, Nugroho et al. 2011).

The morphological appearance of KGM in the IPN hydrogels were confirmed by SEM micrographs of the hydrogel's cross section. Whilst all hydrogels' surfaces showed smooth interfacial morphologies, the cross section of KGM containing hydrogels appeared to have

porous structures. The porous structure and the formation of crosslinking in the semi-IPN and graft-conetwork have profound effects on the hydrogel's EWC and bound water. The decrease in bound water in graft-conetwork compared to semi-IPN with the same concentration of KGM may relate to the changes in the chemistry of KGM when Ce(IV) was added into the formulation.

The KGM content in both semi-IPN and graft-conetwork hydrogels quantified using toluidine blue staining (which stains high molecular weight sugars such as heparin) (Smith, Mallia et al. 1980) confirmed the presence of KGM in the hydrogels. This also showed that the formation of crosslinked KGM in graft-conetworks with higher concentration of Ce(IV) may have altered KGM chemical composition, thus resulting in reduced KGM content compared to semi-IPN. This was confirmed by ^{13}C NMR spectroscopy with the decrease of KGM's assignment peaks at 62, 71, 75, and 102 ppm in full IPN compared to semi-IPN which had no Ce(IV).

The phase transition of semi-IPN and graft-conetwork hydrogels was measured using DSC. P(NVP) and PEGDA are rigid polymers with T_g at 158 and 54°C, respectively (Priola, Gozzelino et al. 1993; Cauich-Rodriguez, Deb et al. 1996). The polymerisation of P(NVP-co-PEGDA) gave a broad curve with two shoulder peaks at 143, and 153°C, and a narrow peak at 143°C, depicting the presence of different chemical compositions in the copolymerisation. The shape of the peak for semi-IPN with 24% (w/v) KGM was similar to P(NVP-co-PEGDA) with shoulder peak at 143°C and a narrow peak at 153°C. The increasing concentrations of KGM and the addition of Ce(IV) in graft-conetwork significantly increase the T_g of the hydrogels. T_g value for semi-IPN with 35% (w/v) KGM was higher compared to semi-IPN with 14 and 24% (w/v), which indicated the existence of stronger interactions in the system and the shifting of phase transition with increasing concentration of KGM. The similar trend was also observed in graft-conetwork with 14 and 24% (w/v) KGM. From the

thermograms in Figure 5.9 it was shown that only semi-IPN with 35% (w/v) KGM and graft-conetwork with 14% (w/v) KGM and 1% (w/v) Ce(IV) displayed a distinct peak that would be indicative for full IPN. The endothermic peaks for graft-conetwork with 24% (w/v) KGM initiated using 0.5 and 1% (w/v) Ce(IV) appeared to be very broad and showed sign of degradation with exothermic peaks at around 290°C as was seen with crosslinked KGM with higher concentrations of Ce(IV) which was mentioned in the previous chapter. The broad peak and higher T_g were concluded to be induced by the formation of crosslinks in KGM and its interaction with P(NVP-co-PEGDA). The endothermic peaks for graft-conetwork of 14% (w/v) KGM with 1% Ce(IV) and graft-conetwork of 24% (w/v) KGM with 0.5 and 1% (w/v) Ce(IV) displayed complex mixture of copolymerisation with the appearance of shoulder on the broad peaks. Exothermic peak was observed in both graft-conetwork of 24% (w/v) KGM with 0.5 and 1% (w/v) Ce(IV). The endothermic and exothermic peaks for both graft-conetwork of 24% (w/v) KGM with 0.5 and 1% (w/v) Ce(IV) appeared to be in the same range with T_g around 151 and 142°C and exothermic peaks at about 310 and 318°C, respectively. This result also confirmed that the presence of Ce(IV) may strongly influenced the conformational changes in the IPN and affected hydrogel's thermal behavior.

Further in this chapter, correlation between the changes in the chemical composition of KGM in semi-IPN and graft-conetwork with water interaction were investigated using EWC and free water measurement. The EWC of a hydrogel is of a great interest for controlled release application and degradation. Hydrogel swells due to the increase in its segmental mobility of polymeric chains when water diffuses into the network of polymers. The expansion in the size of the hydrogel due to swelling also affects the distance between the polymeric chain, which may be influential in cell-material interactions. The EWC for semi-IPN decreased from 95 to 86% with increasing concentrations of KGM from 14, 24 to 35% (w/v) whereas the EWC for all graft-conetwork hydrogels were in the range of 82-85%. The EWC for 35%

(w/v) KGM semi-IPN was similar to graft-conetwork, reflecting the correlation with a tighter, denser gel morphology resulted from higher concentration of KGM with the formation of crosslinked KGM in P(NVP-co-PEDGA) network by Ce(IV).

The state of water molecules within the hydrogels was probed by DSC. Water molecules can be classified as bound water or free water based on heating experiment on hydrated samples. Unlike bound water which involves hydrogen bonding, free water has good mobility inside the hydrogel since it has no interaction with the polymer and was associated with a sharp endothermic peak appearing around $0^{o}C$ which similar pure water in terms of transition temperatures, enthalpies and DSC curves (Kim, Lee et al. 2004). The amount of free water in the hydrogel was approximately calculated as the melting endothermic energy for pure water per mg of sample.The melting point of free water in all samples appeared to be above $0^{o}C$, due to the presence of dense polymeric network chains in the hydrogel, not due to the binding of water to the polymer as bound water did not show any endothermic peak in the temperature range of -70 to $0^{o}C$ (Kim, Lee et al. 2004).

From these observations, it is clear that the increase in EWC is attributed mainly to the free and bound water content in the hydrogel. Another factors that could have been contributing to this effect are the presence of crosslinks in the network that limited the content and binding of water with the hydrogel and the ionic repulsion of $-COO^-$ ions, where dissociation of hydrogen bonding induce the increase of bound water in the hydrogel (Mahdavinia, Pourjavadi et al. 2004). It was also found that the increase of crosslinks in the hydrogels did not only reduced EWC and the presence of free water in the hydrogels, but also changing KGM's chemical structure and content inside the hydrogel confirmed by ^{13}C NMR and toluidine blue staining, which was widely used to identify the presence of high molecular weight sugar such as heparin in a substance (Smith, Mallia et al. 1980).

Clearly, the difference in the structure and chemical properties of these materials produces

changes in biological activities of the cells. Thus, semi-IPN have higher EWC, free water and KGM content compared to graft-conetwork, where the KGM was crosslinked by addition of Ce(IV). The consequence of the formation of crosslinks in the IPN led to the decrease of EWC, which may relate to the mitogenic effect of P(NVP)-co-DEGBAC on fibroblasts viability (Smith, Rimmer et al. 2006). Also, the formation of crosslink in the IPN led to the increase of T_g and phase separation as were observed in DSC thermograms.

This study also showed that, in common with most non-charged hydrogels, the graft-conetwork of KGM was not good for keratinocyte and fibroblast attachment even in the presence of i3T3 and fibronectin. There are a number of factors that affect cell adhesion onto polymer; polymeric surface charge, the presence of specific surface chemistry (i.e. peptides or alkyl amines) water content and structure and the type of cells (Lydon, Minett et al. 1985; Schneider, English et al. 2004). The link between water content of hydrogel on cell adhesion had been described where high water content disabled protein adsorption onto the polymer and discourage cell attachment (Rimmer, German et al. 2005). Cells require integrin interactions or the presence of adsorbed proteins to attach onto polymeric surface. Integrins are cell surface receptor that anchor cells to the ECM and transduce signals to regulate cell functions such as adhesion, migration, differentiation and proliferation. Integrins also regulate cytoskeletal organization. The presence of proteins such as fibronectin, laminin or vitronectin is required to enhance cell attachment onto some surfaces (Nuttelman, Mortisen et al. 2001) but of course these proteins must be adsorbed in active conformations. Approaches such as amine functionalization and tethering with RGD peptides help to improve cell attachment and growth (Rimmer, Johnson et al. 2007; Perlin, MacNeil et al. 2008; Shahbuddin, Park et al. 2009) to hydrogels.

The results present in this chapter suggest that the biological activities of semi-IPN and graft-conetwork are not controlled only by the chemical structure of the polymer but also by the

amount of free water present in the hydrogel. Also, the biological effects on the stimulation and inhibition of fibroblasts and keratinocyte viability are the results of a dynamic interaction between the cells and the gels via cell specific receptors (i.e. lectin). The effect also might be attributed to hydrogel's ability to absorb mitogen from the medium and acting as a reservoir to the cells (Smith, Rimmer et al. 2006). The hydrogel may also function as a diffuser for cell metabolic waste and at the same time supplying nutrients to the cells. The detailed mechanism of action clearly would require further studies but given graft-conetwork advantageous in stimulating fibroblasts viability, this could be potentially useful for wound healing.

5.4 Conclusions.

The semi-IPN and graft-conetwork hydrogels were prepared successfully from P(NVP), PEGDA and KGM via free radical polymerisation using HMPP and Ce(IV) as initiators. The experimental results from FTIR, DSC, ^{13}C NMR, EWC, free water content, toluidine blue staining and biological studies using MTT assay reveal that conformational changes in full IPN hydrogels resulting in lesser EWC, free water and KGM content play significant roles in affecting the biological activities of skin cells. The measurement of DSC confirmed that graft-conetwork possessed broader peak compared to semi IPNs, owing to the formation of crosslinks in the bipolymers. The synergistic interactions and formation of crosslinks initiated by HMPP and Ce(IV) was also confirmed by FTIR, where both semi-IPN and graft-conetwork displayed all characteristic peaks assigned to P(NVP-co-PEGDA) and KGM except for the peak at 1727 cm^{-1}, which shifted to 1635 cm^{-1}. It is also worth noting that the ability of hydrogel to absorb water decreased with the formation of crosslinks in the hydrogel.

Chapter 6. The effect of KGM, xanthan and KGM-xanthan blend hydrogel for cell transportation.

6.1 Introduction.

There are relatively few publications on how to transport cultured cells for clinical use as discussed in (Eves, Baran et al. 2011). For long term storage of cells, these are stored in liquid nitrogen. Cells can be transported frozen in liquid nitrogen, especially where there is a short delivery time window, however, this is both challenging and expensive (Day and Stacey 2007). Also, some researchers have reported cryopreservation of cells to be unreliable due to detrimental effects of dimethyl sulfoxide (DMSO), which is not suitable for cell therapies and linked to cell membrane damage (Volden, Haugen et al. 1980) and apoptosis (Cao, Li et al. 2007). Cryopreservation in liquid nitrogen requires equipment and also is labor intensive and requires that the cells during transport to be kept frozen (Chen, Zhang et al. 2009).

Polysaccharides of different origins such as pectin, galactomannan, dextran, alginate, chitosan or xanthan both individually or combined have great potential in assisting cell transportation due to their ability to maintain cell viability and they are biocompatible, inexpensive and abundant in nature (Mano, Silva et al. 2007; Farris, Schaich et al. 2009). Polysaccharide based hydrogels have gained significant interest as carriers and substrates to assist cell transportation compared to conventional cryopreservation methods. For example, alginate was found to support the short term preservation of corneal epithelial cells (Wright, Cave et al. 2012), and hMSC and mESC at room temperature in air tight containers with minimal medium content (Chen, Zhang et al. 2009). These transported cells were found to have similar levels of cell viability and expression of stem cell markers, proliferation rates and morphology as the stored cells.

Polysaccharides such as carrageenan and xanthan form strong helical confirmation structures with specific cations (Sato, Norisuye et al. 1984) while konjac glucomannan is a linear

polysaccharide with D-mannose and D-glucose in its structure (Fan, Zhu et al. 2007). The differences in mechanical properties and structure of these polysaccharide polymers enable the design of two skin scaffold layers for wound healing treatment (Almeida, Mueller et al. 2013). Although these polysaccharides individually may able to form hydrogels, often the hydrogels are either too hydrophilic – absorbing all medium in the well plate or very weak which makes the maintenance of the hydrogel's integrity very difficult. Blending two or more polysaccharides into a hydrogel provides better structural integrity and function that would be useful for the transportation of cells.

As mentioned earlier, KGM is a water soluble natural polysaccharide derived from the tuber of *Amorphophallus konjac* Koch which is composed of β-(1→4)-linked D-mannose and D-glucose with acetylated branches at every 19 molecules (Huang, Takahashi et al. 2002). KGM hydrogel has been demonstrated to maintain fibroblasts and ADMSC viability in unchanged media for up to 20 days, which is an attractive quality for cell transportation and preservation of cell viability (Shahbuddin, Shahbuddin et al. 2013).

On the other hand, xanthan is a microbial polysaccharide of bacterium *Xanthomonas campestris*, which consists of a cellulose backbone of (β-(1→4)-D-glucopyranose glucan with trisaccaride brances of (3→1)-α linked D-mannopyranose-(2→1)-β-D-glucoronic acid-(4→1)β-mannopyranose (Figure 6.1) (Sandford and Baird 1983). The confirmation is also an anti-parallel, double stranded helix which is less polydispersed than hydrocolloid and does not gel on its own (Li, Qi et al. 2009; Almeida, Mueller et al. 2013). The blend of Xanthan and KGM is particularly interesting, as the combination produced a synergistic interaction with good physiochemical and mechanical properties (Williams, Day et al. 1991; Goycoolea, Morris et al. 1995). It also produced a stronger gel compared to each material alone and was 4 times stronger than the xanthan-locus bean gum blend (Williams, Day et al. 1991).

The aim of this study was to examine the potential of KGM, xanthan and a KGM-xanthan

blend to assist cell transportation ideally across the whole of the UK and possibly Europe as previously investigated by Eves et. al (Eves, Baran et al. 2011). The gold standard for cell culture is incubation in a well maintain environment of $37^{\circ}C$, 5% CO_2 and 95% O_2 with bicarbonate buffer to maintain the pH to be around 7.4 (Eves, Baran et al. 2011). Usually patients have to travel to receive effective treatment which can be inconvenient, time consuming and expensive (Eves, Baran et al. 2011). Cell survival up to 24 hours is essential for transportation as usually that amount of time is required for travelling inside the country while 48 and 72 hours, would enable cell transportation across European continent and to other parts of across the world (Eves, Baran et al. 2011).

Chapter 3 discussed KGM's ability to maintain fibroblasts and ADMSC culture in unchanged media up to 20 days (Shahbuddin, Shahbuddin et al. 2013) and to stimulate fibroblast viability and proliferation when placed in direct contact with the hydrogels. These findings led to the investigation of the potential use of KGM, KGM blends and crosslinked hydrogel for cell transportation. The chapter discusses very brief on the basic characterization of KGM and KGM-xanthan blend hydrogels and also examined the potential of these hydrogels (and crosslinked KGM) to maintain cell viability during the transportation up until 24 hours with mechanical stimulation. In this experiment, to mimic the mechanical trauma and variation in temperature outside the incubator, the cells in a 12 well plate were placed in direct contact with the hydrogels and placed inside the incubator (as control) and outside the incubator on a rocking shaker subjected to an upward and downward movements with a minimum speed of 4 rpm.
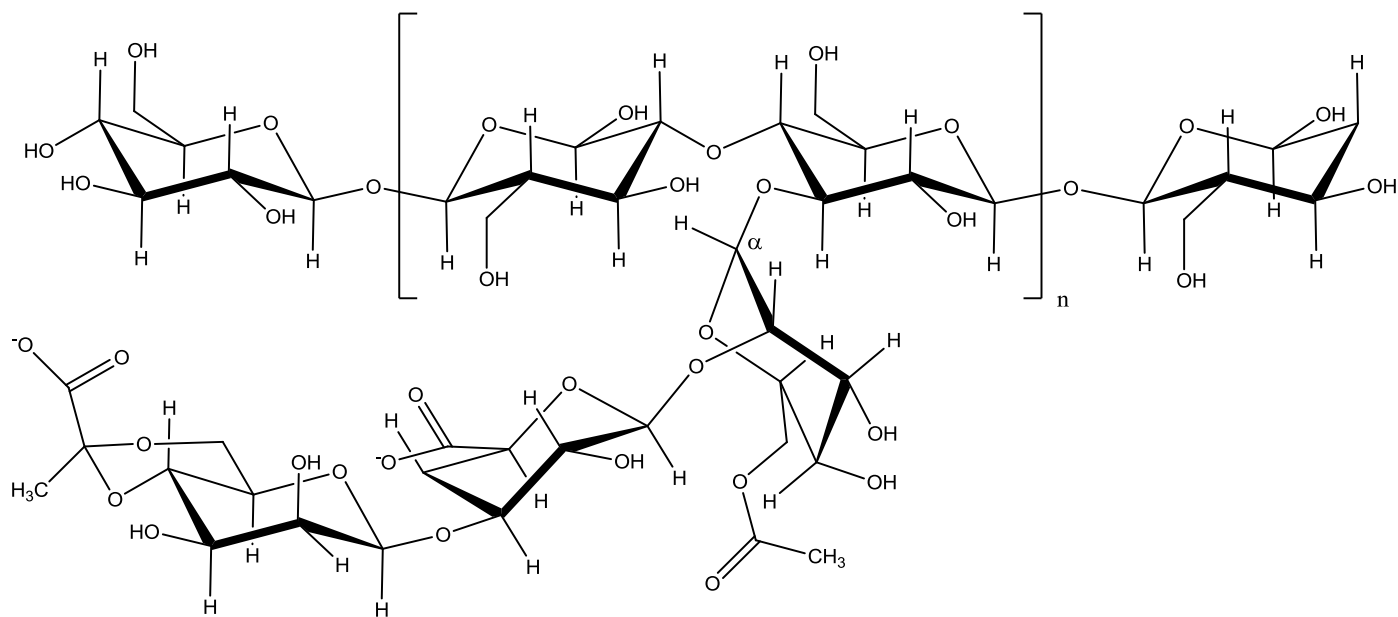
A) Xanthan gum
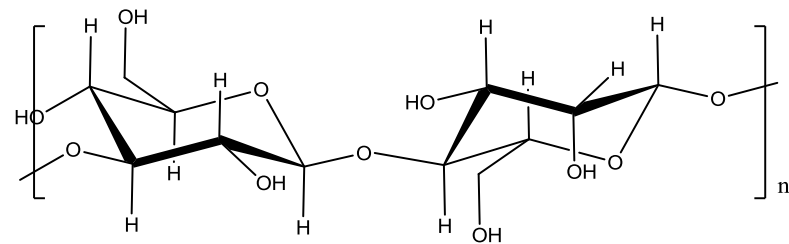
B) Konjac glucomannan

Figure 6.1 Chemical structures of (A) xanthan gum and (B) KGM.

6.2 Results.

6.2.1 Characterization of KGM, xanthan and KGM-xanthan blend hydrogels.

The physical appearance of KGM, xanthan and KGM-xanthan blend hydrogels are shown in Figure 6.2. The picture shows that a blend of KGM-xanthan had better physical integrity than each material on its own which might be attributed to the synergistic interaction between KGM and xanthan as was reported previously (Williams, Day et al. 1991; Li, Qi et al. 2009).
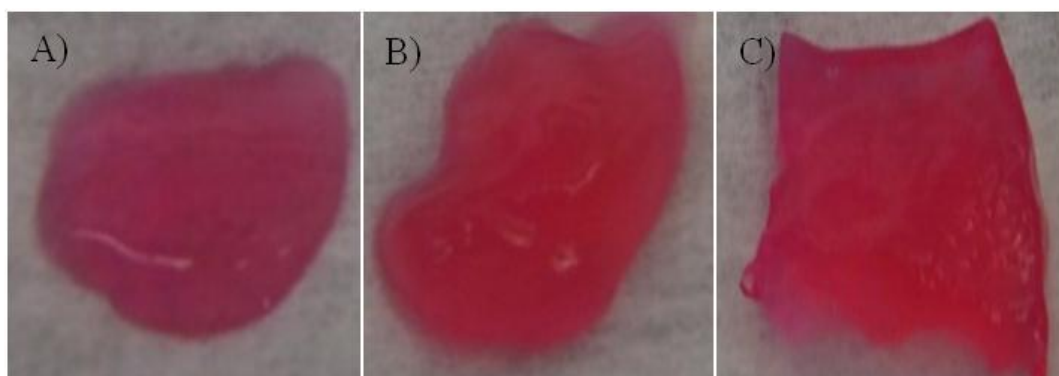
Figure 6.2 The physical appearance of (A) KGM, (B) xanthan and (C) KGM-xanthan blend hydrogels**.**

The chemical structures of the hydrogels were investigated using FTIR, where the conformational changes and intermolecular interaction of each polymer in the binary blend were measured. The IR spectra of each polymer with its characteristic bands are shown in Figure 6.3. All polymers show the characteristic absorption band of OH- at around 3400-3500 cm^{-1}. The characteristic absorption bands of the mannose in KGM located at 745 and 875 cm^{-1} were observed in the KGM and also in blend KGM-xanthan hydrogel as was mentioned by Mathlouthi et al. (Mathlouthi and Koenig 1986).. The deformation of water molecules which are bound water of crystallization was observed in all hydrogels at 1647 cm^{-1}, and was confirmed by Gao et. al (2001) and Zhang et. al (2001) (Gao and Zhang 2001; Zhang,

Yoshimura et al. 2001). The band positons of KGM and xanthan was also shifting to lower wave number, indicating a gradual increase of intermolecular hydrogen boinds between KGM and xanthan. This was more marked at 1250 cm^{-1} at KGM/xanthan blend where the assignment shifted from 1247 cm^{-1} in KGM and 1261 cm^{-1} for xanthan spectra, This could also indicate the changes and association of KGM-xanthan blends with newly formed hydrogen bonds (Li, Qi et al. 2009). Another possibility to the shifting of peak may be due to bound water in xanthan-KGM chain association with respect to the pure components. The peaks at 1424 and 1144 cm^{-1} in KGM-xanthan blend retain the characteristic peak from KGM while 1372 cm^{-1} retain the peak from xanthan. Table 6.1 summarises the IR spectra peaks of KGM, xanthan and KGM-xanthan hydrogels
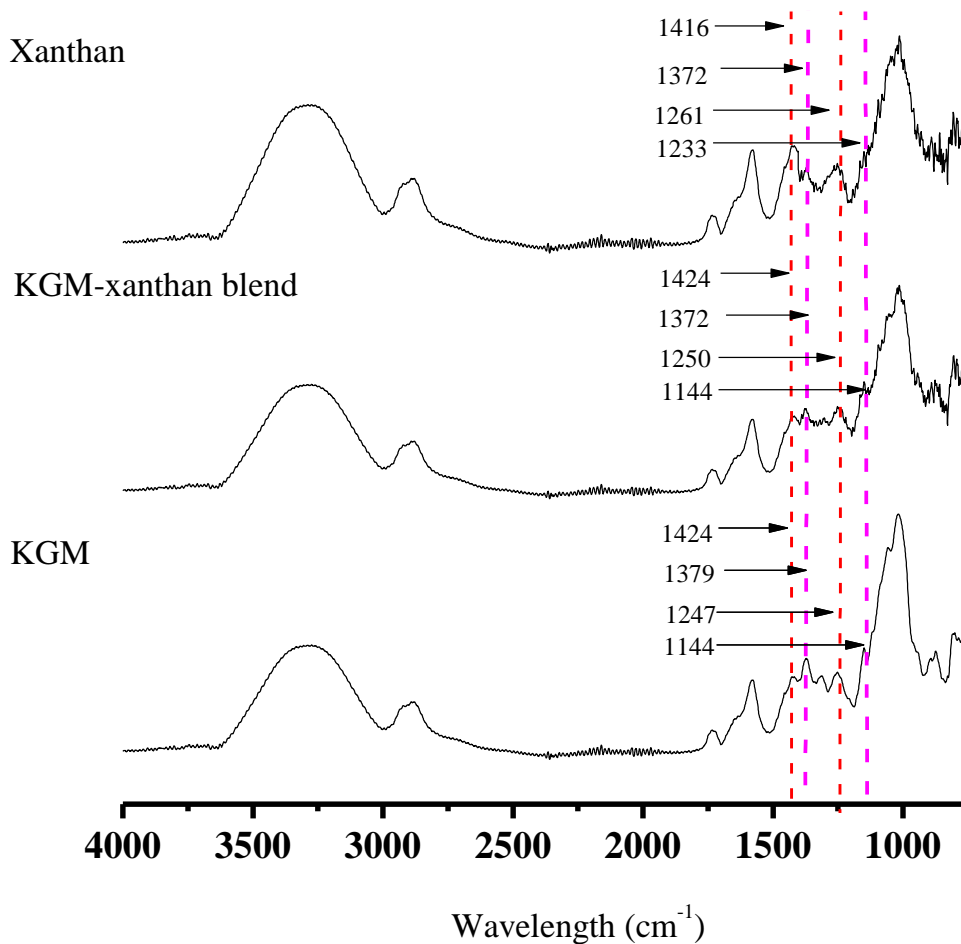
.

Figure 6.2 FTIR spectra of KGM, xanthan and KGM-xanthan blend hydrogels. The line (red) indicate characteristic peak in xanthan and (purple) indicate characteristic peak of KGM.

Table 6.1　　A summary of the peaks observed in FTIR spectra in Figure 6.2

Peak (cm^{-1})	Assignments	KGM	Xanthan	KGM-xanthan blend	Reference
3397-3430	-OH-	√	√	√	(Dumitriu, Magny et al. 1994; Kačuráková and Mathlouthi 1996; Li, Qi et al. 2009; Xu, Luo et al. 2009; Widjanarko, Nugroho et al. 2011)
2953	-CH$_2$- in C-CH$_3$	√	√	√	(Williams, Day et al. 1991; Dumitriu, Magny et al. 1994; Kačuráková and Mathlouthi 1996; Xiao, Liu et al. 2001; Widjanarko, Nugroho et al. 2011)
1730	C=O	√			(Williams, Day et al. 1991; Kačuráková and Mathlouthi 1996; Xiao, Liu et al. 2001; Chen, Liu et al. 2005)
1640	β-1,4 linked glucose in glucomannan		√	√	(Williams, Day et al. 1991; Li, Qi et al. 2009; Xu, Luo et al. 2009; Widjanarko, Nugroho et al. 2011)
1375	-CH$_2$-	√	√	√	(Mathlouthi and Koenig 1986; Száraz and Forsling 2000; Pandey and Pitman 2003; Vaaler 2008; Widjanarko, Nugroho et al. 2011)
1240-1260	C-O-C stretch	√	√	√	(Williams, Day et al. 1991; Dumitriu, Magny et al. 1994; Widjanarko, Nugroho et al. 2011)
1150-1140	-CH$_2$-	√			(Williams, Day et al. 1991; Dumitriu,

			241	Magny et al. 1994; Guo, Huang et al. 1996; Xiao, Liu et al. 2001)
1050	C-O	√	√	(Dumitriu, Magny et al. 1994; Widjanarko, Nugroho et al. 2011)
941				
891	-CH- in mannose		√	(Mathlouthi and Koenig 1986; Hua, Zhang et al. 2004; Li, Qi et al. 2009; Xu, Luo et al. 2009; Widjanarko, Nugroho et al. 2011)
872	-CH- in mannose	√		(Mathlouthi and Koenig 1986; Hua, Zhang et al. 2004; Li, Qi et al. 2009; Xu, Luo et al. 2009; Widjanarko, Nugroho et al. 2011)
	-CH- in mannose	√		(Hua, Zhang et al. 2004; Xu, Luo et al. 2009; Widjanarko, Nugroho et al. 2011)
745	-CH- in mannose	√		(Mathlouthi and Koenig 1986; Hua, Zhang et al. 2004; Widjanarko, Nugroho et al. 2011)

6.2.2 The effect of KGM, xanthan and KGM-xanthan blend hydrogels on the transportation of fibroblasts.

KGM, xanthan and the blend hydrogel of KGM-xanthan significantly increased cell viability after 24 hr in an incubator but not outside the incubator subjected to an upward and downward movement by a rocking machine for a specific time (Figure 6.3). A significant increase in cell viability outside the incubator was observed only with KGM not xanthan or KGM-xanthan blend hydrogels after 18 and 24 hr.

6.2.3 The effect of KGM and crosslinked KGM hydrogels on the transportation of fibroblasts.

The effect of KGM and crosslinked KGM hydrogels with increasing concentration of Ce(IV) on the transportation of fibroblasts outside the incubator is shown in Figure 6.4. Both KGM and crosslinked KGMs with (1% (w/v) KGM with $1x10^{-3}$ % (w/v) Ce(IV)) significantly increased fibroblast viability both within the incubation and outside incubation conditions after 24 hr.
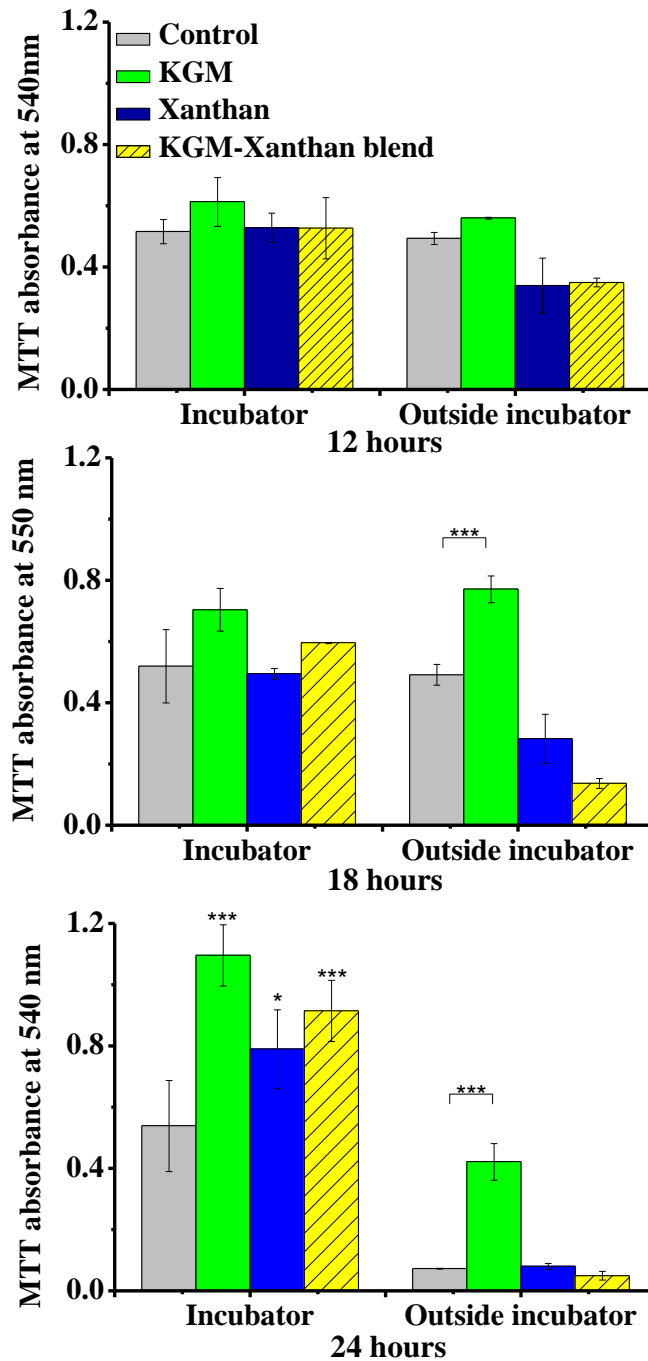
Figure 6.3 The effect of KGM, xanthan and KGM-xanthan blend hydrogels for the transportation of fibroblasts, where the cells outside of the incubator is subjected to an upward and downward movements using a rocking machine. Cell viability was measured after 12, 18 and 24 hr using MTT assay. 1×10^5 fibroblasts were cultured in 1 mL of DMEM with 10% FCS. The results were compared to control cells without KGM. Results shown are mean $\pm$SD, (n=2), ***p<0.001 highly significant, **p<0.01 very significant and *p<0.05 significant compared to control.

Figure 6.4 The effect of KGM and crosslinked KGM for the transportation of fibroblasts, where the cells outside of the incubator is subjected to an upward and downward movements using a rocking machine. Cell viability was measured after 12, 18 and 24 hours using MTT assay. $1x10^5$ fibroblasts were cultured in 1 mL of DMEM with 10% The results were compared to control cells without KGM. Results shown are mean $\pm$SD, (n=1), ***p<0.001 highly significant, **p<0.01 very significant and *p<0.05 significant compared to control.
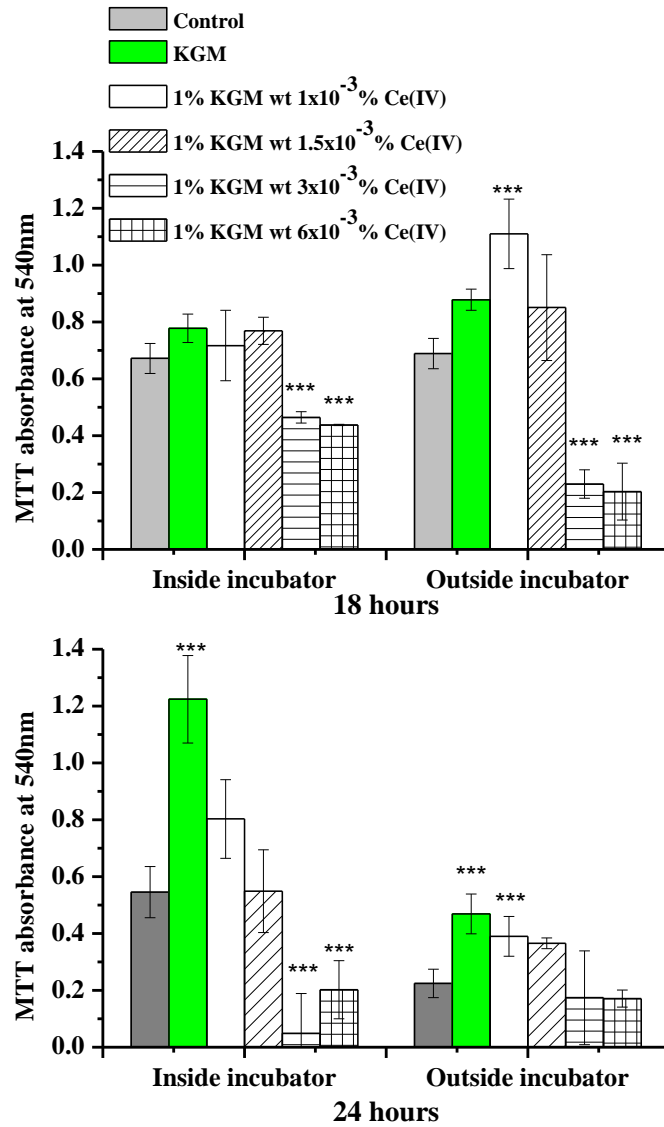
6.3 Discussion.

There were no apparent differences in the molecular confirmations of KGM, xanthan and KGM-xanthan blend hydrogels, noting that the intermolecular interaction between KGM and xanthan was mainly physical. Also, the chemical configuration and structures of both polymers were similar with an abundance of hydroxyl groups at the backbone and branches. Although there were no differences except the peaks at 2028 and 2159 cm^{-1} in xanthan and KGM-xanthan blend hydrogels, the occurrence of hydrogen bonds in the synergistic interaction between KGM and xanthan was suggested by Li et al. (2009). This supports the difference in xanthan physical integrity and stability when in combination with KGM (Almeida, Mueller et al. 2013).

The results shown in Figure 6.3 show that KGM and crosslinked KGM ((1% (w/v) KGM wt 1x10^{-3} % (w/v) Ce(IV)) were able to stimulate and maintain cell viability within an incubator and also outside of incubation conditions. The latter begins to mimic the transportation of cells.

In this chapter, the synthesis of KGM-xanthan blend hydrogel was explored where the synergistic interaction between these two polymers formed stronger hydrogel compared to each material alone. Also, further in this chapter, the potential use of KGM, KGM-xanthan blend and crosslinked KGM in assisting the transportation of fibroblasts was explored. KGM, xanthan, crosslinked KGM (1% (w/v) KGM with increasing concentration of Ce(IV) and KGM- xanthan blend were prepared and used to aid cell transportation in laboratory conditions and outside of an incubator with continous upward and downward movements of shear stress of 4 rpm using a rocking machine. All, KGM, xanthan and KGM-xanthan blend hydrogels stimulated the increase of cell viability inside an incubator after 18 and 24 hours, however only KGM was abled to maintain 50% of cell viability at outside the incubator subjected to continous shear stress for 24 hours. The ability of KGM to suppor cell viability

after 24 hours of shear stress at outside incubator condition reveal greater potential of this polysaccharide for cell transportation studies, supported by previous study which shown KGM's ability to maintain fibroblasts and ADMSC in nutrient deprived condition up to 20 days (Shahbuddin, Shahbuddin et al. 2013)

KGM and crosslinked KGM (1 % (w/v) with $1x10^{-3}$% (w/v) Ce(IV)) were both stimulatory to fibroblast viability in both conditions. It was unknown why KGM and crosslinked KGM were stimulatory to fibroblast viability when placed at outside the incubator with mechanical stimulations compared to KGM-xanthan blend and xanthanhydrogels.

The stimulatory activity of KGM, xanthan and KGM-xanthan blend hydrogels on fibroblast viability in incubator may be related to cell's recognition ability, its interaction with different type of sugars (glucomannan, xanthan) and changes in the microenvironment due to contact with the hydrogel. The results shown in this chapter are particularly interesting and may be useful for further application in cell transportation across U.K. and Europe. It is necessary to conduct more studies and investigation to explore the exact benefit of these particular polysaccharides.

6.4 Conclusions.

Blend hydrogel of KGM-xanthan formed stronger material compared to each hydrogel on its own and able to stimulate and maintain fibroblast viability within an incubator, not at outside incubator with mechanical stimulations. However, KGM and crosslinked KGM were able to stimulate fibroblast viability in both conditions, and this support earlier finding on KGM's ability to stimulate and sustain fibroblast viability in unchanged medium condition up to 20 days.

Chapter 7. The effect of KGM hydrogels on the migration of skin cells.

7.1 Introduction.

In tissue engineering and regenerative medicine, biomaterials designed as templates with biophysical, chemical and mechanical cues to guide cellular behaviour and function to facilitate restoration of structure and function of damaged tissue (Langer 1995; Yannas 2000). Conductive biomaterials that support cellular adhesion, migration and proliferation would be greatly beneficial in acellular tissue repair/regeneration approaches (Yannas, Tzeranis et al. 2010). Biologically derived materials such as collagens from animal tissues and plant's polysaccharide have been extensively explored in the area of guided tissue regeneration (GTR) of skin and offer advantageous of cellular recognition, such as receptor-binding ligands and susceptibility to ECM degradation and remodelling mediated by cell-secreted proteases (Yannas 2000; Lutolf and Hubbell 2005).

Cell migration is essential for a variety of physiological and pathological processes such as wound healing, embryogenesis, cancer metastasis, immune surveillance and inflammation and angiogenesis (Lauffenburger and Horwitz 1996; Sternlicht and Werb 2001). Some materials, either synthetic, natural or combination of both, may need to be modified with specific cell recognition sequences to ensure good cell interaction with these scaffolds. This also can be achieved by adding concentrations of soluble signal factors or ligands that specifically bound to the ECM to promote positive cellular responses that would be beneficial for tissue regeneration (Lauffenburger and Horwitz 1996). The directional cell migration towards soluble signal factors is often referred as chemotaxis, whereas the migration towards an ECM gradient is referred as haptotaxis (Carter 1967). Cell migration in response to a chemoattractant requires at least five events; i) ligand-receptor interaction at the membrane surface, ii) intracellular signal transduction, iii) modification of cytoskeleton, vi) force

generation and v) cyclic establishment and release of adhesive contacts (Mow, Tran-Son-Tay et al. 1994). The transition of adherent cells to migration is often triggered by quantitative or qualitative alterations of ECMs and growth factors (Li, Fan et al. 2004).

Cellular migration is also a fundamental prerequisite for wound healing as during injury the cells at the wound edge will be the first to be in contact with human serum that would trigger cells to migrate into the defective site by dynamic regulation of their cytoskeleton (Sternlicht and Werb 2001). Cell migration can be characterized by the formation of stable and reoriented microtubules involving actin and tubulin and the formation of focal adhesions (Goulimari, Kitzing et al. 2005; Zhang, Bothe et al. 2006).
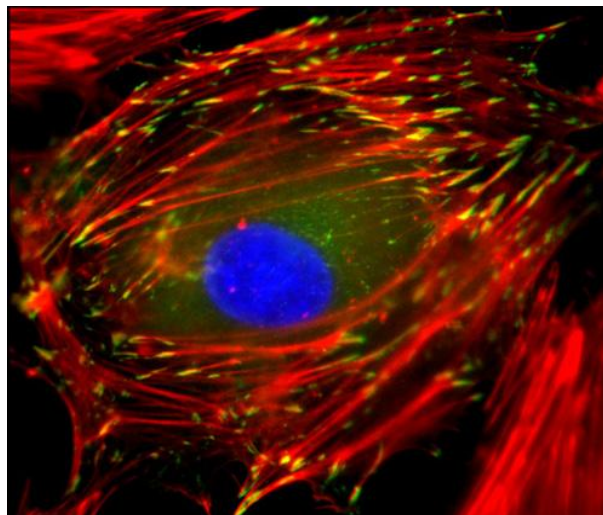

Figure 7.1 Fluorescent micrograph of endothelial cell's focal adhesion anchoring complexes (green), actin filament bundles (red), and nuclei on an extracellular matrix substrate. These structures provide mechanical forces to influence cellular adhesion, migration and morphology (Lele, Thodeti et al. 2006).

In particular, fibroblasts play a pivotal role in tissue repair by functioning as synthesizer cells to deposit collagen-rich matrix and signalling cells to secrete growth factors that are important for cellular communication during the repair process (Falanga 2005; Buonomo, Giacco et al. 2011). Delays in fibroblast function, such as caused by type 2 diabetes would affect normal wound healing process, resulting in chronic non-healing wound. For example,

the migration of adult diabetic fibroblasts was reported to be 75% slower compared to normal fibroblasts (Lerman, Galiano et al. 2003).

The measurement of cell migration can be conducted using a scratch assay which is particularly cheap, easy and well developed assay for the study of cell migration *in vitro* (Liang, Park et al. 2007). In this assay, an artificial gap is created on a confluent cell monolayer to observe the migration of cells to fill the denuded area and establish a new cell-cell contact (Liang, Park et al. 2007). The rate of cell migration is determined by image analysis that compares the size of denuded area from the beginning and the time of interval until the gap is closed (Liang, Park et al. 2007). This assay is advantageous for the study of cell migration as it mimics the extent of cell migration *in vivo* and is suitable to study the regulation of cell interaction with ECM and cell-cell interaction (Liang, Park et al. 2007). There are other methods to study cell migration such as a Boyden chamber, microfluidic-based systems and Electrin cell-substrate impedance sensing (ECIS). The Boyden chamber is not suitable for tracking individual cells, but relatively cheap compared to microfluidic-based system and ECIS which require nanofabrication facilities that are difficult to set up (Liang, Park et al. 2007).

It is also important to eliminate cell proliferation in the scratch assay as usually after 12-48 hours, most cells will enter mitosis. Many researchers have used Mitomycin C to inhibit cell proliferation in the study of cell migration (Li, Fan et al. 2004). Mitomycin C is a bifunctional alkylating agent and a potent DNA crosslinker that inhibits DNA synthesis, nuclear division and cell proliferation (Hoorn, Wagner et al. 1995). It is also a widely used as antibiotic because of its lack of toxicity with potent antitumor activity (Crooke and Bradner 1976; Doll, Weiss et al. 1985). Mitomycin C works by interacting with DNA and inhibits the synthesis of DNA, *in vivo* and *in vitro* by forming crosslinks between the complementary DNA strands (Ueda and Komano 1984). It is produced by a strain of actinomyces,

Streptomyces caepitosus and contains three different anti cancer moieties namely, quinone, urethane and aziridine groups (Wakaki, Marumo et al. 1958). Mitomycin C is used in glaucoma filtration surgery to reduce scarring by inhibit fibroblast proliferation (Daniels, Occleston et al. 1999). The effect of mitomycin C was reported to be dependent on the concentrations and duration of exposure to this antimetabolite (Remers and Vyas 1989). It is important to note that mitomycin C can arrest fibroblast proliferation after a single exposure to mitomycin C (Daniels, Occleston et al. 1999) However, mitomycin C is not able to stop fibroblasts from continuing to express growth factors, or forming ECM, which may explained why scars and restenosis occurred despite topical application of mitomycin C (Daniels, Occleston et al. 1999).

Cell integrins provide traction for cellular movement and also function as transmitters for ECM guidance signals (Lauffenburger and Horwitz 1996). The migration is more complicated in 3D compared to planar surface of 2D due to the complex environment of the ECM (Lauffenburger and Horwitz 1996). To overcome biophysical resistance of ECM, biologically derived materials offer the advantages of cellular recognition and degradation mediated by cell-secreted proteases (Lutolf and Hubbell 2005). In a previous chapter, KGM has shown strong affinity to mannose receptors and lectins that are implicated in the stimulation and proliferation of skin cells (Shahbudin, Shahbuddin et al. 2013). KGM's ability to mediate fibroblasts and keratinocytes proliferation would be very beneficial in the treatment of wounds, particularly in the promotion of collagen production by stimulation of fibroblast proliferation and reduction of skin contraction, by KGM's inhibition on keratinocyte proliferation as 40% of skin contraction are caused by keratinocytes which will later be discussed in Chapter 8 (Chakrabarty, Heaton et al. 2001; Shahbudin, Shahbuddin et al. 2013).

In this chapter, optimization of the effect of different concentrations of mitomycin C on skin

cells was conducted before further investigations on KGM and KGM hydrogels' ability to direct cellular migration in a 2D scratch assay.

7.2 Results.

7.2.1 The effect of mitomycin C on fibroblast proliferation.

Figure 7.2 shows the effect of mitomycin C on fibroblasts after 30 min, 24 and 72 hours in culture. There was no cytotoxic effect with 1-100 µg.mL^{-1} mitomycin C after 30 min. The effectiveness of mitomycin C to inhibit fibroblast proliferation was measured using the MTT assay after 24 and 72 hours and compared with the controls. The results show that the addition of 10-100 µg.mL^{-1} mitomycin C for 30 mins (which was subsequently washed away) significantly inhibited the proliferation of fibroblasts.

7.2.2 The effect of mitomycin C and KGM on the proliferation of fibroblasts.

An investigation on the correlation between mitomycin C's effect on fibroblast proliferation and migration was conducted. Figure 7.3 shows that 1-100 µg.mL^{-1} mitomycin C effectively inhibited fibroblast proliferation and KGM stimulation of fibroblast viability after 3 and 5 days. The MTT absorbance of cells treated with 100 µg.mL^{-1} mitomycin C showed a significant decrease in cell proliferation compared to control and those with lower concentrations of mitomycin C after 1, 3 and 5 days. The result also shows that the addition of 10 mg.mL^{-1} KGM into the culture treated with mitomycin C also did not improve cell proliferation.

7.2.3 The effect of mitomycin C and KGM on the migration of fibroblasts.

To study migration it is necessary to eliminate as much proliferative activity of the cells as possible. Accordingly 10 µg.mL^{-1} of mitomycin C was used as this as successfully inhibited

fibroblast proliferation as mentioned earlier (Daniels, Occleston et al. 1999). Using phase contrast microscopy, the effect of mitomycin C and KGM on the migration of fibroblasts in a scratch wound assay was measured using ImageJ. The measurement was calculated as the percentage of covered area/total scratch area and the distance of the cells movement towards closing the scratch area. Results in Figure 7.4 shows that cells treated with mitomycin C covered less area after 8 hours compared to non-treated cells. Significant difference of % covered area and rate of migration can be seen in the control of mitomycin C treated and non-treated cells (p<0.1). There were no differences in the % of covered area and the rate of cell migration of the mitomycin C non-treated cells cultured with 1-10 mg.mL^{-1} concentrations of KGM. However, a declining trend of migration of mitomycin C treated fibroblasts was observed with 10 mg.mL^{-1} of KGM.
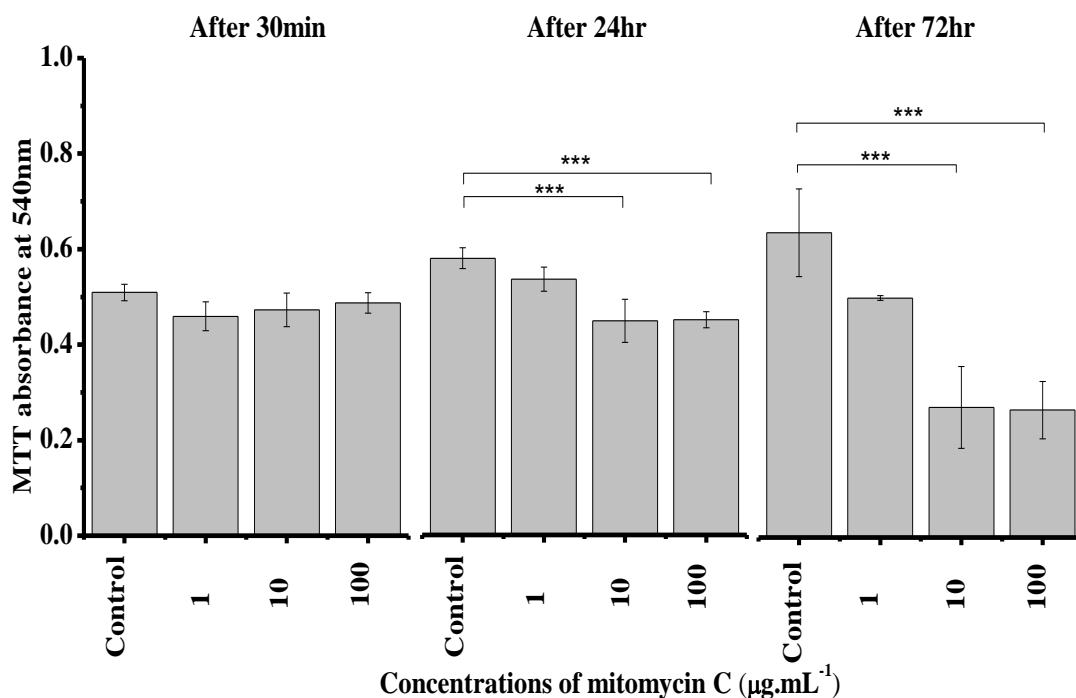

Figure 7.2 The effect of varying concentrations of mitomycin C on human dermal fibroblasts after 30 mins, 24 hours and 72 hours. 1×10^5 fibroblasts in 1mL of 10% DMEM were cultured in 12 well plates overnight before being treated with concentrations of mitomycin C for 30 mins. Inhibition of cell proliferation after 24 and 72 hrs could be seen with cells treated with 10 and 100 µg.mL^{-1} mitomycin C. (n=2), ***p<0.001 highly significant, **p<0.01 very significant and *p<0.05 significant compared to control.

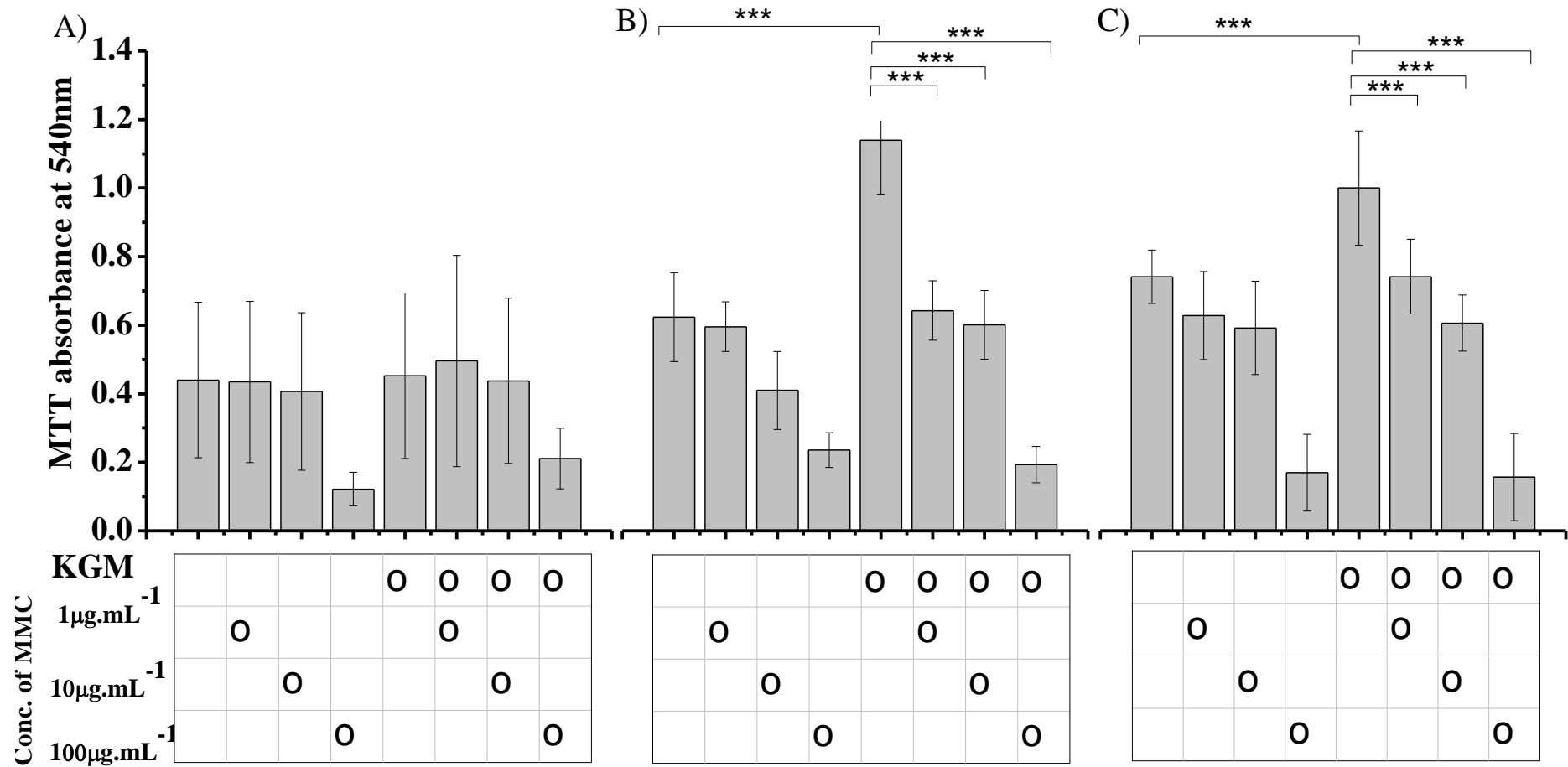**Figure 7.3** 1×10^5 fibroblasts in 1mL of 10% DMEM were cultured in 12 well plates overnight before treatment with concentrations of mitomycin C for 30 mins. Then, the cells were washed with PBS to remove any mitomycin C in the culture media. Fresh medium was added into the culture and 10 mg of KGM was added to respective samples. Cell proliferation was measured using MTT assay after A) 1, B) 3 and C) 5 days. (n=2), ***p<0.001 highly significant, **p<0.01 very significant and *p<0.05 significant compared to control.

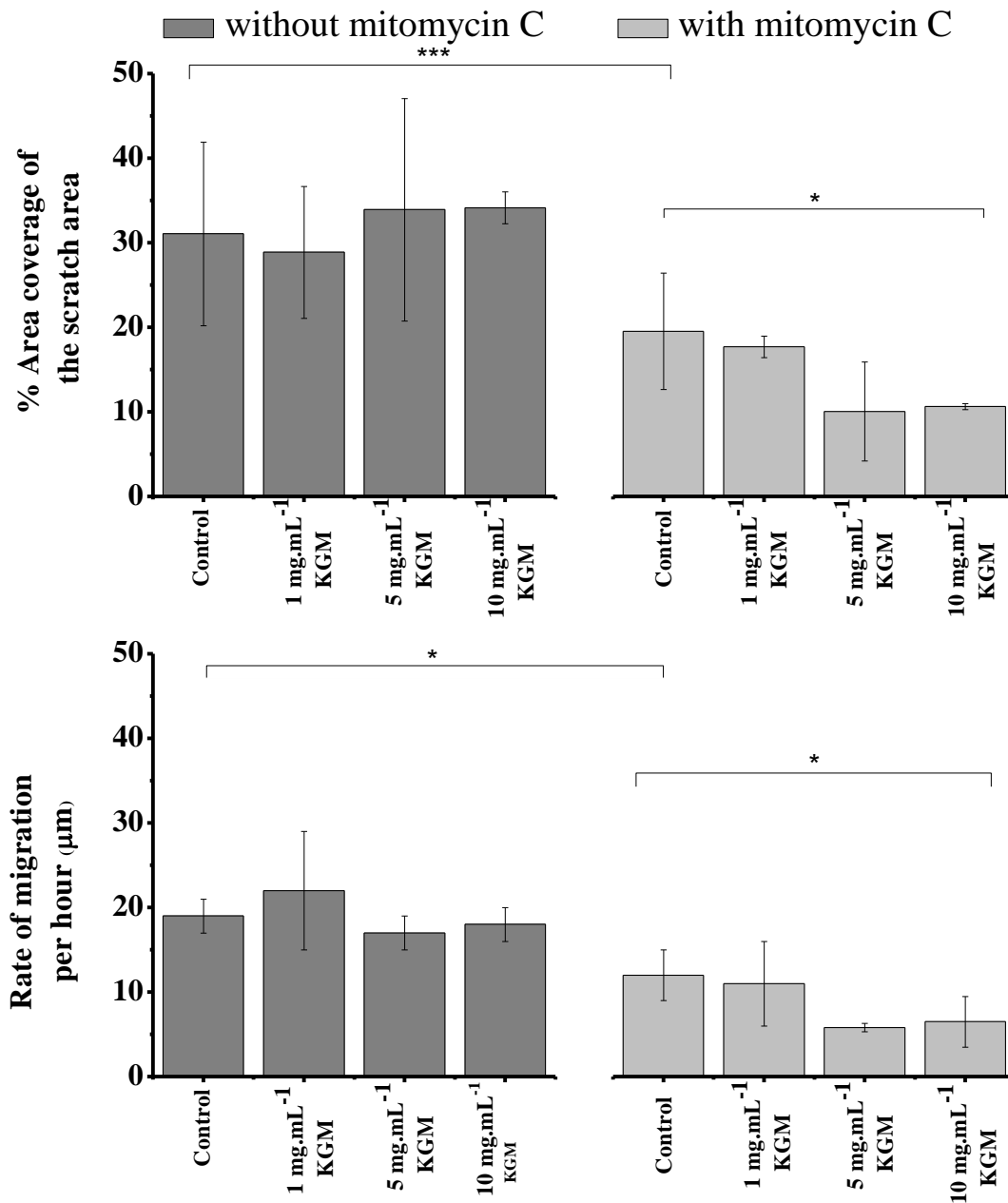**Figure 7.4** The effect of mitomycin C on the % of covered area and fibroblast rate of migration after 15 hours of culture with concentrations of KGM. 1×10^5 fibroblasts in 1 mL of 10% DMEM were cultured in 12 well plates overnight before being treated with concentrations of mitomycin C for 30 mins. (n=2), ***p<0.001 highly significant, **p<0.01 very significant and *p<0.05 significant compared to control.
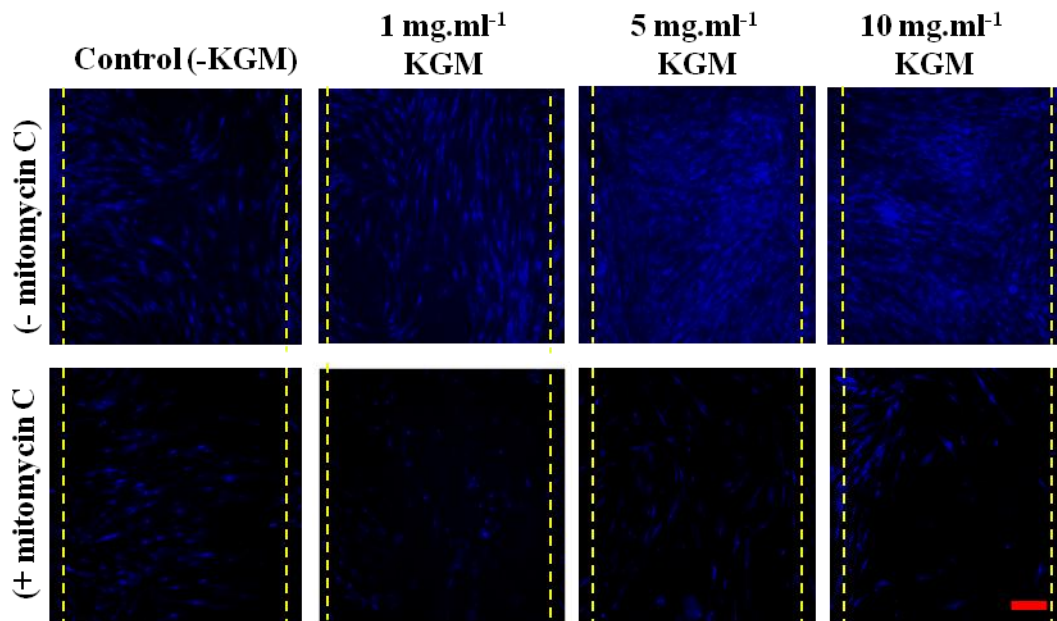
Figure 7.5 Micrographs of nuclei stained (using DAPI) mitomycin C treated and non-treated fibroblast migration in the scratch assay after 36 hours. (Scale bar: 100 μm).

Photomicrographs in Figure 7.5 show an inhibition of fibroblast migration by mitomycin C. Clearly without mitomycin C, KGM was able to stimulate fibroblast proliferation and this was observed with complete coverage of the denuded area. There is no difference in the rate of migration of non-treated cells with different concentrations of KGM as measured in Figure 7.4. However, less migration was observed in mitomycin C treated fibroblasts with 10 mg.mL^{-1} of KGM compared to control and those with lower concentrations of KGM.

7.2.4 The effect of mitomycin C on the proliferation of keratinocytes

Figure 7.6 shows that treatment with 10 and 100 μg.mL^{-1} mitomycin C for an hour effectively inhibited keratinocyte proliferation after 24 and 72 hours compared to control and 1 μg.mL^{-1} as measured by MTT assay. All cells were viable after 1 hr of treatment, and a reduction in cell proliferation in >1 μg.mL^{-1} mitomycin C treated cells was seen after 24 and 72 hr post treatment. 100 μg.mL^{-1} mitomycin C treated cells completely inhibited keratinocyte viability after 24 and 72 hours. This result provides information that a 10 μg.mL^{-1} dosage and 1 hr

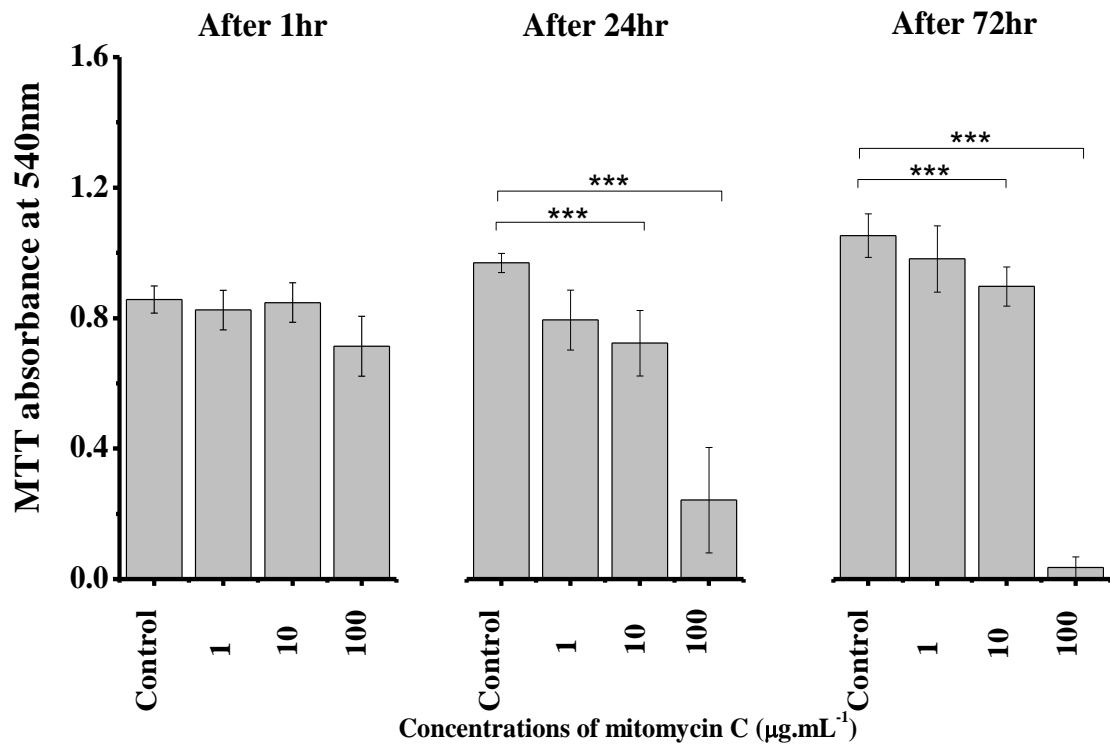incubation time to affectively inhibit keratinocyte proliferation for migration studies.

Figure 7.6 The effect of varying concentrations of mitomycin C on keratinocyte proliferation after 1, 24 and 72 hours.1 mL of 1×10^5 keratinocytes co-cultured with 5×10^4 i3T3 in 10% Greens' in 12 well plates overnight before treatment with mitomycin C at different concentrations for an hour. The effect of mitomycin C on the proliferation of keratinocytes after 1, 24 and 72 hours post treatment with mitomycin C was measured using the MTT assay. (n=3), ***$p<0.001$ highly significant, **$p<0.01$ very significant and *$p<0.05$ significant compared to control.

7.2.5 The effect of soluble KGM on the migration of keratinocytes treated with mitomycin C.

The effect of soluble KGM on the migration of keratinocytes treated with 300 μL of 10 μg.mL^{-1} mitomycin C for 1 hour in terms of % of the coverage in the scratch area and the

rate of migration after 0, 24 and 48 hours were measured using ImageJ (Figure 7.7). There was no significant difference in the % of the coverage area and the rate of migration of control with those treated with mitomycin C and cultured with KGM at 1, 5 and 10 mg.mL^{-1} concentrations although there was a declining trend in keratinocyte's rate of migration and % coverage area with higher concentrations of KGM (Figure 7.8).

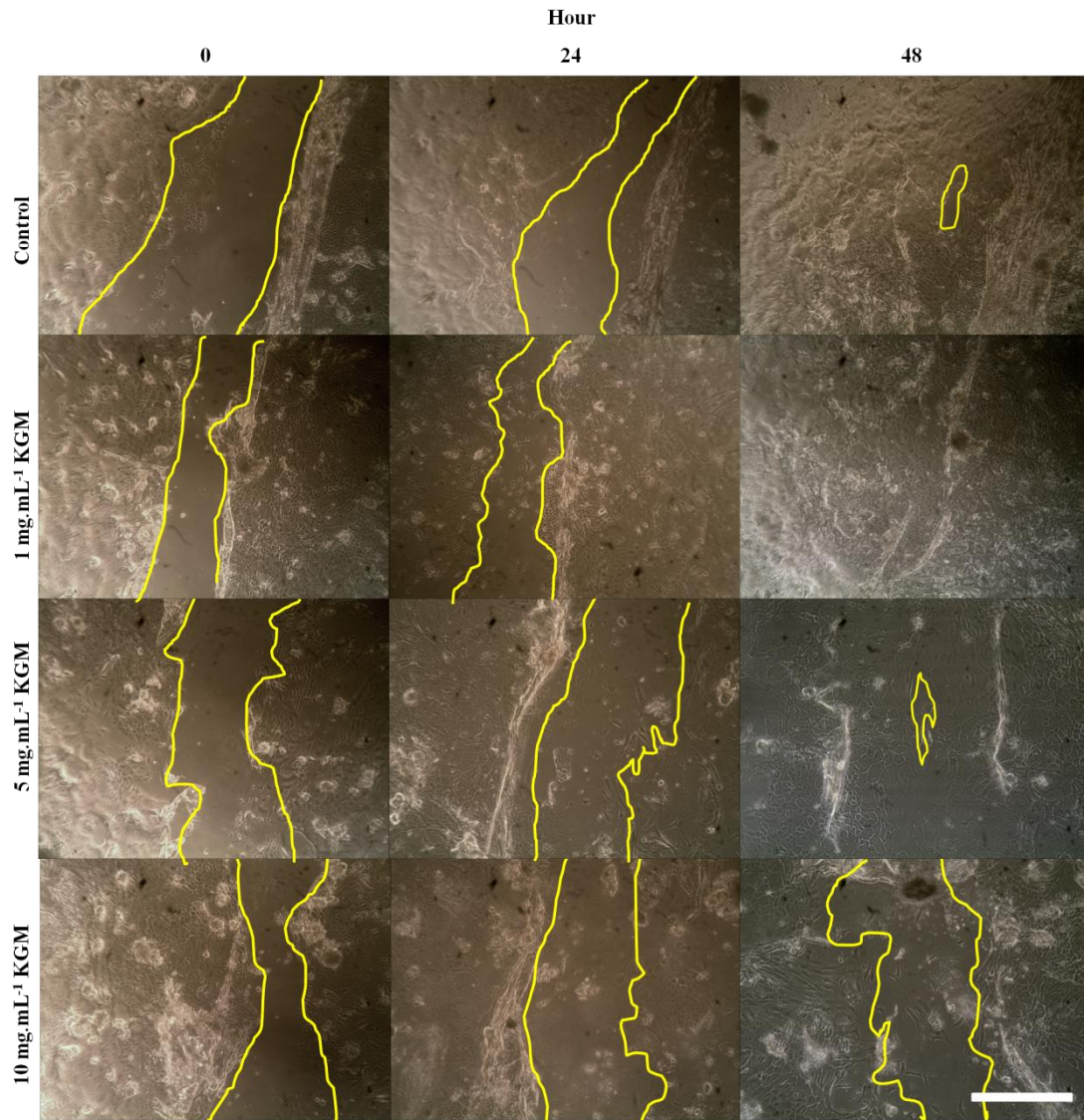**Figure 7.7** Micrographs of effect of direct contact of increasing concentrations of KGM on the migration of keratinocytes on TCP after 0, 24 and 48 hours photographed under phase contrast microscopy for image analysis. 1 mL of 1x10^5 keratinocytes co-cultured with 5x10^4 i3T3 in 10% Greens' in 12 well plate for overnight before treated with 10 μg.mL^{-1} mitomycin C for an hour. (Scale bar: 500 μm).
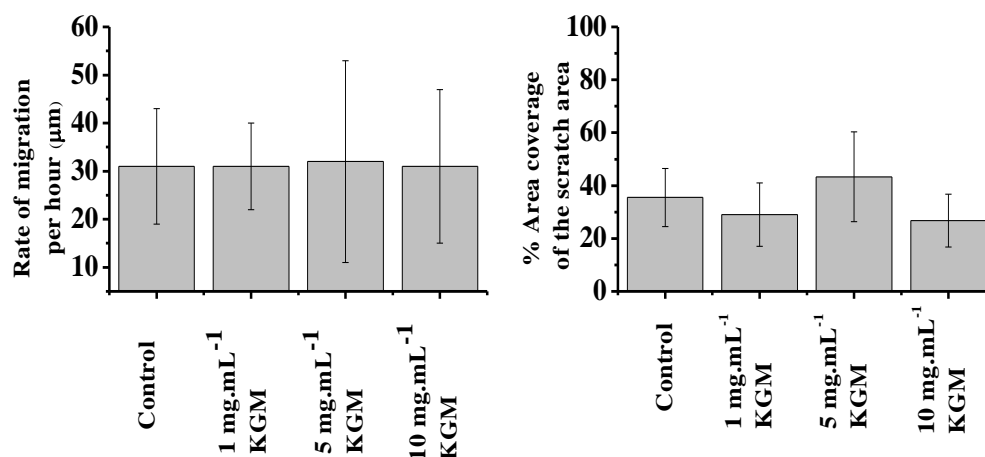
Figure 7.8 1 mL of $1x10^5$ keratinocytes co-cultured with $5x10^4$ i3T3 in 10% Greens' in 12 well plate for overnight before treated with 300 μL of 0.1 μg.mL^{-1} mitomycin C for an hour. Concentrations of KGM 1, 5 and 10 mg.mL^{-1} were added after and the effect of post treatment with mitomycin C and addition of KGM on keratinocyte migration after 24 hours was measured using ImageJ.(n=2), ***$p<0.001$ highly significant, **$p<0.01$ very significant and *$p<0.05$ significant compared to control.

7.2.6 The effect of crosslinked KGM hydrogels on the migration of fibroblasts.

The effect of 0.5 and 1% (w/v) crosslinked KGM with $1x10^{-3}$% (w/v) Ce(IV) on the migration of mitomycin C treated fibroblasts in a scratch assay after 0, 5 and 24 hours was measured using ImageJ (Figure 7.9). Quantitative measurements on the % covered area and the rate of migration of the cells in direct contact with the hydrogels after 8 hours showed a trend in the increment in the rate of migration and % covered area when compared to the control (Figure 7.9) but this was not significantas this is only one experiment it would require repetition.

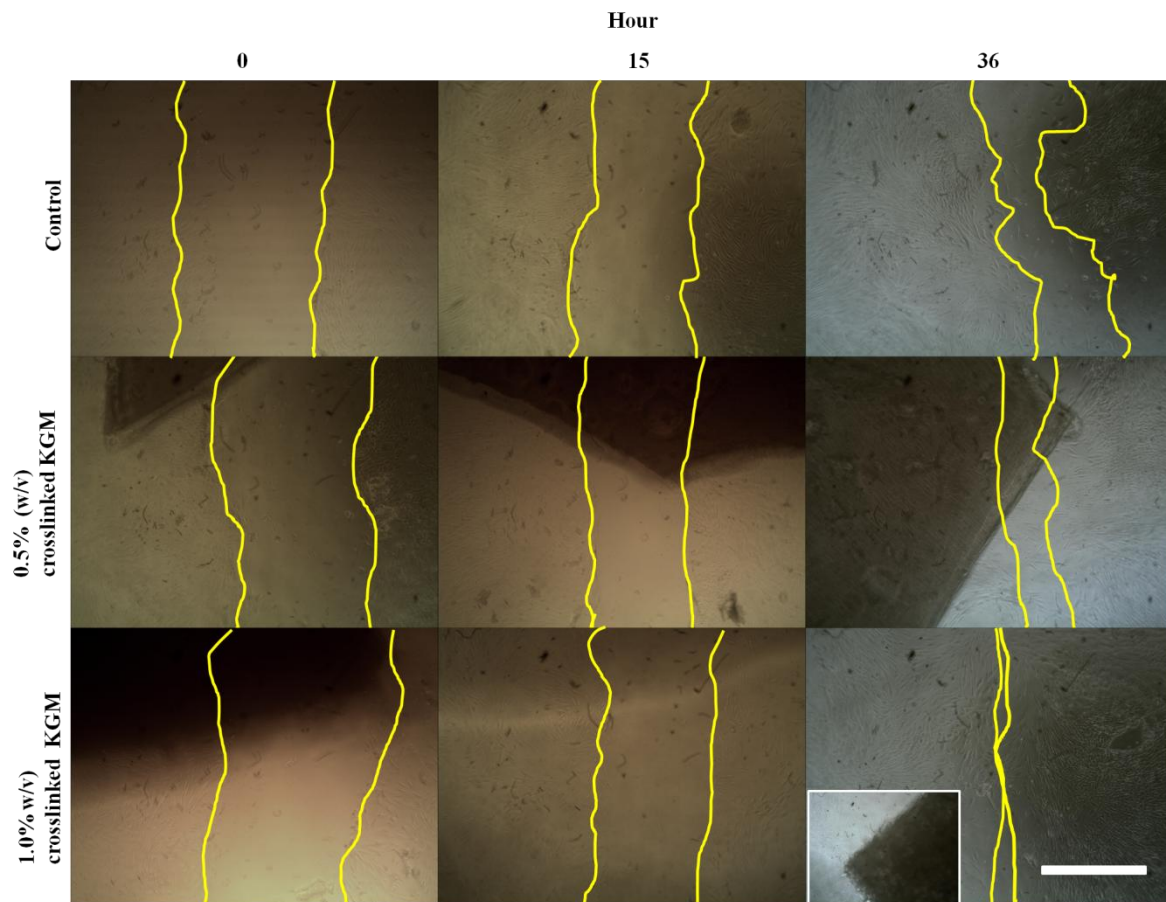**Figure 7.9**   Micrographs of effect of direct contact of crosslinked KGM on the migration of fibroblasts on TCP after 0, 15 and 24 hours photographed under phase contrast microscopy for image analysis. (Scale bar: 500 μm).
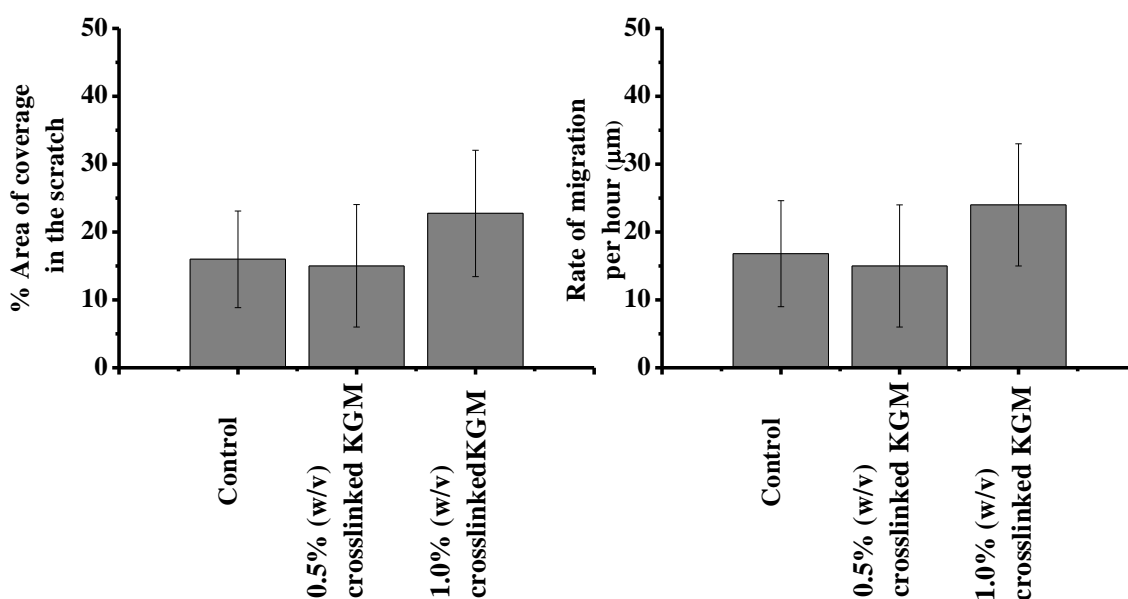
Figure 7.10 The percentage of the covered area and the rate of fibroblast migration in the scratch wound assay after 15 hours. 1 mL of 1×10^5 fibroblasts in 10% DMEM were cultured in 12 well plates overnight before treatment with 300 µL of 0.1 µg.mL^{-1} mitomycin C for an hour. (n=1), ***p<0.001 highly significant, **p<0.01 very significant and *p<0.05 significant compared to control.

7.2.7 The effect of semi IPN and graft-conetworks hydrogels on the migration of fibroblasts.

The effect of KGM hydrogels on the migration of fibroblasts treated with 300 µL of 10 µg.mL^{-1} mitomycin C for 30 min in terms of % of the coverage in the scratch area and length of migration per hour are shown in Figure 7.10. There were significant differences in the % of covered area and the rate of cell migration in direct contact with graft-conetwork hydrogels compared to control and those placed in direct contact with P(NVP-co-PEGDA) and semi IPNs.
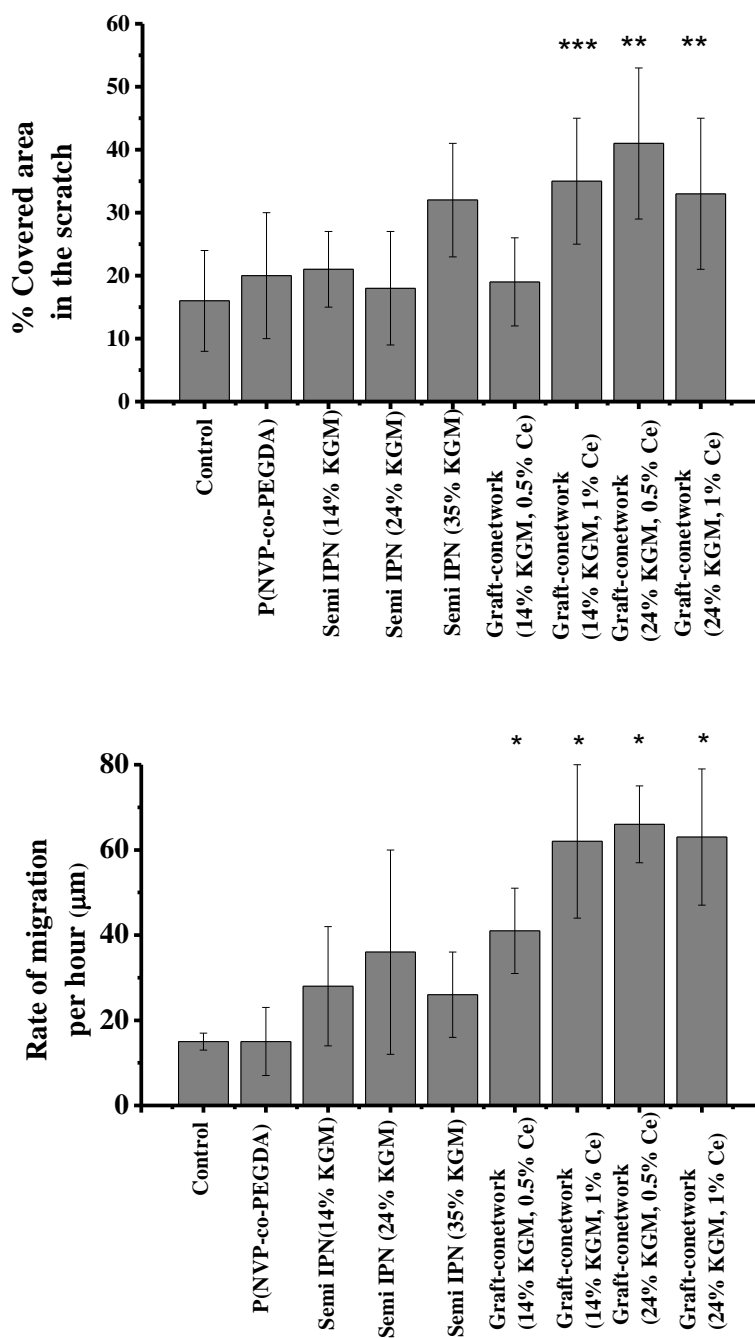
Figure 7.11 The effect of semi-IPN and graft-conetwork hydrogels on fibroblasts in the % of covered area and the rate of migration on scratch assay after 15 hours. 1 mL of 1×10^5 fibroblasts in 10% DMEM were cultured in 12 well plate for overnight before treated with 300 μL of 10 μg.mL^{-1} mitomycin C for an hour. (n=3), ***p<0.001 highly significant, **p<0.01 very significant and *p<0.05 significant compared to control.
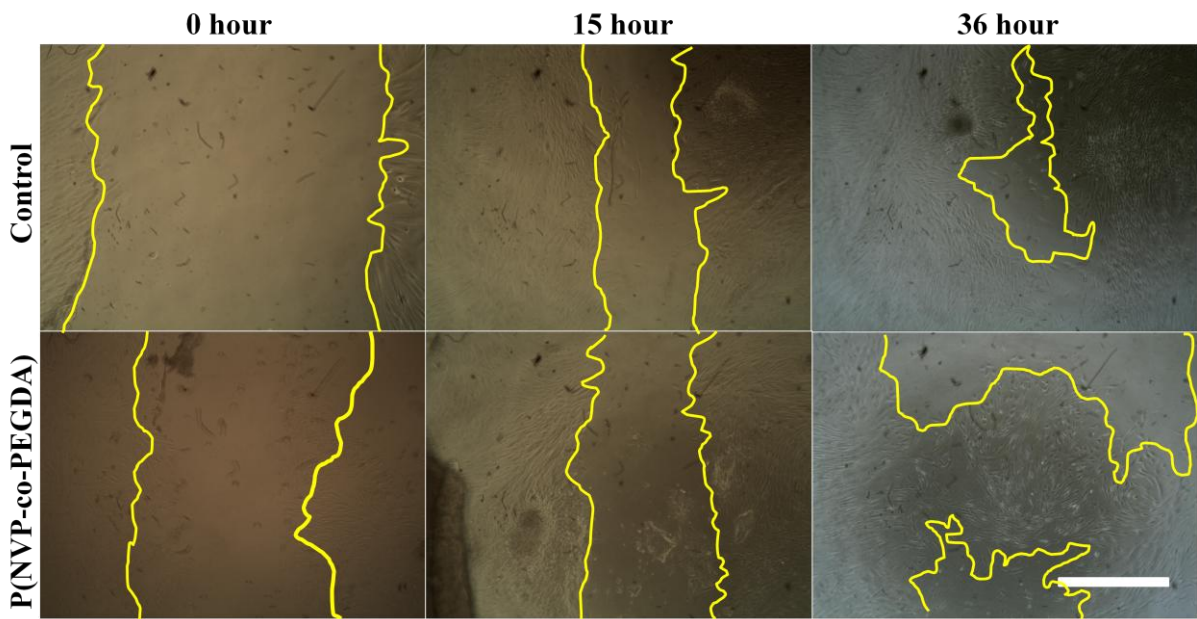
Figure 7.12A Micrographs of effect of direct contact of P(NVP-co-PEGDA) on the migration of fibroblasts on TCP after 0, 15 and 24 hours photographed under phase contrast microscopy for image analysis. (Scale bar: 500 μm).

Figure 7.12B Micrographs of effect of direct contact of semi-IPN hydrogels on the migration of fibroblasts on TCP after 0, 15 and 24 hours photographed under phase contrast microscopy for image analysis. (Scale bar: 500 μm).

Figure 7.12C Micrographs of effect of direct contact of graft-conetwork hydrogels on the migration of fibroblasts on TCP after 0, 15 and 24 hours photographed under phase contrast microscopy for image analysis. (Scale bar: 500 μm).

7.2.8 The effect of semi-IPN and graft-conetwork hydrogels on the migration of keratinocytes treated with mitomycin C.

The effect of KGM hydrogels on the migration of keratinocytes treated with 300 μL of 10 μg.mL^{-1} mitomycin C for 1 hr in terms of % of the covered area and the rate of migration are shown in Figure 7.11. There were significant differences in the % of the covered area and the rate of migration of when graft-conetwork hydrogels were placed in direct contact with the cells compared to control cells and those placed in adjacent with P(NVP-co-PEGDA) and semi IPNs.
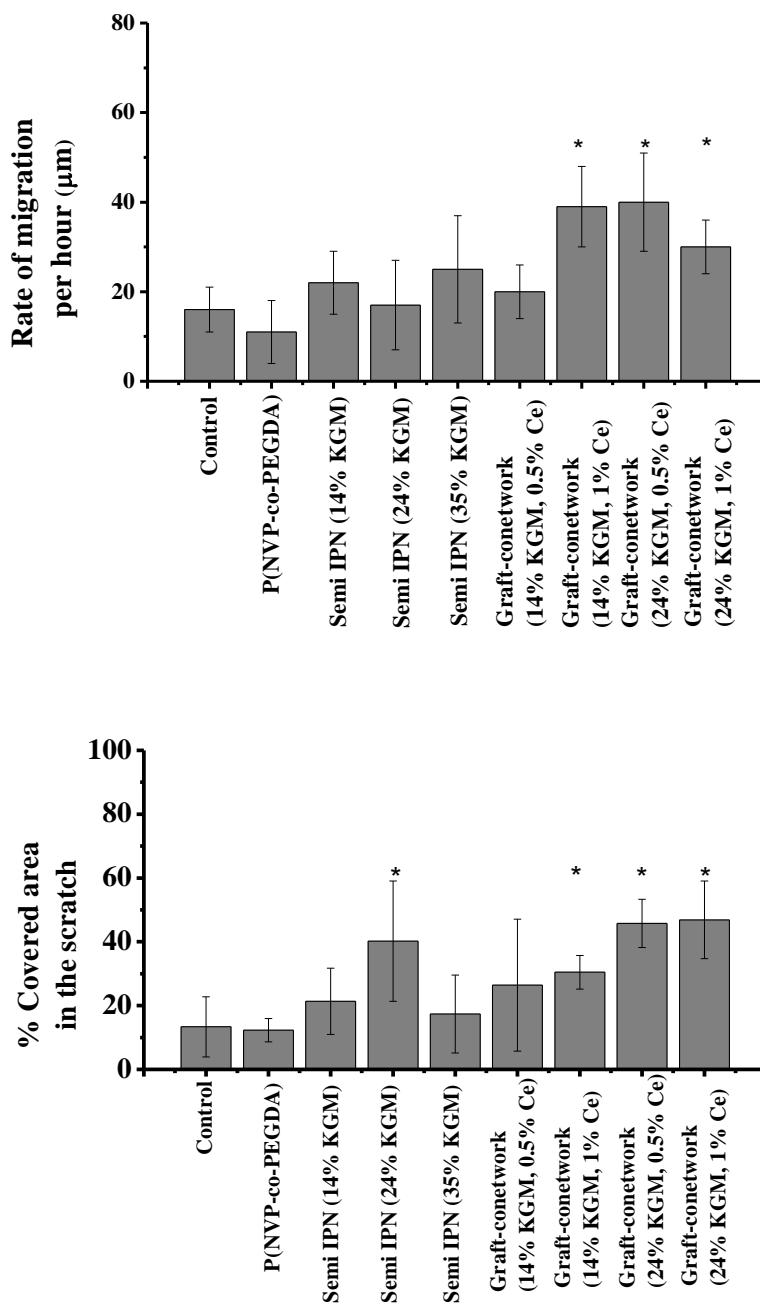
Figure 7.13 The effect of post treatment with mitomycin C and semi-IPN and graft-conetwork hydrogels on keratinocyte migration after 24 hrs measured using ImageJ. Graft-conetworks (14% (w/v) KGM with 1% (w/v) Ce (IV) and 24% KGM with 0.5 and 1% (w/v) Ce(IV)) significantly affect the migration of keratinocytes. 1 mL of 1×10^5 keratinocytes co-cultured with 5×10^4 i3T3 in 10% Greens' in 12 well plate for overnight before treated with 300 μL of 10 μg.mL^{-1} mitomycin C for an hour. Then, the hydrogels were put adjacents to the cells. (n=2), ***p<0.001 highly significant, **p<0.01 very significant and *p<0.05

significant compared to control.
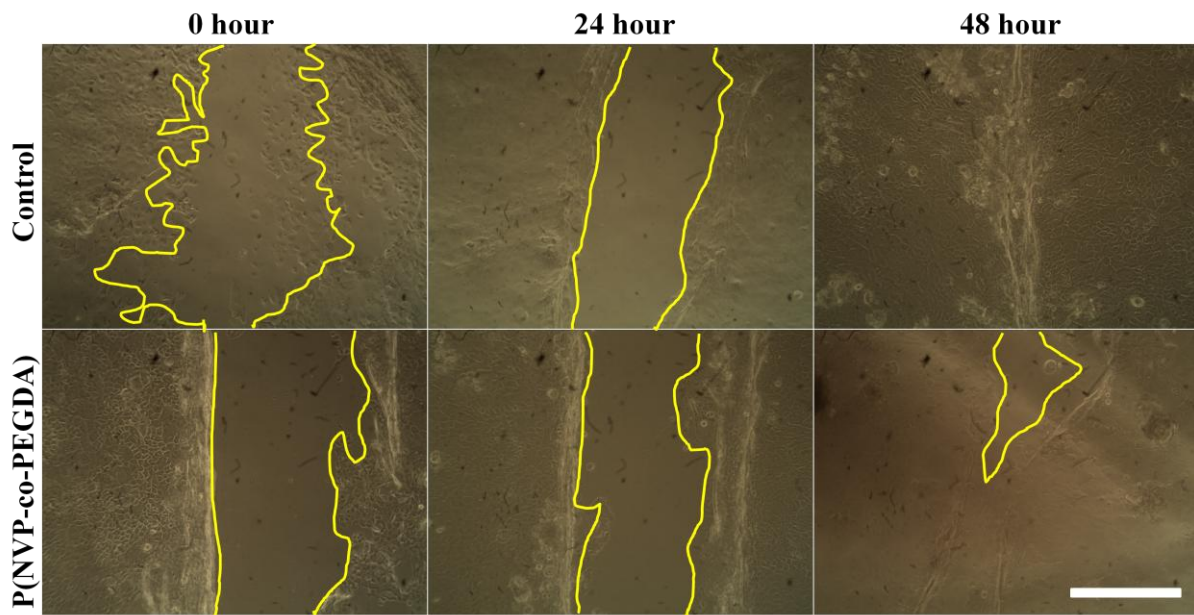
Figure 7.14A Micrographs of effect of direct contact of control (without hydrogel) and P(NVP-co-PEGDA) on the migration of keratinocytes on TCP after 0, 24 and 48 hours photographed under phase contrast microscopy for image analysis. (Scale bar: 500 μm).
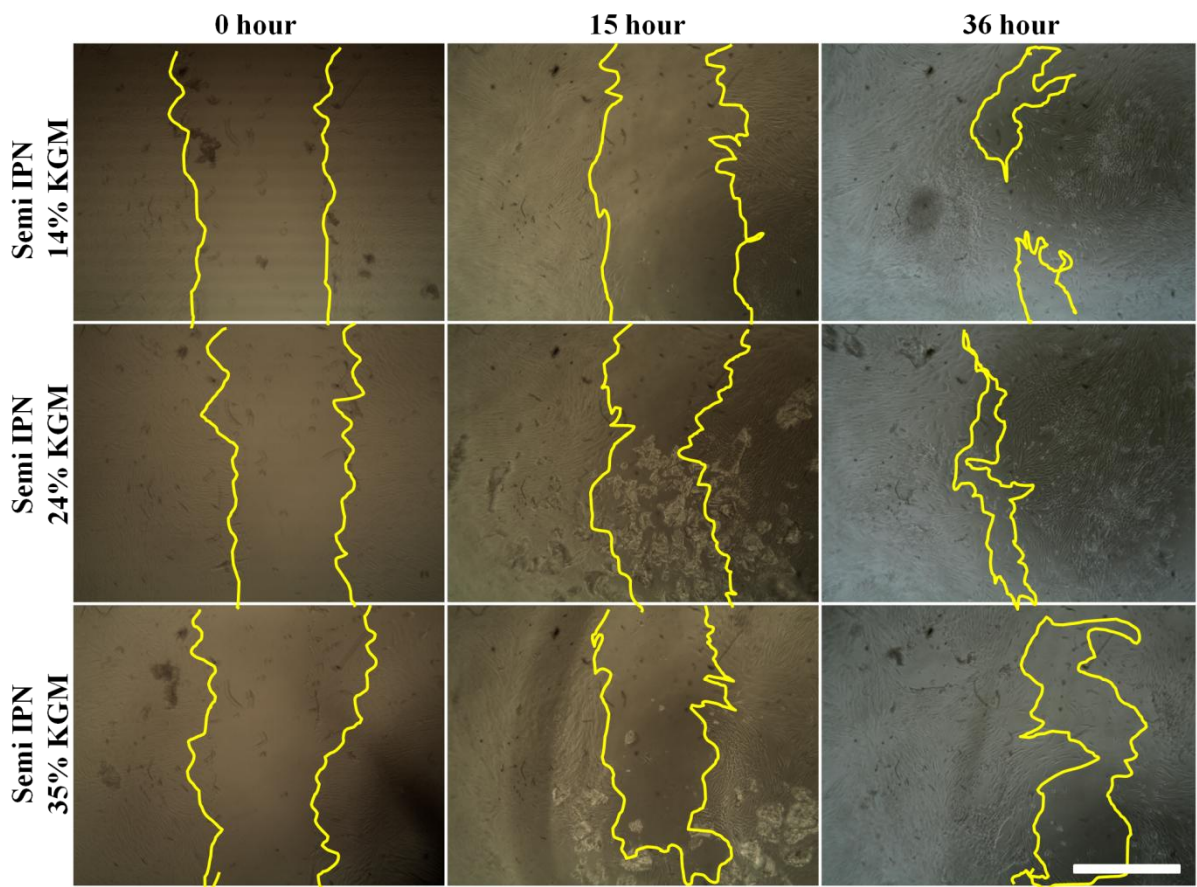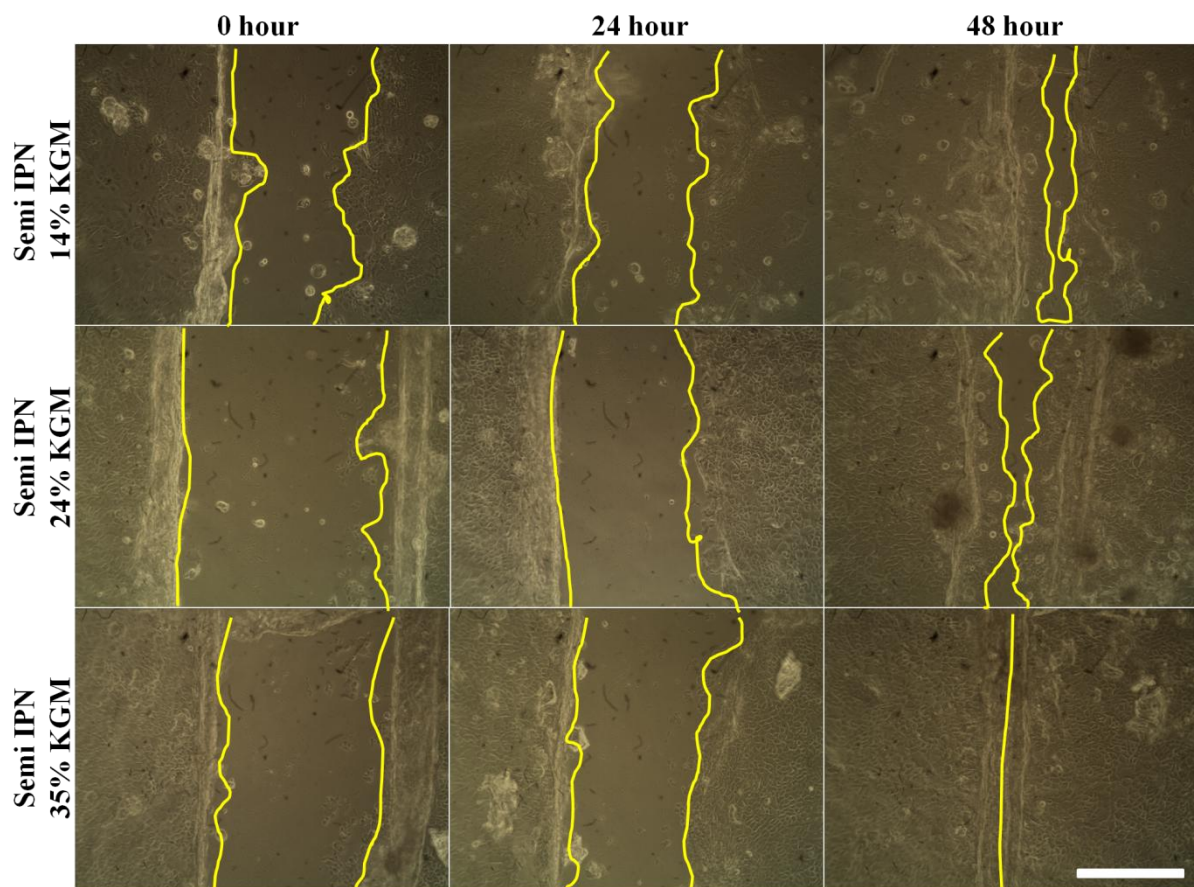
Figure 7.14B Micrographs of effect of direct contact of semi-IPN hydrogels on the migration of keratinocytes on TCP after 0, 24 and 48 hours photographed under phase contrast microscopy for image analysis. (Scale bar: 500 μm).
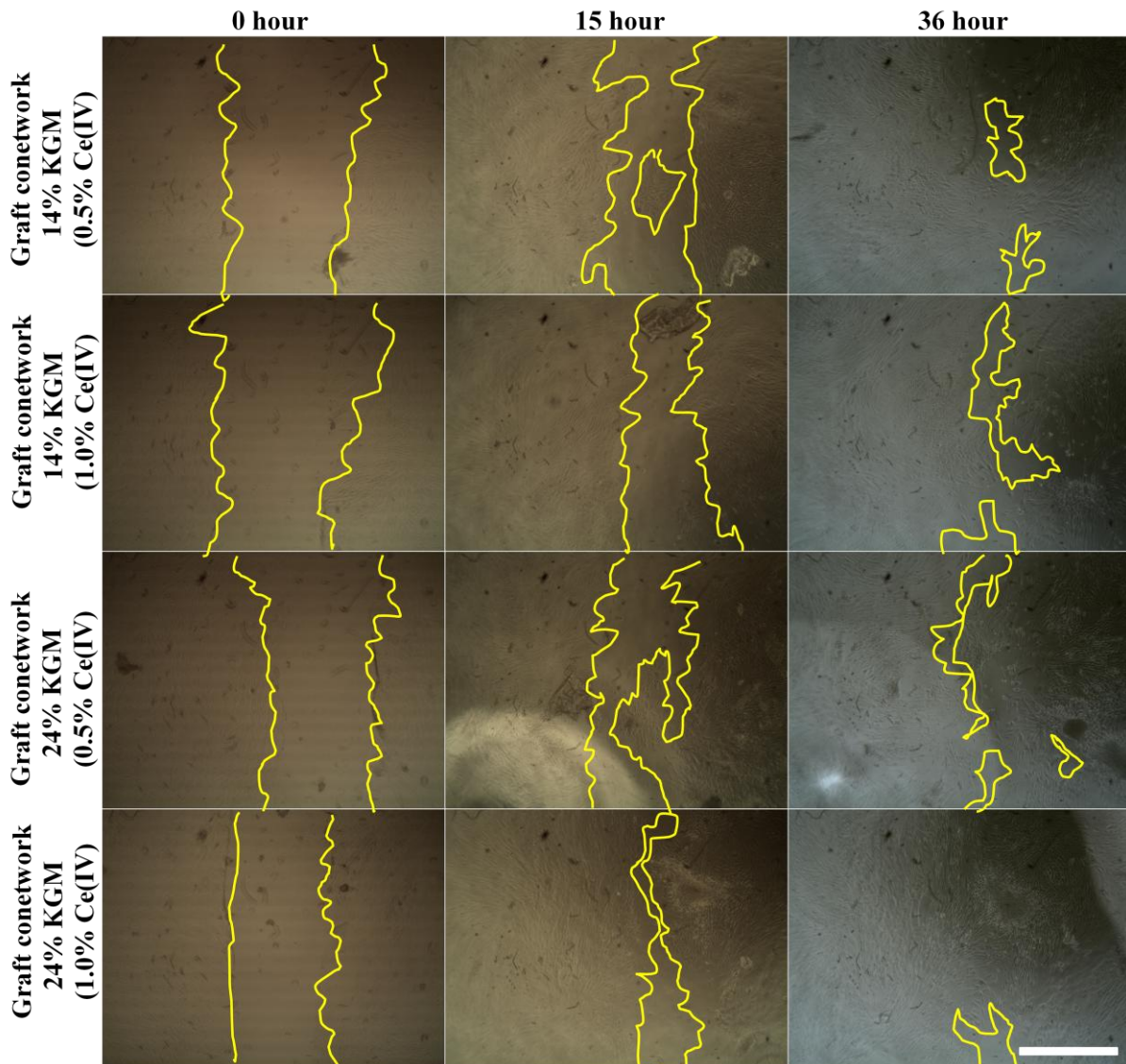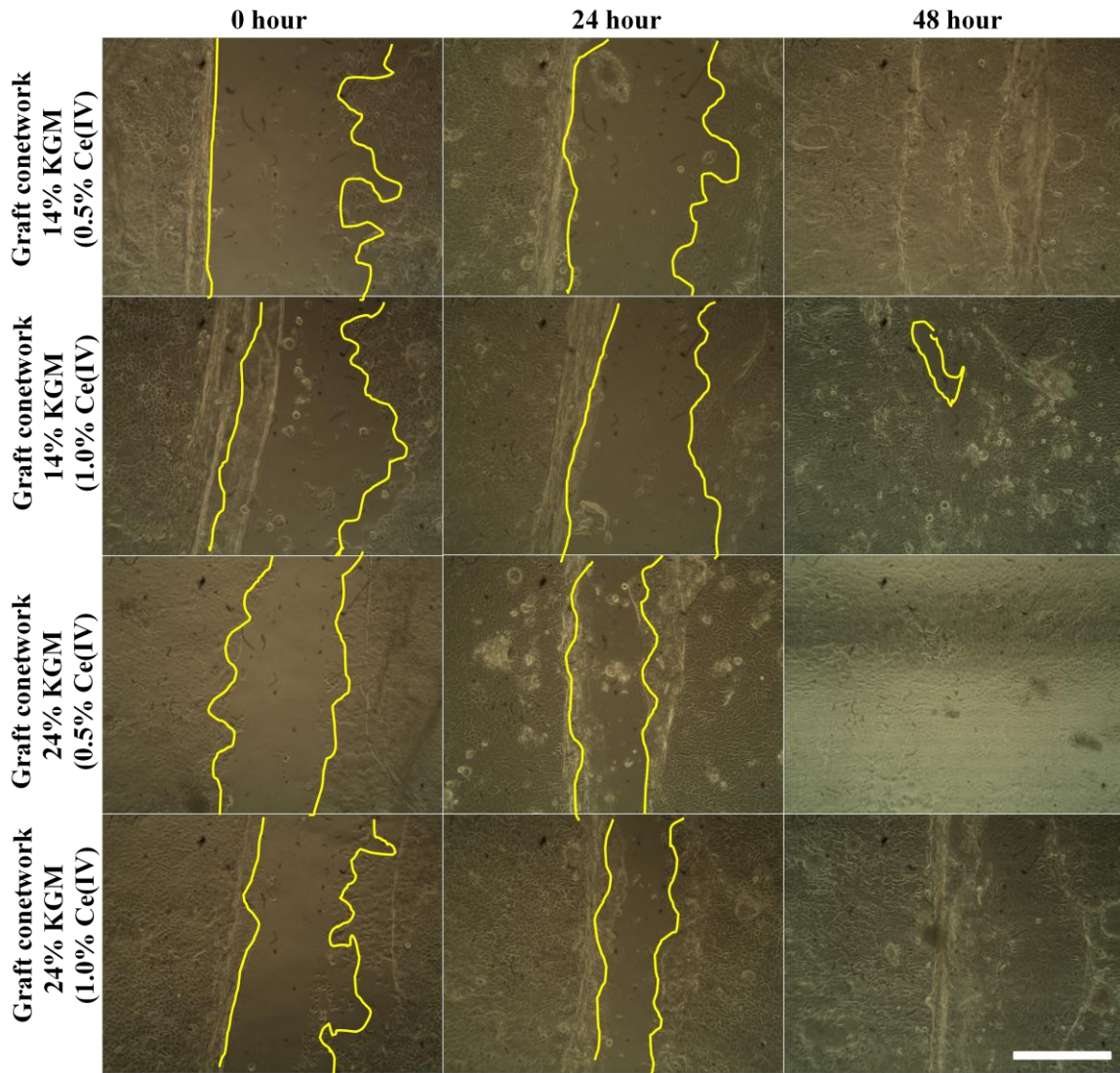

Figure 7.14C Micrographs of effect of direct contact of graft-conetwork hydrogels on the migration of keratinocytes on TCP after 0, 24 and 48 hours photographed under phase contrast microscopy for image analysis. (Scale bar: 500 μm).

7.2.9 The effect of semi-IPN and graft-conetwork hydrogels on the migration of fibroblasts and keratinocytes.

Confirmation of KGM hydrogels' biological activities on mitomycin C treated fibroblasts and keratinocytes were measured using the MTT assay and Live/Dead staining. Figure 7.15 shows the viability of fibroblasts in direct contact with KGM hydrogels in a scratch assay after 36 hours in culture. There was no significant differences in the viability of fibroblasts which were placed in direct contact with P(NVP-co-PEGDA) and KGM hydrogels compared to control, therefore this eliminates any effect of KGM on cell proliferation. On the other hand, photomicrographs of Live and Dead staining of the fibroblast cultures with semi and full IPNs in Figure 7.17 did not show any evidence of dead cells. .

Figure 7.16 shows that the direct contact of keratinocytes with semi and full IPNs, significantly reduced cell viability when compared to control and P(NVP-co-PEGDA). This shows that the presence of KGM in the hydrogels inhibited keratinocyte viability as previously mentioned with soluble KGM. The reduction in keratinocyte proliferation was consistent with Live/Dead staining in Figure 7.18, where more dead cells were observed in cell culture with KGM containing hydrogels.
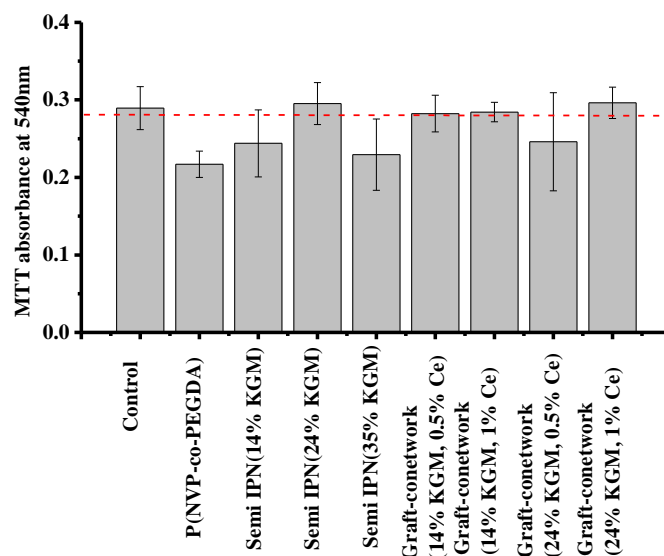
Figure 7.15   There were no significant changes in the metabolic activities of fibroblasts when semi IPNs and graft-conetworks were put adjacent to the cells in scratch assay after 48 hours in culture, indicating that the hydrogels did not stimulate the proliferation of fibroblasts. (n=3), ***p<0.001 highly significant,   **p<0.01 very significant and *p<0.05 significant compared to control.
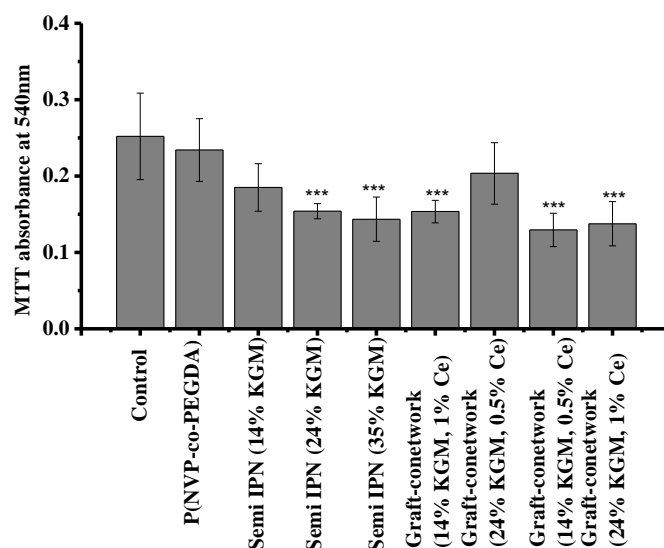

Figure 7.16   Keratinocyte metabolic activity was reduced when KGM containing hydrogels, semi-IPN and graft-conetwork were put in direct contact with the cells in the scratch assay after 48 hours. 1 mL of 1×10^5 keratinocytes co-cultured with 5×10^4 i3T3 in 10% Greens' in 48 well plate for overnight before treated with 300 μL of 0.1 μg.mL^{-1} mitomycin C for an hour. Then, the hydrogels were put adjacently to the cells. (n=2), ***p<0.001 highly significant, **p<0.01 very significant and *p<0.05 significant compared to control.
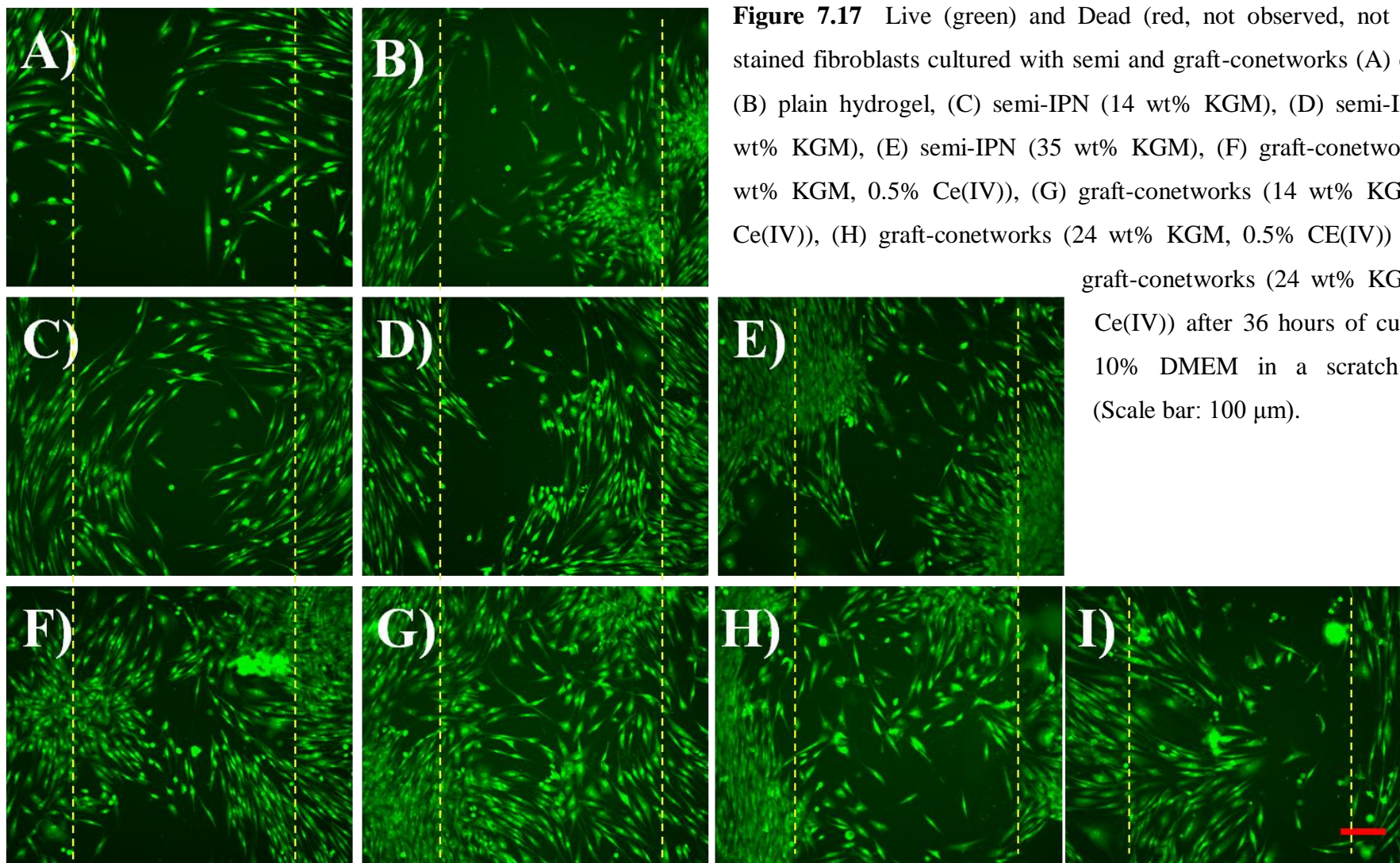
Figure 7.17 Live (green) and Dead (red, not observed, not shown) stained fibroblasts cultured with semi and graft-conetworks (A) control, (B) plain hydrogel, (C) semi-IPN (14 wt% KGM), (D) semi-IPN (24 wt% KGM), (E) semi-IPN (35 wt% KGM), (F) graft-conetworks (14 wt% KGM, 0.5% Ce(IV)), (G) graft-conetworks (14 wt% KGM, 1% Ce(IV)), (H) graft-conetworks (24 wt% KGM, 0.5% CE(IV)) and (I) graft-conetworks (24 wt% KGM, 1% Ce(IV)) after 36 hours of culture in 10% DMEM in a scratch assay. (Scale bar: 100 μm).
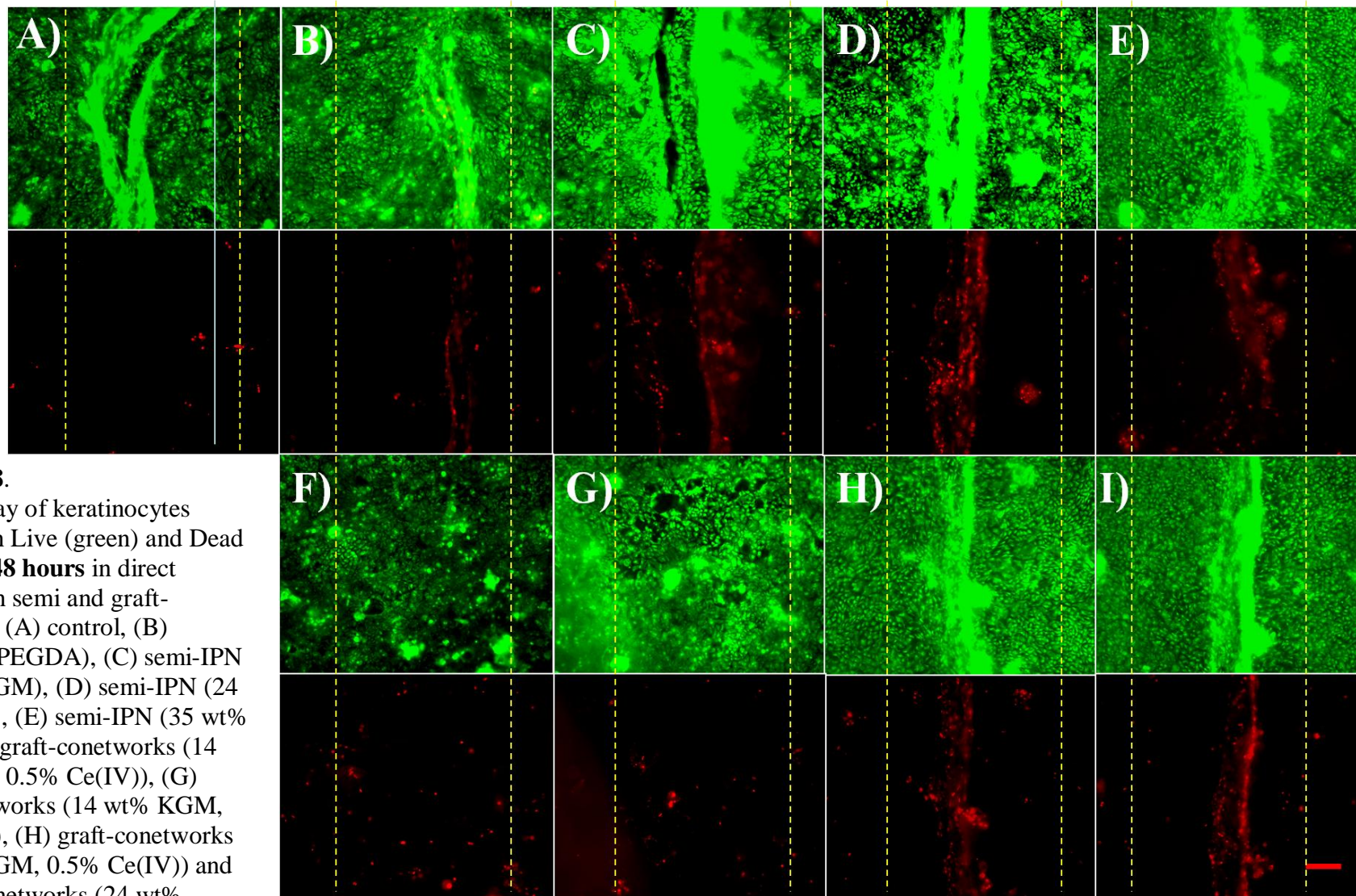
Figure 7.18. Scratch assay of keratinocytes stained with Live (green) and Dead (red) after **48 hours** in direct contact with semi and graft-conetworks (A) control, (B) P(NVP-co-PEGDA), (C) semi-IPN (14 wt% KGM), (D) semi-IPN (24 wt% KGM), (E) semi-IPN (35 wt% KGM), (F) graft-conetworks (14 wt% KGM, 0.5% Ce(IV)), (G) graft-conetworks (14 wt% KGM, 1% Ce(IV)), (H) graft-conetworks (24 wt% KGM, 0.5% Ce(IV)) and (I) graft-conetworks (24 wt% KGM, 1% Ce(IV)) in 10% Greens. (Scale bar: 100 µm).

7.3 Discussion.

Cell-cell interactions play a very important role in tissue homeostasis and wound healing. This chapter discusses the potential influence of KGM and KGM containing hydrogels on the migration of fibroblasts and keratinocytes in 2D culture. The migration of skin cells in wound scratch assays was quantified using image analysis at different time points of 0, 15, 24, 36 and 48 hours. All migration studies included mitomycin C to eliminate any effect of KGM on cell proliferation which would have made the interpretation of these experiments challenging. Investigation of the effectiveness of mitomycin C to inhibit cellular proliferation was conducted and it was found that incubation with 1, 10 and 100 $\mu g.mL^{-1}$ mitomycin C for 30 minutes or 1 hour successfully inhibited fibroblast and keratinocyte proliferation respectively. Treatment of 30 minutes also inhibited KGM stimulation of fibroblast proliferation. The mitomycin C dosage of 20-50 $\mu g.mL^{-1}$ was clinically relevant as higher dosages were found to induce apoptosis and cell death in fibroblasts *in vitro* (Crowston, Akbar et al. 1998; Daniels, Occleston et al. 1999).

The migration of mitomycin C treated and non-treated fibroblasts were investigated in the presence and absence of soluble KGM. The results showed that mitomycin C not only inhibited fibroblast migration, but also inhibited the KGM stimulatory effect on proliferation. Further investigation of the migration of mitomycin C treated fibroblasts in direct contact with crosslinked KGM and IPN hydrogels was also conducted. The results showed that both crosslinked KGM hydrogels with 0.5 and 1% (w/v) KGM increased the fibroblasts rate of migration by (+25%) and the % of covered area in the scratch assay compared to control without the hydrogels.

Graft-conetwork hydrogels with 14 and 24% (w/v) KGM significantly increased mitomycin C treated fibroblast and keratinocyte rate of migration and % of covered area compared to P(NVP-co-PEGDA), semi-IPN and control after 24 and 48 hours. Then, confirmation of cell

proliferation and viability were conducted using MTT assay and Live/Dead staining at the end of the experiments to confirm the effectiveness of mitomycin C on the cells and hydrogel's biological activity to inhibit keratinocyte viability.

The result of MTT assay of fibroblasts in direct contact with both semi and graft-conetwork showed no difference in cell proliferation with the control and P(NVP-co-PEGDA), confirming that the number of cells in all samples were the same. The Live/Dead staining of all samples also showed the absence of dead cells consistent with earlier results on cytocompatibility.

In the experiment with keratinocytes, the MTT assay of the cells in direct contact with both semi and graft-conetwork hydrogels were lower compared to those of positive control (with P(NVP-co-PEGDA) and negative control (without hydrogel). Live/Dead staining of keratinocytes showed that the cells in direct contact with semi-IPN and graft-conetwork had more dead cells compared to both positive and negative controls indicating that both types of hydrogels were biologically active to inhibit keratinocyte viability.

The summary of the effect of KGM hydrogels on the migration of skin cells is shown in Table 7.1

Table 7.1 A summary of the effect of hydrogels on the migration of mitomycin C treated fibroblasts and keratinocytes. (↑: increase, NS = no significant effect; n.a: not assessed).

	Effect on fibroblast migration	Effect on keratinocyte migration
Soluble KGM	NS	NS
Crosslinked hydrogels	↑ (25%)	n.a
Semi-IPN hydrogels	NS	NS
Graft-conetwork hydrogels	↑ (50%)	↑ (50%)

7.4 Conclusion.

In conclusion, soluble KGM did not stimulate migration of fibroblasts or keratinocytes once treated with mitomycin C and neither did semi-IPN hydrogels. In contrast, crosslinked hydrogels and graft-conetworks hydrogels did stimulate migration of fibroblasts and keratinocytes.

Chapter 8. The effect of KGM and KGM hydrogels on the reepithelisation and contraction of tissue engineered skin.

8.1 Introduction.

Wound healing is a repair process to restore structure and functionality of skin that involves concerted efforts of different types of cells. In this process phases of inflammation, granulation and remodelling overlap before a wound his completely healed (Desmoulière, Chaponnier et al. 2005). Reepithelisation is a remodelling process of the epidermal defect site to restore skin structure where cells from the wound edges migrate over the area and cells within the wound begin to produce new extracellular matrix (ECM) for reepithelisation. Scarring and contraction of the skin are common with wound healing. Researchers use several methods to prevent scarring with pharmaceutical approaches such as mitomycin C (Liu, Siriwardena et al. 2008), D-penicillamine (Weiss and M. 1981), hydrogels (Murakami, Aoki et al.) and suppression of TGFβ (Chipev and Simon 2002; Ferguson and O'Kane 2004). The use of hydrogels to prevent scarring and wound contraction is not new (Murakami, Aoki et al. ; Choi and Chung 2003). Based on the results of KGM inhibition of keratinocyte proliferation, it was then hypothesized that this could benefit wound healing by prevention of tissue contraction and scarring. A previous study by Harrison et. al showed that the contraction of tissue engineered skin based on human dermis appeared to be related to the differentiation status of the keratinocytes, tissue engineered skin contracting more as the keratinocytes differentiated (Harrison, Gossiel et al. 2006).

In this chapter, experiments were focused on the ability of KGM and KGM hydrogels to stimulate fibroblast proliferation, form a secure dermal-epidermal junction and inhibit contraction of tissue engineered (TE) skin.

The TE skin model used throughout the study was based on the method developed by the MacNeil group in the University of Sheffield. It is based on sterilized de-epidermised acellular human dermis (DED), obtained with informed consent from patients in the age range of 25-60 undergoing elective breast reductions and abdominoplasty surgeries at the Royal Hallamshire Hospital (Ghosh, Boyce et al. 1997; Ralston, Layton et al. 1997; Chakrabarty, Dawson et al. 1999). The skin was soaked in 0.1N sodium chloride overnight and then extensively washed to make it acellular. The DED was then cultured with human keratinocytes and fibroblasts in 3:1 ratio onto the papillary surface for 2 days before exposed to an air-liquid interface (ALI). This model was used in the investigation of pharmaceutical approaches to reduce contraction and to investigate melanoma invasion in skin (Eves, Layton et al. 2000; Eves, Katerinaki et al. 2003; Harrison, Gossiel et al. 2006). In studies of contraction this model also showed that keratinocytes were responsible for 40% of skin contraction over 10 days period and that this effect was not significantly altered by the presence of fibroblasts (Ralston, Layton et al. 1997; Chakrabarty, Heaton et al. 2001). In another study of keratinocyte induced contraction of collagen gels, it was found that the keratinocytes on their own were able to contract gels when seeded either on the top or through the gel (Souren, Ponec et al. 1989). However, keratinocytes cultured through the gel required greater number of cells in order to stimulate an equal degree of contraction caused by keratinocytes which seeded on the top of the gel (Souren, Ponec et al. 1989).

Keratinocyte culture *in vitro* is highly dependent on their co-culture with human dermal fibroblasts, where keratinocytes will lose its proliferative capacity and rapidly undergo terminal differentiation (Werner, Krieg et al. 2007). In the contraction of collagen gels, co-culture of keratinocytes and fibroblasts contract more compared to single culture of each cell (Souren, Ponec et al. 1989). The contraction of keratinocyte-fibroblasts co-cultured on collagen gels was also proportional to the increase in serum concentration up to 10% , which

may suggest cellular responsiveness to cytokines, growth factors and molecules present in the serum (Souren, Ponec et al. 1989). Whereas one can study growth of keratinocytes on collagen and look at contraction of collagen gels, human DED provides a more physiologically relevant matrix as it consists of mature crosslinked collagen (Harrison, Gossiel et al. 2006). The method of sterilization using glycerol, ethylene glycol and gamma radiation significantly affect the quality of DED and influenced the ability of keratinocyte to achieve contraction with greater degree of contraction being seen with pliable dermal matrices (Ghosh, Boyce et al. 1997; Chakrabarty, Heaton et al. 2001). Therefore to eliminate these factors in the experiments in this chapter, the DED was obtained aseptically and used without sterilization. Furthermore, animal skin consists of a layer called '*panniculus carnosus*' which is a skin flap that attach to the reticular dermis and is separated from superficial of underlying muscle, causing the wound healing of animal skin to have relatively less scarring, (Billingham and Medawar 1955). Animal models also do not show abnormalities such as keloid and hypertropic scarring as is seen in human (Aksoy, Vargel et al. 2002). Furthermore, the degree of wound contracture and epithelisation in animal models are different compared to human (Stavrou, Haik et al. 2009).

The ultimate goal of wound healing is to rapidly complete regeneration of functional skin that includes all skin appendages such as hair follicles, sweat glands and layers (dermal, epidermal and subcutaneous), without any scar formation. Yannas (2000) proposed the ideal induction of skin regeneration which requires two steps; blocking of wound contraction and the presence of a neo-scaffold as topological template for the synthesis of newly formed stroma to assist with skin regeneration over a period of time (Yannas 2000). As earlier studies have shown KGM hydrogels to stimulate fibroblast proliferation while retarding keratinocyte proliferation, it was interesting to see to what extent these gels would influence the formation of tissue engineered skin and it's contraction in the 3D skin model.

8.2 Results.

8.2.1 Histological Characterisation of TE Skin.

Histological assessment of TE skin used throughout this study using H&E staining is shown in Figure 8.1. The skin composites used in this study were made of aseptically obtained DED that was seeded with keratinocytes and fibroblasts in a 3:1 ratio at an air-liquid interface (ALI). Haematoxylin and Eosin staining is the simplest method to assess histological changes on tissue architecture embedded in paraffin wax sections. These combination of stains highlight cell nuclei in blue/black while cytoplasm and connective tissue in pink.
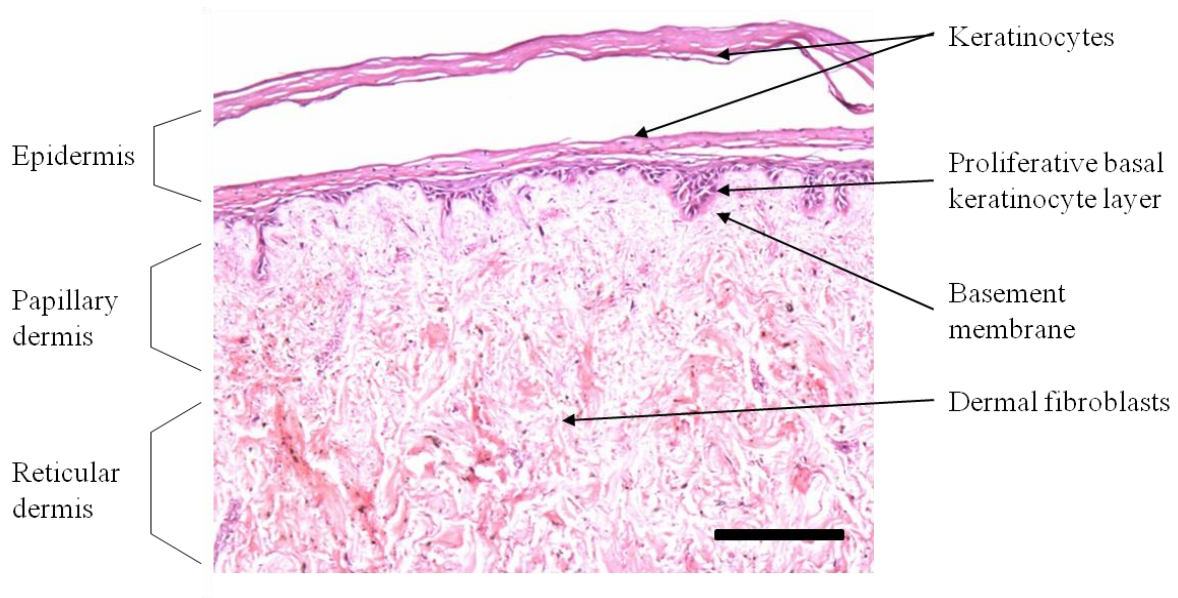
Figure 8.1   H&E stained TE skin shows distinct layer of epidermis and dermis. (Scale bar: 100 µm).

8.2.2 The effect of soluble KGM on the reepithelisation and stimulation of fibroblast proliferation in the dermal region.

In this section, the effect of soluble KGM in different concentrations (1 and 5 mg.mL^{-1}) after 14 days on TE skin section was observed and quantified. KGM was added to the culture medium 24 hrs after being exposed to ALI. The thickness of the basal layer of keratinocytes and the epidermal-dermal junction and the population of cells per 10,000 μm^2 in the dermal region of TE skin were measured using ImageJ. Following culture on day 14, all skin composites showed well differentiated keratinized layers shown in Figure 8.3. There were no difference in the thickness of the basal layer of cells and epidermal layer on control and those cultured with concentrations of KGM. However, the highest concentration of KGM (5 mg.ml^{-1}), showed the highest cell density per 10000 μm^2 in the dermal region with (4.8± 2.9) cells followed by 1 mg.mL^{-1} with (4.1± 2.6) compared to control (2.5±1.8). The histology of TE skin with H&E staining shows more cells density in the dermal region of TE skin cultured with 5 mg.ml^{-1} KGM compared to control and 1 mg.ml^{-1} KGM, suggesting KGM's stimulation on fibroblast proliferation as was reported earlier in Chapter 3.

KGM stimulation of fibroblast proliferation in the dermal region of TE skin was particularly interesting for wound healing. Figure 8.3 shows the histology of TE skin stained with H&E with obvious separation of fibroblasts and keratinocytes at papillary and dermal layers.
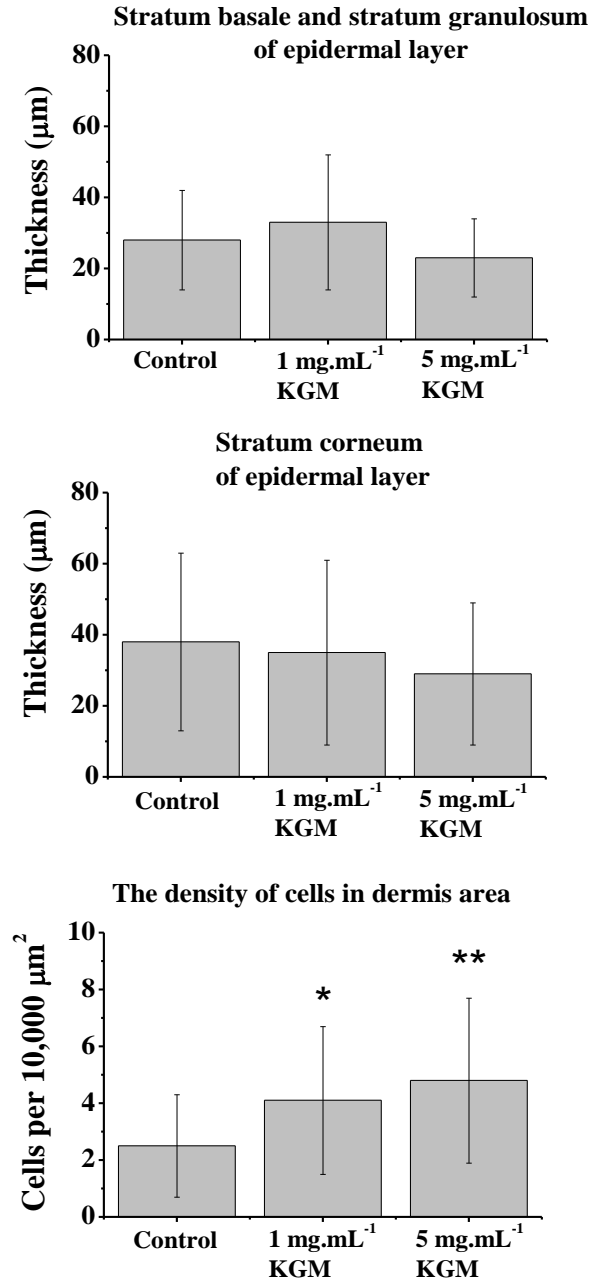
Figure 8.2 The effect of KGM powder (1 and 5 mg.mL^{-1}) on the thickness of proliferating (stratum basale and stratum granulosum) and differentiated epithelium (stratum corneum) layer of a TE skin and on the number of cells in the dermal region per 10,000 μm^2 of a TE skin after 14 days of culture in 10% Greens' medium measured using ImageJ. (n=3), ***p<0.001 highly significant, **p<0.01 very significant and *p<0.05 significant compared to control.
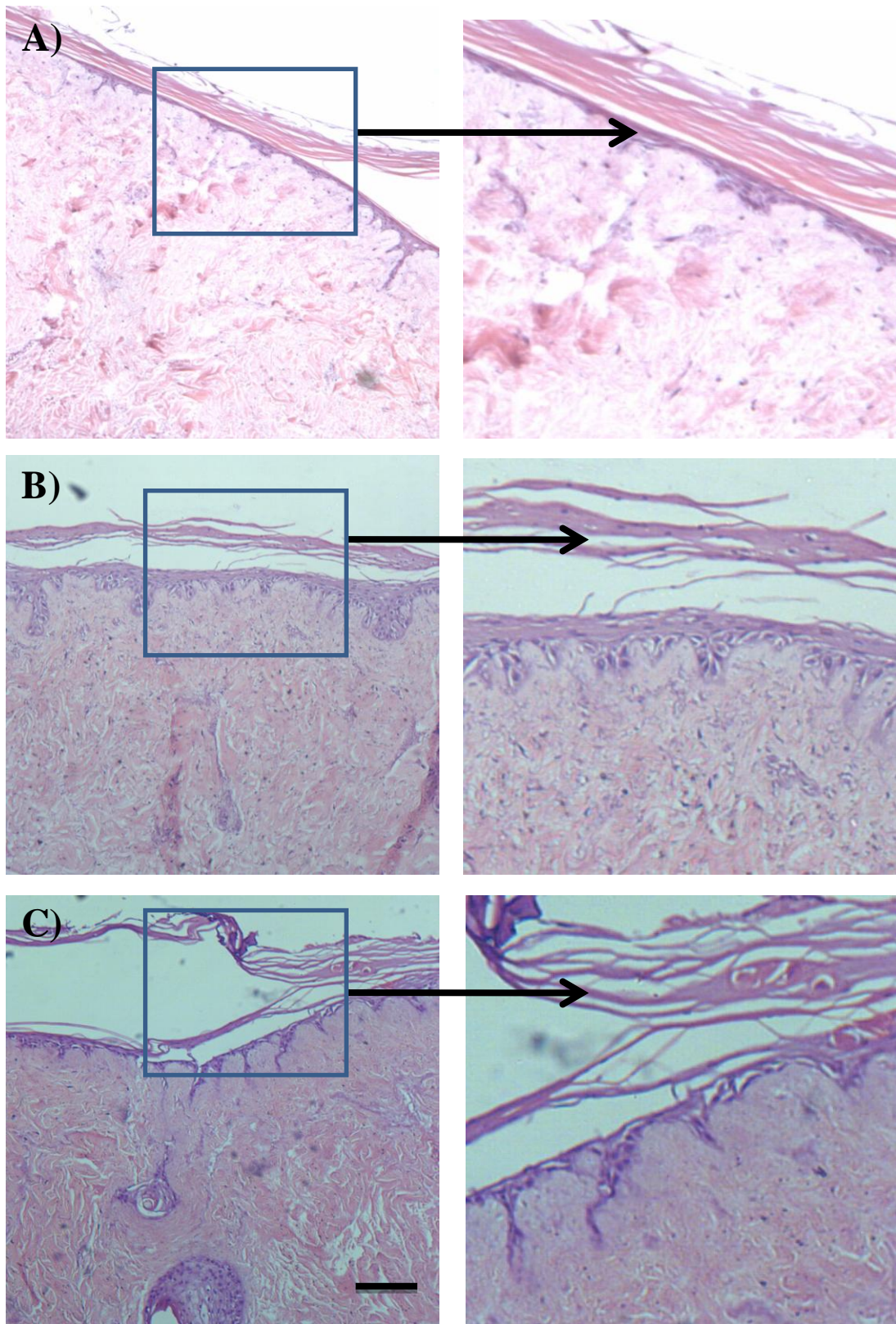
Figure 8.3 Micrographs of H&E stained TE skin cultured with concentrations of KGM (A) control, (B) 1 mg.mL^{-1} and (C) 5 mg.mL^{-1} (after 14 days culture with 10% Greens' medium. Left: 2x magnification of the area in the TE skin samples). (Scale bar: 100 μm).

8.2.3 The effect of KGM powder on the contraction of TE skin.

The effect of soluble KGM at different concentrations on the reduction of TE skin contraction was then measured using image analysis after 1, 3, 9 and 12 days of culture in ALI and shown in Figure 8.4. The graph shows a decreasing trend in the contraction of TE skin with higher concentration of KGM but this did not reach statistical significance. The changes in size of TE skin supplemented with concentrations of KGM after 3, 5, 9 and 14 days of culture are shown in Figure 8. 5.
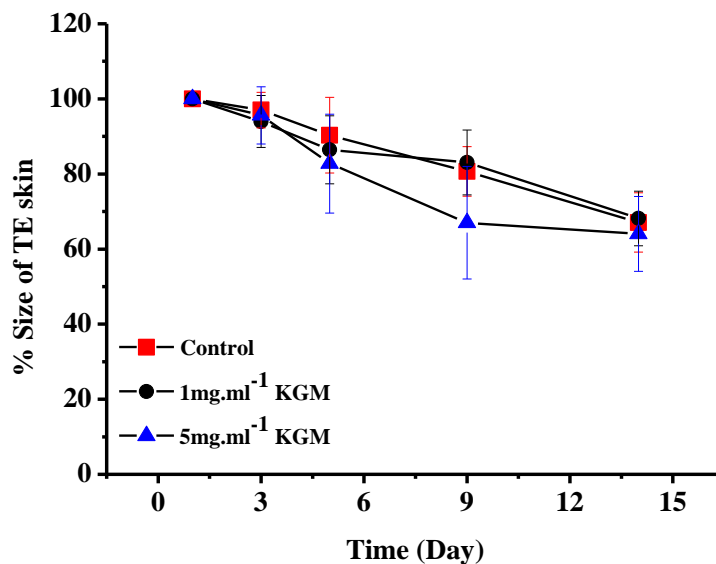
Figure 8.4 Measurement on the effect of different concentrations of KGM on the contraction of TE skin after 14 days in ALI measured using ImageJ. (n=3), ***$p<0.001$ highly significant, **$p<0.01$ very significant and *$p<0.05$ significant compared to control.
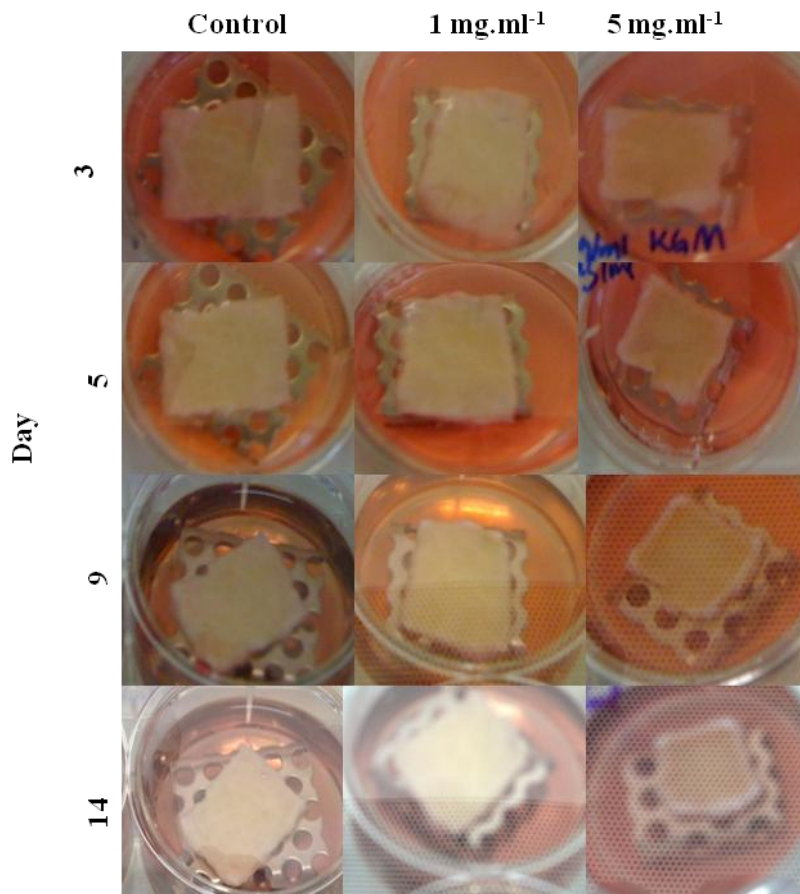
Figure 8.5 Micrographs of the appearance of TE skin with 1 and 5 mg.mL^{-1} KGM after 3, 5, 9 and 14 days in ALI.

8.2.4 The effect of crosslinked KGM with Ce(IV) on the reepithelisation, contraction and viability of TE skin.

Attempts to investigate the effect of 0.5 and 1% (w/v) crosslinked KGM hydrogels on the reepithelisation, viability and contraction of TE skin were conducted for 7, 14 and 21 days. Figure 8.6 shows the histological appearances of epidermal and dermal sections of the TE skin when the hydrogels were placed in direct contact. All samples showed good reepithelisation and segregation of dermal and epidermal layers. From the micrographs, it was obvious that the addition of 1% crosslinked KGM by day 14 led to a higher number of keratinocytes and a more secure epidermal-dermal junction. There were also more cells evident within the dermis. Higher number of cell density also was observed at day 7 and 21 on TE skin with 1% (w/v) crosslinked KGM.

ImageJ was then used to measure the thickness of proliferating keratinocyte layer and cell density in the dermal region of TE skin, which then confirmed the latter observation (Figure 8.7). The figures show that there were no differences in the thickness of stratum corneum, stratum granulosum, and stratum basale of epidermal layer of TE skin with the addition of crosslinked KGM compared to the control. However, a higher cell density was seen in the dermis on TE skin with 1% (w/v) crosslinked KGM compared to 0.5% (w/v) crosslinked KGM and the controls The effect of these hydrogels on the contraction of TE skin was measured using image analysis by comparing the images on day 7, 14 and 21 to day 0 (Figure 88). The results in Figure 8.8 shows that 0.5 and 1.0% (w/v) crosslinked KGM significantly inhibited the contraction of TE skin compared to the controls by 10-15%. The effect of KGM hydrogels on the viability of TE skin was then measured using Alamar Blue ^{TM} assay (Figure 8.9). The results show a significant reduction in the viability of TE skin with 1.0% (w/v) crosslinked KGM at day 7 and 14 compared to 0.5% (w/v) crosslinked KGM and the control.

This suggests a relationship between the inhibition of contraction of TE skin by KGM and KGM reducing the viability of the skin cells.
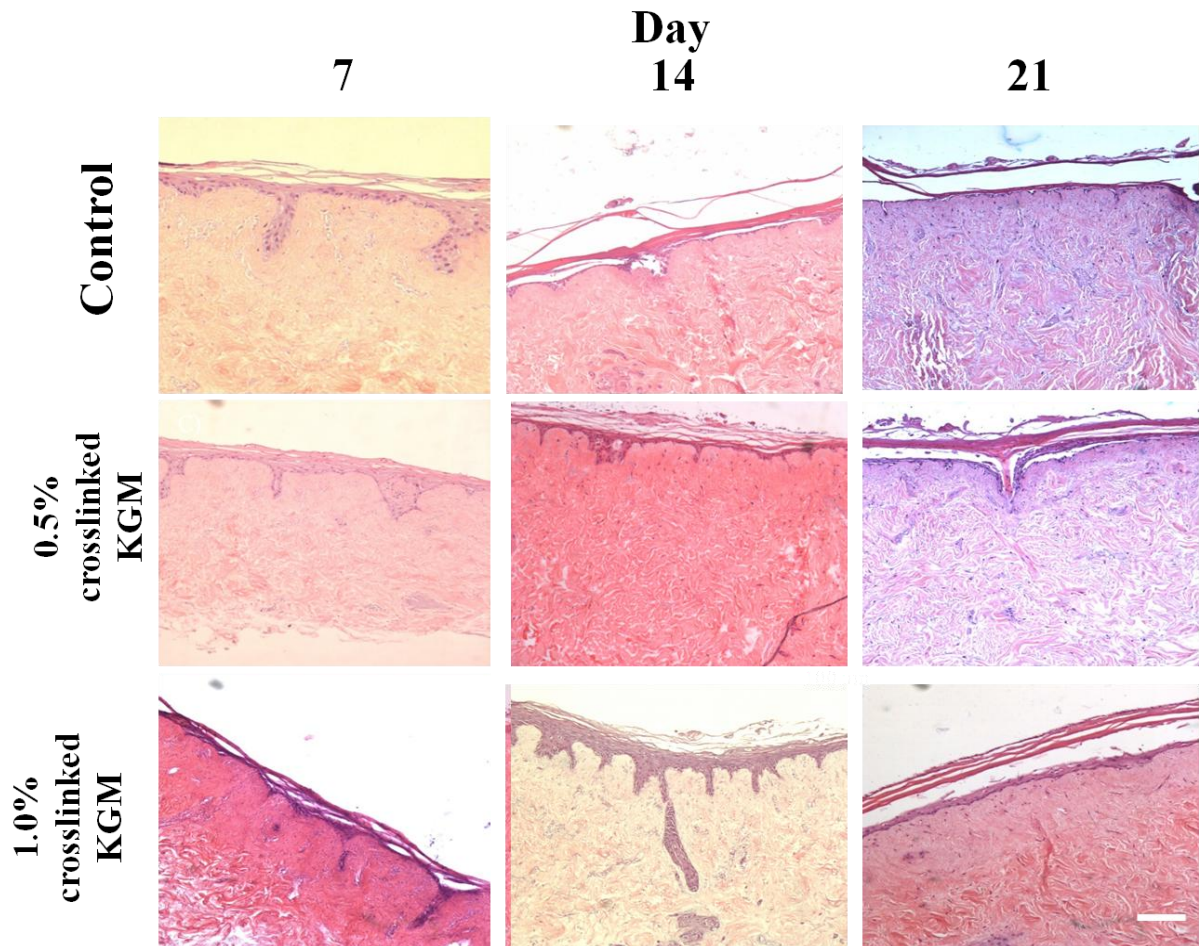
Figure 8.6 Micrographs of H&E stained TE skin cultured with 0.5 and 1% (w/v) crosslinked KGM hydrogels after 7, 14 and 21 days culture with 10% Greens' medium. (Scale bar:100 µm).
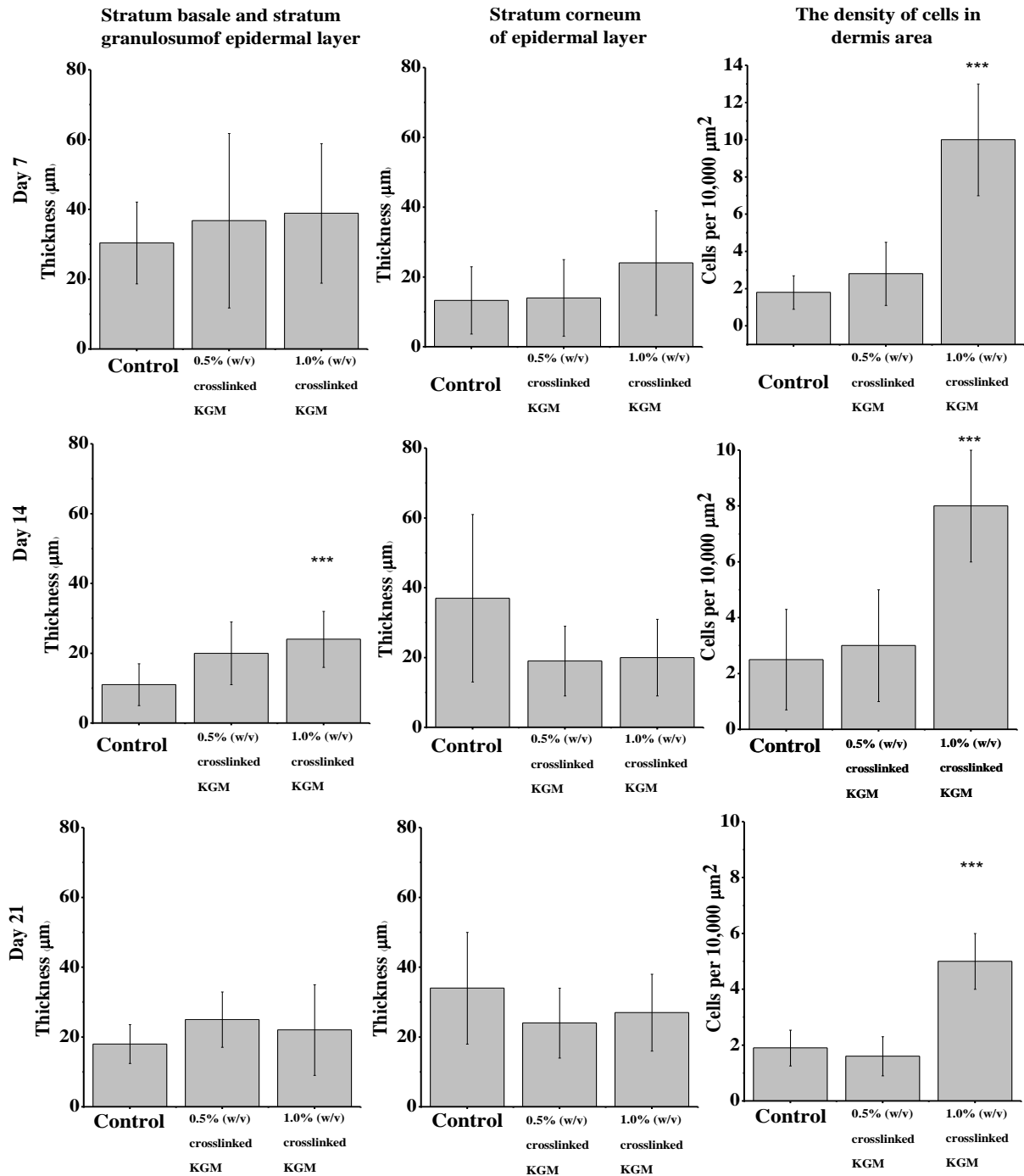
Figure 8.7 The effect of 0.5 and 1% (w/v) crosslinked KGM wt 1×10^{-3} Ce(IV) hydrogels on the thickness of proliferating (stratum basale and stratum granulosum) and differentiated epithelium (stratum corneum) layer of a TE skin and on the number of cell population in dermal region per 10,000 μm^2 of a TE skin after 7, 14 and 21 days of culture in 10% Greens' medium measured using ImageJ. (n=3), ***p<0.001 highly significant, **p<0.01 very significant and *p<0.05 significant compared to control.
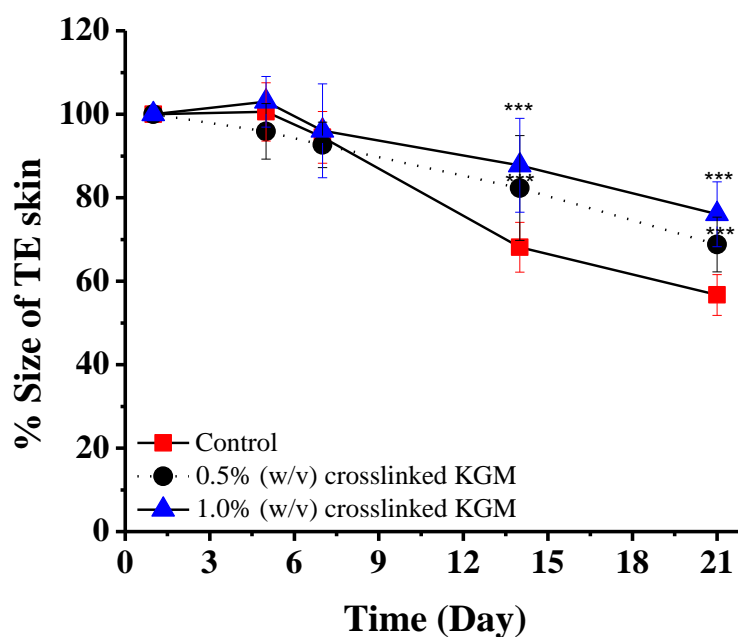
**Figure 8.8** Measurement of the contraction of TE skin model in direct contact with 0.5 and 1% (w/v) crosslinked KGM with $1 \times 10^{-3}\%$ Ce(IV) after 1, 5, 7, 14 and 21 days measured using Alamar Blue ^{TM} (n=2), ***p<0.001 highly significant, **p<0.01 very significant and *p<0.05 significant compared to control.
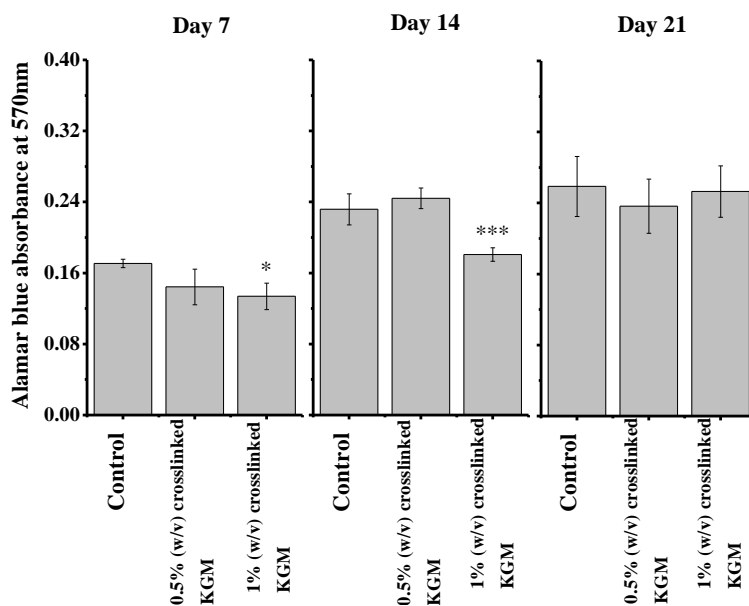
Figure 8.9 Measurement of the viability of TE skin in ALI with 0.5 and 1 % (w/v) crosslinked KGM after 7, 14 and 21 days in ALI with 10% Greens' measured using Alamar Blue ^{TM} (n=2), ***$p<0.001$ highly significant, **$p<0.01$ very significant and *$p<0.05$ significant compared to control.

8.2.5 The effect of graft-conetwork (24% (w/v) KGM wt 1% (w/v) Ce(IV)) and crosslinked KGM hydrogels on the reepithelisation, contraction and viability of TE skin.

The effects of graft-conetwork (24% KGM with 1% Ce(IV)) (w/v) hydrogel after 14 days in ALI on the reepithelisation, contraction and viability of TE skin were observed and quantified using ImageJ and Alamar Blue ^{TM} assay. These experiments show the effects of graft conetworks on the DED – unfortunately this was at a time in the laboratory when skin supplies from elective operations were very poor and towards the end of my PhD. Hence it would have been ideal to have introduced a plain hydrogel without KGM (e.g. P(NVP-co-PEGDA)) as a control but this was not possible at this time. However, the results show clear effects of both the 1% crosslinked KGM and the 24% graft-conetwork hydrogels on this DED model.

Figure 8.10 shows the histological appearances of epidermal and dermal sections of the TE skin when the hydrogels (crosslinked and graft-conetwork) were placed on the upper section of the skin at ALI after 14 days. All samples showed good reepithelisation and segregation of dermal and epidermal layers as was observed in control samples. From the micrographs, it was obvious 1.0% (w/v) crosslinked KGM and graft-conetwork (24% (w/v) KGM with 1% (w/v) Ce(IV) hydrogels had thicker layer of proliferating keratinocyte (stratum basale and stratum granulosum) and a higher number of cell density compared to control and 0.5% (w/v) KGM crosslinked hydrogel.
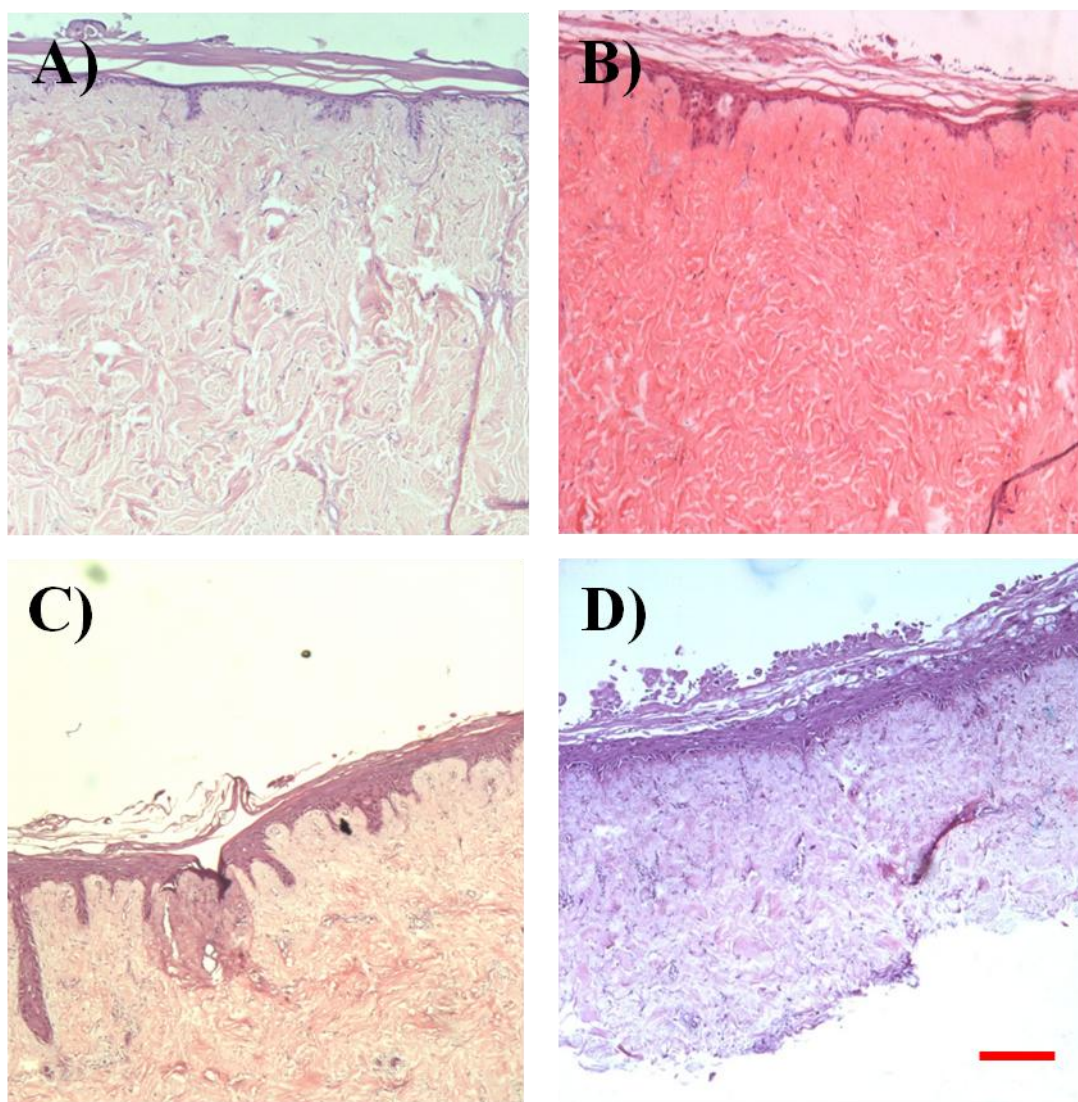
Figure 8.10 Micrographs of H&E stained TE skin cultured with (A) Control (without hydrogel), (B) 0.5% (w/v) crosslinked KGM with 1×10^{-3} % (w/v) Ce(IV), (C) 1.0% (w/v) crosslinked KGM with 1×10^{-3} % (w/v) Ce(IV) and (D) Graft-conetwork of 24% (w/v) KGM with 1% (w/v) Ce(IV) after 14 days in ALI and cultured with 10% Greens' medium. (Scale bar: 100 μm).

The thickness of the layers of proliferating keratinocytes and the number of cells in the dermis were then quantified using image analysis and shown in Figure 8.11. The figure shows that both crosslinked KGM and graft-conetworks hydrogels did not affect the thickness of proliferating keratinocytes but significantly increased the cell density in the dermis, confirming the observations in Figure 8.10.

The effect of graft-conetworks and crosslinked KGM hydrogels on the inhibition of the contraction of TE skin after 7 and 14 days was then measured using ImageJ and presented in Figure 8.12. The graph shows that both crosslinked KGM and graft-conetworks hydrogels significantly inhibited the contraction of TE skin after 14 days in ALI. The relationship between inhibition of contraction and the viability of TE skin was then measured using Alamar Blue [TM] where the result and these observations are shown in Figure 8.13 and 8.14.

Figure 8.13 shows that only TE skin with 1% (w/v) crosslinked KGM after 14 days in ALI had a significant reduction in viability compared to the control and TE skin with graft conetworks. There was no difference in the viability of TE skin with crosslinked KGM and graft-conetworks hydrogels at day 7 and 21, indicating that proliferating keratinocytes were most active at day 14. The change in color from dark blue to pink from Alamar Blue [TM] reduction in oxidation is shown in Figure 8.14. TE skin with crosslinked KGM appeared blue compared to control and TE skin with graft-conetworks with light pink and purple respectively.
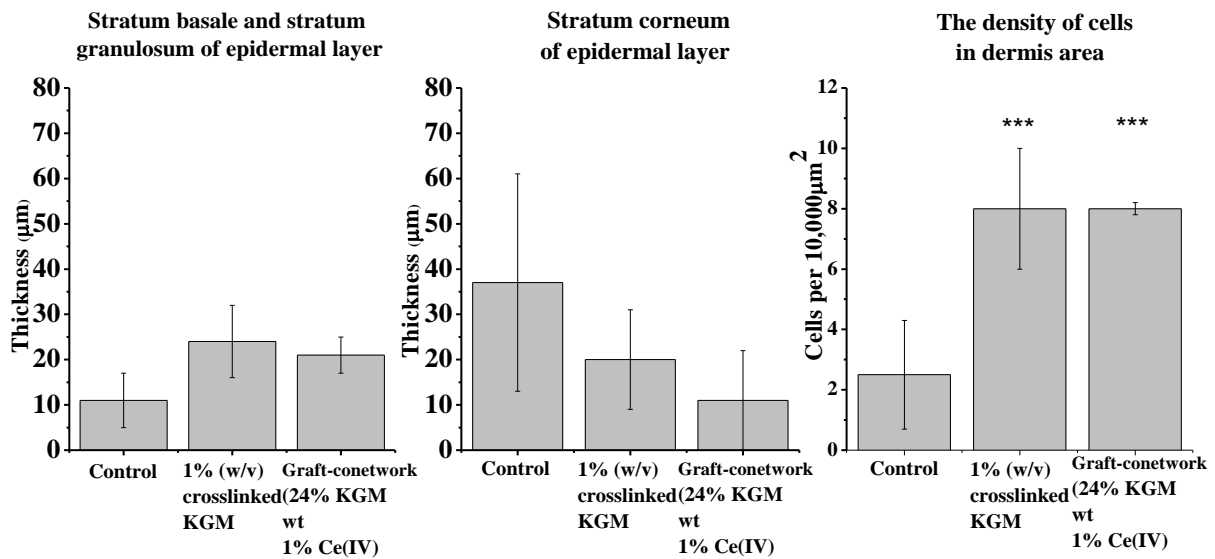
Figure 8.11 The effect of crosslinked KGM (0.5 and 1% (w/v) KGM) and graft-conetwork (24% (w/v) KGM with 1% (w/v) Ce(IV)) hydrogels on the thickness of proliferating (stratum basale and stratum granulosum) and differentiated epithelium (stratum corneum) layers of a TE skin and on the number of cell population in dermal region per 10,000 μm^2 of a TE skin after 14 days in ALI with 10% Greens' measured using ImageJ analysis. (n=3), ***p<0.001 highly significant, **p<0.01 very significant and *p<0.05 significant compared to control.
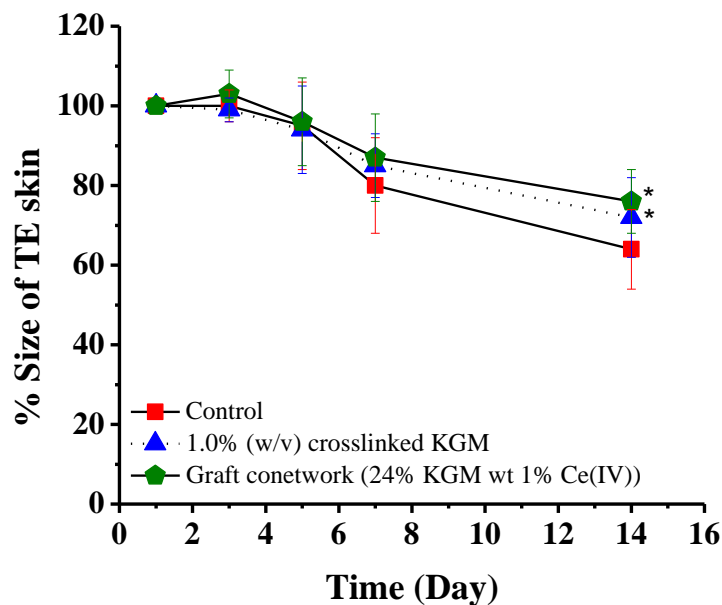
Figure 8.12 Measurement of the contraction of TE skin in direct contact with 1% (w/v) crosslinked KGM and graft-conetwork hydrogels for 14 days in ALI with 10% Greens' measured using imageJ analysis (n=3), ***p<0.001 highly significant, **p<0.01 very significant and *p<0.05 significant compared to control.
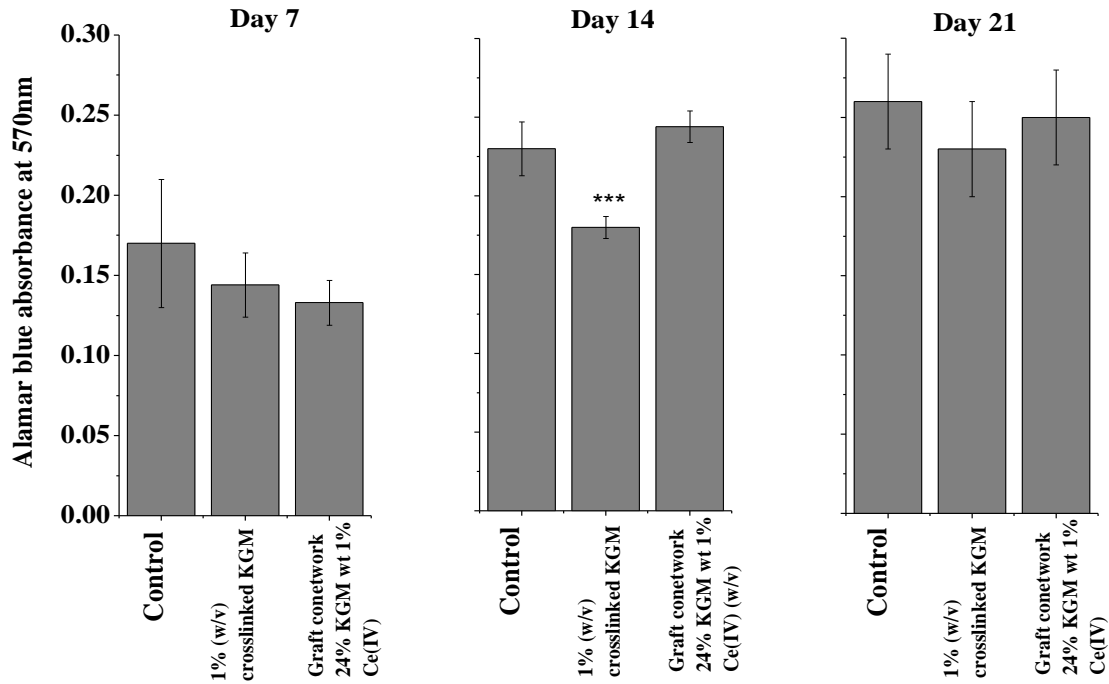
Figure 8.13 Measurement of the viability of TE skin at an ALI with 1% (w/v) crosslinked KGM and graft-conetworks hydrogels after 7, 14 and 21 days in ALI with 10% Greens' measured using Alamar Blue ™ (n=2), ***p<0.001 highly significant, **p<0.01 very significant and *p<0.05 significant compared to control.
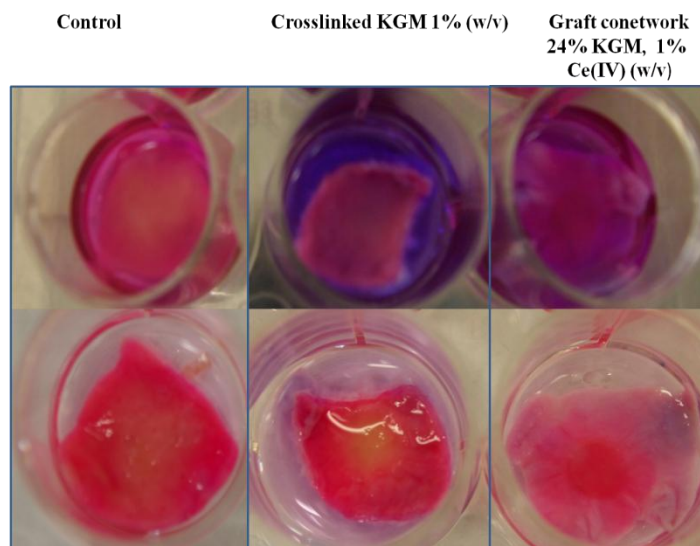
Figure 8.14 Micrographs of the viability of TE skin with 1% (w/v) crosslinked KGM and graft-conetworks hydrogels after 14 days in ALI with 10% Greens' measured using Alamar Blue [TM].
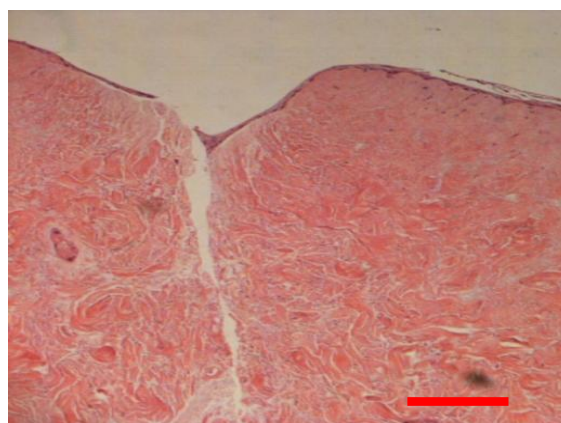
Figure 8.15 Micrograph of the incision in TE skin for wound model after 5 days in culture with keratinocytes and fibroblasts in 3:1 ratio at ALI with 10% Greens'. (Scale bar: 100 μm).

8.2.6 The effect of crosslinked KGM and graft-conetwork hydrogels on the reepithelisation, contraction and viability of wounded TE skin.

In this section, the effect of crosslinked KGM (0.5 and 1% (w/v) KGM with 1×10^{-3}% (w/v) Ce(IV)) and graft-conetwork (24% (w/v) KGM with 1% (w/v)Ce(IV)) on the reepithelisation and contraction of wounded TE skin was investigated and measured using ImageJ and Alamar Blue ^{TM} assay. The wound was created after 5 days of initial seeding of fibroblasts and keratinocytes (3:1) on DED and is shown in Figure 8.15.

Reepithelisation of wounded TE skin after 14 days was observed using H&E staining and is shown in Figure 8.16. There was no evident effect of the addition of the hydrogels on wound healing in this model. However, it should be noted that the incisional cuts used healed rapidly within 14 days in all cases. The figure also shows that all TE skin shows good reepithelisation with evidence of cell migration into the void with formation of keratinized layers. In this study, the inhibition of the contraction of wounded TE skin was also investigated (Figure 8.17 8.19). Figure 8.17 shows that the addition of KGM and graft-conetworks hydrogels significantly inhibited skin contraction compared to the controls while not preventing it completely. The micrographs of the reduction in the size of TE skin with crosslinked KGM and graft-conetworks hydrogels during 14 days period are shown in Figure 8.18. The relationship between wounded TE skin contraction and viability was then investigated and shown in Figure 8.19, 8.20 and 8.21(Also refer to Figure 8.17). These figures show that wounded TE skin with 1% (w/v) crosslinked KGM had significantly low viability at day 14 compared to the control and wounded TE skin with graft-conetworks hydrogels. Observation in Figure 8.20 shows that the color of Alamar Blue ^{TM} appeared to be pale violet for both samples with 0.5 and 1% (w/v) crosslinked KGM compared to control and graft-conetworks hydrogel with shades of pink. The figure 8.20 (C and D) show that the incisions at both TE skins were completely healed, although having differences in viability.

The figure also shows that whilst crosslinked KGM and graft-conetworks hydrogels inhibited the contraction of wounded TE skin, the viability of TE skin with graft-conetworks hydrogel was higher than TE skin with crosslinked KGM which suggests that the inhibition of proliferating keratinocyes was less active in TE skin with graft-conetworks. A clearer observation of completely healed wounded TE skin with crosslinked KGM and graft-conetworks hydrogels is shown in Figure 8.21 (C and D).

Although previously the void area of wounded TE skin with graft-conetworks did not show any abnormality, hyperkeratosis was observed in the other areas of the epidermis. Hyperkeratosis is the thickening of keratinized layer of epidermis which is a general reaction in response to injury either by mechanical, chemical, electrical or thermal stimuli. The photomicrographs of the formation of hyperkeratosis on the epidermal area are shown in Figure 8.22. The pictures suggest that in wounded TE skin, the graft-conetworks hydrogels had different biological properties compared to crosslinked KGM and the controls, in which their wounded TE skin had a normal epidermis.
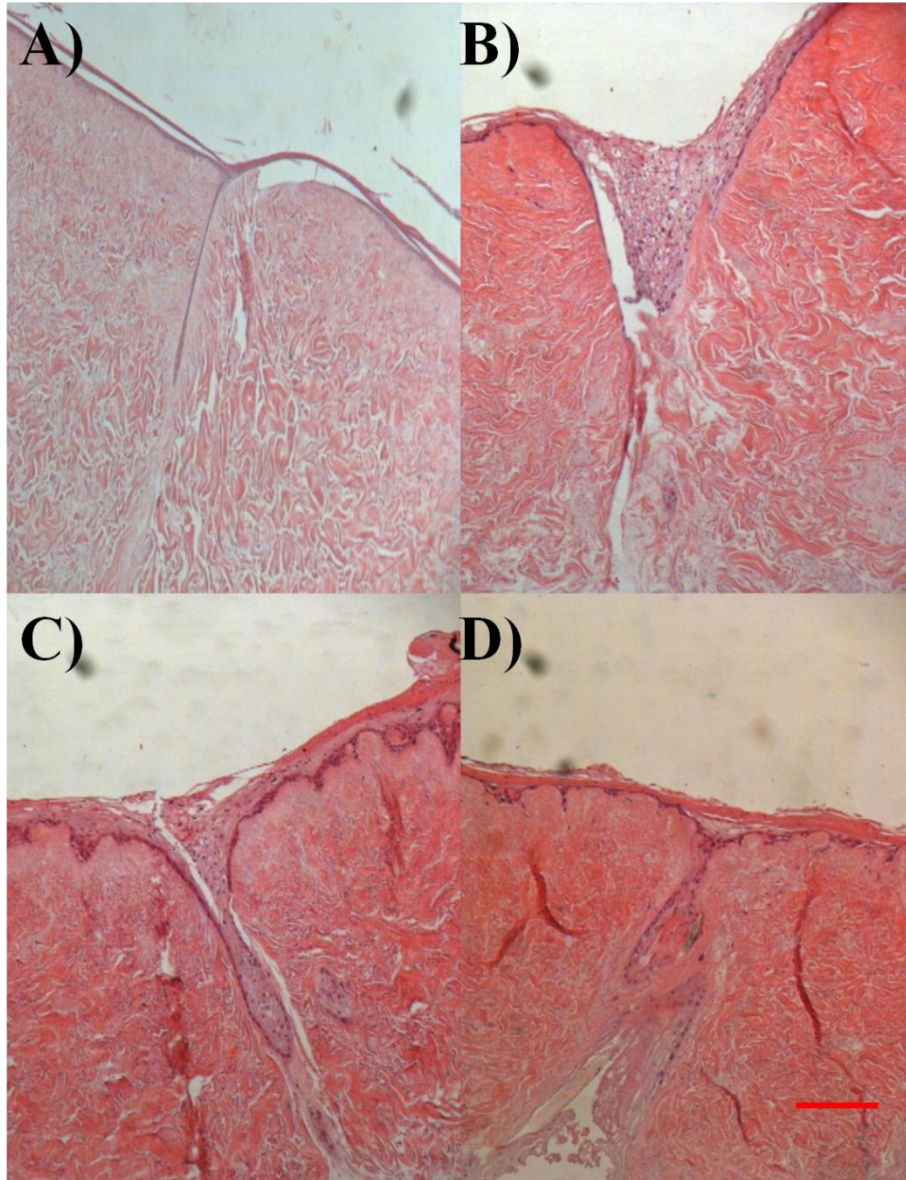
Figure 8.16 Microphotographs of H&E stain TE skin wound model (A) control (B) 0.5% (w/v) crosslinked KGM (C) 1.0% (w/v) crosslinked KGM and (D) Graft-conetwork of 24% (w/v) KGM wt 1% (w/v) Ce(IV). The photographs showed no difference in the reepithelisation of TE skin with migrating keratinocytes into the void area after incision at day 5. (Scale bar: 100 μm).
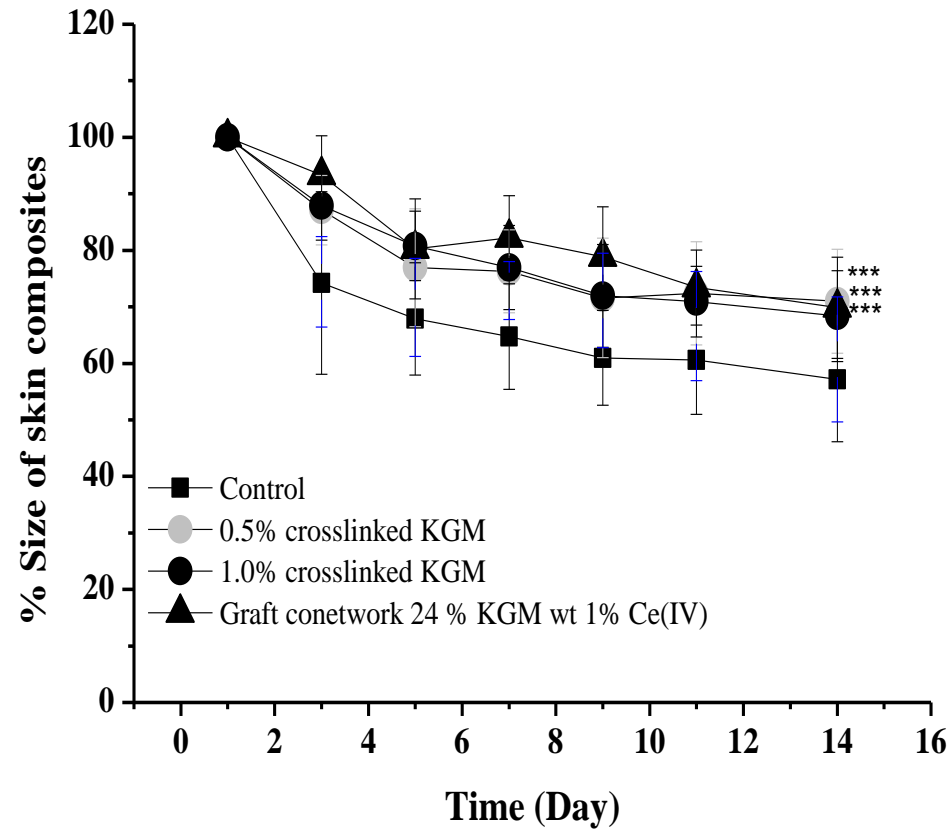
Figure 8.17 Measurement of the contraction of wounded TE skin in direct contact with crosslinked KGM with Ce(IV) and graft-conetwork hydrogels up until 14 days in ALI with 10% Greens' measured using image analysis (n=3), ***p<0.001 highly significant, **p<0.01 very significant and *p<0.05 significant compared to control .
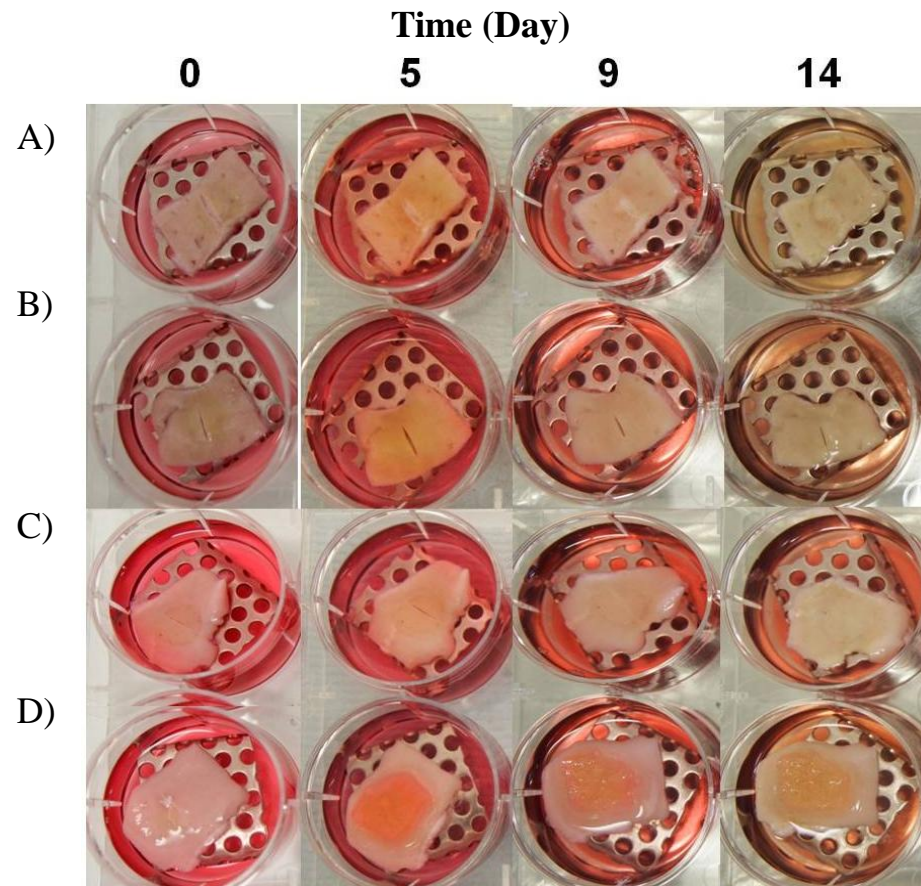
Figure 8.18 Micrographs of the effect of KGM hydrogels on the reepithelisation of a wound on TE skin with (A) control, (B) 0.5 % (w/v) crosslinked KGM, (C) 1% (w/v) crosslinked KGM and (D) graft-conetworks hydrogel (24% (w/v) KGM and 1% (w/v) Ce(IV) after 0, 5, 9 and 14 days in ALI with 10% Greens'. Note that at C and D, the wounds had completely healed.
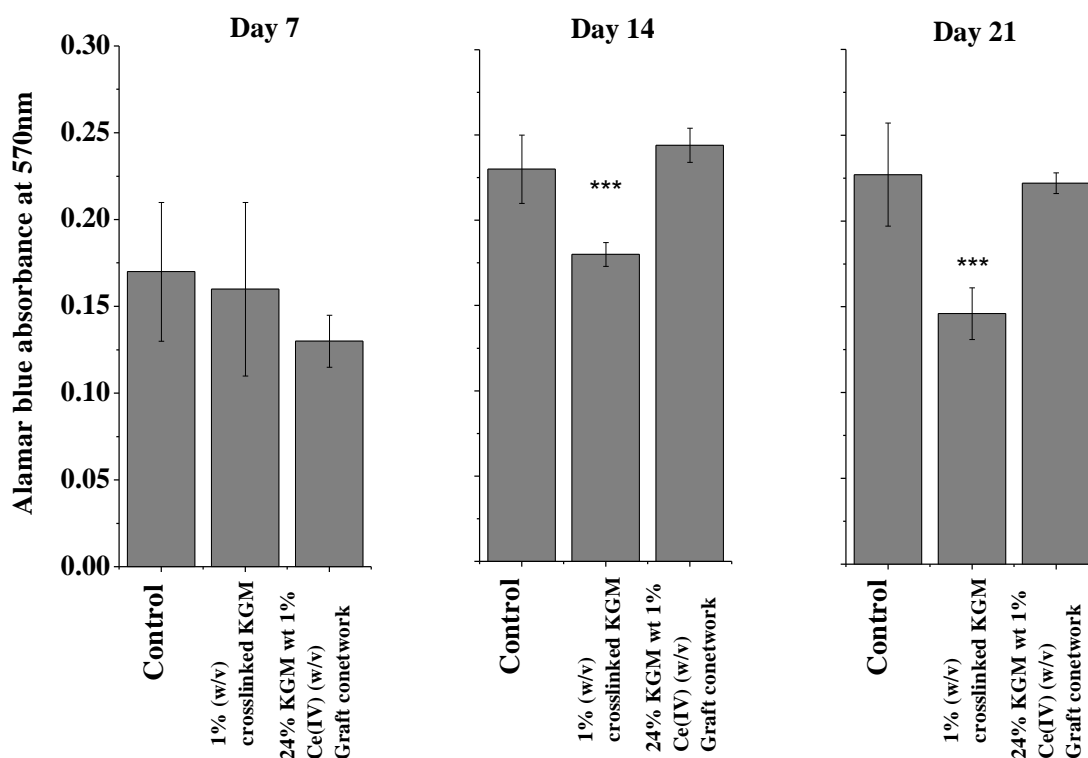
Figure 8.19 Measurement of the viability of wounded TE skin in ALI with 1 % (w/v) crosslinked KGM and graft-conetworks hydrogels after 7, 14 and 21 days in ALI with 10% Greens' measured using Alamar Blue [TM] (n=2), ***p<0.001 highly significant, **p<0.01 very significant and *p<0.05 significant compared to control.
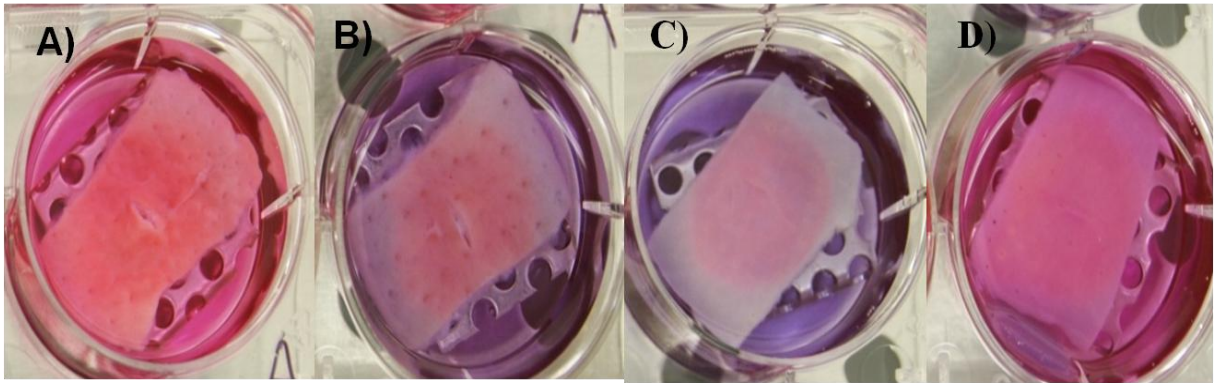
Figure 8.20   Micrographs of the effect of KGM hydrogels on the reepithelisation of a wound on TE skin with (A) control, (B) 0.5 % (w/v) crosslinked KGM, (C) 1% (w/v) crosslinked KGM and (D) graft-conetworks hydrogel (24% (w/v) KGM and 1% (w/v) Ce(IV) after 14 days in ALI with 10% Greens' measured using Alamar Blue assay. Note that in C and D, the wounds had completely healed.
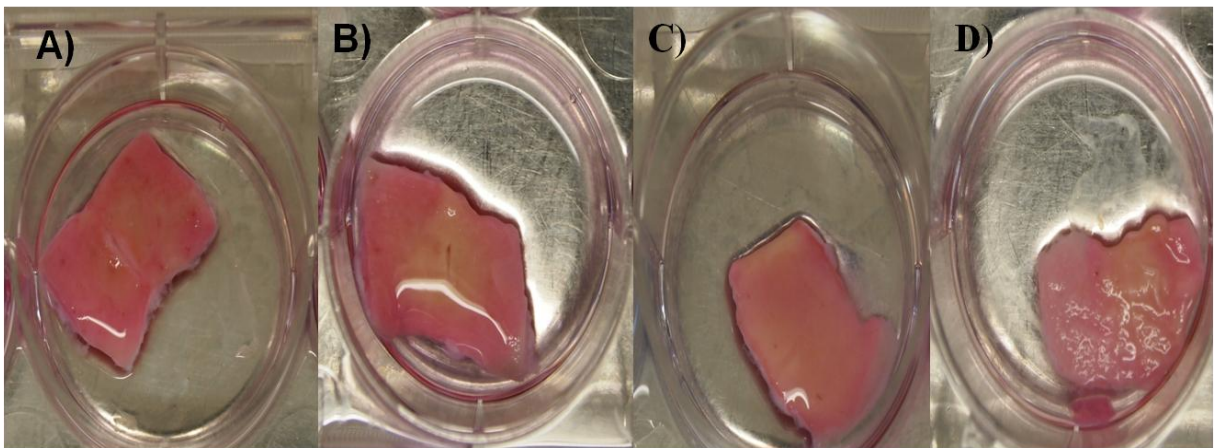
Figure 8.21   Micrographs of the effect of KGM hydrogels on the reepithelisation of a wound on TE skin with (A) control, (B) 0.5 % (w/v) crosslinked KGM, (C) 1% (w/v) crosslinked KGM and (D) graft-conetworks hydrogel (24% (w/v) KGM and 1% (w/v) Ce(IV) after 14 days in ALI with 10% Greens'. Note that C and D, the wounds had completely healed and the TE skin showed appearance of yellowish and pink indicating healthier physiology of a skin.

+ graft-conetworks
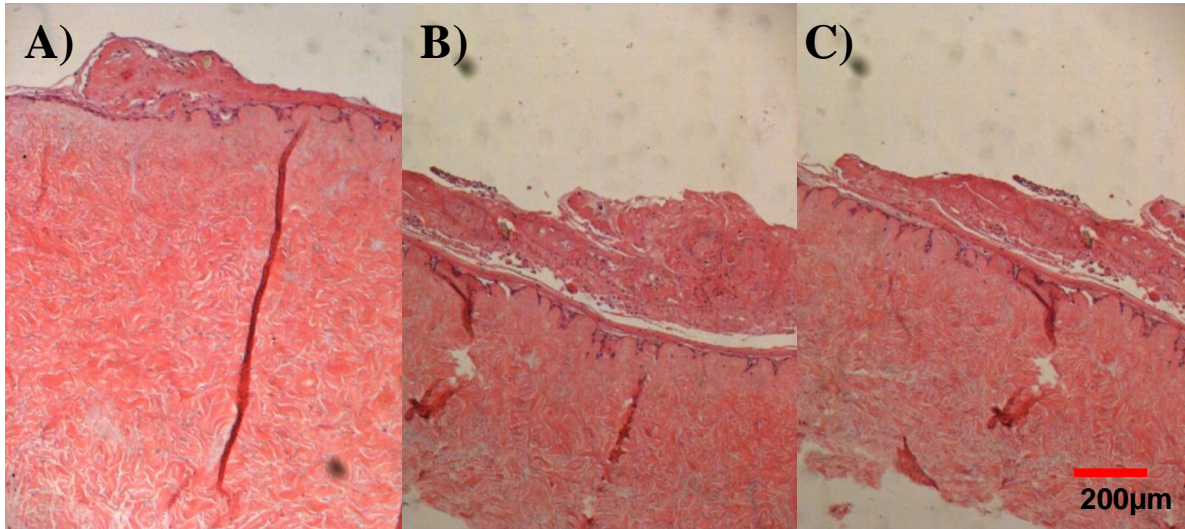
Figure 8.22 (A-C) The formation of hyperkeratosis in TE skin wound model with graft-conetwork hydrogel of 24% (w/v) KGM wt 1% (w/v) Ce(IV) after 14 days from the same triplicate experiment. (Scale bar: 200 µm).

8.3 Discussion.

This chapter has provided several useful pointers to the potential therapeutic benefits of KGM and KGM hydrogels on TE skin, specifically stimulation of fibroblast proliferation, improvement of the epidermal/dermal junction and a slight reduction in the extent of skin contraction. The hydrogels, crosslinked KGM (1% (w/v) KGM) wt 1×10^{-3}% (w/v) Ce(IV) and graft-conetwork (24% (w/v) KGM wt 1% (w/v) Ce(IV) significantly reduced the contraction of TE skin populated with fibroblasts and keratinocytes without disrupting the formation of the dermal and epidermal layers. The relationship between the reduction in skin contraction and cellular viability was then measured using Alamar Blue^{TM}, where the color changed from blue to pink demonstrated the presence of active mitochondrial reduction-oxidation activities. It showed that the presence of KGM hydrogels on the TE skin surfaces reduced cell viability compared to the control (without KGM). It was hard to verify which cells might be contributing to this effect, due to complex synergistic behaviour of fibroblast and keratinocyte (Werner, Krieg et al. 2007). It was possible that KGM's effect on the inhibition of keratinocyte proliferation might be responsible for reducing the contraction as it has previously been shown that keratinocytes can contract the DED model by as much as 40% over 14 days (Ralston, Layton et al. 1997; Chakrabarty, Heaton et al. 2001).

Whilst KGM hydrogels show remarkable effects on the stimulation of cell density in the dermis, their relationship to the reduction of TE skin contraction is still unknown. Although Alamar Blue ^{TM} assay suggested inhibition of proliferating keratinocytes by KGM could contribute to the reduction of contraction, further investigations on the effect of cytokines and MMP expressions should be taken into account to fully understand the mechanism of skin contraction.

Preliminary studies on the reepithelisation of wounded TE skin models treated with KGM hydrogels indicated that all samples promoted cell migration and reepithelisation. Observations on wounded TE skin after 14 days at an ALI showed that 1% crosslinked KGM and graft-conetworks hydrogels improved healing with closed gaps and appeared pinkish, indicating they were   in good condition compared to the controls and those with 0.5% crosslinked KGM. Although there were differences in the viability of TE skin with 1% crosslinked KGM and graft-conetworks hydrogels, it was possible that the increased viability of TE skin with graft-conetworks hydrogels was because of hyperkeratosis.

Hyperkeratosis is seen in psoriasis where there appears to be premature differentiation of keratinocytes producing many layers in a basket weave (Bos, De Rie et al. 2005). It has previously been noted in this model when matrix metalloproteinases (MMP) were inhibited with Galardin, a broad spectrum inhibitor for MMP (Chakrabarty, Heaton et al. 2001). There are also other factors such as the differences between normal and wounded skin's expression/suppression of cytokines, sensitivities to T-cell activation, and down regulation processes (Bos, De Rie et al. 2005).

There was a problem with the wound model. It was difficult to make a standard incision and control the area of the wound. This really requires a better wound model and further studies to investigate the effects of the hydrogels on cell migration. It is hoped that this preliminary will receive further investigation in a better wound model.

8.4 Conclusions.

This chapter extends the previous work on KGM hydrogels on skin cells using 2D cell culture and wound scratch assays. In this chapter the effects were studied on a 3D tissue engineered skin model. The results show that all KGM hydrogels used in this study were biocompatible, the majority of them actually improved the epidermal/dermal junction and at the same time promoted fibroblast proliferation. The crosslinked hydrogel, which are biodegradable, and graft conetworks, which are non-biodegradable, are interesting materials for wound healing as both are easy to handle, and apply to different types of wound. The non-degradable material would require removing, whereas the degradable material would not. The latter could avoid the need for frequent changes of dressings and avoid disrupting newly formed skin. While time did not permit extensive studies of the effects of the hydrogels on this model the results are clearly encouraging and merit further investigation into these plant derived hydrogels capable of promoting wound healing.

Chapter 9. Final discussion and Future works.

In summary this thesis explores the use of KGM, and the development of KGM hydrogels for wound healing applications and presents some of the challenges faced during experiments with these gels in 2D cell culture and TE skin. The results provide insights into the use of KGM for the treatment of wounds and also unexpectedly for cell transportation.

The aim of this project was to demonstrate the potential of KGM in the development of hydrogels for wound healing and cell transportation applications.

To achieve this, a series of objectives were identified: 1) to examine and characterize the biological properties of KGM on skin cells, 2) to investigate the potential of KGM for cell transportation, 3) to develop biodegradable crosslinked KGM and non-degradable semi-IPN and graft-conetworks hydrogels, 4) to investigate the biological effects of KGM hydrogels on skin cells, TE skin and wound model.

Cytotoxicity testing showed that KGM is very stimulatory to fibroblast proliferation but inhibitory to keratinocyte proliferation and also able to support both fibroblasts and ADMSC cell culture in unchanged medium up to 20 days. The results on fibroblasts and keratinocytes were also observed with crosslinked KGM and graft-conetworks hydrogels, indicating that both hydrogels were biologically active. Cytotoxicity testing on these hydrogels is very important to determine the extend of Ce(IV) concentrations that would be safe for cell before further testing on TE skin and wound model.

The data emerging from the characterizations and biological activities of different species of KGM, Glc:Man ratio and fractions of *A. konjac* Koch at different molecular weights on the biological activities unleashed the potential of KGM as drug delivery vehicle and hydrogels with specific functions. It is also noteworthy to clarify and investigate more on the role of MR and lectins, as it will not only increase understanding of cellular interactions and signalling, but more importantly could also lead to new treatment strategies for several

human pathologies, particularly diabetic wound healing.

Initially the attempts were made to produce KGM hydrogels of crosslinked KGM with properties that would benefit wound healing. However, the nature of this hydrogel that breaks easily makes experimental with skin cells in 2D difficult, especially when removing the medium out from the well plate. Therefore, improvements to produce materials with greater strength and mechanical properties were conducted by adding P(NVP) crosslinked with PEGDA to form semi-IPN and graft-conetworks hydrogels. These non-degradable hydrogels have different biological and chemical properties, where semi-IPN had higher EWC and KGM content compared to graft-conetworks hydrogels. Semi-IPN are inert while graft-conetworks hydrogels promoted cell migration and stimulate fibroblast proliferation. Although graft-conetworks hydrogels had remarkable properties for wound healing, both skin cells (keratinocytes and fibroblasts) were not able to successfully attach and proliferate onto the hydrogel.

Both degradable and non-degradable hydrogels presented in this thesis are equally important for wound healing. There are number of areas where further works could be carried out to improve the understanding of the results presented in this thesis and to explore more potential KGM hydrogels for wound healing applications. A more detailed study on the characterizations of the synthesized hydrogels would also be advantageous to further understand the factors that influence cell-cell and cell-material interactions. However, it would be necessary that the hydrogels to be produced in sterile environment and aseptically ready to be used on wounded skin.

One of the most interesting applications for the hydrogel is for cell transportation across Europe as was previously highlighted by Eves et. al (2006). The results in chapter 6 show that KGM and crosslinked KGM were able to increase and maintain fibroblast viability outside the incubator, that mimicked transportation condition. The experiment performed in this

study were conducted using only one type of cell, fibroblasts and performed within the lab condition, at inside and outside the incubator subjected to shear stress. It would be interesting to test the effect of these hydrogels on a different type of cells such as ADMSC. Further experiment should also be conducted to compare the ability of these hydrogels with different parameters that would be similar to transportation condition such as variation in temperature, CO_2 and O_2 supplies.

The data on the effects of KGM and KGM hydrogels on the reepithelisation of TE skin and wounded TE skin was promising but requires further investigation. Although the results in this section were very brief, due to limitation of time for PhD research and lack of skin supplies, it would be necessary in the future to conduct more repeat experiments before going further into animal testing *in vivo* for wound healing application. There was also some limitation to the TE skin model used in this research due to non-standardized dermal samples from various donors. All skin samples are collected on an anonymous basis under an HTA research tissue bank licence so it is not possible to relate skin to donor details. In addition to this, further experiments would also need to be carried out to look at a range of biological effects that include collagen production and promotion/inhibition of different type of cytokines. Improvements in the TE skin model to assess the effect of the hydrogels in the reepithelisation and wound healing should also need to be taken into consideration as skin consists of more than just fibroblasts and keratinocytes. Other cells, such as melanocytes, macrophages and neutrophils that found in skin should also be included in the future skin model. Although this model has been used for many years in Professor MacNeil's group in studying skin contracture, it would be interesting to develop a fully functional skin that consist all type of skin cells with dermal architecture and basal membrane that mimic real skin.

A major drawback in the production of TE skin is the accessibility of skin biopsies for DED and cell extractions. Cultured epithelial autologous grafts are usually produced from keratinocytes at low passages (1 to 2). However, these keratinocytes rapidly lose their proliferative capabilities and differentiate early when cultured *in vitro* under inappropriate conditions. It is necessary to maintain keratinocyte culture in a condition that allow good proliferation by delaying their terminal differentiation, to maintain their capacity to act like normal skin epithelial cells once grafted on a patient as to ensure the long term regeneration of the epidermis (Bisson, Rochefort et al. 2013). Other considerations such as the use of mouse i3T3 for feeder layer and foetal calf serum should also be considered in order to prevent transmission of viruses, mycoplasma contamination and protein diseases such as bovine spongiform e. (BSE).

One of the interesting findings presented in this thesis was that the use of graft-conetworks hydrogels on TE skin led to a reduction in the rate of contraction over period of 14 days. Earlier, graft-conetworks hydrogels were shown to stimulate fibroblasts and inhibit keratinocyte proliferation and stimulate migration of both cell types in a wound scratch assay. As discussed earlier, further studies on the effect of graft-conetworks hydrogels on collagen synthesis and cytokines production on TE skin would be needed before proceeding to animal or clinical studies.

10. References

Abercrombie, M., M. H. Flint, et al. (1956). "Wound Contraction in Relation to Collagen Formation in Scorbutic Guinea-pigs." Journal of Embryology and Experimental Morphology **4**(2): 167-175.

Adderley, U. (2010). "Managing wound exudate and promoting healing." British Journal of Community Nursing, Vol. 15, Iss. 3 Suppl, 01 Mar 2010, pp S15 - S20 **15**(3): 15-20.

Ahn, S. J., J. Costa, et al. (1996). "PicoGreen Quantitation of DNA: Effective Evaluation of Samples Pre-or Psost-PCR." Nucleic Acids Research **24**(13): 2623-2625.

Aksoy, M. H., I. Vargel, et al. (2002). "A New Experimental Hypertrophic Scar Model in Guinea Pigs." Aesthetic Plastic Surgery **26**(5): 388-396.

Al-Ghazzewi, F. H. and R. F. Tester (2010). "Effect of konjac glucomannan hydrolysates and probiotics on the growth of the skin bacterium Propionibacterium acnes in vitro." International Journal of Cosmetic Science **32**(2): 139-142.

Almeida, N., A. Mueller, et al. (2013). "Rheological Studies of Polysaccharides for Skin Scaffolds." Journal of Biomedical Materials Research Part A: n/a-n/a.

Alonso-Sande, M., D. Teijeiro-Osorio, et al. (2009). "Glucomannan, a promising polysaccharide for biopharmaceutical purposes." European Journal of Pharmaceutics and Biopharmaceutics **72**(2): 453-462.

Alpesh, P. and K. Mequanint (2011). "Hydrogel Biomaterials, Biomedical Engineering - Frontiers and Challenges, ."

Angele, M. K., M. W. Knöferl, et al. (1999). "Trauma-hemorrhage delays wound healing potentially by increasing pro-inflammatory cytokines at the wound site." Surgery **126**(2): 279-285.

Astarie-Dequeker, C., E.-N. N'Diaye, et al. (1999). "The Mannose Receptor Mediates Uptake of Pathogenic and Nonpathogenic Mycobacteria and Bypasses Bactericidal Responses in Human Macrophages." Infection and Immunity **67**(2): 469-477.

Atiyeh, B. S., S. N. Hayek, et al. (2005). "New technologies for burn wound closure and healing--review of the literature." Burns **31**(8): 944-56.

Bae, M., R. A. Gemeinhart, et al. (2010). "Fabrication of poly(ethylene glycol) hydrogel structures for pharmaceutical applications using electron beam and optical lithography." J. Vac. Sci. Technol. **28**(6): 24.

Becker, J. W., G. N. Reeke, et al. (1976). "New evidence on the location of the saccharide-binding site of concanavalin A." Nature **259**(5542): 406-409.

Berger, J., M. Reist, et al. (2004). "Structure and interactions in covalently and ionically crosslinked chitosan hydrogels for biomedical applications." European Journal of Pharmaceutics and Biopharmaceutics **57**(1): 19-34.

Billingham, R. E. and P. B. Medawar (1955). "Contracture and intussusceptive growth in the healing of extensive wounds in mammalian skin." J Anat 89: 114 **89**: 114.

Bisson, F., E. Rochefort, et al. (2013). "Irradiated Human Dermal Fibroblasts Are as Efficient as Mouse Fibroblasts as a Feeder Layer to Improve Human Epidermal Cell Culture Lifespan." Int. J. Mol. Sci **14**(3): 4684-4704.

Biswas, A., M. Bharara, et al. (2010). "Use of sugar on the healing of diabetic ulcers: a review." J Diabetes Sci Technol **4**(5): 1139-45.

Blaschek, W., J. Kasbauer, et al. (1992). "Pythium aphanidermatum: culture, cell wall composition, and isolation and structure of antitumour storage and solubilised cell-wall (l→3) (l→6)-β-D-glucans." Carbohyd Res. **231**: 293-307.

Blasi, F. and P. Carmeliet (2002). "uPAR: a versatile signalling orchestrator." Nat Rev Mol Cell Biol **3**(12): 932-943.

Blokzijl, W. and J. B. F. N. Engberts (1993). "Hydrophobic Effects. Opinions and Facts." Angewandte Chemie International Edition in English **32**(11): 1545-1579.

Bo Chen, Bernice Wright, et al. (2012). "A novel alternative to cryo-preservation for the short term storage of stem cells for use in cell therapy using alginate encapsulation." Tissue Engineering Part C: Methods. .

Bohn, J. A. and J. N. BeMiller (1995). "(1-3)-*B*-d-Glucans as biological response modifiers: a review of structure-functional activity relationships." Carbohydrate Polymers **28**(1): 3-14.

Bohn, J. A. and J. N. BeMiller (1995). "(1->3)-B-D-Glucans as biological response modifiers: a review of structure-functional activity relationships." Carbohydrate Polymers **28**(1): 3-14.

Bos, J. D., M. A. De Rie, et al. (2005). "Psoriasis: dysregulation of innate immunity." British Journal of Dermatology **152**(6): 1098-1107.

Bradshaw, C. E. (2011). "An in vitro comparison of the antimicrobial activity of honey, iodine and silver wound dressings." Bioscience Horizons.

Brannon-Peppas, L. and N. A. Peppas (1990). "Dynamic and equilibrium swelling behaviour of pH-sensitive hydrogels containing 2-hydroxyethyl methacrylate." Biomaterials **11**(9): 635-644.

Braun, S. and S. Werner (2006). Wound Healing. Encyclopedic Reference of Genomics and Proteomics in Molecular Medicine, Springer Berlin Heidelberg**:** 2008-2011.

Breasted, J. H. (1930). The Edwin Smith Surgical Papyrus. Chicago, Univ. Chicago Press.

Brenda, E., A. r. Marques, et al. (1995). "Action of papain, sugar, minoxidil, and glucan on excisional wounds in rats." Current Therapeutic Research **56**(12): 1285-1297.

Bundle, D. R. and N. M. Young (1992). "Carbohydrate-protein interactions in antibodies and lectins." Current Opinion in Structural Biology **2**(5): 666-673.

Buonomo, R., F. Giacco, et al. (2011). "PED/PEA-15 controls fibroblast motility and wound closure by ERK1/2-dependent mechanisms." Journal of Cellular Physiology **227**(5): 2106-2116.

Cao, X.-G., X.-X. Li, et al. (2007). "Responses of Human Lens Epithelial Cells to Quercetin and DMSO." Investigative Ophthalmology & Visual Science **48**(8): 3714-3718.

Carter, S. B. (1967). "Haptotaxis and the Mechanism of Cell Motility." Nature **213**: 256-260.

Cascone, M. G., N. Barbani, et al. (2001). "Bioartificial polymeric materials based on polysaccharides." J. Biomater. Sci. Polym. **12**: 267-81.

Cauich-Rodriguez, J. V., S. Deb, et al. (1996). "Characterization of hydrogel blends of poly(vinyl pyrrolidone) and poly(vinyl alcohol-vinyl acetate)." Journal of Materials Science: Materials in Medicine **7**(5): 269-272.

Černáa, M., A. S. Barros, et al. (2003). "Use of FT-IR spectroscopy as a tool for the analysis of polysaccharide food additives." Carbohydrate Polymers **51**(4): 383-389.

Cescutti, P., C. Campa, et al. (2002). "Structure of the oligomers obtained by enzymatic hydrolysis of the glucomannan produced by the plant Amorphophallus konjac." Carbohydrate Research **337**(24): 2505-2511.

Cha, Y. and C. G. Pitt (1990). "The biodegradability of polyester blends." Biomaterials **11**(2): 108-112.

Chakrabarty, K. H., R. A. Dawson, et al. (1999). "Development of autologous human dermal–epidermal composites based on sterilized human allodermis for clinical use." British Journal of Dermatology **141**(5): 811-823.

Chakrabarty, K. H., M. Heaton, et al. (2001). "Keratinocytes driven contraction of reconstructed human skin." Wound Repair and Regeneration **9**(2): 95-106.

Chao, Y.-C., S.-K. Su, et al. (2013). "Preparation and Application of PEG/PVP Copolymers." Journal of Polymers and the Environment **21**(1): 160-165.

Chen, L.-G., Z.-L. Liu, et al. (2005). "Synthesis and properties of degradable hydrogels of konjac glucomannan grafted acrylic acid for colon-specific drug delivery." Polymer **46**(16): 6274-6281.

Chen, X., L. Zhang, et al. (2009). "Novel Sulfated Glucomannan-Barium-Alginate Microcapsules in Islet Transplantation: Significantly Decreased the Secretion of Monocyte Chemotactic Protein 1 and Improved the Activity of Islet in Rats." Transplantation Proceedings **41**(10): 4307-4312.

Chenal, T., X. Olonde, et al. (2007). "Controlled polyethylene chain growth on magnesium catalyzed by lanthanidocene: A living transfer polymerization for the synthesis of higher dialkyl-magnesium." Polymer **48**(7): 1844-1856.

Chipev, C. C. and M. Simon (2002). "Phenotypic differences between dermal fibroblasts from different body sites determine their responses to tension and TGFbeta1." BMC Dermatol **2**: 13.

Chirife, J., G. Scarmato, et al. (1982). "Scientific basis for use of granulated sugar in treatment of infected wounds." The Lancet **319**(8271): 560-561.

Choi, S. and M.-H. Chung (2003). "A review on the relationship between aloe vera components and their biologic effects." Seminars in Integrative Medicine **1**(1): 53-62.

Chua, M., K. Chan, et al. (2012). "Methodologies for the extraction and analysis of konjac glucomannan from corms of Amorphophallus konjac K. Koch." Carbohydrate Polymers **87**(3): 2202-2210.

Church, D., S. Elsayed, et al. (2006). "Burn Wound Infections." Clinical Microbiology Reviews **19**(2): 403-434.

Clohisy, D. R., Z. Bar-Shavit, et al. (1987). "1,25-Dihydroxyvitamin D3 modulates bone marrow macrophage precursor proliferation and differentiation. Up-regulation of the mannose receptor." Journal of Biological Chemistry **262**(33): 15922-15929.

Colucci, G., J. G. Moore, et al. (1999). "cDNA cloning of FRIL, a lectin from Dolichos lablab, that preserves hematopoietic progenitors in suspension culture." Immunology **96**(2): 646-650.

Connolly, M. L., J. A. Lovegrove, et al. "Konjac glucomannan hydrolysate beneficially modulates bacterial composition and activity within the faecal microbiota." Journal of Functional Foods **2**(3): 219-224.

Corkhill, P. H., C. J. Hamilton, et al. (1989). "Synthetic hydrogels VI. Hydrogel composites as wound dressings and implant materials." Biomaterials **10**(1): 3-10.

Crooke, S. T. and W. T. Bradner (1976). "Mitomycin C: a review." Cancer Treatment Reviews **3**(3): 121-139.

Crowston, J. G., A. N. Akbar, et al. (1998). "Antimetabolite-induced apoptosis in Tenon's capsule fibroblasts." Investigative Ophthalmology & Visual Science **39**(2): 449-54.

Currie, L. J., R. Martin, et al. (2003). "A comparison of keratinocyte cell sprays with and without fibrin glue." Burns **29**(7): 677-685.

Dai, Y. H., X. L. Sun, et al. (2012). "A Polymer Gel Electrolyte Based on P (MMA-NVP) for Quasi-Solid-State Dye-Sensitized Solar Cell." Advanced Materials Research **347**: 124-127.

Dam, T. K. and C. F. Brewer (2010). "Lectins as pattern recognition molecules: The effects of epitope density in innate immunity." Glycobiology **20**(3): 270-279.

Daniels, J. T., N. L. Occleston, et al. (1999). "Effects of Antimetabolite Induced Cellular Growth Arrest on Fibroblast-Fibroblast Interactions." Experimental Eye Research **69**(1): 117-127.

Day, J. and G. Stacey (2007). Long-Term Ex Situ Conservation of Biological Resources and the Role of Biological Resource Centers. Cryopreservation and Freeze-Drying Protocols, Humana Press. **368:** 1-14.

Dergunov, S. and G. Mun (2009). "Gamma-irradiated chitosan-polyvinyl pyrrolidone hydrogels as pH-sensitive protein delivery system. ." Radiation Physics and Chemistry **78**(1): 65-68.

Desmoulière, A., C. Chaponnier, et al. (2005). "Tissue repair, contraction, and the myofibroblast.

12." Wound Repair and Regeneration **13**(1): 7-12.

Doll, D. C., R. B. Weiss, et al. (1985). "Mitomycin: ten years after approval for marketing." Journal of Clinical Oncology **3**(2): 276-86.

Drury, J. L. and D. J. Mooney (2003). "Hydrogels for tissue engineering: scaffold design variables and applications." Biomaterials **24**(24): 4337-4351.

Dumitriu, S., P. Magny, et al. (1994). "Polyionic Hydrogels Obtained by Complexation between Xanthan and Chitosan: Their Properties as Supports for Enzyme Immobilization." Journal of Bioactive and Compatible Polymers **9**(2): 184-209.

Eaglstein, W. H. (2001). "Moist Wound Healing with Occlusive Dressings: A Clinical Focus." Dermatologic Surgery **27**(2): 175-182.

East, L. and C. M. Isacke (2002). "The mannose receptor family." Biochimica et Biophysica Acta (BBA) - General Subjects **1572**(2): 364-386.

Eichler, M. J. and M. A. Carlson (2006). "Modeling dermal granulation tissue with the linear fibroblast-populated collagen matrix: A comparison with the round matrix model." Journal of Dermatological Science **41**(2): 97-108.

Esseku, F. and M. C. Adeyeye (2010). "Bacteria and pH-sensitive polysaccharide-polymer films for colon targeted delivery." Critical Reviews in Therapeutic Drug Carrier Systems **28**(5): 395-445.

Eves, P., M. Baran, et al. (2011). "Establishing a Transport Protocol for the Delivery of Melanocytes and Keratinocytes for the Treatment of Vitiligo." Tissue Engineering Part C: Methods **17**(4): 375-382.

Eves, P., E. Katerinaki, et al. (2003). "Melanoma invasion in reconstructed human skin is influenced by skin cells--investigation of the role of proteolytic enzymes." Clin Exp Metastasis **20**(8): 685-700.

Eves, P., C. Layton, et al. (2000). "Characterization of an in vitro model of human melanoma invasion based on reconstructed human skin." Br J Dermatol **142**(2): 210-22.

Eves, P. C., A. J. Beck, et al. (2005). "A chemically defined surface for the co-culture of melanocytes and keratinocytes." Biomaterials **26**(34): 7068-7081.

Fahie, M. A. and D. Shettko (2007). "Evidence-Based Wound Management: A Systematic Review of Therapeutic Agents to Enhance Granulation and Epithelialization." Veterinary Clinics of North America: Small Animal Practice **37**(3): 559-577.

Falanga, V. (2005). "Wound healing and its impairment in the diabetic foot." The Lancet **366**(9498): 1736-1743.

Falanga, V., K. Faria, et al. (2007). Bioengineered skin constructs. Principles of Tissue Engineering (Third Edition). Burlington, Academic Press**:** 1167-1185.

Fan, J., K. Wang, et al. (2008). "In vitro evaluations of konjac glucomannan and xanthan gum mixture as the sustained release material of matrix tablet." Carbohydrate Polymers **73**(2): 241-247.

Fan, L., H. Zhu, et al. (2007). "Structure and properties of blend fibers prepared from alginate and konjac glucomannan." Journal of Applied Polymer Science **106**(6): 3903-3907.

Farris, S., K. M. Schaich, et al. (2009). "Development of polyion-complex hydrogels as an alternative approach for the production of bio-based polymers for food packaging applications: a review." Trends in Food Science & Technology **20**(8): 316-332.

Farris, S., K. M. Schaich, et al. (2009). "Development of polyion-complex hydrogels as an alternative approach for the production of bio-based polymers for food packaging

applications: a review." Trends in Food Science & Technology **20**(8): 316-332.

Ferguson, M. and S. O'Kane (2004). "Scar-free healing: from embryonic mechanisms to adult therapeutic intervention." Philos Trans R Soc Lond B Biol Sci **359**(1445): 839-50.

Fodor, W. (2003). "Tissue engineering and cell based therapies, from the bench to the clinic: the potential to replace, repair and regenerate." Reprod Biol Endocrinol **1**: 102.

Forrest, R. D. (1982). "Early history of wound treatment." J R Soc Med. **75**(3): 198-205.

Freitas, A. R., L. Gaffo, et al. (2014). "Miscibility studies on polychloroprene/natural rubber (PCP/NR) blends by dilute solution viscometry (DSV) and scanning electronic microscopy (SEM) methods." Journal of Molecular Liquids **190**(0): 146-150.

Gao, S. and L. Zhang (2001). "Molecular Weight Effects on Properties of Polyurethane/Nitrokonjac Glucomannan Semiinterpenetrating Polymer Networks." Macromolecules **34**(7): 2202-2207.

Garbuz, N., R. Zhbankov, et al. (1973). "Investigation of cellulose derivatives containing C≡C bond by IR spectroscopy." Journal of Applied Spectroscopy **19**(1): 898-902.

Garfein, E. S., D. P. Orgill, et al. (2003). "Clinical applications of tissue engineered constructs." Clinics in Plastic Surgery **30**(4): 485-498.

Ghosh, M. M., S. Boyce, et al. (1997). "A comparison of methodologies for the preparation of human epidermal-dermal composites." Annals of plastic surgery **39**(4): 390-404.

Gidley, M. J., A. J. McArthur, et al. (1991). "13C NMR characterization of molecular structures in powders, hydrates and gels of galactomannans and glucomannans." Food Hydrocolloids **5**(12): 129-140.

Goldstein, I. J., C. E. Hollerman, et al. (1965). "Protein-Carbohydrate Interaction. II. Inhibition Studies on the Interaction of Concanavalin A with Polysaccharides*." Biochemistry **4**(5): 876-883.

Gomaa, K., J. Kraus, et al. (1992). "Antitumour and immunological activity of aB1-3/1-6 glucan from *Glomerella cingulata*." Journal of Cancer Research and Clinical Oncology **118**(2): 136-140.

Gouin, J.-P. and J. K. Kiecolt-Glaser "The Impact of Psychological Stress on Wound Healing: Methods and Mechanisms." Immunology and Allergy Clinics of North America **31**(1): 81-93.

Goulimari, P., T. M. Kitzing, et al. (2005). "Ga12/13 Is Essential for Directed Cell Migration and Localized Rho-Dia1 Function." Journal of Biological Chemistry **280**(51): 42242-42251.

Gow, N. A. R., F. L. van de Veerdonk, et al. (2012). "Candida albicans morphogenesis and host defence: discriminating invasion from colonization." Nat Rev Micro **10**(2): 112-122.

Goycoolea, F. M., E. R. Morris, et al. (1995). "Screening for synergistic interactions in dilute polysaccharide solutions." Carbohydrate Polymers **28**(4): 351-358.

Griffith, L. G. and G. Naughton (2002). "Tissue Engineering--Current Challenges and Expanding Opportunities." Science **295**(5557): 1009-1014.

Griffiths, P. and J. A. De Haseth (2007). Fourier Transform Infrared Spectrometry. Hoboken, New Jersey, John Wiley & Sons, Inc.

Guo, Q., J. Huang, et al. (1996). "Miscibility of poly(N-vinyl-2-pyrrolidone) with poly(hydroxyether of phenolphthalein) and polyacrylonitrile." European Polymer Journal **32**(4): 423-426.

Gupta, A., R. K. Gupta, et al. (2009). "Targeting cells for drug and gene delivery: Emerging applications of mannans and mannan binding lectins." Journal of Scientific and Industrial Research **68**(6): 465-483.

Hampton, S. (2004). "A guide to managing the surrounding skin of chronic, exuding wounds." http://www.nursingtimes.net/a-guide-to-managing-the-surrounding-skin-of-

chronic-exuding-wounds/200076.article **Last assessed at 16th March 2013.**

Hanninen, O. and M. Farago, and Monos E. (1983). "Ignaz Philipp Semmelweis, the prophet of bacteriology " Infect Control. **(Sept-Oct) 4**(5): 367-70.

Hansbrough, J. F., D. W. Mozingo, et al. (1997). "Clinical trials of a biosynthetic temporary skin replacement, dermagraft-transitional covering, compared with cryopreserved human cadaver skin for temporary coverage of excised burn wounds." J Burn Care Rehabil **18**(43-51).

Harrison, C., F. Gossiel, et al. (2006). "Use of an in vitro model of tissue-engineered skin to investigate the mechanism of skin graft contraction." Tissue Eng **12**(11): 3119-33.

He, S., M. J. Yaszemski, et al. (2000). "Injectable biodegradable polymer composites based on poly(propylene fumarate) crosslinked with poly(ethylene glycol)-dimethacrylate." Biomaterials **21**(23): 2389-2394.

Healy, C. and J. Boorman (1989). "Comparison of E-Z Derm and Jelonet dressings for partial skin thickness burns." Burns Incl Therm Inj **15**(1): 52-4.

Henderson, N. C., A. C. Mackinnon, et al. (2006). "Galectin-3 regulates myofibroblast activation and hepatic fibrosis." Proceedings of the National Academy of Sciences of the United States of America **103**(13): 5060-5065.

Hespanhol, R. C., M. d. N. C. Soeiro, et al. (2005). "The Expression of Mannose Receptors in Skin Fibroblast and Their Involvement in Leishmania (L.) amazonensis Invasion." Journal of Histochemistry & Cytochemistry **53**(1): 35-44.

Higa, O. Z., S. O. Rogero, et al. (1999). "Biocompatibility study for PVP wound dressing obtained in different conditions." Radiation Physics and Chemistry **55**(5-6): 705-707.

Hoffman, A. S. (2002). "Hydrogels for biomedical applications." Advanced Drug Delivery Reviews **54**(1): 3-12.

Holgersson, J., A. Gustafsson, et al. (2005). "Characteristics of protein-carbohydrate interactions as a basis for developing novel carbohydrate-based antirejection therapies." Immunol Cell Biol **83**(6): 694-708.

Honardoust, H. A., G. Jiang, et al. (2006). "Expression of Endo180 is spatially and temporally regulated during wound healing." Histopathology **49**(6): 634-648.

Hong, Y., T. V. Chirila, et al. (1997). "Effect of crosslinked poly(1-vinyl-2-pyrrolidinone) gels on cell growth in static cell cultures." Bio-Medical Materials and Engineering **7**(1): 35-47.

Hoorn, C. M., J. G. Wagner, et al. (1995). "Toxicity of Mitomycin C Toward Cultured Pulmonary Artery Endothelium." Toxicology and Applied Pharmacology **130**(1): 87-94.

Hua, Y. F., M. Zhang, et al. (2004). "Structural characterization of a 2-O-acetylglucomannan from Dendrobium officinale stem." Carbohydrate Res **339**: 2219-2224.

Huang, L., R. Takahashi, et al. (2002). "Gelation Behavior of Native and Acetylated Konjac Glucomannan." Biomacromolecules **3**(6): 1296-1303.

Imaz, A. and J. Forcada (2008). "N-vinylcaprolactam-based microgels: Effect of the concentration and type of cross-linker." Journal of Polymer Science Part A: Polymer Chemistry **46**(8): 2766-2775.

Irache, J. M., H. H. Salman, et al. (2008). "Mannose-targeted systems for the delivery of therapeutics." Expert Opinion on Drug Delivery **5**(6): 703-724.

Isaac, C., M. B. Mathor, et al. (2009). "Pentoxifylline modifies three-dimensional collagen lattice model contraction and expression of collagen types I and III by human fibroblasts derived from post-burn hypertrophic scars and from normal skin." Burns **35**(5): 701-706.

Jacon, S. A., M. A. Rao, et al. (1993). "The isolation and characterization of a water extract of konjac flour gum." Carbohydrate Polymers **20**(1): 35-41.

Jakupec, M. A., P. Unfried, et al. (2005). Pharmacological properties of cerium compunds Reviews of Physiology, Biochemistry and Pharmacology. O. Krayer, E. Lehnartz, A. v. Muralt and H. H. Weber, Springer Berlin Heidelberg. **153:** 101-111.

Jansen, K. M. and G. K. Pavlath (2006). "Mannose receptor regulates myoblast motility and muscle growth." <u>J Cell Biol</u> **174**(3): 403-13.

Janzekovic, Z. (1970). "A New Concept in the Early Excision and Immediate Grafting of Burns." <u>The Journal of Trauma and Acute Care Surgery</u> **10**(12): 1103-1108.

Jhon, M. S. and J. D. Andrade (1973). "Water and hydrogels." <u>Journal of Biomedical Materials Research</u> **7**(6): 509-522.

Jones, I., L. Currie, et al. (2002). "A guide to biological skin substitutes." <u>British Journal of Plastic Surgery</u> **55**(3): 185-193.

Joseph, H. (2004). Chapter 1 - Wound Healing. <u>Small Animal Surgery Secrets (Second Edition)</u>. Philadelphia, Hanley & Belfus**:** 1-6.

Kačuráková, M., P. Capek, et al. (2000). "FT-IR study of plant cell wall model compounds: pectic polysaccharides and hemicelluloses." <u>Carbohydrate Polymers</u> **43**(2): 195-203.

Kačuráková, M. and M. Mathlouthi (1996). "FTIR and laser-Raman spectra of oligosaccharides in water: characterization of the glycosidic bond." <u>Carbohydrate Research</u> **284**(2): 145-157.

Kačurákováa, M. and R. H. Wilson (2001). "Developments in mid-infrared FT-IR spectroscopy of selected carbohydrates." <u>Carbohydrate Polymers</u> **44**(4): 291-303.

Kamigaito, M., Y. Maeda, et al. (1993). "Living cationic polymerization of isobutyl vinyl ether by hydrogen chloride/Lewis acid initiating systems in the presence of salts: in-situ direct NMR analysis of the growing species." <u>Macromolecules</u> **26**(7): 1643-1649.

Kato, K. and K. Matsuda (1969). <u>Agric. Biol. Chem.</u> **33**: 1446.

Kilic, A. (2001). "Healing of diabetic ulcers with granulated sugar." <u>Plast Reconstr Surg</u> **108**: 585.

Kim, S. J., K. J. Lee, et al. (2004). "Water Behavior of Poly(acrylic acid)/ Poly (acrylonitrile) Semi-Interpenetrating Polymer Network Hydrogels." <u>High Performance Polymers</u> **16**(4): 625-635.

Klima, J., L. Lacina, et al. (2009). "Differential regulation of galectin expression/reactivity during wound healing in porcine skin and in cultures of epidermal cells with functional impact on migration." <u>Physiol Res.</u> **58**(6): 873-874.

Knutson, R., L. Merbitz, et al. (1981). "Use of sugar and povidone-iodine to enhance wound healing: five year's experience." <u>South Med J</u> **74**: 1329 - 35.

Ko, Y. C., B. D. Ratner, et al. (1981). "Characterization of hydrophilic–hydrophobic polymeric surfaces by contact angle measurements." <u>Journal of Colloid and Interface Science</u> **82**(1): 25-37.

Kobayashi, M., I. Ando, et al. (1995). "Structural study of poly(vinyl alcohol) in the gel state by high-resolution solid-state 13C NMR spectroscopy." <u>Macromolecules</u> **28**(19): 6677-6679.

Kohn, J., Abramson, S. and Langer, R. (2004). Bioresorbable and bioerodible materials. <u>Biomaterials Science</u>. D. R. Buddy, Academic Press**:** 115-127.

Kojima, T., K. Tabata, et al. (1986). "Molecular weight dependence of the antitumor activity of Schizophyllan." <u>Argic. Biol. Chem</u> **50**: 231-232.

Kollet, O., J. G. Moore, et al. (2000). "The plant lectin FRIL supports prolonged in vitro maintenance of quiescent human cord blood CD34(+) CD38 (-low)/SCID repopulating stem cells." <u>Experimental Hematology</u> **28**(6): 726-736.

Kolybaba, M., Tabil, L. G., Panigrahi, S., Crerar, W. J., Powell, T., Wang, B., Inn, Q., et al.. (2003). "Biodegradable Polymers : Past , Present , and Future. Biodegradation." **0300(03),**(1-15.).

Kulicke, W.-M., A. I. Lettau, et al. (1997). "Correlation between immunological activity, molar mass, and molecular structure of different (1->3)-B-D-glucans." Carbohydrate Research **297**(2): 135-143.

Kuroyanagi, Y., K. Kubo, et al. (2004). "Establishment of Banking System for Allogeneic Cultured Dermal Substitute." Artificial Organs **28**(1): 13-21.

Labsky, J., B. Dvorankova, et al. (2003). "Mannosides as crucial part of bioactive supports for cultivation of human epidermal keratinocytes without feeder cells." Biomaterials **24**(5): 863-872.

Lam, C. X., D. W. Hutmacher, et al. (2009). "Evaluation of polycaprolactone scaffold degradation for 6 months in vitro and in vivo." Journal of Biomedical Materials Research Part A **90**(3): 906-919.

Langer, R. (1995). "Biomaterials and biomedical engineering." Chemical Engineering Science **50**(24): 4109-4121.

Langer, R. S. and N. A. Peppas (1981). "Present and future applications of biomaterials in controlled drug delivery systems." Biomaterials **2**(4): 201-214.

Lauffenburger, D. and A. Horwitz (1996). "Cell migration: a physically integrated molecular process." Cell **84**(3): 359-69.

Lawrence, W. T. (1998). "Physiology of the acute wound." Clin Plast Surg. **25**(3): 321-40.

Laws, D. D., H. Bitter, et al. (2002). "Solid-State NMR Spectroscopic Methods in Chemistry." Angewandte Chemie International Edition **41**(17): 3096-3129.

Lee, B. S., B. C. Chun, et al. (2001). "Structure and Thermomechanical Properties of Polyurethane Block Copolymers with Shape Memory Effect." Macromolecules **34**(18): 6431-6437.

Lee, K. Y. and D. J. Mooney (2001). "Hydrogels for tissue engineering." Chem Rev. **101**: 1869-79.

Lee, P. Y., E. Cobain, et al. (2007). "Thermosensitive Hydrogel PEG-PLGA-PEG Enhances Engraftment of Muscle-derived Stem Cells and Promotes Healing in Diabetic Wound." Mol Ther **15**(6): 1189-1194.

Lee, S. J., S. Evers, et al. (2002). "Mannose Receptor-Mediated Regulation of Serum Glycoprotein Homeostasis." Science **295**(5561): 1898-1901.

Lele, T., C. Thodeti, et al. (2006). "Force meets chemistry: analysis of mechanochemical conversion in focal adhesions using fluorescence recovery after photobleaching." J Cell Biochem **97**(6): 1175-83.

Lemieux, R. U. (1993). "How Proteins recognize and bind oligosaccharides." Acs Symposium Series **519**: 5-18.

Leo, M. a. Z., V. I.. (1961). Great Ideas in the History of Surgery. New York, Bailliere, Tindall & Cox

Lerman, O. Z., R. D. Galiano, et al. (2003). "Cellular Dysfunction in the Diabetic Fibroblast: Impairment in Migration, Vascular Endothelial Growth Factor Production, and Response to Hypoxia." The American Journal of Pathology **162**(1): 303-312.

Leung, M. Y. K., C. Liu, et al. (2004). "Chemical and biological characterization of a polysaccharide biological response modifier from Aloe vera L. var. chinensis (Haw.) Berg." Glycobiology **14**(6): 501-510.

Levy, G. B. and H. P. Frank (1955). "Determination of molecular weight of polyvinylpyrrolidone. II." Journal of Polymer Science **17**(84): 247-254.

Lewandowska, K. (2011). "Miscibility and interactions in chitosan acetate/poly(N-vinylpyrrolidone) blends." Thermochimica Acta **517**(12): 90-97.

Li, J., Y.-P. Zhang, et al. (2003). "Angiogenesis in wound repair: Angiogenic growth factors and the extracellular matrix." Microscopy Research and Technique **60**(1): 107-114.

Li, Q., W. Qi, et al. (2009). "Preparation and characterization of enzyme-modified konjac

glucomannan/xanthan blend films." J Biomater Sci Polym Ed **20**(3): 299-310.

Li, W., J. Fan, et al. (2004). "Mechanism of Human Dermal Fibroblast Migration Driven by Type I Collagen and Platelet-derived Growth Factor-BB." Molecular Biology of the Cell **15**(1): 294-309.

Li, Y., J. Rodrigues, et al. (2012). "Injectable and biodegradable hydrogels: gelation, biodegradation and biomedical applications." Chemical Society Reviews **41**(6): 2193-2221.

Liang, C.-C., A. Y. Park, et al. (2007). "In vitro scratch assay: a convenient and inexpensive method for analysis of cell migration in vitro." Nature Protocols **2**: 329-333.

Liang, C. Y. and R. H. Marchessault (1959). J. Polym. Sci **37**(385).

Liang, C. Y. and R. H. Marchessault (1959 (a)). J. Polym. Sci. **39**(269).

Lionelli, G. T. and W. T. Lawrence (2003). "Wound dressings." Surgical Clinics of North America **83**(3): 617-638.

Lis, H. and N. Sharon (1998). "Lectins: Carbohydrate-specific proteins that mediate cellular recognition." Chemical Reviews **98**(2): 637-674.

Lisle, J. (2002). "Use of sugar in the treatment of infected leg ulcers." Br J Community Nurs **7**(6 Suppl): 46.

Liu, L., D. Siriwardena, et al. (2008). "Australia and New Zealand survey of antimetabolite and steroid use in trabeculectomy surgery." J Glaucoma **17**(6): 423-30.

Liu, T.-l., J.-c. Miao, et al. "Cytocompatibility of regenerated silk fibroin film: a medical biomaterial applicable to wound healing." Journal of Zhejiang University - Science B **11**(1): 10-16.

Liu, V. and S. Bhatia (2002). "Three-Dimensional Photopatterning of Hydrogels Containing Living Cells." Biomedical Microdevices **4**(4): 257-266.

Lloyd, A. W., R. G. A. Faragher, et al. (2001). "Ocular biomaterials and implants." Biomaterials **22**(8): 769-785.

Lu, Y., L. Zhang, et al. (2004). "Structure, properties and biodegradability of water resistant regenerated cellulose films coated with polyurethane/benzyl konjac glucomannan semi-IPN coating." Polymer Degradation and Stability **86**(1): 51-57.

Lutolf, M. P. and J. A. Hubbell (2005). "Synthetic biomaterials as instructive extracellular microenvironments for morphogenesis in tissue engineering

" Nature Biotechnology **23**: 47-55.

Lydon, M. J., T. W. Minett, et al. (1985). "Cellular interactions with synthetic polymer surfaces in culture." Biomaterials **6**(6): 396-402.

MacNeil, S. (2007). "Progress and opportunities for tissue-engineered skin." Nature **445**: 874-880.

Maeda, M., H. Shimahara, et al. (1980). "Studies of mannan and related-compounds 5. Detailed examination of the branched structure of konjac glucomannan." Agric. Biol. Chem. **2**(44): 245-252.

Mahdavinia, G. R., A. Pourjavadi, et al. (2004). "Modified chitosan 4. Superabsorbent hydrogels from poly(acrylic acid-co-acrylamide) grafted chitosan with salt- and pH-responsiveness properties." European Polymer Journal **40**(7): 1399-1407.

Mano, J. F., G. A. Silva, et al. (2007). "Natural origin biodegradable systems in tissue engineering and regenerative medicine: present status and some moving trends." Journal of The Royal Society Interface **4**(17): 999-1030.

Mansur, H. S., C. M. Sadahira, et al. (2008). "FTIR spectroscopy characterization of poly (vinyl alcohol) hydrogel with different hydrolysis degree and chemically crosslinked with glutaraldehyde." Materials Science and Engineering: C **28**(4): 539-548.

Markowska, A. I., K. C. Jefferies, et al. "Galectin-3 Protein Modulates Cell Surface Expression and Activation of Vascular Endothelial Growth Factor Receptor 2 in

Human Endothelial Cells." Journal of Biological Chemistry **286**(34): 29913-29921.

Martino, F., E. Martino, et al. (2005). "Effect of dietary supplementation with glucomannan on plasma total cholesterol and low density lipoprotein cholesterol in hypercholesterolemic children." Nutrition, Metabolism and Cardiovascular Diseases **15**(3): 174-180.

Marvin E, L. (1998). "Prevention and treatment of diabetic foot wounds." Journal of WOCN **25**(3): 129-146.

Masaidova, G., A. Yakunina, et al. (1966). "rogovin ZA. Structure and properties of cellulose and its derivatives. CXCVI. Synthesis of cellulose ethers containing CC triple bonds." Vysokomolekulyarnye Soedineniya **8**: 865-869.

Mathlouthi, M. and J. L. Koenig (1986). "Vibrational spectra of carbohydrates." Advances in Carbohydrate Chemistry and Biochemistry **44**: 7-89.

Matsuda, K., S. Suzuki, et al. (1990). "Influence of glycosaminoglycans on the collagen sponge component of a bilayer artificial skin." Biomaterials **11**(5): 351-355.

Mayo, S. J., J. Bogner, et al. (1997). *Amorphophallus*. The genera of *Araceae*., Royal Botanic Gardens, Kew**:** 235-239. .

McGreal, E. P., J. L. Miller, et al. (2005). "Ligand recognition by antigen-presenting cell C-type lectin receptors." Current Opinion in Immunology **17**(1): 18-24.

Metcalfe, A. D. and M. W. J. Ferguson (2007). "Bioengineering skin using mechanisms of regeneration and repair." Biomaterials **28**(34): 5100-5113.

Metcalfe, A. D. and M. W. J. Ferguson (2007). "Tissue engineering of replacement skin: the crossroads of biomaterials, wound healing, embryonic development, stem cells and regeneration." Journal of The Royal Society Interface **4**(14): 413-437.

Mi, F.-L., S.-S. Shyu, et al. (2003). "Chitin/PLGA blend microspheres as a biodegradable drug delivery system: a new delivery system for protein." Biomaterials **24**(27): 5023-5036.

Miadoková, E., S. Svidová, et al. (2006). "Diverse biomodulatory effects of glucomannan from Candida utilis." Toxicology in Vitro **20**(5): 649-657.

Milani, M., D. Drobne, et al. (2007). "How to study biological samples by FIB/SEM." Modern Research and Educational Topics in Microscopy. A. MÃ©ndez-Vilas and J. DÃaz (Eds.): 787-794.

Mokoena, T. and S. Gordon (1985). "Human macrophage activation. Modulation of mannosyl, fucosyl receptor activity in vitro by lymphokines, gamma and alpha interferons, and dexamethasone." J Clin Invest **75**(2): 624-31.

Moore, J., C. Fuchs, et al. (1997). "A new red kidney bean lectin called FRIL specifically stimulates proliferation of 3T3 fibroblasts transfected with the Flk2/Flt3 receptor." Blood **90**: 1366a.

Moore, J. G., C. A. Fuchs, et al. (2000). "A new lectin in red kidney beans called PvFRIL stimulates proliferation of NIH 3T3 cells expressing the Flt3 receptor." Biochimica et Biophysica Acta (BBA) - General Subjects **1475**(3): 216-224.

Moore, O., L. Smith, et al. (2001). "Systematic review of the use of honey as a wound dressing." BMC Complementary and Alternative Medicine **1**(1): 2.

Moshaverinia, A., N. Roohpour, et al. (2009). "Effects of N-vinylpyrrolidone (NVP) containing polyelectrolytes on surface properties of conventional glass-ionomer cements (GIC)." Dental Materials **25**(10): 1240-1247.

Mow, V., R. Tran-Son-Tay, et al. (1994). Mechanics of Cell Locomotion. Cell Mechanics and Cellular Engineering, Springer New York**:** 459-478.

Mumtaz, M., C. Labrugère §, et al. (2009). "Synthesis of Polyaniline Nano-Objects Using Poly(vinyl alcohol)-, Poly(ethylene oxide)-, and Poly[(N-vinyl pyrrolidone)-co-(vinyl alcohol)]-Based Reactive Stabilizers." Langmuir **25**(23): 13569-13580.

Murakami, K., H. Aoki, et al. "Hydrogel blends of chitin/chitosan, fucoidan and alginate as healing-impaired wound dressings." Biomaterials **31**(1): 83-90.

Nguyen, K. T. and J. L. West (2002). "Photopolymerizable hydrogels for tissue engineering applications." Biomaterials **23**(22): 4307-4314.

Nik, M. and M. Otto (1990). "Towards an optimized MTT assay." Journal of Immunological Methods **130**(1): 149-151.

Nikonenko, N. A., D. K. Buslov, et al. (2005). "Spectroscopic manifestation of stretching vibrations of glycosidic linkage in polysaccharides." Journal of Molecular Structure **752**(13): 20-24.

Nuttelman, C. R., D. J. Mortisen, et al. (2001). "Attachment of fibronectin to poly(vinyl alcohol) hydrogels promotes NIH3T3 cell adhesion, proliferation, and migration." Journal of Biomedical Materials Research **57**(2): 217-223.

Odian, G. (1981). Principles of polymerization, John Wiley & Sons, Inc.

Odian, G. (2004). Principles of Polymerization. New York, Wiley-Interscience.

Onishi, N., S. Kawamoto, et al. (2007). "Dietary Pulverized Konjac Glucomannan Suppresses Scratching Behavior and Skin Inflammatory Immune Responses in NC/Nga Mice." Int Arch Allergy Immunol **144**(2): 95-104.

Pandey, K. and A. Pitman (2003). "FTIR studies of the changes in wood chemistry following decay by brown-rot and white-rot fungi." International biodeterioration & biodegradation **52**(3): 151-160.

Pavlov, M. P., J. F. Mano, et al. (2004). "Fibers and 3D Mesh Scaffolds from Biodegradable Starch-Based Blends: Production and Characterization." Macromolecular Bioscience **4**(8): 776-784.

Peattie, R. A., A. P. Nayate, et al. (2004). "Stimulation of in vivo angiogenesis by cytokine-loaded hyaluronic acid hydrogel implants." Biomaterials **25**(14): 2789-2798.

Peppas, N., R. Langer, et al. (1995). Tissue regeneration templates based on collagen-glycosaminoglycan copolymers. Biopolymers II, Springer Berlin Heidelberg. **122:** 219-244.

Peppas, N. A., P. Bures, et al. (2000). "Hydrogels in pharmaceutical formulations." European Journal of Pharmaceutics and Biopharmaceutics **50**(1): 27-46.

Peppas, N. A. and J. J. Sahlin (1996). "Hydrogels as mucoadhesive and bioadhesive materials: a review." Biomaterials **17**(16): 1553-1561.

Perez-Rigueiro, J., M. Elices, et al. (2007). "Similarities and Differences in the Supramolecular Organization of Silkworm and Spider Silk." Macromolecules **40**(15): 5360-5365.

Perkins, R. G., I. R. Davidson, et al. (2006). "Low-temperature SEM imaging of polymer structure in engineered and natural sediments and the implications regarding stability." Geoderma **134**(1â€"2): 48-55.

Perlin, L., S. MacNeil, et al. (2008). "Production and performance of biomaterials containing RGD peptides." Soft Matter **4**(12): 2331-2349.

Phan, T. T., L. Sun, et al. (2003). "Dietary compounds inhibit proliferation and contraction of keloid and hypertrophic scar-derived fibroblasts in vitro: therapeutic implication for excessive scarring." J Trauma **54**: 1212-1224.

Pieper, B. and M. H. L. Caliri (2003). "Nontraditional wound care: A review of the evidence for the use of sugar, papaya/papain, and fatty acids." Journal of WOCN **30**(4): 175-183.

Priola, A., G. Gozzelino, et al. (1993). "Properties of polymeric films obtained from u.v. cured poly(ethylene glycol) diacrylates." Polymer **34**(17): 3653-3657.

Queen, D., J. Evans, et al. (1987). "Burn wound dressings - a review." Burns **13**: 218 - 228.

Ralston, D. R., C. Layton, et al. (1997). "Keratinocytes contract human dermal extracellular

matrix and reduce soluble fibronectin production by fibroblasts in a skin composite model." British Journal of Plastic Surgery **50**(6): 408-415.

Rault, I., V. Frei, et al. (1996). "Evaluation of different chemical methods for cross-linking collagen gel, films and sponges. ." J. Mater. Sci. Mater. Med. **7**: 215-21.

Razzak, M. T., D. Darwis, et al. (2001). "Irradiation of polyvinyl alcohol and polyvinyl pyrrolidone blended hydrogel for wound dressing." Radiation Physics and Chemistry **62**(1): 107-113.

Remers, W. A. and D. M. Vyas (1989). "Structure-activity comparison of mitomycin C and mitomycin A analogues (review)." Anticancer Res. **9**(4): 1095-9.

Rimmer, S. (2011). Biomedical hydrogels: Biochemistry, manufacture and medical applications. Synthesis of hydrogels for biomedical applications: control of structure and properties. S. Rimmer, Woodhead Publishing Limited**:** 269.

Rimmer, S., M. J. German, et al. (2005). "Synthesis and properties of amphiphilic networks 3: preparation and characterization of block conetworks of poly(butyl methacrylate-block-(2,3 propandiol-1-methacrylate-stat-ethandiol dimethacrylate))." Biomaterials **26**(15): 2219-2230.

Rimmer, S., C. Johnson, et al. (2007). "Epithelialization of hydrogels achieved by amine functionalization and co-culture with stromal cells." Biomaterials **28**(35): 5319-5331.

Risbud, M., A. Hardikar, et al. (2000). "Growth modulation of fibroblasts by chitosan-polyvinyl pyrrolidone hydrogel: implications for wound management?" J Biosci **25**(1): 25-31.

Robinson, B. V., F. M. Sullivan, et al. (1990). PVP:a critical review of the kinetics and toxicology of polyvinylpyrrolidone (povidone). Lewis Publishers.

Rodriguez, F. (1996). Principles of polymer systems, Taylor & Francis New York.

Ross, D., A. Phipps, et al. (1993). "The use of cerium nitrate-silver sulphadiazine as a topical burns dressing." British Journal of Plastic Surgery **46**(7): 582-584.

Ruszova, E., S. Pavek, et al. (2008). "Photoprotective effects of glucomannan isolated from Candida utilis." Carbohydrate Research **343**(3): 501-511.

Sadeghi, M. and M. Yarahmadi (2011). "Synthesis and Properties of Biopolymer based on Carboxymethyl Cellulose-g-Poly (N-vinylpyrollidin-co-2-Acrylamido-2-methyl propan Sulfonic Acid as Superabsorbent hydrogels." Oriental Journal of Chemistry **27**(1): 13-21.

Sandford, P. A. and J. Baird (1983). The Polysaccharides. New York, NY, Academic Press.

Sato, T., T. Norisuye, et al. (1984). "Double-stranded helix of xanthan: dimensional and hydrodynamic properties in 0.1 M aqueous sodium chloride." Macromolecules **17**(12): 2696-2700.

Schneider, G. B., A. English, et al. (2004). "The effect of hydrogel charge density on cell attachment." Biomaterials **25**(15): 3023-3028.

Schwentker, A., Y. Vodovotz, et al. (2002). "Nitric oxide and wound repair: role of cytokines?" Nitric Oxide **7**(1): 1-10.

Shahbuddin, M., A. Bullock, et al. (2013). "Glucomannan-poly(N-vinyl pyrrolidinone) bicomponent hydrogels for wound healing." Journal of Materials Chemistry B.

Shahbuddin, M., H. Park, et al. (2009). "Investigation of Cell-Matrix Interactions Using a FRET Technique." Bull. Korean Chem. Soc. **30**(8): 1817.

Shahbuddin, M., D. Shahbuddin, et al. (2013). "High molecular weight plant heteropolysaccharides stimulate fibroblasts but inhibit keratinocytes." Carbohydrate Research.

Sheikh, H., H. Yarwood, et al. (2000). "Endo180, an endocytic recycling glycoprotein related to the macrophage mannose receptor is expressed on fibroblasts, endothelial cells and macrophages and functions as a lectin receptor." Journal of Cell Science **113**(6): 1021-

1032.

Shevchenko, R. V., S. L. James, et al. (2010). "A review of tissue-engineered skin bioconstructs available for skin reconstruction." Journal of The Royal Society Interface **7**(43): 229-258.

Silvetti, A. N. (1981). "An Effective Method of Treating Long-Enduring Wounds and Ulcers by Topical Application of Nutrients." J. Dermatol, Surg. Oncol. **7**: 501-508.

Smith, L. E., S. Rimmer, et al. (2006). "Examination of the effects of poly(N-vinylpyrrolidinone) hydrogels in direct and indirect contact with cells." Biomaterials **27**(14): 2806-2812.

Smith, P. K., A. K. Mallia, et al. (1980). "Colorimetric method for the assay of heparin content in immobilized heparin preparations." Analytical Biochemistry **109**(2): 466-473.

Snyder, P. W., J. Mecinović, et al. (2011). "Mechanism of the hydrophobic effect in the biomolecular recognition of arylsulfonamides by carbonic anhydrase." Proceedings of the National Academy of Sciences **108**(44): 17889-17894.

Son, Y. K., J.-H. Kim, et al. (2007). "Preparation and properties of PEG Modified PNVP hydrogel." Macromolecular research **15**(6): 527-532.

Souren, J. M., M. Ponec, et al. (1989). "Contraction of collagen by human fibroblasts and keratinocytes." In Vitro Cellular & Developmental Biology **25**(11): 1039-1045.

Stavrou, D., J. Haik, et al. (2009). "From Traction and Contraction to Wound Closure." Journal of Wound Ostomy & Continence Nursing **36**(4): 365-366 10.1097/WON.0b013e3181aaefa5.

Stein, M., S. Keshav, et al. (1992). "Interleukin 4 potently enhances murine macrophage mannose receptor activity: a marker of alternative immunologic macrophage activation." J Exp Med **176**(1): 287-92.

Stephen, A. M. (1983). Other plant polysaccharides. . The Polysaccharides. G. O. Aspinall. New York, Academic Press. **2**: 97-192.

Sternlicht, M. and Z. Werb (2001). "How matrix metalloproteinases regulate cell behavior." Annu Rev Cell Dev Biol **17**: 463-516.

Suggs, L. J. and A. G. Mikos (1999). "Development of poly(propylene fumarate-co-ethylene glycol) as an injectable carrier for endothelial cells." Cell Transplantation **8**(4): 345-350.

Sutherland, A., R. Tester, et al. (2008). "Glucomannan hydrolysate (GMH) inhibition of Candida albicans growth in the presence of Lactobacillus and Lactococcus species." Microbial Ecology in Health and Disease **20**(3): 127-134.

Sylvester, M. F., I. V. Yannas, et al. (1989). "Collagen banded fibril structure and the collagen-platelet reaction." Thrombosis Research **55**(1): 135-148.

Száraz, I. and W. Forsling (2000). "A spectroscopic study of the solvation of 1-vinyl-2-pyrrolidone and poly(1-vinyl-2-pyrrolidone) in different solvents." Polymer **41**(13): 4831-4839.

Szolnoky, G., Z. Bata-Csorgo, et al. (2001). "A Mannose-Binding Receptor is Expressed on Human Keratinocytes and Mediates Killing of Candida albicans." J Invest Dermatol **117**(2): 205-213.

Taylor, P. R., S. Gordon, et al. (2005). "The mannose receptor: linking homeostasis and immunity through sugar recognition." Trends in Immunology **26**(2): 104-110.

Taylor, P. R., S. Gordon, et al. (2005). "The mannose receptor: linking homeostasis and immunity through sugar recognition." Trends Immunol **26**(2): 104-10.

Tejero-Trujeque, R. (2001). "How do fibroblasts interact with the extracellular matrix in wound contraction?" J Wound Care **10**(6): 237-42.

Thimma, R. T., N. S. Reddy, et al. (2003). "Synthesis and characterization of guar gum-graft-

polyacrylonitrile." <u>Polymers for Advanced Technologies</u> **14**(10): 663-668.

Tizard, I. R., R. H. Carpenter, et al. (1989). "The biological activities of mannans and related complex carbohydrates." <u>Mol Biother</u> **1**(6): 290-6.

Tizard, I. R., R. H. Carpenter, et al. (1989). "The biological activities of mannans and related complex carbohydrates." <u>Molecular biotherapy</u> **1**(6): 290-6.

Toita, S., N. Morimoto, et al. (2011). "Functional cycloamylose as a polysaccharide-based biomaterial: Application in a gene delivery system." <u>Biomacromolecules</u> **11**(2): 397-401.

Topham, J. (2002). "Why do some cavity wounds treated with honey or sugar paste heal without scarring?" <u>J Wound Care</u> **11**(2): 53-5.

Tye, R. J. (1989). "Industrial and non-food uses for carrageenan." <u>Carbohydrate Polymers</u> **10**(4): 259-280.

Ueda, K. F. and T. Komano (1984). "Sequence-specific DNA damage induced by reduced mitomycin C and 7-N-(p-hydroxyphenyl)mitomycin C." <u>Nucleic Acid Research</u> **12**(17): 6673-83.

Vaaler, D. A. G. e. (2008). "Yield-increasing additives in kraft pulping: Effect on carbohydrate retention, composition and handsheet properties."

van Apeldoorn, A. A., Y. Aksenov, et al. (2005). "Parallel high-resolution confocal Raman SEM analysis of inorganic and organic bone matrix constituents." <u>Journal of The Royal Society Interface</u> **2**(2): 39-45.

Varki A, C. R, et al. (1999). <u>Essentials of glycobiology</u> Cold Spring Harbor Laboratory Press, USA.

Vickers, N. J., S. L. McArthur, et al. (2008). "Ceric Ammonium Nitrate Initiated Grafting of PEG to Plasma Polymers for Cell-Resistant Surfaces." <u>Plasma Processes and Polymers</u> **5**(2): 192-201.

Vijayasekaran, S., T. Chirila, et al. (1996). "Poly(1-vinyl-2-pyrrolidinone) hydrogels as vitreous substitutes: histopathological evaluation in the animal eye." <u>J Biomater Sci Polym Ed</u> **7**(8): 685-96.

Vijayasekaran, S., T. V. Chirila, et al. (1996). "Poly(I-vinyl-2-pyrrolidinone) hydrogels as vitreous substitutes: Histopathological evaluation in the animal eye." <u>Journal of Biomaterials Science, Polymer Edition</u> **7**(8): 685-696.

Volden, G., H. Haugen, et al. (1980). "Reversible cellular damage by dimethyl sulfoxide reflected by release of marker enzymes for intracellular fractions." <u>Archives of Dermatological Research</u> **269**(2): 147-151.

Vuksan, V., D. J. Jenkins, et al. (1999). "Konjac-mannan (glucomannan) improves glycemia and other associated risk factors for coronary heart disease in type 2 diabetes. A randomized controlled metabolic trial." <u>Diabetes Care</u> **22**(6): 913-919.

Vuksan, V., J. L. Sievenpiper, et al. (2000). "Beneficial effects of viscous dietary fiber from Konjac-mannan in subjects with the insulin resistance syndrome: results of a controlled metabolic trial." <u>Diabetes Care</u> **23**(1): 9-14.

Vuksan, V., J. L. Sievenpiper, et al. (2001). "Konjac-Mannan and American Ginsing: Emerging Alternative Therapies for Type 2 Diabetes Mellitus." <u>Journal of the American College of Nutrition</u> **20**(suppl 5): 370S-380S.

Wade, C., S. E. Wolf, et al. (2010). "Loss of Protein, Immunoglobulins, and Electrolytes in Exudates From Negative Pressure Wound Therapy." <u>Nutrition in Clinical Practice</u> **25**(5): 510-516.

Wagner, D. K. and P. G. Sohnle (1995). "Cutaneous defenses against dermatophytes and yeasts." <u>Clinical Microbiology Reviews</u> **8**(3): 317-35.

Wakaki, S., H. Marumo, et al. (1958). "Isolation of new fractions of antitumor mitomycins. ." <u>Antibiot Chemother.</u> **8**: 228-240.

Wasser, S. (2003). "Medicinal mushrooms as a source of antitumor and immunomodulating polysaccharides." Applied Microbiology and Biotechnology **60**(3): 258-274.

Weiss, J. F. and B. M. (1981). "The effect of penicillamine on posttraumatic vitreous proliferation." Am J Ophthalmol **92**: 925-627.

Wen, X., T. Wang, et al. (2008). "Preparation of konjac glucomannan hydrogels as DNA-controlled release matrix." International Journal of Biological Macromolecules **42**(3): 256-263.

Werner, S., T. Krieg, et al. (2007). "Keratinocyte-Fibroblast Interactions in Wound Healing." J Invest Dermatol **127**(5): 998-1008.

White, R. and K. F. Cutting (2006). "Modern exudate management: a review of wound treatments." http://www.worldwidewounds.com/2006/september/White/Modern-Exudate-Mgt.html **Last assessed March 2013**.

Whitney, S. E. C., J. E. Brigham, et al. (1998). "Structural aspects of the interaction of mannan-based polysaccharides with bacterial cellulose." Carbohydrate Research **307**(34): 299-309.

Wichterle, O. and D. Lim (1960). "Hydrophilic Gels for Biological Use." Nature **185**(4706): 117-118.

Widjanarko, S. B., A. Nugroho, et al. (2011). "Functional interaction components of protein isolates and glucomannan in food bars by FTIR and SEM studies
" African Journal of Food Science **5**(1): 12-21.

Widjanarko, S. B., A. Nugroho, et al. (2011). "Functional interaction components of protein isolates and glucomannan in food bars by FTIR and SEM studies
" African Journal of Food Science **5**(1): 12-21.

Williams, I. R. and T. S. Kupper (1996). "Immunity at the surface: Homeostatic mechanisms of the skin immune system." Life Sciences **58**(18): 1485-1507.

Williams, P. A., D. H. Day, et al. (1991). "Synergistic interaction of xanthan gum with glucomannans and galactomannans." Food Hydrocolloids **4**(6): 489-493.

Winter, G. D. (1962). "Formation of the scab and the rate of epithelization of superficial wounds in the skin of the young domestic pig." Nature **193**(4812): 293-4.

Wollenberg, A., M. Mommaas, et al. (2002). "Expression and Function of the Mannose Receptor CD206 on Epidermal Dendritic Cells in Inflammatory Skin Diseases." J. Invest Dermatol **118**(2): 327-334.

Wollenberg, A., M. Mommaas, et al. (2002). "Expression and Function of the Mannose Receptor CD206 on Epidermal Dendritic Cells in Inflammatory Skin Diseases." **118**(2): 327-334.

Wolter, T. P., E. M. Noah, et al. (2005). "The use of Integra® in an upper extremity avulsion injury." British Journal of Plastic Surgery **58**(3): 416-418.

Wright, B., R. A. Cave, et al. (2012). "Enhanced viability of corneal epithelial cells for efficient transport/storage using a structurally-modified calcium alginate hydroge." Regenative Medicine **7**(3): 295-307.

Xiao, C., S. Gao, et al. (2000). "Blend films from chitosan and konjac glucomannan solutions." Journal of Applied Polymer Science **76**(4): 509-515.

Xiao, C., S. Gao, et al. (2000). "Blend films from konjac glucomannan and sodium alginate solutions and their preservative effect." Journal of Applied Polymer Science **77**(3): 617-626.

Xiao, C., H. Liu, et al. (2001). "Characterization of poly(vinylpyrrolidone)-konjac glucomannan blend films." Journal of Applied Polymer Science **81**(5): 1049-1055.

Xu, C., X. Luo, et al. (2009). "Preparation and characterization of polylactide/thermoplastic konjac glucomannan blends." Polymer **50**(15): 3698-3705.

Yamaguchi, Y., V. J. Hearing, et al. (2005). "Mesenchymal-epithelial interactions in the skin:

Aiming for site-specific tissue regeneration." Journal of Dermatological Science **40**(1): 1-9.

Yannas, I. V. (2000). "Synthesis of organs: In vitro or in vivo?" Proceedings of the National Academy of Sciences **97**(17): 9354-9356.

Yannas, I. V. (2005). "Similarities and differences between induced organ regeneration in adults and early foetal regeneration." J R Soc Interface. **2**(5): 403-417.

Yannas, I. V., E. Lee, et al. (1989). "Synthesis and characterization of a model extracellular matrix that induces partial regeneration of adult mammalian skin." Proceedings of the National Academy of Sciences **86**(3): 933-937.

Yannas, I. V., D. S. Tzeranis, et al. (2010). "Biologically active collagen-based scaffolds: advances in processing and characterization." Philosophical Transactions of the Royal Society A: Mathematical, Physical and Engineering Sciences **368**(1917): 2123-2139.

Yeganeh, H. and M. R. Mehdizadeh (2004). "Synthesis and properties of isocyanate curable millable polyurethane elastomers based on castor oil as a renewable resource polyol." European Polymer Journal **40**(6): 1233-1238.

Yeh, S.-L., M.-S. Lin, et al. "Partial hydrolysis enhances the inhibitory effects of konjac glucomannan from Amorphophallus konjac C. Koch on DNA damage induced by fecal water in Caco-2 cells." Food Chemistry **119**(2): 614-618.

Yu, H., A. Huang, et al. (2006). "Characteristics of konjac glucomannan and poly(acrylic acid) blend films for controlled drug release." Journal of Applied Polymer Science **100**(2): 1561-1570.

Zhang H, G. C., Wu H, Fan L, Li F, Yang F, Yang Q. (2007). "Immobilization of derivatized dextran nanoparticles on konjac glucomannan/chitosan film as a novel wound dressing." Biofactors(30(4)

): 227-40.

Zhang, H., M. Yoshimura, et al. (2001). "Gelation behaviour of konjac glucomannan with different molecular weights." Biopolymers **59**(1): 38-50.

Zhang, J., S. D. Tachado, et al. (2005). "Negative regulatory role of mannose receptors on human alveolar macrophage proinflammatory cytokine release in vitro." Journal of Leukocyte Biology **78**(3): 665-674.

Zhang, Q. Z., W. R. Su, et al. (2010). "Human gingiva-derived mesenchymal stem cells elicit polarization of m2 macrophages and enhance cutaneous wound healing." Stem Cells **28**(10): 1856-68.

Zhang, Y.-q., B.-j. Xie, et al. (2005). "Advance in the applications of konjac glucomannan and its derivatives." Carbohydrate Polymers **60**(1): 27-31.

Zhang, Z. G., I. Bothe, et al. (2006). "Interactions of primary fibroblasts and keratinocytes with extracellular matrix proteins: contribution of alpha2beta1 integrin." Journal of cell science **119**(Pt 9): 1886-1895.

Zhao, S., M. Cao, et al. "Synthesis and characterization of thermo-sensitive semi-IPN hydrogels based on poly(ethylene glycol)-co-poly(Îμ-caprolactone) macromer, N-isopropylacrylamide, and sodium alginate." Carbohydrate Research **345**(3): 425-431.